



**Using mouse models to learn about
mitochondrial DNA point mutations in
ageing and disease**

Holly Baines

BSc (Hons) MRes

This thesis is submitted for the degree of Doctor of Philosophy at
Newcastle University

Wellcome Trust Centre for Mitochondrial Research

Institute of Neuroscience

Newcastle University

October 2014

Author's Declaration

This thesis is submitted for the degree of Doctor of Philosophy at Newcastle University. The research was conducted in the Wellcome Trust Centre for Mitochondrial Research, Institute of Neuroscience, and is my own work if not stated otherwise. The research was completed under the supervision of Professor D.M. Turnbull and Dr Laura Greaves from September 2011 to October 2014.

I certify that none of the material offered in this thesis, with the exception of my MRes results as cited in Chapter 3, has been previously submitted by me for a degree or any other qualification at any other university.

Abstract

Mitochondrial DNA (mtDNA) point mutations clonally expand and result in focal respiratory chain deficiency in tissues of patients with mitochondrial disease and to a lesser extent in normal human ageing. The consequences of mtDNA point mutations upon cellular processes and the mechanisms involved in mitochondrial disease heterogeneity and progression as well as age-related tissue dysfunction, however still remain unknown. The aim of this thesis was to further our understanding of clonally expanded mtDNA point mutations in ageing and the mechanisms associated with disease heterogeneity, using mice that harbour mtDNA point mutations.

Characterisation of mitochondrial dysfunction in the *PolgA*^{+/*mut*} mouse colon provided evidence for a conserved mechanism for the clonal expansion of somatic mtDNA point mutations by random genetic drift, without any selective constraints, resulting in age-related respiratory chain deficiency in colonic crypts of both *PolgA*^{+/*mut*} mice and ageing humans. Preliminary data examining the gene expression profile of respiratory chain deficient colonic crypts revealed potential alterations in processes concerning: the cell cycle and proliferation; DNA maintenance and repair; cell adhesion and tight junction formation; the adaptive immune response and energy metabolism. Such changes hold a number of potentially interesting associations with the development of colorectal cancer and the pathogenesis of inflammatory bowel disease.

Using histochemical and mtDNA genome analysis, the m.5024C>T tRNA^{Ala} mouse was shown to be a fairly good model of a pathogenic mt-tRNA point mutation in disease. Results demonstrated that the m.5024C>T mutation was pathogenic; mice displayed phenotypic evidence of respiratory chain deficiency; aged mice displayed evidence of disease progression; different tissues showed different biochemical thresholds and there was a selective loss of the mutation in actively dividing cells.

These observations have important implications for the role of mtDNA point mutations in ageing and potential mechanisms that govern mitochondrial disease presentation, progression and transmission.

Acknowledgements

Firstly I would like to thank my supervisors Professor Doug Turnbull and Dr Laura Greaves for their continuous guidance and support throughout my PhD, without which I would not have been able to reach this stage. I would also like to thank them for their constant encouragement and inspiring words, especially when lab work became very frustrating and experiments required continuous optimisation.

I would also like to thank those whom I have collaborated with throughout my PhD, and their contributions to this thesis as outlined in the relevant sections. Primarily I would like to thank Dr James Stewart and Professor Nils-Göran Larsson (Max Planck Institute for Biology of Ageing, Cologne, Germany) for providing the *PolgA*^{+/*mut*} mice used in chapter 3 and the m.5024C>T tRNA^{Ala} mice used in chapter 5. I would further like to thank James Stewart for helping with the purifying selection statistics and for the continuous information and scientific discussions regarding the m.5024C>T tRNA^{Ala} mutant mice. I am also very grateful to Dr Graham Smith (Newcastle University) for completing the RNA bioinformatic analysis in chapter 4 as well as Craig Stamp (Newcastle University) for designing the in silico model used in chapter 3 and the Hue Saturation Value colour space model in chapter 5. I would also like to thank Dr Laura Greaves for performing the long-range PCR discussed in chapter 3.

I would like to thank Lynne and Chris in the animal house (Newcastle University) for their help with maintaining and sacrificing the *PolgA*^{mut/*mut*} and *PolgA*^{+/*mut*} mouse colony.

Huge thanks to various member of the Mitochondrial research group, who have given vast amounts of support over the years. I would particularly like to thank Alexia and Phil for listening to me complain when lab work was not going to plan as well as John for helping me with my stats and computer related queries. I would also like to thank Mrs Debra Jones and Mrs Hazel Glass for all of their incredible assistance and support.

Thanks to all of my family for their constant encouragement, support and interest in my work and publications, despite the fact they had no idea about science or what I was talking about.

Lastly I am grateful to the MRC for my studentship and the opportunity to complete this PhD.

Table of contents

Contents

Chapter 1. Introduction	6
1.1 Mitochondria	6
1.1.1 Mitochondrial structure	6
1.1.2 OXPHOS and synthesis of ATP	8
1.1.3 Other mitochondrial functions	12
1.2 The mitochondrial genome	13
1.2.1 Mammalian MtDNA transcription and replication	15
1.2.2 Mammalian mtDNA repair mechanisms	21
1.2.3 Maternal inheritance and the mtDNA bottleneck	22
1.2.4 MtDNA mutagenesis	23
1.2.5 Heteroplasmy	24
1.2.6 The threshold effect	24
1.2.7 Clonal expansion	26
1.2.8 Mitotic segregation	30
1.3 Mitochondrial disease	30
1.3.1 Mt-tRNA point mutations	32
1.4 Ageing	33
1.4.1 Evolutionary theories of ageing	34
1.4.2 Molecular theories of ageing	35
1.4.3 Mitochondrial dysfunction and ageing	37
1.5 Mouse models of mitochondrial dysfunction	40
1.5.1 TFAM knockout mice	40
1.5.2 The MtDNA mutator mouse	41
1.5.3 Mouse models of mtDNA disease	44

1.6	The colon.....	48
1.6.1	Structure of the colon	48
1.6.2	Functions of the colon	49
1.7	The colon: a model stem cell tissue for studying mtDNA mutations	50
1.7.1	Clonally expanded somatic mtDNA point mutations in the human colon .	50
1.7.2	Random mtDNA mutagenesis and selective constraints	52
1.8	Aims and objectives	54
Chapter 2.	Materials and Methods	56
2.1	Equipment and consumables.....	56
2.1.1	Equipment	56
2.1.2	Consumables	57
2.2	Solutions and chemicals.....	57
2.2.1	Solutions.....	57
2.2.2	Chemicals.....	59
2.3	Animals	61
2.3.1	Heterozygous (PolgA ^{+/mut}) mice	61
2.3.2	M.5024C>T tRNA ^{Ala} mice.....	61
2.3.3	Breeding of homozygous (PolgA ^{mut/mut}) and heterozygous (PolgA ^{+/mut}) mice	63
2.4	Tissue preparation	64
2.4.1	Frozen Tissue	64
2.5	Histological and Histochemical staining procedures	65
2.5.1	Haematoxylin and Eosin staining procedure.....	65
2.5.2	Dual cytochrome c oxidase (COX)/ succinate dehydrogenase (SDH) histochemistry	65
2.5.3	Cresol violet acetate alcoholic staining procedure.....	67
2.6	Molecular Biology Techniques	67
2.6.1	Isolation of total DNA from mouse tissue	67

2.6.2	Isolation of total RNA from colonic crypts	68
2.6.3	Polymerase Chain Reaction (PCR) for $PolgA^{mut/mut}$ genotyping	68
2.6.4	PCR amplification of the entire mitochondrial genome	69
2.6.5	PCR amplification of the m.5024 region of the mouse mtDNA genome for sequencing.....	70
2.6.6	PCR amplification of the m.5024 region of the mouse mtDNA genome for pyrosequencing	71
2.6.7	Long-range PCR of single colonic crypts	72
2.6.8	Agarose Gel electrophoresis	72
2.6.9	PCR clean up, cycle sequencing and DNA precipitation for mtDNA sequencing.....	73
2.6.10	M.5024C>T mutation quantification using pyrosequencing	74
2.6.11	RNA quantification and quality control.....	75
2.7	Bioinformatic analysis	75
2.7.1	RNA sequencing data.....	75
2.8	In silico modelling	76
Chapter 3. Results: Age-related clonally expanded somatic mtDNA mutations are similar in the colon of $PolgA^{+/mut}$ mice and humans.....		79
3.1	Introduction	79
3.1.1	Somatic mtDNA point mutations in ageing mitotic tissues.....	79
3.1.2	Overview of animal models	79
3.2	Aims	82
3.3	Results	82
3.3.1	Respiratory chain deficiency in $PolgA^{+/mut}$ mouse colonic crypts.....	82
3.3.2	MtDNA genome analysis of $PolgA^{+/mut}$ mouse colonic crypts.....	84
3.4	Discussion	98
3.4.1	Future work	102
3.5	Conclusion	102

Chapter 4. Results: How does age-related mitochondrial respiratory chain dysfunction affect the gene expression profile of colonic crypts and what are the potential functional effects of this upon cellular processes?	104
4.1 Introduction	104
4.1.1 Stem cell ageing	104
4.1.2 Mitochondria and stem cell ageing	105
4.1.3 Mouse models	106
4.2 Aim of the study	107
4.3 Experimental procedures	107
4.4 Results	110
4.4.1 Significant differentially expressed genes in PolgA ^{+/-mut} COX deficient colonic crypts	111
4.4.2 Gene set enrichment analysis	125
4.5 Discussion	130
4.5.1 Potential implications for aberrant cell growth and tumorigenesis in colonic crypts	131
4.5.2 Potential implications for epithelial permeability and the pathogenesis of inflammatory bowel disease in the colon	133
4.5.3 Potential implications for the immune response and sensitivity to bacterial infection in colonic crypts	134
4.5.4 Future work	135
4.6 Conclusion	136
Chapter 5. Results: M.5024 C>T tRNA ^{Ala} mutation: a candidate allele for modelling mitochondrial disease in mice.	138
5.1 Introduction	138
5.1.1 Models of mtDNA disease	138
5.1.2 Mouse models of mtDNA disease	139
5.2 Breeding of mice harbouring specific mtDNA point mutations	140
5.3 Can dual COX/SDH histochemistry in the colonic epithelium be used as an early experimental screening tool for evidence of mitochondrial dysfunction and	

identifying potential pathogenic mtDNA point mutations in the breeding of mice harbouring specific mtDNA point mutations?	142
5.3.1 Identification of a candidate allele and breeding of mice with a m.5024 C>T tRNA ^{Ala} mutation.....	143
5.3.2 Early molecular characterisation of m.5024C>T tRNA ^{Ala} mutant mice...	144
5.4 Aims of the study	146
5.5 Results.....	146
5.5.1 Do young tRNA ^{Ala} mutant mice routinely display phenotypic evidence of mitochondrial dysfunction in the colonic epithelium?.....	146
5.5.2 Is the m.5024C>T mutation pathogenic? Segregation of the m.5024C>T mutation with COX deficiency in colonic crypts of young mutant tRNA ^{Ala} mice.	150
5.5.3 Is there evidence of respiratory chain deficiency in post-mitotic tissues of young m.5024C>T tRNA ^{Ala} mutant mice?	156
5.5.4 Does mitotic segregation affect m.5024C>T heteroplasmy across different tissues of young tRNA ^{Ala} mutant mice?.....	160
5.5.5 Do aged m.5024C>T tRNA ^{Ala} mutant mice show evidence of enhanced mitochondrial dysfunction and a progressive mtDNA disease phenotype?.....	161
5.6 Discussion	181
5.6.1 Future work	187
5.7 Conclusions	189
Chapter 6. Final Discussion	191
6.1 Segregation of mtDNA point mutations: why is there a selective loss?.....	192
6.2 The colon: a model replicative tissue.....	194
6.3 Use of mouse models	195
6.4 Implications for ageing and disease.	195
6.5 Concluding remarks	196
Chapter 7. Appendices	199
7.1 Appendix A: Mice used in this study.....	199

7.2	Appendix B: Primer sequences and positions for molecular biology techniques	203
7.3	Appendix C-Somatic mtDNA point mutations detected in the <i>PolgA</i> ^{+/<i>mut</i>} mouse colonic crypts.	209
7.4	Appendix D: Incidence of COX deficiency in different tissues of mutant and control tRNA ^{Ala} mice	220
Chapter 8.	References	222

List of figures

Figure 1-1: Schematic representation of mitochondrial structure.....	8
Figure 1-2: The OXPHOS system.....	10
Figure 1-3: The human mitochondrial genome.....	14
Figure 1-4: The machinery involved in mtDNA replication.....	21
Figure 1-5: Heteroplasmic mtDNA mutations and the threshold effect.	25
Figure 1-6: Clonal expansion of a mutant mtDNA molecule in mitotic tissues by random intracellular drift.	29
Figure 1-7: Structural arrangement of the colonic crypt.....	49
Figure 2-1: Germline mtDNA mutagenesis and breeding strategy using <i>PolgA</i> ^{+/<i>mut</i>} female mice to segregate specific mtDNA mutations into mouse lineages.	62
Figure 2-2: Breeding strategy to establish an ageing colony of <i>PolgA</i> ^{mut/<i>mut</i>} , <i>PolgA</i> ^{+/<i>mut</i>} and <i>PolgA</i> ^{+/+} mice.....	64
Figure 2-3: Example gel electrophoresis image gel following Polg PCR for genotyping.	69
Figure 3-1: Respiratory chain deficiency in colonic crypts of ageing <i>PolgA</i> ^{+/<i>mut</i>} mice. .	84
Figure 3-2: Absence of large scale mtDNA deletions in <i>PolgA</i> ^{+/<i>mut</i>} mouse single colonic crypts.....	85
Figure 3-3: Detection of somatic mtDNA mutations in <i>PolgA</i> ^{+/<i>mut</i>} colonic crypts.....	87
Figure 3-4: The frequency, type and location of somatic mtDNA point mutations in <i>PolgA</i> ^{+/<i>mut</i>} mouse COX positive and COX deficient colonic crypts.....	88
Figure 3-5: MtDNA mutations occur randomly in <i>PolgA</i> ^{+/<i>mut</i>} mouse colonic crypts.	89
Figure 3-6: Gene type, location and clonal expansion of somatic mtDNA point mutations in COX deficient colonic crypts in the ageing <i>PolgA</i> ^{+/<i>mut</i>} mouse and human colon.....	92
Figure 3-7: Genetic consequences of somatic mtDNA point mutations in the <i>PolgA</i> ^{+/<i>mut</i>} mouse colon.	94
Figure 3-8: Positional mutation frequency and mutation distribution by codon position and gene reveals an absence of evidence for purifying selection on somatic mtDNA point mutations in <i>PolgA</i> ^{+/<i>mut</i>} colonic crypts.....	95
Figure 3-9: Respiratory chain deficiency in ageing <i>PolgA</i> ^{mut/<i>mut</i>} mouse colon.	97
Figure 3-10: Random genetic drift can explain the clonal expansion of mtDNA point mutations and the incidence of COX deficiency in colonic crypt stem cells of ageing mice.....	97

Figure 4-1: Combined COX/SDH histochemistry and Cresyl violet acetate alcoholic staining on colon sections for the identification of COX deficient and COX positive colonic crypts during laser microdissection.	109
Figure 4-2: RIN output images showing the relative proportion of 28S:18S in a sample.	110
Figure 4-3: Genes that were significantly differentially expressed, with the highest log fold change in the COX deficient crypts versus the COX positive crypts.....	113
Figure 4-4: The fraction of genes expressed in biological pathways at different pathway completeness's for (a) KEGG pathways and (b) Reactome pathways.	114
Figure 4-5: Gene ontology categories of the significant DE genes in COX deficient colonic crypts compared to COX positive colonic crypts.....	115
Figure 5-1: Germline mtDNA mutagenesis and breeding strategy using <i>PolgA</i> ^{+/<i>mut</i>} female mice to segregate specific mtDNA mutations into mouse lineages.	141
Figure 5-2: Dual COX/SDH histochemistry screen on colonic epithelium of a mouse lineage created via the <i>PolgA</i> ^{+/<i>mut</i>} breeding strategy.....	143
Figure 5-3: Clover leaf structure of the human and mouse mt-tRNA ^{Ala}	144
Figure 5-4: Molecular characterization of young tRNA ^{Ala} mutant mice.	145
Figure 5-5: Respiratory chain deficiency in colonic epithelial tissue of young m.5024C>T tRNA ^{Ala} mutant mice.	148
Figure 5-6: The magnitude of COX deficiency in the colon correlates with m.5024C>T tail heteroplasmy in young tRNA ^{Ala} mutant mice.....	149
Figure 5-7: Normal COX activity in colonic epithelial tissue of young control mice..	150
Figure 5-8: Sequencing electropherograms illustrating the presence of the m.5024C>T mutation in COX positive and deficient colonic crypts from mutant tRNA ^{Ala} mice....	152
Figure 5-9: Pathogenicity and segregation of the m.5024C>T mutation with COX deficiency in single colonic crypts from young tRNA ^{Ala} mutant mice.	155
Figure 5-10: M.5024C>T heteroplasmy in single colonic crypts from young control animals.	156
Figure 5-11: COX/SDH histochemistry on heart tissue from control and mutant m.5024C>T tRNA ^{Ala} mutant mice.	158
Figure 5-12: COX/SDH histochemistry on skeletal muscle from control and m.5024C>T tRNA ^{Ala} mutant mice.	159
Figure 5-13: M.5024C>T heteroplasmy in different tissues of young mutant tRNA ^{Ala} and control mice.....	161

Figure 5-14: Respiratory chain deficiency in the colonic epithelium of 65 and 70 week old m.5024C>T tRNA ^{Ala} mutant mice.....	163
Figure 5-15: Absence of correlation between the magnitude of COX deficiency in the colon and the m.5024C>T tail heteroplasmy in aged (65 and 70 week old) mutant tRNA ^{Ala} mice.....	164
Figure 5-16: Respiratory chain deficiency in the colonic smooth muscle of 65 and 70 week old m.5024C>T tRNA ^{Ala} mutant mice.	165
Figure 5-17: Example image outputs generated using the HSV colour space model for the accurate detection and quantification of COX deficiency in colonic smooth muscle and heart fibers of aged tRNA ^{Ala} mutant mice.....	166
Figure 5-18: Respiratory chain deficiency in the heart of 70 week old m.5024C>T tRNA ^{Ala} mutant mice.....	168
Figure 5-19: COX/SDH histochemistry on skeletal muscle tissue from 70 week old m.5024C>T tRNA ^{Ala} mutant mice.	169
Figure 5-20: The effect of m.5024C>T tail heteroplasmy and tissue variability on the incidence of COX deficiency in aged mutant tRNA ^{Ala} mice.	171
Figure 5-21: COX/SDH histochemistry on aged WT control mouse muscle tissues. ...	172
Figure 5-22: The m.5024C>T heteroplasmy in the colon compared to the tail in aged (65 and 70 week old) tRNA ^{Ala} mutant mice.....	173
Figure 5-23: M.5024C>T heteroplasmy in different tissues of 70 week old mutant tRNA ^{Ala} mice.....	175
Figure 5-24: Example gel electrophoresis image following the pyrosequencing PCR of single colonic crypts from 65 week old tRNA ^{Ala} mutant mice.....	175
Figure 5-25: M.5024C>T heteroplasmy in single colonic crypts from 70 week old mutant tRNA ^{Ala} mice.....	177
Figure 5-26: Example sequencing electropherograms demonstrating the presence of the m.5024C>T mutation in colonic smooth muscle fibers of aged mt5024C>T tRNA ^{Ala} mutant mice.	179
Figure 5-27: Segregation of the m.5024C>T mutation with COX deficiency in colonic smooth muscle fibers of 70 week old mutant tRNA ^{Ala} mice.....	181
Figure 6-1: The accumulation of mtDNA point mutations in colonic crypts is affected by the incidence of clonal expansions.....	194

List of Tables

Table 3-1: A comparison of the location, types and frequency of mtDNA point mutations in COX positive and COX deficient colonic crypts from <i>PolgA</i> ^{+/<i>mut</i>} mice and aged humans (Greaves, Elson et al. 2012).	90
Table 4-1: RNA concentration and RIN scores for each COX positive and COX deficient sample from the 5 <i>PolgA</i> ^{+/<i>mut</i>} mouse samples.	110
Table 4-2: Significant DE genes mapped to biological pathways in both KEGG and Reactome.	116
Table 4-3: Significant DE genes mapped to KEGG pathways alone.	120
Table 4-4: Significant DE genes mapped to Reactome pathways alone.	122
Table 4-5: Cellular pathways identified in Reactome that are broadly upregulated and broadly downregulated in COX deficient colonic crypts compared to COX positive..	126
Table 4-6: Cellular pathways mapped to KEGG that are broadly upregulated and broadly downregulated in COX deficient colonic crypts compared to COX positive..	128

Publications

Baines, H. L., Stewart, J. B., Stamp, C., Zupanic, A., Kirkwood, T. B. L., Larsson, N. G., Turnbull, D. M. and Greaves, L.C. (2014). "Similar patterns of clonally expanded somatic mtDNA mutations in the colon of heterozygous mtDNA mutator mice and ageing humans." *Mechanisms of Ageing and Development* 139(1): 22-30.

Baines, H. L., D. M. Turnbull, D. M. and Greaves, L.C. (2014). "Human stem cell aging: Do mitochondrial DNA mutations have a causal role?" *Aging Cell* 13 (2): 201-205.

Abbreviations

ADP	Adenosine diphosphate
AMP	Antimicrobial protein
ANF	Atrial natriuretic factor
ATP	Adenosine Triphosphate
C	Cytochrome c
Ca ²⁺	Calcium
CoA	Coenzyme A
COX	Cytochrome <i>c</i> oxidase
CP	Codon position
CM	Cristae membrane
Dels	Deletions
DNA	Deoxyribonucleic acid
DE	Differentially expressed
DAB	Diaminobenzidine
D-loop	Displacement loop
dN	Number of non-synonymous substitutions per site
dS	Number of synonymous substitutions per site
DA	Dopaminergic
ETC	Electron transport chain
EtOH	Ethanol
FDR	False discovery rate
FGF	Fibroblast growth factor
FC	Fold change
Fe-S	Iron-sulphur
GO	Gene ontology

GSEA	Gene set enrichment analysis
HSP	Heavy strand promoter
HSV	Hue Saturation Value
Ig	Immunoglobulin
IBD	Inflammatory bowel disease
IBM	Inner boundary membrane
IMM	Inner mitochondrial membrane
Ins	Insertions
LHON	Leber's hereditary optic neuropathy
LSP	Light strand promoter
LP-BER	Long patch base excision repair
MHC	Major histocompatibility complex
MCAD	Medium-chain acyl-Coenzyme A Dehydrogenase
mRNA	Messenger ribonucleic acid
MMR	Mismatch repair
MtDNA	Mitochondrial DNA
MELAS	Mitochondrial encephalopathy, lactic acidosis and stroke-like episodes
MFTA	Mitochondrial Free Radical Theory of Ageing
mtSSB	Mitochondrial single stranded DNA binding protein
mTERF	Mitochondrial termination factors
MERRF	Myoclonic epilepsy with ragged red fibers
NK	Natural killer cells
NGS	Next generation sequencing
NBT	Nitro blue tetrazolium

Non-syn	Non-synonymous
Nseen	Number of genes in a given pathway expressed in the RNA sequencing dataset
O _H	Origin of heavy strand replication
O _L /OriL	Origin of light strand replication
OXPPOS	Oxidative phosphorylation
OriZ	Broad zone
PCR	Polymerase chain reaction
PEN	Polyethylenenaphthalate
Pi	Inorganic phosphate
PEO	Progressive external ophthalmoplegia
PGC1- α	Peroxisome proliferator-activated receptor gamma, coactivator 1 alpha
PolgA	Catalytic subunit of polymerase gamma
PolgB	Accessory subunit of polymerase gamma
<i>PolgA</i> ^{+/<i>mut</i>}	Heterozygous polymerase gamma mutator mouse
<i>PolgA</i> ^{<i>mut/mut</i>}	Homozygous polymerase gamma mutator mouse
POLG/Poly	Mitochondrial polymerase gamma
POLRMT	Mitochondrial ribonucleic acid polymerase
PPAR γ	Peroxisome proliferator-activated receptor γ
PMS	Phenazine methosulphate
Pway size	Number of genes mapping to a pathway
PSQ	Pyrosequencing

Q	Ubiquinone
QH2	Ubiquinol
RIN	RNA integrity number
RITOLS	Ribonucleotide incorporation throughout the lagging strand
RFLP	Restriction fragment length polymorphism
ROS	Reactive Oxygen species
RNA	Ribonucleic acid
SDH	Succinate dehydrogenase
SKM	Skeletal muscle
SN	Substantia Nigra
SP-BER	Single patch base excision repair
SS	Single stranded
Syn	Synonymous
TCA	Tricarboxylic acid cycle
TFAM	Transcription factor A
TFB1M	Mitochondrial transcription factor B1
TFB2M	Mitochondrial transcription factor B2
TFEM	Mitochondrial elongation factor
TNF	Tumor necrosis factor
tRNA	Transfer ribonucleic acid
VDAC	Voltage dependent anion channel
VLCAD	Very-Long-chain acyl-CoA Dehydrogenase
WT	Wild-type
W/V	Weight/ volume

Chapter 1

Chapter 1. Introduction

1.1 Mitochondria

Mitochondria are dynamic, intracellular organelles found in all nucleated mammalian cells that have a variety of roles, of which the production of adenosine triphosphate (ATP) by the process of oxidative phosphorylation (OXPHOS) is a dominant function. Mitochondria also play a critical role in intermediary metabolism (citric acid cycle, β oxidation), iron-sulphur (Fe-S) cluster biogenesis (van der Giezen and Tovar 2005), reactive oxygen species (ROS) production (Starkov 2008), regulation of cytosolic calcium (Ca^{2+}) ion concentration (Pozzan, Magalhães et al. 2000) apoptosis (Newmeyer and Ferguson-Miller 2003) and the urea cycle. Mitochondria are commonly believed to have evolved from free-living Eubacteria, through the process of endosymbiosis. Endosymbiosis was originally believed to comprise two successive events ('serial hypothesis'), involving the initial formation of the cell nucleus from Archaeobacterium followed by the incorporation of Eubacteria into primitive eukaryotic cells (Margulis 1971). An alternative theory, known as the 'hydrogen hypothesis' however, proposes that the eukaryotic nucleus and the mitochondrion were created simultaneously by the fusion of hydrogen-requiring Archaeobacterium and hydrogen-producing Eubacteria (Martin and Müller 1998). In either case, endosymbiosis occurs and the majority of genes from the Eubacteria (proto-mitochondrion) were transferred to the cell nucleus, creating a long-term, co-dependent relationship between the two (symbiosis).

1.1.1 Mitochondrial structure

Electron microscope studies reveal that mitochondria are generally elongated, rod-shaped structures or oval, circular organelles that measure 1-4 μm in length and 0.3-0.7 μm in diameter (Palade 1953). The size and number of mitochondria within tissues varies widely according to the cell type and the metabolic activity of the tissue, with mitochondria migrating to and clustering at sites of high energy consumption, such as neuronal axons and synapses (Morris and Hollenbeck 1993; Li, Okamoto et al. 2004). As such mitochondrial biogenesis is closely correlated to the ATP requirements of a cell, and this is primarily regulated by peroxisome proliferator-activated receptor γ (PPAR γ) and co-factor 1 α (PGC1- α).

Given that still electron microscope images were always used to depict mitochondria, these organelles were originally believed to be static structures within the cell.

However, it is now known that mitochondria are highly dynamic and undergo budding, fission and fusion, forming intracellular networks within a cell (Carroll 1989). In addition to fission and fusion mitochondrial dynamics also encompasses the process of mitophagy, whereby dysfunctional or undesirable mitochondria are selectively targeted for degradation via lysosomes (Kim, Rodriguez-Enriquez et al. 2007).

Mitochondria are double-membraned structures, comprising an outer and inner mitochondrial membrane, which form a small intermembrane space and enclose a large, internal matrix (Figure 1-1) (Palade 1953). The mitochondrial matrix houses multiple copies of the mitochondrial genome, enzymes of intermediary metabolism, transcription and translation machinery and it is the site of Fe-S cluster formation.

The outer mitochondrial membrane is equivalent to a normal cell membrane. It consists of a lipid bilayer punctuated by a number of protein channels, known as porin. Porin is a voltage dependent anion channel (VDAC), which functions to allow the movement of small molecules and ions, <5000 Daltons, between the cell cytoplasm and the intermembrane space of the mitochondria (Alberts 2002).

The inner mitochondrial membrane (IMM) was originally believed to be a continuous, closed membrane that folded forming invaginations, known as cristae, into the mitochondrial matrix. It is now known, however, that the IMM actually comprises two components: the inner boundary membrane (IBM) and the cristae membrane (CM), which are connected through tubular cristae junctions (Freya and Mannellab 2000). The IMM is an extremely protein rich lipid bilayer, comprising ~75% proteins (Ardail, Privat et al. 1990), and is largely impermeable to small solutes and polar molecules, with the exception of O₂, CO₂, H₂O and NH₃. The most abundant protein complexes are those involved in OXPHOS, which are primarily located in the CM (Vogel, Bornhövd et al. 2006). As such the CM is highly specialised to perform OXPHOS, which is further facilitated by the large surface area created through folding of the membrane into cristae. The CM is further enriched for mitochondrial translation products. The IBM forms close interactions with the outer membrane, and as such is enriched in proteins concerned with mitochondrial import (Vogel, Bornhövd et al. 2006). The IMM lipid components constitute ~25% of the membrane and include phosphatidylcholine, phosphatidylethanolamine and cardiolipin (Fleischer 1961), which provide electrochemical insulation, essential for OXPHOS.

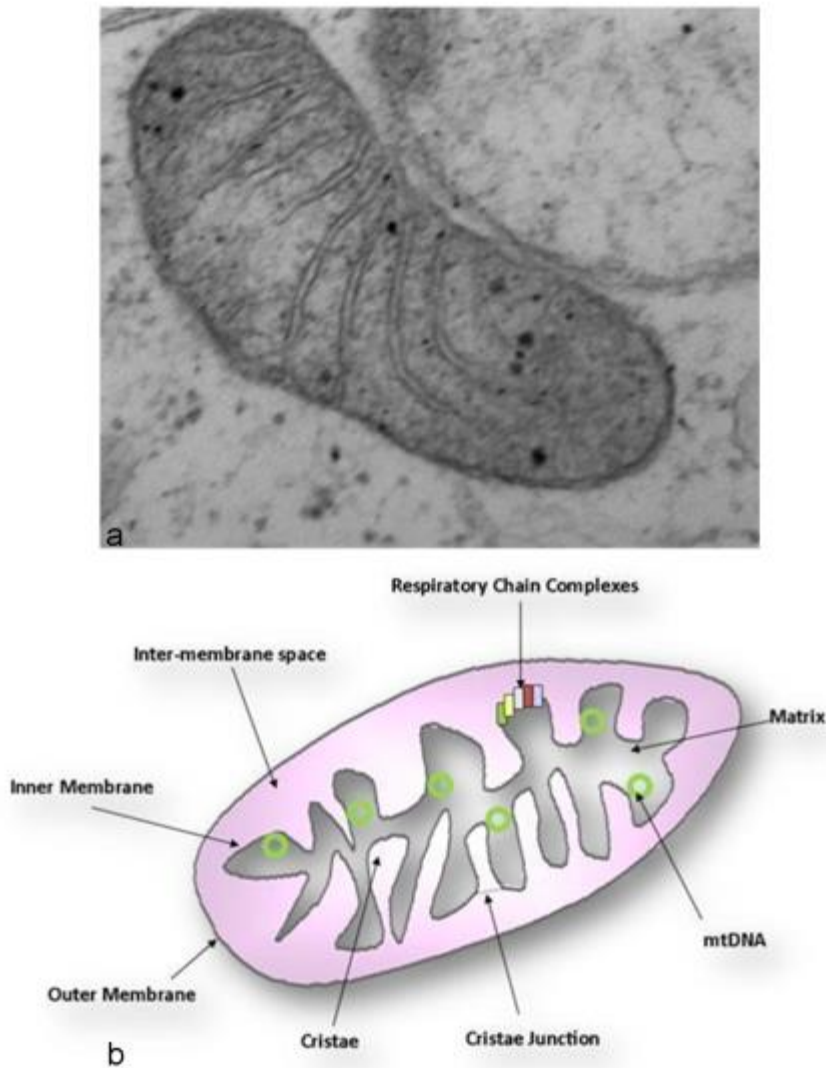


Figure 1-1: Schematic representation of mitochondrial structure.

(a) Electron micrograph image of a single mitochondria in situ and (B) a simplified representation of the structure of mitochondria displaying the key features. Images courtesy of Dr Amy Reeve and Dr Eve.Simcox.

1.1.2 *OXPHOS and synthesis of ATP*

OXPHOS is the process by which cellular ATP is generated, resulting from the transfer of electrons from intermediary products of the citric acid cycle/ tricarboxylic acid (TCA) cycle and β oxidation, to oxygen via a series of electron carriers (Hatefi 1985).

The production of ATP is initiated by the process of glycolysis in the cell cytoplasm, where glucose is broken down, in the presence of oxygen, into pyruvate, 2 molecules of ATP and 2 molecules of NADH. Pyruvate is subsequently transported across the outer and inner mitochondrial membranes into the mitochondrial matrix for decarboxylation by pyruvate dehydrogenase to produce acetyl Coenzyme A (CoA). One NADH and one CO_2 molecule are produced during the conversion of pyruvate to acetyl CoA. Acetyl

CoA is a key substrate for the TCA cycle, during which it becomes oxidized to CO₂ alongside the reduction of NAD⁺ and FADH⁺ to NADH and FADH₂. NADH and FADH₂ function as electron carriers and are fundamental to the OXPHOS pathway.

The OXPHOS system is located in the CM and consists of five transmembrane protein-lipid enzyme complexes (Complexes I-V) and two electron carriers, coenzyme Q (ubiquinone) and cytochrome *c* (Hatefi 1985) (Figure 1-2). Electrons from NADH and FADH₂, derived from the TCA cycle and β oxidation, are shuttled along the respiratory chain, otherwise known as electron transport chain (ETC), from Complex I to Complex IV, and are subsequently transferred to oxygen to be reduced to water. At complexes I, III and IV, the transfer of electrons results in the translocation of protons (H⁺ ions) from the mitochondrial matrix to the intermembrane space, creating a protonic electrochemical gradient. Protons move down this electrochemical gradient, through ATP synthase (Complex V), which provides a hydrophilic channel across the IMM. As protons flow through ATP synthase, adenosine diphosphate (ADP) is phosphorylated to give ATP in an energetically unfavourable reaction (Hatefi 1985). One ATP molecule is generated for approximately 3 protons that pass through ATP synthase.

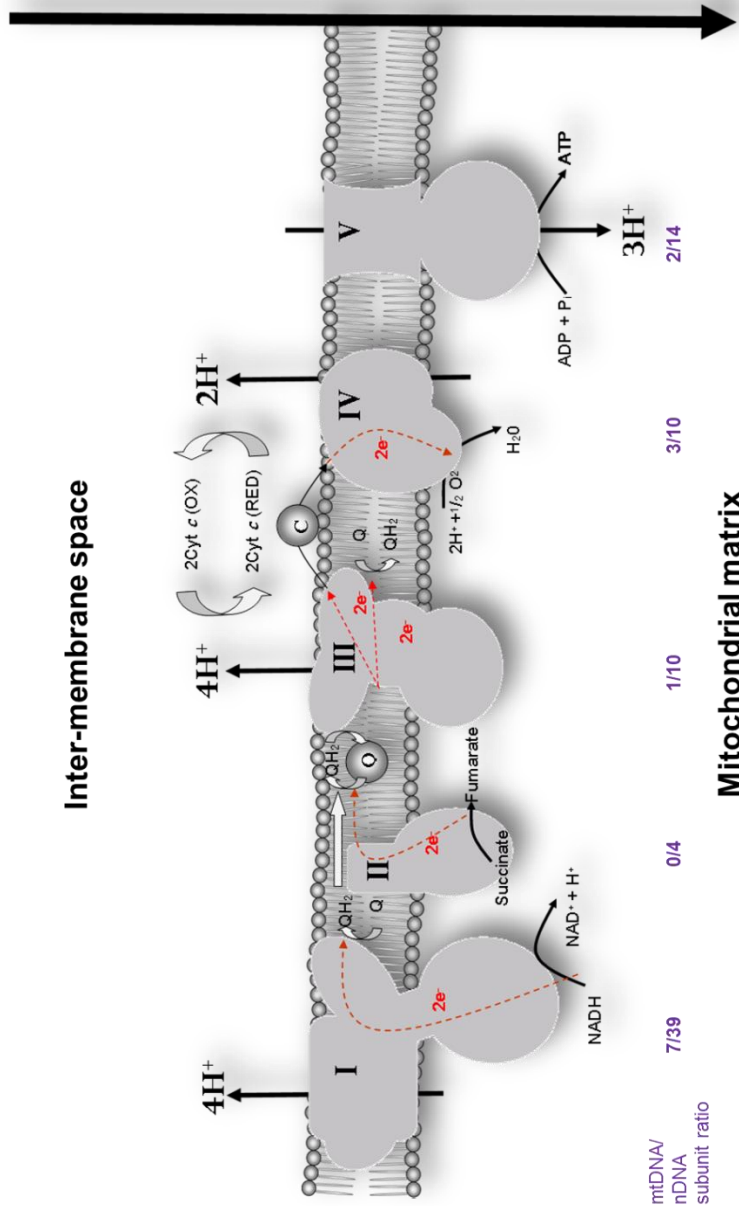


Figure 1-2: The OXPHOS system.

The five transmembrane enzyme complexes of the mitochondrial respiratory chain are located in the CM of the IMM. Mitochondrial DNA encodes essential subunits of complexes I, III, IV and V, but complex II is entirely encoded by nuclear DNA (Morris 1995). The ratio of mitochondrial: nuclear encoded subunits are shown below each complex. Electrons (in red) feed into the electron transport chain at Complex I (via NADH) and Complex II (via FADH₂). Complex I transfers 2 electrons from NADH to ubiquinone (Q), which is coupled with the translocation of 4 protons to the intermembrane space (Hatefi 1985). Complex II catalyzes the oxidation of succinate to fumarate and the reduction of ubiquinone to ubiquinol (QH₂) using FADH₂ (Hägerhäll 1997). Complex III then re-oxidizes ubiquinol to ubiquinone and transfers the electrons to cytochrome *c* (*c*), which is coupled to the transmembrane translocation of 2 protons (Hatefi 1985). Cytochrome *c* is a small heme protein located in the intermembrane space, which serves to carry an electron from Complex III to Complex IV. Complex IV is the terminal component of the electron transport chain and catalyzes the transfer of electrons to oxygen, reducing it to water. The reduction of oxygen requires the transfer of 4 electrons, resulting in the translocation of 4 protons to the intermembrane space (Brändén, Gennis et al. 2006). Complex V converts ADP and inorganic phosphate (Pi) to ATP as protons move down the electrochemical gradient created by complexes I, III and IV. Complex V comprises two components: F₁ the ATP synthase and F₀ the proton translocator. The movement of protons through F₀ is proposed to cause rotation of a Y chain in F₁ which subsequently causes conformational changes in β chains of F₁ and the synthesis of ATP (Noji, Yasuda et al. 1997). The production of one molecule of ATP is associated with the flow of ~3 protons through ATP synthase (Ferguson 2010). Image adapted courtesy of Dr Eve Simcox.

Regulation of OXPHOS is principally controlled by the relative concentrations of ADP and substrates available, as well as the mitochondrial membrane potential (-180mv). As such when mitochondrial matrix concentrations of ADP are high, ATP is synthesised (Chance 1956) and oxygen is consumed by the ETC to restore the electrochemical gradient (state III respiration). Low concentrations of ADP in the matrix are associated with low oxygen consumption and the mitochondrial membrane potential is maintained as protons are not moving through ATP synthase to generate ATP (state IV respiration) (Chance 1956). ATP production is therefore regulated by the balance between state III and IV respiration.

Intramitochondrial Ca^{2+} concentration is also believed to regulate ATP synthesis, as Ca^{2+} has been found to activate a number of mitochondrial enzymes, including pyruvate dehydrogenase, NAD isocitrate dehydrogenase and possibly ATP synthase (Tarasov, Griffiths et al. 2012). Activation of these dehydrogenases by increased concentrations of Ca^{2+} is proposed to increase the levels of NADH and FADH_2 electron carriers available to the ETC, thus increasing OXPHOS (Denton 2009). Given that an increase in intramitochondrial Ca^{2+} is linked to muscle contraction, the concentration of Ca^{2+} inside mitochondria can therefore couple ATP synthesis with the energy demands of the cell (Denton 2009). Furthermore Ca^{2+} can also directly bind to ATP synthase (Hubbard and McHugh 1996) and binding of a calcium sensing protein (S100A1) has also been shown to increase ATP production (Boerries, Most et al. 2007).

1.1.2.1 *Respiratory chain supercomplexes*

Complexes of the respiratory chain do not exist as single entities, distributed irregularly throughout the IMM but instead have been shown to associate and form supercomplexes in both yeast and mammalian mitochondria (Schägger and Pfeiffer 2000). In mammalian mitochondria complex I associates and forms a supercomplex with the majority of complex III and four copies of complex IV (Schägger and Pfeiffer 2000), giving rise to a network of respiratory chain complexes known as the 'respirasome'. Such respirasomes are indeed functional and have been shown to respire, given that they can transfer electrons from NADH to oxygen (Acín-Pérez, Fernández-Silva et al. 2008). In the same study blue native PAGE further demonstrated that unsurprisingly supercomplexes do not form if one of the components is not present

(Acín-Pérez, Fernández-Silva et al. 2008). Complex I, which forms in multiple stages, is fundamental in the construction of respirasomes, providing a framework for the collective integration of subunits of complexes III and IV, which assemble independently (Moreno-Lastres, Fontanesi et al. 2012; Winge 2012). Respirasome activation is achieved upon the final assembly and activation of complex I, when the catalytic subunit of NADH dehydrogenase is incorporated (Moreno-Lastres, Fontanesi et al. 2012; Winge 2012). Indeed, the formation of respirasomes is believed to enhance efficiency of the ETC and the OXPHOS process, as the association of respiratory chain complexes would enable specific substrates to be directed to specific complexes, enhancing catalytic activity (Schägger and Pfeiffer 2000) as well as preventing electron leakage, especially from complex III, and the formation of superoxide radicals (Winge 2012). Given the structural connections and relationships between complexes in respirasomes, a single genetic defect could indeed affect the activity of multiple respiratory chain complexes, particularly in complexes I, III and IV. Undoubtedly this has significant implications for understanding mitochondrial defects in disease processes and ageing.

1.1.3 Other mitochondrial functions

1.1.3.1 Iron homeostasis and Fe-S cluster biogenesis

Mitochondria also have a central role in iron homeostasis, with the majority of intracellular iron used by mitochondria for the synthesis of haem and Fe-S cluster biogenesis (Wang and Pantopoulos 2011). Mitochondrial proteins are essential in the formation of Fe-S clusters, providing frameworks for their initial formation (Isu1/2) and facilitating development of the clusters (Grx5 and Abcb7) (Wang and Pantopoulos 2011). Fe-S clusters are fundamental in many cellular processes including OXPHOS, the catalysis of enzymatic reactions and the sensing and regulation of mitochondrial iron homeostasis. The mitochondrial electron transport chain houses up to 12 different Fe-S clusters, which serve as electron carriers by cycling between the Fe²⁺ and Fe³⁺ form, as well as contributing to complexes I and III (Schultz and Chan 2001).

1.1.3.2 ROS production

Mitochondria are known to possess up to 10 different sites of ROS production, predominantly located within the mitochondrial ETC. Complexes I and III serve as the major sites of ROS production (Turrens and Boveris 1980; Sugioka, Nakano et al. 1988), where the loss of a single electron reduces molecular oxygen, resulting in the

production of a superoxide radical (O_2^-) (Starkov 2008). The deleterious effects of mitochondrial derived ROS in oxidative stress and damage are well-documented and are believed to have a role in ageing (see section 1.4.2.1). However, ROS also serve as essential signalling molecules in many physiological and cellular pathways including cell proliferation, differentiation, autophagy and anti-tumorigenic responses such as apoptosis and senescence (Valko, Leibfritz et al. 2007).

1.1.3.3 *Calcium homeostasis*

Given the negative mitochondrial membrane potential (-180mv) created by the ETC, mitochondria are ideal organelles for the uptake and sequestration of Ca^{2+} ions and as such play a key role in the regulation of intracellular Ca^{2+} concentration, with mitochondria capable of absorbing up to 1000nmol Ca^{2+} per mitochondrial protein (Kirichok, Krapivinsky et al. 2004). Mitochondrial Ca^{2+} uptake therefore has significant implications for multiple cellular processes and pathways in which Ca^{2+} serves as a key signalling molecule, including cellular communication (Hofer, Curci et al. 2000), apoptosis (Orrenius, Zhivotovsky et al. 2003), ATP production and its regulation (Tarasov, Griffiths et al. 2012), metabolism and the TCA cycle (Duchen 2000).

1.1.3.4 *Apoptosis*

Mitochondrial Ca^{2+} overload in a cell is one mechanism by which mitochondria play a fundamental role in apoptosis to remove damaged cells and aid normal tissue turnover. Mitochondria have also been proposed to contribute to programmed cell death through a number of other mechanisms including: the release of cytoxic proteins, such as cytochrome *c* (Liu, Kim et al. 1996) and apoptosis-inducing factor (Susin, Lorenzo et al. 1999); a rapid reduction in the mitochondrial membrane potential (Goldstein, Waterhouse et al. 2000); ROS production (Fleury, Mignotte et al. 2002); opening of the permeability transition pore (Zamzami and Kroemer 2001) and mitochondrial network fragmentation (Newmeyer and Ferguson-Miller 2003).

1.2 **The mitochondrial genome**

Mitochondria are the only extra nuclear source of DNA within a cell (Nass 1966), which is located within the mitochondrial matrix. The mitochondrial genome (mtDNA) is a covalently closed, double stranded molecule comprising a heavy strand, which is rich in guanine residues, and a light strand, rich in cytosine residues. The human mitochondrial genome is a 16 596 base pair (bp) molecule of DNA, encoding 37 genes, which include: 13 protein encoding genes for essential subunits of the respiratory chain

(Figure 1-2); 2rRNAs (12s and 16s) and 22tRNAs (Figure 1-3) (Anderson, Bankier et al. 1981). The remaining proteins of the respiratory chain (~77) are encoded by nuclear DNA and are imported into mitochondria from the cytoplasm. As such mitochondria rely on both the nuclear and mitochondrial genomes for control. MtDNA displays an organization of extreme economy, as virtually all of the genome has a distinct coding function, with tRNA genes scattered in between rRNA and protein encoding genes (Figure 1-3)(Anderson, Bankier et al. 1981). There is an absence of introns and termination codons are created via polyadenylation of mRNAs after transcription (Anderson, Bankier et al. 1981).The primary non-coding region of the genome is the displacement loop (D-loop), a ~1,100 bp region that contains key control elements for transcription and replication of mtDNA, including the origin of heavy-strand (O_H) replication (Shadel and Clayton 1997).

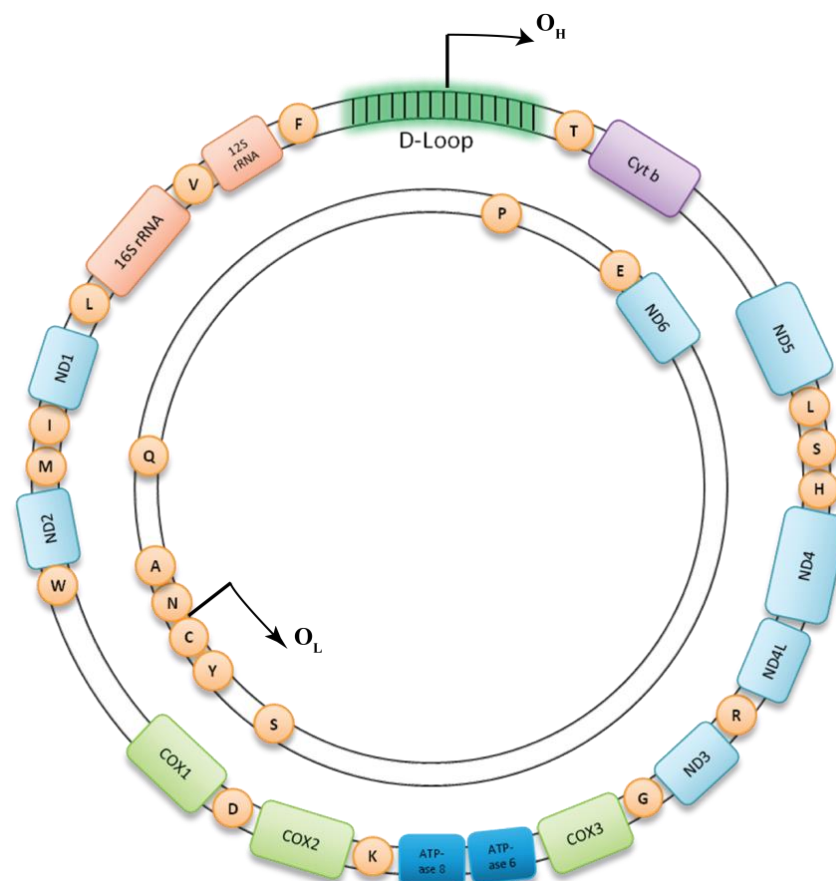


Figure 1-3: The human mitochondrial genome.

The human mtDNA genome is covalently closed 16, 596 bp molecule, comprising a heavy strand and a light strand. MtDNA encodes 37 genes: 13 essential polypeptides, 2rRNAs and 22tRNAs. The outer heavy strand houses 12 of the protein encoding genes, including: 5 subunits of complex I (ND1-5), one subunit of complex III (CytB), 3 subunits of complex IV (COX1-3) and 2 subunits of complex V (ATPase 6 &8). The ND6 subunit of complex I is located on the inner light strand. The mtDNA genome is an example of extreme economy, with tRNA genes interspersed between the protein encoding genes. The only non-coding region is the D-loop, in which the origin of H strand replication (O_H) is located. The origin of light strand replication (O_L) is also displayed. Image (adapted) courtesy of Dr Casey Wilson.

Mitochondrial genetics is examined throughout this thesis in the context of mouse models. The human and mouse mitochondrial genomes are extremely homologous, in terms of both sequence and the genes encoded for, as well as the organization and location of tRNA, rRNA and protein encoding genes in both genomes (Bibb, Van Etten et al. 1981). The mouse mitochondrial genome is a slightly smaller molecule of 16, 259 bp, which is principally due to a smaller D-loop (879bp) that is 243 nucleotides smaller than the human mitochondrial D-loop (Bibb, Van Etten et al. 1981). Indeed it is the D-loop which is the most dissimilar in sequence between the two genomes. However, given that the D-loop contains no open reading frames, this divergence conveys very little difference in function (Bibb, Van Etten et al. 1981). The only other features that are specific to mouse mtDNA are the initiation and termination codons required for translation (see section 1.2.1.1.2).

Mitochondria contain multiple copies of the mtDNA genome. Given that a somatic mammalian cell contains numerous mitochondria, cells within the human body are believed to contain thousands of copies of the mtDNA genome (10^3 - 10^4) (Lightowlers, Chinnery et al. 1997). Whilst this is true for many somatic human cells, there are however notable exceptions, such as stem cells in which copy number is estimated to be ~200 mtDNA molecules (Coller, Khrapko et al. 2001). MtDNA is present within cells as compacted nucleoprotein complexes, known as nucleoids, which are estimated to contain between 2 and 10 molecules of mtDNA (Kukat and Larsson 2013). Nucleoids have been identified to contain 21 proteins. Mitochondrial transcription factor A (TFAM) is a principal component of nucleoids, which, through its ability to bind, bend and wrap mtDNA, is also fundamental in their formation (Kukat and Larsson 2013). Other proteins include those with a role in mtDNA replication and transcription, such as the mitochondrial TWINKLE helicase, as well as proteins that are generally housed within the IMM, such as ANT1 and prohibitin, indicating that mtDNA is associated with the inner mitochondrial membrane (Falkenberg, Larsson et al. 2007).

1.2.1 *Mammalian MtDNA transcription and replication*

1.2.1.1 *Transcription*

Mammalian mtDNA transcription and replication are principally controlled at the D-loop, which houses three promoter sites for the initiation of mtDNA transcription: two promoters on the heavy strand (HSP1 and HSP2) and one on the light strand (LSP). A full length transcript is produced when transcription is initiated at HSP2, however only

2rRNAs and 2 of the mt-tRNAs (tRNA^{Phe} and tRNA^{Val}) are transcribed when initiation occurs at HSP1 (Rebelo, Dillon et al. 2011). Both rRNA genes, 14 of the tRNA genes and all protein encoding genes, except mt-*ND6* are transcribed from the heavy strand of mtDNA, with the other 8 tRNAs and the mt-*ND6* protein encoding gene transcribed from the light strand. Transcription of mtDNA occurs in both directions and results in a single polycistronic precursor RNA. Polycistronic precursors are subsequently processed into the 12S and 16S rRNAs, tRNAs and a number of mRNAs, which are then polyadenylated prior to translation (Clayton 1991).

The machinery necessary for mammalian mtDNA transcription includes the mtRNA polymerase (POLRMT), TFAM and mitochondrial transcription factor B1/B2 (TFB1M/TFB2M) (Falkenberg, Gaspari et al. 2002). Transcription can be initiated by either mitochondrial transcription factors in combination with POLRMT and TFAM, however TFB2M has been shown to be over 10 times more efficient than TFB1M (Falkenberg, Gaspari et al. 2002). TFAM is a fundamental component of the transcription machinery, initiating transcription through binding of its carboxyl terminal tail to one of the promoter regions, which stimulates a conformational change in mtDNA, enabling the binding of POLRMT (Fisher, Topper et al. 1987; Dairaghi, Shadel et al. 1995). TFAM also acts as a regulator of the POLRMT/TFB2M and POLRMT/TFB2M complexes (Falkenberg, Gaspari et al. 2002) and expression of TFAM is highly correlated with mtDNA copy number (Larsson, Wang et al. 1998). Following transcription initiation, elongation occurs by POLRMT, with the aid of mitochondrial elongation factor (TEFM). Further details of the mammalian transcription machinery and factors required can be found in the following two reviews (Falkenberg, Larsson et al. 2007; Rebelo, Dillon et al. 2011).

1.2.1.1.1 Transcription termination

Termination of mammalian transcription is instigated by mitochondrial termination factors (mTERF), of which four have been identified (Falkenberg, Larsson et al. 2007). MTERF1 is the most characterized, having been shown to bind a 28bp region in tRNA^{Leu (UUR)} and terminate the transcription of the short transcript initiated at HSP1, thus regulating the proportion of mRNA to rRNA (Roberti, Bruni et al. 2006). MTERF1 is believed to act through bending, unwinding and melting of the DNA duplex, followed by base flipping to stabilise binding of the termination factor (Yakubovskaya, Mejia et al. 2010). Termination of the long transcript initiated from the HSP2 promoter is less well understood, with research having only identified proteins that are able to bind to

the H2 termination region. Leucine rich pentatricopeptide-repeat containing protein (LRPPRC) is the most characterized of these, having been shown as essential for the expression of mtDNA encoded COX subunits and a key regulator of mtDNA transcription (Gohil, Nilsson et al. 2010). The other three homologues of mTERF1 are less well characterised and their exact functions still remain to be clarified. It has been proposed that MTERF2 acts as a positive regulator of transcription, whilst mTERF3 is a transcriptional repressor and mTERF4 is proposed to regulate transcription through binding to the D-loop (Rebelo, Dillon et al. 2011).

1.2.1.1.2 Mitochondrial translation

Mitochondria have their own unique translation system with different wobble rules, enabling the decoding of all mRNAs and the synthesis of proteins using only the 22tRNAs encoded by mtDNA, with no evidence for the importation of nuclear encoded tRNAs from the cell cytoplasm (Anderson, Bankier et al. 1981; Bibb, Van Etten et al. 1981). The mechanism by which mitochondrial translation occurs is largely based on our understanding of bacterial translation, with protein synthesis comprising three stages: initiation, elongation and termination (Smits, Smeitink et al. 2010)

Mammalian mitochondrial tRNAs are shorter than bacterial and cytosolic tRNAs, but the majority of them display the classic cloverleaf structure, comprising 4 stems and 3 loops: an acceptor stem, a dihydrouridine stem/loop, a TΨC-stem/loop and an anticodon stem/loop. Decoding of all mRNAs by the 22 tRNAs is thought to be achieved by a “two out of three” method, whereby the base in the first anticodon position in mRNA (corresponding to the third codon position of DNA) conveys little significance (Barrell, Anderson et al. 1980). As such there are 8 individual tRNAs that are each capable of recognising a U in the first anticodon position of mRNA, which in some cases can be distinguished between a purine and a pyrimidine base, enabling the decoding of up to 60 codons (Barrell, Anderson et al. 1980).

Translation of mammalian mitochondrial mRNAs occurs on mitoribosomes, consisting of a large 39S and a small 28S subunit along with the two mt-rRNAs (12S and 16S), which are located within the mitochondrial matrix (Smits, Smeitink et al. 2010).

Mammalian mitoribosomes are unique and differ from other ribosomes in that they have a fairly low rRNA content, but high protein content, with proteins proposed to have specific mitochondrial functions (Smits, Smeitink et al. 2010). In addition to tRNAs, rRNAs and mitoribosomes mitochondrial translation also requires nuclear encoded

initiation, elongation and translation termination factors as well as mitochondrial aminoacyl-tRNA synthetases and methionyl-tRNA transformylase, which are needed to initiate translation (Smits, Smeitink et al. 2010).

Translation of nuclear encoded mRNA is most commonly initiated by the presence of an AUG codon; however the translation of mitochondrial genes in humans is predominantly initiated by the presence of an AUA or AUU codon (Anderson, Bankier et al. 1981). In general mitochondrial translation is terminated when mitochondrial termination factor 1a (mtRF1a) recognises a UAA and UAG codon within the mRNA (Barrell, Anderson et al. 1980; Anderson, Bankier et al. 1981). However, in mammalian mitochondria AGA or AGG also occur once at the end of two mitochondrial ORFs, effectively acting as hungry codons that promote non-canonical translation termination (Temperley, Richter et al. 2010). Irrespective, only a single translation release factor, mtRF1a, is required to recognise and terminate translation from all 13 open reading frames. Decoding of mRNA in mice is not dissimilar to that in humans, with the only unique features being that AUN serves as the translation initiation codon, where any of the four nucleotides can occur in the third position, and UAA serves as the termination codon for translation (Bibb, Van Etten et al. 1981).

1.2.1.2 *Mitochondrial DNA replication*

1.2.1.2.1 Models of mtDNA replication

Mammalian mtDNA is constantly turned over and is replicated autonomously, independent of nuclear DNA and the cell cycle (Bogenhagen and Clayton 1977). Two different models for mammalian mtDNA replication have been proposed: the asynchronous (strand displacement) model (Clayton 1982) and the synchronous model (Holt, Lorimer et al. 2000).

In the asynchronous model, mtDNA replication is highly dependent upon mtDNA transcription, as replication initiation at the origin of H strand replication (O_H) requires RNA primers produced from transcription initiation at the LSP. Synthesis of the leading (heavy) strand then advances clockwise, two thirds of the way around the genome until it displaces the origin of L strand replication (O_L). Exposure of the L strand as a single stranded template activates synthesis of the lagging (light) strand in the opposite direction (Clayton 1982). MtDNA daughter molecules are then ligated to form closed, circular molecules and superhelical turns are introduced to give the final product of replication known as C mtDNA (Clayton 1982). It has been proposed that the

replication of mtDNA molecules in this manner would take 1 hour (Clayton 1982). Indeed this is a slow rate for DNA replication and this is thought to be attributable to the low water content in the mitochondrial matrix (Hackenbrock 1968) .

Study of mtDNA replication intermediates by 2D agarose gel electrophoresis revealed that two different types of replication intermediates were produced, which displayed different sensitivity to single-strand nuclease digestion (Holt, Lorimer et al. 2000). Such a discovery was highly suggestive of a synchronous model of mammalian mtDNA replication, whereby synthesis of the leading and lagging strand are coupled and occur symmetrically (Holt, Lorimer et al. 2000). In this way mtDNA replication occurs bidirectionally and not only initiates at the O_H , but can initiate at multiple replication forks within a broad zone (OriZ), which encompasses parts of the genome encoding cytochrome b and subunits 5 and 6 of NADH dehydrogenase (Bowmaker, Yang et al. 2003). The same study demonstrated that the O_H can actually cause arrest of the replication fork and serve as a termination site for mtDNA replication (Bowmaker, Yang et al. 2003).

More recently a different method for mtDNA replication in vertebrates has been suggested, known as RITOLS (ribonucleotide incorporation throughout the lagging strand) (Yasukawa, Reyes et al. 2006). This model proposes that whilst the leading strand is synthesised, RNAs are incorporated into the lagging strand, which are later converted to DNA (Yasukawa, Reyes et al. 2006). Thus there is a delay between the synthesis of the leading and lagging strand of mtDNA and as such this model is not dissimilar to the asynchronous model of replication.

A firm conclusion regarding the mechanism of mammalian mtDNA replication is yet to be made, with experimental evidence from the study of replication intermediates supporting the existence of all methods. Indeed it has been suggested that the mechanism selected for mtDNA replication is highly dependent upon the cell type, mtDNA copy number and the required rate of mtDNA synthesis, with the asynchronous model preferred in cells that require rapid replication compared to the synchronous model, which may be preferred by cells in a steady state (Holt, Lorimer et al. 2000; Yasukawa, Reyes et al. 2006).

1.2.1.2.2 MtDNA replication machinery

Even though mtDNA is self-replicating and replication is principally controlled at the D-loop, the proteins and machinery required for mtDNA replication are in fact all

nuclear encoded. Mammalian mtDNA replication machinery is known as the mitochondrial replisome, which comprises three main proteins: the mtDNA polymerase gamma (Poly γ), the mitochondrial TWINKLE DNA helicase and mitochondrial single-stranded DNA binding protein (mtSSB) (Falkenberg, Larsson et al. 2007).

For mtDNA to be replicated the double stranded DNA must be unwound to give the two, complementary single strands (ss) of DNA. TWINKLE is the mitochondrial replicative helicase enzyme responsible for the ATP dependent unwinding of the DNA duplex, in the 5' to 3' direction (Korhonen, Gaspari et al. 2003), to give ssDNA (Figure 1-4). Stabilization of ssDNA is achieved by the mtSSB, a 13-16kDa protein (Kaguni 2004), which the ssDNA wraps around (Figure 1-4). MtSSB enhances the helicase activity of TWINKLE, via protein-protein interactions and in turn triggers the activity of Poly γ , initiating DNA synthesis (Figure 1-4) (Korhonen, Gaspari et al. 2003).

Poly γ is an RNA dependent DNA polymerase, which consists of a Poly γ A catalytic domain and the Poly γ B accessory subunit. The catalytic domain has a molecular mass of 140kDa (Gray and Tai Wai 1992) and has 3'-5' exonuclease activity and 5' deoxyribose phosphate lyase activity (Pinz and Bogenhagen 1998; Kaguni 2004). Poly γ B is a smaller protein (55kDa) that associates with Poly γ A to form a heterotrimer (Poly γ AB₂) in mammalian cells (Figure 1-4) (Yakubovskaya, Chen et al. 2006). The Poly γ B subunit binds to double stranded DNA greater than 45bp in length, and functions to enhance DNA and nucleotide binding, thereby increasing the catalytic and processing activity of Poly γ A (Kaguni 2004). Poly γ is a high fidelity polymerase enzyme, which efficiently selects and incorporates nucleotides into the growing DNA strand whilst eliminating errors due to its proofreading activity conveyed by the 3'-5' exonuclease (Kaguni 2004). Unlike other DNA polymerases, Poly γ therefore has a role in replication, repair and recombination (Kaguni 2004). The activity of Poly γ is dependent upon POLRMT, which provides the RNA primers necessary for mtDNA replication initiation at the O_H (Shadel and Clayton 1997) and potentially the O_L.

Whilst Poly γ , TWINKLE and mtSSB form the core components of mammalian mtDNA replication machinery, it has been proposed that other enzymatic activities may be required for/or facilitate mtDNA replication. Ribonuclease H1, has been proposed to have a role in the removal of primers from the O_H and O_L (Cerritelli, Frolova et al. 2003) and a mitochondrial topoisomerase, encoded by TOP1mt, is necessary to alleviate

some of the torsional force created during the replication of closed, circular mtDNA molecules (Zhang, Barceló et al. 2001).

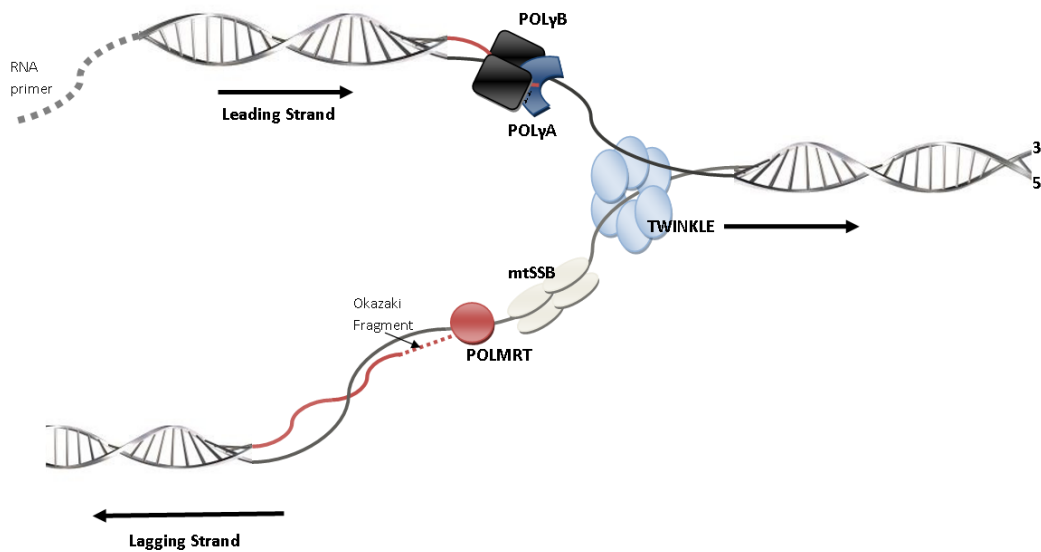


Figure 1-4: The machinery involved in mtDNA replication.

The mitochondrial TWINKLE helicase unwinds double stranded mtDNA in the 5' to 3' direction to give two single stranded molecules of DNA. mtSSB stabilizes DNA in the single stranded form and activates the Poly holoenzyme to synthesise the complementary strand of mtDNA. Image courtesy of Dr Eve Simcox.

1.2.2 Mammalian mtDNA repair mechanisms

Mammalian mtDNA is to some extent protected from damage by mtDNA associated proteins, which have been shown to provide protection against mutagenic insults caused by x-rays and hydrogen peroxide, equivalent to that provided by histones, (Guliaeva, Kuznetsova et al. 2006). Furthermore the packaging of mtDNA into nucleoids, results in the covering and protection of large amounts of mtDNA by TFAM. Nonetheless, mtDNA, just like nuclear DNA, is exposed to intrinsic and extrinsic harmful agents that induce DNA damage. Originally it was believed that mammalian mitochondria, lacked any form of repair enzymes or mechanisms to deal with DNA damage, as UV induced pyrimidine dimers were not removed from mtDNA (Clayton DA 1974) nor were certain types of alkylation damage (Miyaki, Yatagai et al. 1977). However, it is now known that mammalian mitochondria do indeed share many of the same repair mechanisms as nuclear DNA.

It is well established that mammalian mitochondria possess the single-patch base excision repair (SP-BER) pathway for the removal of modified nucleotides and single base lesions caused by oxidative damage, spontaneous hydrolysis and alkylation. SP-

BER involves DNA glycosylase enzymes to remove the modified base (Bogenhagen 1999), AP endonucleases to remove the resulting abasic site (Tomkinson, Bonk et al. 1988) and lyase activity of mtDNA polymerase γ and mtDNA ligase III to seal the DNA nick and complete the DNA repair (Bogenhagen 1999). Evidence for the removal of photo induced lesions in yeast mitochondria (Prakash 1975) and alkylation damage in human mitochondria (Cai, Xu et al. 2005) have also been documented.

More recently it has also been identified that mtDNA repair pathways actually include long patch BER (LP-BER), with flap endonuclease and DNA2 nuclease/ helicase activity, for the removal of oxidised lesions involving more than 2 nucleotides (Liu, Qian et al. 2008; Zheng, Zhou et al. 2008). Mismatch repair (MMR) has also been identified in mammalian mitochondria for the removal of misincorporated bases and slippage errors caused by Poly during mtDNA replication (Mason, Matheson et al. 2003; de Souza-Pinto, Mason et al. 2009) and there is increasing evidence for the repair of double strand breaks in mammalian mitochondria by homologous recombination and non-homologous end joining, as detailed in (Liu and Demple 2010).

Targeted degradation of damaged mtDNA has also been hypothesised as a mechanism by which mitochondria can remove high levels of mtDNA damage. This was supported with the discovery of a novel endo-exonuclease in the mitochondrial matrix (Davies, Hershman et al. 2003) and the more recent discovery that oxidative lesions in mtDNA are selectively targeted for degradation to prevent their copying during mtDNA replication and mutagenesis (Shokolenko, Venediktova et al. 2009).

1.2.3 Maternal inheritance and the mtDNA bottleneck

Inheritance of mtDNA is unique in that it is not subject to Mendelian inheritance but is inherited strictly through the maternal lineage. Sperm mitochondria are diluted out by the vast number of mitochondria present in the maternal oocyte and following fertilisation sperm mitochondria are targeted selectively for degradation by ubiquitination and autophagy in the oocyte cytoplasm (Al Rawi, Louvet-Vallée et al. 2011), with any remaining paternal mitochondria inactivated by proteolysis during preimplantation development (Cummins, Wakayama et al. 1997; Sutovsky, Moreno et al. 2000). Only one incidence of paternally inherited mtDNA has ever been reported, where a patient presented with a deletion in mt-ND2, that was found to be of paternal origin and absent from the maternal haplotype (Schwartz and Vissing 2002).

Pathogenic mtDNA mutations are transmitted from mother to child if present in the maternal germline (Giles, Blanc et al. 1980), with the risk of transmission governed by the heteroplasmy of the mutation (Larsson, Tulinius et al. 1992). Indeed the type of mtDNA defect further influences the risk of transmission, with mtDNA deletions rarely transmitted from mother to offspring (Larsson, Eiken et al. 1992) whilst the transmission of mtDNA point mutations is much more common. The maternal transmission of a mtDNA mutation can result in offspring with substantial variability in heteroplasmy for the same mutation (Taylor and Turnbull 2005), which is due to a phenomenon known as the “genetic bottleneck”. Mammalian oocytes contain ~100,000 copies of mtDNA, whereas the primordial germ cell from which they originated contains a much lower number of mtDNA genomes, ~200 (Cree, Samuels et al. 2008). As such there is the selective replication and amplification of only a small number of specific mtDNA molecules during oogenesis. The molecular mechanisms involved in the “genetic bottleneck” remain to be elucidated; however the bottleneck is believed to exist to act as a constraint on the germline transmission of pathogenic mtDNA mutations. Indeed studies performed in mice have demonstrated that pathogenic mtDNA mutations are subject to strong purifying selection in the mammalian germline, limiting the transmission of severe mutations in protein-encoding genes (Fan, Waymire et al. 2008; Stewart, Freyer et al. 2008). However, despite such selective mechanisms pathogenic mtDNA mutations and low level heteroplasmic mutations are still frequently inherited through the maternal lineage (He, Wu et al. 2010).

1.2.4 *MtDNA mutagenesis*

As mentioned above mtDNA, is subject to harmful intrinsic and extrinsic noxious agents that induce DNA damage and can result in mutations of the mtDNA genome. MtDNA mutations can present as point mutations, deletions, insertions and large-scale rearrangements. The incidence of damage to the mtDNA genome is substantially higher than to the nuclear genome, with the mtDNA mutation rate estimated to be 10-17 fold higher than nuclear DNA (Neckelmann, Li et al. 1987; Wallace, Ye et al. 1987). This was originally believed to be due to a lack of DNA repair mechanisms (Clayton 1982) coupled with a lack of protective histones (Richter C 1988). However, it is now known that mitochondria do indeed share many of the same DNA repair mechanisms as the nuclear genome (Liu and Demple 2010) and the protective role of histones is actually rather dubious, with certain experimental evidence suggesting that histones can intensify DNA damage rather than protect against it (Liang and Dedon 2001).

MtDNA point mutations are principally thought to arise from endogenous replication errors caused by Poly through the misincorporation and miscopying of bases (Zheng, Khrapko et al. 2006). Indeed mtDNA Poly is thought to have a greater error rate than other DNA polymerase enzymes (Kunkel 1986). Unrepaired oxidized lesions are also a cause of mtDNA mutations, with mtDNA being shown to contain a higher incidence of the common oxidized lesion, 8-hydroxydeoxyguanosine, occurring every 1 in 8000 bases, compared to 1 in 130 000 bases in nuclear DNA (Richter C 1988). As such the substantial mutation rate of the mtDNA genome is also believed to be attributable to the close proximity of the mtDNA genome to the ETC in the IMM and the site of ROS production (Richter C 1988). The formation of mtDNA deletions is believed to arise from one of two proposed mechanisms: either during slippage replication (Shoffner, Lott et al. 1989) or during the repair of DNA damage, caused by double-strand breaks (Krishnan, Reeve et al. 2008).

1.2.5 *Heteroplasmy*

Given the high copy number of mtDNA within mitochondria, a mixture of both wild-type (WT) mtDNA and mutant mtDNA can exist within a cell, giving rise to a state known as heteroplasmy (Larsson and Clayton 1995). Heteroplasmy is often expressed as the percentage of mtDNA genomes that harbour a mutation within a cell, and is an important determining factor in the clinical presentation of mitochondrial DNA disease. When all of the mtDNA in a given cell is identical, this is known homoplasmy, such that a cell can be homoplasmic WT or homoplasmic mutant.

1.2.6 *The threshold effect*

MtDNA mutations are highly recessive (Sciaccio M 1994), which coupled with the high copy number of mtDNA in a cell, means that a cell can tolerate a fairly high level of mtDNA defects and still maintain normal mitochondrial function. It is well established, however that once a mutant mtDNA molecule is present within a cell, it can clonally expand and become the dominant genome. It is only when a mutant mtDNA molecule clonally expands and reaches a critical threshold level that normal mitochondrial function can no longer be maintained, a biochemical defect in the respiratory chain occurs and a mutant phenotype is observed (Figure 1-5). The critical threshold level differs according to the individual, the cell type (Johns 1995), the metabolic demand of the tissue, the mutation type and the amount of residual WT mtDNA. However, in general a mutant phenotype is observed when the level of mtDNA deletion exceeds ~60% in a cell (Sciaccio M 1994) and ~85% for mtDNA point mutations, with the

critical threshold level for certain tRNA mutations exceeding 90% (Boulet L 1992; Chomyn, Martinuzzi et al. 1992).

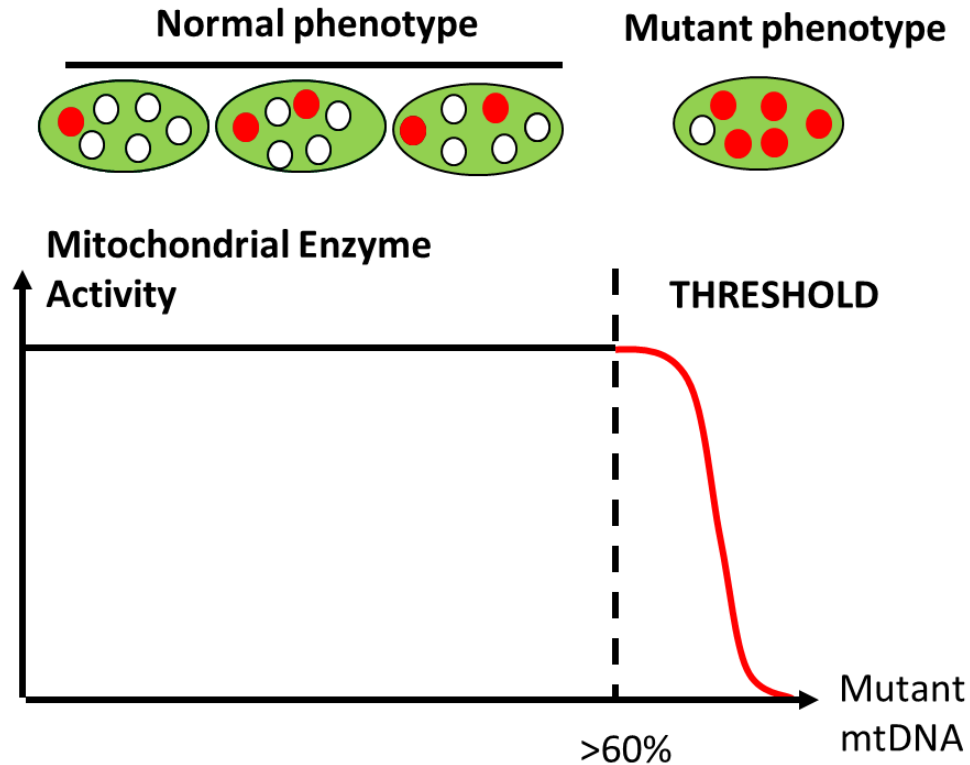


Figure 1-5: Heteroplasmic mtDNA mutations and the threshold effect.

Heteroplasmic mtDNA mutations can be tolerated by a cell and normal mitochondrial functional maintained, until a critical threshold level of mutant mitochondria is reached, which is usually in excess of 60% heteroplasmy. The green ovals represent individual mitochondria within a cell, containing WT mtDNA (white circles) and mutant mtDNA (red circles).

The mutant phenotype that ensues when a biochemical defect arises in the respiratory chain can routinely be identified in tissues using a histochemical assay for the activity of cytochrome *c* oxidase (COX), complex IV of the respiratory chain, and succinate dehydrogenase (SDH), complex II (Old and Johnson 1989). Given that the catalytic subunits of complex IV, which are essential for its assembly, are encoded by mtDNA, mtDNA defects often result in a loss of COX activity. SDH is entirely nuclear encoded and as such is unaffected by mtDNA defects. Using this assay sections are firstly incubated with COX medium which comprises 3, 3'-diaminobenzidine (DAB), cytochrome *c* and catalase. DAB acts as an electron donor in the ETC, reducing cytochrome *c*, which in turn is then oxidised by COX. The loss of an electron from DAB induces oxidative polymerization and the cyclization of DAB, which results in the

formation of a brown, insoluble, indamine polymer in cells that harbour normal COX activity (Old and Johnson 1989). Endogenous peroxidase activity, which may interfere with the formation of the brown polymer, is inhibited by the inclusion of catalase in the reaction medium. The SDH medium used comprises nitro blue tetrazolium (NBT), phenazine methosulphate (PMS), sodium azide and sodium succinate. NBT acts as an electron acceptor in the ETC, PMS is used as an efficient electron carrier, enhancing the formation of the final product, sodium azide acts as a terminal respiratory chain inhibitor and sodium succinate serves as the substrate in the reaction (Old and Johnson 1989). The reduction of NBT upon gaining an electron results in the formation of an insoluble, microcrystalline, blue formazan. Cells with normal functioning mitochondria and preserved COX activity will therefore oxidize DAB and stain brown and cells with dysfunctional mitochondria will stain negative for COX activity but positive for SDH activity and appear blue upon the reduction of NBT (Muller-Hocker 1989; Old and Johnson 1989). As such this histochemical assay can be readily used to identify cells harbouring mtDNA defects and is commonly used as a screening tool for mitochondrial dysfunction in both disease (Sciaccio M 1994; Kaido, Fujimura et al. 1995) and ageing (Muller-Hocker 1989; Muller-Hocker 1990; Brierley, Johnson et al. 1998; Cottrell, Blakely et al. 2001; Taylor, Barron et al. 2003; Bender, Krishnan et al. 2006). Indeed this assay serves as a fundamental screening tool throughout this thesis.

1.2.7 Clonal expansion

The ability of a mtDNA mutation to clonally expand and become the dominant genome within a cell was first documented in muscle biopsies of patients with mtDNA over 20 years ago (Mita, Schmidt et al. 1989). However the exact mechanism by which a mtDNA mutation clonally expands remains unknown. Several hypotheses have been proposed, however these differ in suitability according to the type of mtDNA defect and the tissue in which the mutant mtDNA molecule is undergoing clonal expansion.

1.2.7.1 Structural mechanisms

The structural mechanisms of clonal expansion suggest that specific structural changes invoked by the mtDNA defect convey a replicative advantage to the mutant mtDNA genome, thus propagating clonal expansion within the cell. As such it was proposed by Wallace in 1992 that a mtDNA genome possessing a large-scale deletion would replicate and proliferate faster in the cell, due to the smaller size, than the larger WT mtDNA molecule, thus driving clonal expansion (Wallace 1989). Indeed this has been supported experimentally in two different studies (Diaz, Bayona-Bafaluy et al. 2002;

Fukui and Moraes 2009). However, the known rate of mtDNA replication (<90 minutes) and the interval between replications (~2 weeks), indicates that a faster mtDNA replication would bear little benefit to a mutant mtDNA molecule (Shadel and Clayton 1997; Korr, Kurz et al. 1998; Kowald and Kirkwood 2000). Furthermore if smaller genomes replicated faster, mtDNA deletions should preferentially accumulate in replicative tissues with a high turnover rate. However, this is not the case, with clonally expanded mtDNA deletions predominantly seen in post-mitotic tissues (Muller-Hocker 1989; Muller-Hocker 1990; Cottrell, Blakely et al. 2001). Clonally expanded mtDNA point mutations prevail in mitotic tissues and indeed the “survival of the smallest” concept and the proposed replicative advantage could not explain the clonal expansion of these mtDNA genomes, where there is no alteration in size (Taylor, Barron et al. 2003; McDonald, Preston et al. 2006; Fellous, McDonald et al. 2009). Moreover, given that multiple stages of the mtDNA replication process are dependent upon ATP it is difficult to understand how a smaller genome, that will undoubtedly have lost genes and therefore proteins that are essential for activity of the ETC, could generate enough energy to facilitate faster mtDNA replication (Kowald and Kirkwood 2000).

Alternatively it has been suggested that mtDNA deletions harbour a replicative advantage due to the loss or inactivation of *cis*-acting regulatory elements that usually repress proliferation (Shoubridge, Karpati et al. 1990). As such enhanced proliferation of deleted mtDNA genomes would ensue leading to their clonal expansion and accumulation within the cell. However, the location of such negative regulatory elements was not specified in this study and it was found that multiple large deletions covering a number of overlapping-regions of the genome accumulate in heart muscle fibers (Khrapko, Bodyak et al. 1999). As such the clonal expansion of deletions cannot simply be dependent upon the loss/ inactivation of one particular part of the genome.

1.2.7.2 *Functional mechanisms*

The functional mechanisms predict that a mtDNA defect in a tRNA or protein-encoding gene causes a functional change, enabling the mutant mtDNA genome to accumulate within the cell. In 1990 Shoubridge offered a mechanism for the clonal expansion of mtDNA deletions based upon the principle that increased oxidative demand in skeletal muscle stimulates mitochondrial biogenesis and proliferation (Williams, Salmons et al. 1986). As such it was suggested that a cell harbouring mutant mtDNA would stimulate increased mtDNA synthesis and mitochondrial proliferation in an attempt to compensate for a reduction in OXPHOS and ATP production thus causing expansion of

the mutant genome (Shoubridge, Karpati et al. 1990). Indeed this is supported by the presence of ragged red fibers (RRF) in skeletal muscle of certain patients with mitochondrial DNA disease, demonstrating the subsarcolemmal accumulation of mitochondria and a potential hyperproliferative response (Shoffner, Lott et al. 1990). This positive feedback mechanism, however would only operate if individual mitochondria harbouring mutant mtDNA were stimulated to proliferate (Kowald and Kirkwood 2000). Indeed such a mechanism is unlikely given that mitochondria exist in a dynamic intracellular network and undergo fission and fusion. Moreover experimental evidence demonstrates that defective mitochondria are selectively degraded by autophagy and not preferentially amplified (Twig, Elorza et al. 2008; Kim and Lemasters 2011).

Alternatively it has been suggested that a mutation in mtDNA actually results in decreased activity of the ETC and decreased ROS production, thereby resulting in less oxidative damage to mitochondrial membranes. As such mitochondria harbouring mutant mtDNA would be targeted less for degradation by lysosomes, than their WT counterparts that would incur more oxidative damage (De Grey 1997). The favoured survival of mutant mtDNA would give the mutant genome a selective advantage, thus facilitating clonal expansion within the cell. This is otherwise known as the “survival of the slowest” mechanism and has been supported by modelling studies (Kowald and Kirkwood 2000). However, again this mechanism disregards the dynamic, reticular network of mitochondria within a cell, the distribution of mtDNA within this network and the compensatory mechanisms that exist for reduced OXPHOS capacity.

1.2.7.3 *Random mechanisms*

Random mechanisms of clonal expansion, unlike the structural and functional mechanisms, propose that replication of the mtDNA genome is actually unbiased. Computer modelling demonstrated that neutral replication, where some mtDNA molecules are randomly replicated and others are randomly lost, coupled with mitotic segregation during cell division, is sufficient for a mtDNA mutation to clonally expand and reach homoplasmy in a dividing cell after a specific number of divisions (Figure 1-6) (Coller, Khrapko et al. 2001). This model was found to match experimental data and successfully predicted the frequency of homoplasmic mtDNA mutations in normal buccal epithelial cells and tumour cells (Coller, Khrapko et al. 2001). However, this model assumed that mtDNA replication was coupled with cell division (Coller,

Khrapko et al. 2001) whereas mtDNA is known to replicate autonomously, independent of the cell cycle.

A second computer modelling study, however, further demonstrated that relaxed replication of the mtDNA genome coupled with random mtDNA replication, can through random intracellular drift, lead to the clonal expansion of mtDNA mutations in single post mitotic cells during the human lifespan (Elson, Samuels et al. 2001). This model again was found to match experimental data, successfully predicting the magnitude of COX deficiency ($\leq 4\%$) caused by clonally expanded mtDNA mutations in human post mitotic tissues (Muller-Hocker 1990; Brierley, Johnson et al. 1998; Cottrell, Blakely et al. 2001). The clonal expansion of mtDNA mutations through random intracellular drift did indeed take a significant number of years and so it was proposed that mtDNA mutations actually occur during childhood or early adulthood and clonally expand throughout an individual's lifetime (Elson, Samuels et al. 2001), which has since been reinforced experimentally using mitochondrial mutation assays (Coller, Khrapko et al. 2005; Greaves 2014).

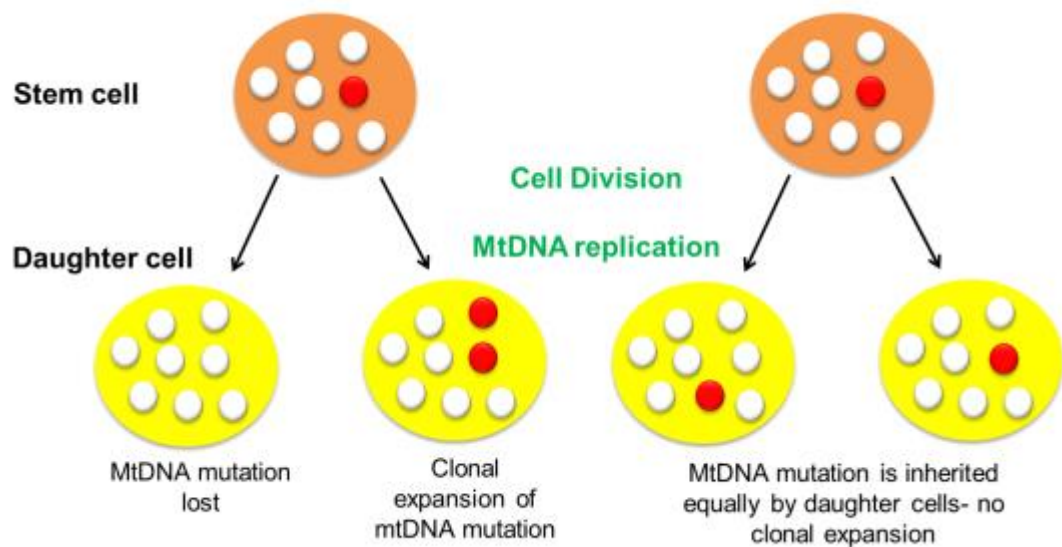


Figure 1-6: Clonal expansion of a mutant mtDNA molecule in mitotic tissues by random intracellular drift.

The mutated mtDNA molecule is shown by the red circle and the WT mtDNA molecules by the white circles. Random genetic drift poses that during stem cell division, the relaxed replication of the mtDNA genome coupled with the fact that a mutant mtDNA molecule may be randomly lost or randomly replicated, can lead to the clonal expansion of the mutant genome when the replicated mutated genomes are both inherited by a daughter cell, as shown in the diagram on the left. Alternatively, during stem cell division, a mutant mtDNA molecule may be evenly distributed between daughter cells, resulting in an absence of clonal expansion, as indicated by the diagram on the right.

Experiments in certain human cell cybrids have shown that some mtDNA mutations do seem to convey a selective advantage and lead to the preferential replication and

amplification of the mutant genome (Shay and Ishii 1990; Yoneda, Chomyn et al. 1992). However, random intracellular drift closely matches the experimental data and incidence of clonally expanded mtDNA mutations that we see in human tissues, and so whilst there are specific exceptions, it may be a more general mechanism for the clonal expansion of mutations in human tissues.

Understanding the mechanisms by which mtDNA mutations clonally expand is essential to facilitate our understanding of the presentation and progression of pathological conditions and disease, as well as the ageing process, with clonally expanded mtDNA mutations documented in a number of ageing human tissues (see section 1.4.3.1.1).

1.2.8 Mitotic segregation

The rate of mtDNA turnover remains poorly understood, however the continuous replication of the mtDNA genome means that mtDNA molecules can segregate in both mitotic and post-mitotic cells, irrespective of the cell cycle. During mitosis mtDNA molecules are randomly segregated between daughter cells, which causes variations in the level of mutant mtDNA. Consequently, mtDNA heteroplasmy can vary considerably between cell lineages and different tissues (Macmillan, Lach et al. 1993), and it is only if the mutation load exceeds the critical threshold level that a mutant phenotype is observed, giving rise to the significant heterogeneity seen with mitochondrial DNA disease. Indeed tissue segregation of mtDNA molecules can also lead to the loss of a mutant mtDNA molecule within a cell population, especially in mitotic tissues with a high cellular turnover. This is characteristic of the m.3243A>G mutation in patients with mtDNA disease that present with lower heteroplasmy in the blood, buccal and hair compared to much higher levels of the mutation in muscle and urine, suggesting a selective loss of the mutation in replicative tissues (Chinnery, Zwiijnenburg et al. 1999; Rahman, Poulton et al. 2001).

1.3 Mitochondrial disease

Pathogenic mutations in mtDNA were first identified in 1988 (Holt, Harding et al. 1988; Wallace 1988). It is now estimated that 1 in 200 people in the UK harbour a pathogenic mtDNA mutation, with ~1 in 10,000 adults presenting with clinically manifesting mitochondrial disease in north east of England (Elliott, Samuels et al. 2008; Schaefer, McFarland et al. 2008). Given the presence of mitochondria in all nucleated mammalian cells, mitochondrial disease is an extremely heterogeneous group of disorders, that affect multiple organ systems and can present at different ages of onset (McFarland,

Taylor et al. 2007). The clinical presentation of the disease is governed by the type of mutation, heteroplasmy and the threshold level, mitotic segregation, the genetic bottleneck and the clonal expansion of the mutation. Neurological and muscle phenotypes are common as organ systems that have a high-energy demand are typically affected in mitochondrial disease. Mitochondrial diseases are a severely debilitating group of disorders, for which there is currently no cure and treatment options purely focus on managing disease symptoms. For further details of the different symptoms and clinical manifestations of mitochondrial DNA disease in both adults and children please refer to the following reviews (Taylor and Turnbull 2005; Tuppen, Blakely et al. 2010).

Successful diagnosis of mitochondrial disease relies on multiple avenues of investigation including histochemical and biochemical analysis as well as whole genome sequencing of mtDNA for the detection of mtDNA point mutations or deletions. Histological evidence of mitochondrial dysfunction, including the presence of ragged red fibres, indicative of subsarcolemmal accumulation of irregular mitochondria, and COX deficiency can frequently be detected in muscle biopsies of patients with mitochondrial DNA disease (Sciacco M 1994; Kaido, Fujimura et al. 1995). COX deficiency can also be detected in certain brain regions of patients with mtDNA disease (Kaido, Fujimura et al. 1995).

Mitochondrial disease is commonly caused by rearrangements in mtDNA or point mutations. Given that a substantial number of proteins involved in OXPHOS and all proteins required for mtDNA replication are nuclear encoded, nuclear gene mutations can also precipitate mitochondrial disease. For example mutations in Poly and TWINKLE have been shown to cause the accumulation of multiple mtDNA deletions (Spelbrink, Li et al. 2001; Van Goethem, Dermaut et al. 2001) and mutations in complex I subunits encoded by nuclear DNA cause Leigh syndrome (Smeitink and Van Den Heuvel 1999). For additional details on mitochondrial respiratory chain disorders caused by different nuclear gene defects please see the following reviews (Shoubridge 2001; DiMauro and Schon 2003). Mitochondrial disease can also be caused by problems with fatty acid metabolism, as seen in Medium-chain acyl-Coenzyme A Dehydrogenase (MCAD) deficiency, which commonly presents as hypoketotic hypoglycaemia and Very-Long-chain acyl-CoA Dehydrogenase (VLCAD) deficiency, characterised by cardiomyopathy (Wilcken 2010).

MtDNA rearrangement disorders are primarily caused by large-scale deletions in mtDNA but can also be caused by duplications. MtDNA deletions typically range from ~1- 8kb in size and can span several genes (Schon, Rizzuto et al. 1989). They commonly occur between the two origins of replication and are flanked by two short (13bp) direct repeats (Samuels, Schon et al. 2004; Bua, Johnson et al. 2006). Single mtDNA deletions, where the same deletion is present in all cells of an affected tissue, commonly cause sporadic mitochondrial disease, such as Kearns-Sayre syndrome (Zeviani, Moraes et al. 1988), Chronic Progressive External Ophthalmoplegia (Moraes, DiMauro et al. 1989) and Pearson syndrome (Rotig, Cormier et al. 1990). The formation of mtDNA deletions is covered in section 1.2.4 and further details concerning the clinical phenotype and mtDNA genotype of these disorders can be found in the following review (Taylor and Turnbull 2005). The presence of multiple mtDNA deletions in cells is generally secondary to a nuclear gene defect, such as mutations in TWINKLE and mtDNA polymerase γ (see above) (Taylor and Turnbull 2005).

Pathogenic point mutations in mtDNA that cause mtDNA disease are typically heteroplasmic and are maternally inherited. Point mutations can occur within protein encoding genes, directly affecting the function of a respiratory chain complex, as seen in Leber's Hereditary Optic Neuropathy, which is caused by complex I defects (LHON) (Johns, Neufeld et al. 1992), rRNA genes or they can occur in tRNA genes, which are detrimental to mitochondrial translation. The emphasis of this thesis is not on mitochondrial disease in general but rather on a mouse model of a specific mt-tRNA point mutation and as such I will only discuss this group of mtDNA point mutations in more detail. For further details on the range of clinical mitochondrial DNA diseases caused by mtDNA point mutations please see the following review (Taylor and Turnbull 2005).

1.3.1 Mt-tRNA point mutations

In spite of the fact that tRNA genes only occupy ~10% of the mtDNA genome (McFarland, Elson et al. 2004), over half of the disease-causing mtDNA point mutations that have been identified occur in mt-tRNA genes and account for the majority of pathogenic mtDNA mutations transmitted from mother to child (Schaefer, McFarland et al. 2008). Unsurprisingly mt-tRNA mutations precipitate a loss in translational function of the tRNA and cells harbouring pathological mt-tRNA commonly show reduced activity and function of respiratory chain complexes, reduced oxygen consumption,

reduced growth rates and increased levels of lactate, given the cells dependence upon glycolysis for energy production (Jacobs 2003).

Two of the most prominent clinical mitochondrial disorders are caused by mt-tRNA mutations: mitochondrial encephalomyopathy, lactic acidosis and stroke like episodes (MELAS), which is caused by the m.3243A>G mutation in mt-tRNA^{Leu (UUR)} (Goto, Nonaka et al. 1990) and myoclonic epilepsy with ragged red fibres (MERRF), which is caused by the m.8344A>G mutation in mt-tRNA^{Lys} (Shoffner, Lott et al. 1990). The m.3243A>G mutation occurs in the dihydrouridine loop of tRNA^{Leu (UUR)}, which is associated with a decrease in the aminoacylation of the tRNA, causing a defective anticodon that leads to impaired translation (Yasukawa, Suzuki et al. 2000). The m.8344A>G mutation occurs in the TΨC loop of tRNA^{Lys} and is similarly associated with an unmodified base in the wobble position of the anticodon, resulting in mistranslation (Yasukawa, Suzuki et al. 2000). Whilst the tRNA mutations precipitating MELAS and MERRF are fairly common within the population, many other mt-tRNA point mutations will only present in one or two families (Majamaa, Moilanen et al. 1998).

Certain correlations can be made between disease presentation in patients and the mt-tRNA gene affected, such that tRNA^{Lys} mutations are often associated with cardiomyopathy, as seen in MERRF, tRNA^{Ser} mutations often resulting in sensorineural deafness and tRNA^{Leu} mutations are commonly associated with myopathy and muscle phenotypes (Jacobs 2003). Specific mt-tRNA mutations, however, still precipitate extremely heterogeneous clinical phenotypes in different patients, which is common in patients with MELAS. Heteroplasmy, mitotic segregation and the limited number of non-specific mitochondrial tRNAs available that cause variation in the proteins synthesised, are amongst some of the explanations offered to describe the diverse clinical symptoms caused by a specific mt-tRNA mutations (Jacobs 2003). However, our understanding of the molecular mechanisms involved in the diversity of mitochondrial DNA diseases caused by mt-tRNA mutations still remains fairly poor. Dissecting such molecular mechanisms is vital for understanding disease progression, maternal transmission, improving disease management and developing new treatments.

1.4 Ageing

Ageing is a stochastic process characterised by the accumulation of molecular damage within cells, resulting in attenuated tissue function during adulthood, reduced fecundity,

enhanced susceptibility to disease and an increased probability of death (Kirkwood 2008). Since the late 19th and 20th century, improvements in sanitation, medicine, housing and education have resulted in a vast increase in life expectancy, accompanied by a reduction in later life mortality (Kirkwood 2008). Consequently, it is becoming crucial to understand the mechanisms involved in the ageing process and the driving factors of age-related frailty and disease, in order to improve the quality of later life in aged individuals. A number of theories, classified as either evolutionary or molecular theories of ageing, have been proposed to explain the ageing process and the causal factors. However, much of the literature and experimental evidence is still fairly dubious, with ageing actually believed to be a multi-factorial process, arising from a combination of different mechanisms acting simultaneously.

1.4.1 *Evolutionary theories of ageing*

Given that different species have different lifespans, evolutionary theories of ageing assert that lifespan and longevity is controlled by the genome and that the ageing process is therefore programmed (Finch and Tanzi 1997). There are three predominant evolutionary theories of ageing, which began with August Weismann in 1889, with the suggestion that all species possess an ‘ageing gene’ and this acts to programme ageing in order to minimise and control population size. Genomic influence on the ageing process became well-recognized when Medawar proposed the Mutation Accumulation theory, suggesting that ageing is driven by the accumulation of deleterious mutations within the genome, that have adverse effects later in life (Medawar 1952). The late-onset adverse effects of genes is a repeated concept in the Antagonistic Pleotropy theory of ageing, which suggests that the selection of favourable genes which convey a reproductive advantage early in life, become detrimental later on (Williams 1957). The Disposable Soma theory of ageing is the third evolutionary theory and alternatively suggests that ageing arises due to metabolic trade-offs between reproduction, cell growth and repair mechanisms in somatic cells (Kirkwood 1977). Given that energy will be pooled into reproductive processes to propagate a species, a lack of energy resources are available for cell maintenance and repair (Kirkwood 1977). As such damage will accumulate within cells and drive the ageing process. However, the prospect that genes govern lifespan and that organisms would select for a process that is not advantageous for their survival and instead leads to ageing, disease and death, is highly unlikely, and is a major argument used against the evolutionary theories of ageing (Kirkwood 1995).

1.4.2 *Molecular theories of ageing*

Molecular theories of ageing propose that ageing is not programmed but rather results from the accumulation of unrepaired molecular damage in somatic cells caused by biochemical and cellular processes. Given that such processes would occur randomly, the molecular theories of ageing are more widely accepted. The molecular theories of ageing essentially focus on the accumulation of damage to DNA, telomeres, proteins and oxidative damage to macromolecules.

Random mutagenesis of chromosomal DNA coupled with the progressive inefficiency of DNA repair mechanisms during the life course of a species (Szilard 1959; Hart 1974), have been proposed as the principle driving factors of DNA damage accumulation within cells, leading to tissue dysfunction with age. The idea that DNA damage is fundamental in cellular ageing is further continued by the telomere hypothesis of cellular ageing (Harley 1992). Given that the activity of telomerase, the enzyme that maintains telomere length, is suppressed in somatic cells, there are only a certain number of cell divisions that a cell can undergo before telomere length decreases below a specific limit and the cell will enter replicative senescence (Harley 1992). Arrested cells therefore begin to accumulate over time, with the lack of functional cells leading to tissue failure. Age-related damage to DNA can further arise from time-dependent, abnormal post-translational cross-linking, which can permanently interfere with normal function (Bjorksten and Tenhu 1990). Protein damage can also ensue from such chemical cross-linking (Bjorksten and Tenhu 1990), which along with age-related disturbances in protein homeostasis and decreased protein turnover within cells (Cuervo 2000) can cause the accumulation of damaged, aggregated proteins within cells. Oxidative damage to DNA, proteins, lipids and macromolecules is a further source of damage accumulation and is well-documented in ageing tissues (Balaban, Nemoto et al. 2005). It was in 1956 that Harman first proposed the free radical theory of ageing to explain oxidative damage (Harman 1956), which later became adapted to the mitochondrial free radical theory of ageing (Harman 1972).

1.4.2.1 *The (mitochondrial) free radical theory of ageing*

According to the free radical theory of ageing, cellular dysfunction arises from irreversible oxidative damage to DNA, proteins and cellular membranes caused by endogenous ROS, namely the superoxide radical and hydroxyl radical, produced during

OXPPOS (Harman 1956). The discovery of the antioxidant superoxide dismutase, the enzyme responsible for metabolising the superoxide radical, in mitochondria (McCord 1969) and the identification of mitochondria as the dominant site of ROS production in a cell (Chance 1979) lead to the adaptation of this theory to the mitochondrial free radical theory of ageing (MFTA) (Harman 1972). It is estimated that ~0.2% of the total oxygen consumed by mitochondria is responsible for ROS production (St-Pierre, Buckingham et al. 2002) and ~90% of total cellular ROS production is attributable to the mitochondrial ETC (Balaban, Nemoto et al. 2005). It is proposed that the close proximity of mtDNA to the ETC and site of ROS production renders mtDNA vulnerable to oxidative damage and mtDNA mutations (Harman 1972). As such the MFTA proposes that mtDNA mutations accumulate throughout life and result in reduced mitochondrial and respiratory chain function (Miquel, Economos et al. 1980). This is proposed to activate a vicious cycle whereby dysfunction of the OXPPOS system causes enhanced ROS production and further damage to mtDNA, leading to the progressive accumulation of mtDNA mutations with age and further oxidative damage, eventually resulting in cell death (Harman 1972).

A fundamental association between ROS, mitochondria and lifespan has been demonstrated in a number of studies that show a reduced production of the superoxide radical in the heart, liver and kidney (Sohal, Svensson et al. 1989) and decreased oxidative damage to proteins (Agarwal and Sohal 1996) in longer lived animals. Pigeons, which live 7 years longer than rats, have also been shown to release ~30% less hydrogen peroxide from mitochondria than rat mitochondria (Herrero and Barja 1997). Furthermore transgenic mouse models demonstrate decreased ROS production and oxidative damage when the antioxidant catalase is targeted to mitochondria (Williams, Van Remmen et al. 1998; Schriener, Linford et al. 2005) and mice defective in manganese superoxide dismutase show increased oxidative damage to DNA and proteins (Williams, Van Remmen et al. 1998).

The mitochondrial theory of ageing is very attractive as mitochondria are the only extra nuclear source of DNA within a cell; the location of mtDNA renders it vulnerable and sensitive to the accumulation of damage (Harman 1972) and mtDNA demonstrates a significantly high mutation rate (Neckelmann, Li et al. 1987). Furthermore normal functioning of the mitochondrial respiratory chain plays a pivotal role within cellular survival and lifespan (Lin, Kaeberlein et al. 2002; Rea, Ventura et al. 2007). Structural

changes in mitochondria are also observed with increasing age, including a decline in number in post-mitotic tissues such as the heart,(Herbener 1976) and brain (Samorajski, Friede et al. 1971) as well as mitochondrial enlargement, cristae abnormalities and vacuolization (Wilson and Franks 1975; Wilson and Franks 1975). Seemingly a number of changes occur within mitochondria with increasing age, and the pivotal role of the ETC for normal cellular function, indicates that such changes in mitochondria and any resulting dysfunction are likely to be detrimental to the cell and contribute to the ageing process.

1.4.3 Mitochondrial dysfunction and ageing

Much of the supporting evidence for the MFTA however is simply correlative, and experimental evidence from recent years actually contests the so called ‘vicious cycle’ hypothesis. According to the vicious cycle ageing tissues should demonstrate a progressive accumulation of mtDNA mutations due to the production of new mtDNA mutations induced by the aggressive production of ROS (Harman 1972). However, ageing tissues tend to present with respiratory chain deficient cells that harbour a single clonally expanded mutant mtDNA molecule, rather than a variety of different mutations (Brierley, Johnson et al. 1998) (see section 1.4.3.1) and studies performed in the mtDNA mutator mouse, which show a progressive accumulation of mtDNA mutations and a premature ageing phenotype, do not show increased ROS production (Kujoth, Hiona et al. 2005; Trifunovic, Hansson et al. 2005) (see section 1.5.3), providing evidence against the ‘vicious cycle’ hypothesis. As such an alternative explanation for the mitochondrial theory of aging has been proposed, suggesting that mtDNA mutations actually arise during early life due to oxidative damage or errors that occur during mtDNA replication, and it is the clonal expansion of these mutations throughout adulthood that results in mitochondrial dysfunction later in life (Elson, Samuels et al. 2001; Greaves 2014). Tissue dysfunction would subsequently arise from defects in energy metabolism, apoptosis and senescence, eventually leading to age-related frailty and disease (Taylor and Turnbull 2005). Age-related respiratory chain dysfunction was reported in 1989 with the discovery that COX deficient cardiomyocytes accumulated in the hearts of subjects over the age of 60 and were indeed absent from young individuals below 20 years of age (Muller-Hocker 1989). COX deficient cells have since been documented in numerous ageing human tissues including skeletal muscle (Muller-Hocker 1990), brain (Cottrell, Blakely et al. 2001), the colon (Taylor, Barron et al.

2003), liver (Fellous, Islam et al. 2009), and stomach (McDonald, Greaves et al. 2008), indicating a role for mitochondrial respiratory chain deficiency in the ageing process.

1.4.3.1 *MtDNA mutations and ageing*

The central focus of this thesis is to examine the role of mtDNA point mutations in ageing mitotic tissues, and so the role of age-related mtDNA deletions will only be examined briefly.

The ‘common deletion’, which spans 4977 nucleotides between the mt-*ATPase8* and mt-*ND5* genes, was the first mtDNA deletion to be discovered in ageing tissues, detected in the heart and multiple regions of the brain of elderly individuals (Cortopassi and Arnheim 1990). The ‘common deletion’ has subsequently been identified in skeletal muscle, the diaphragm, kidney, spleen and liver, with the highest level of the deletion detected in post-mitotic tissues, suggesting that mtDNA deletions accumulate in a tissue specific manner with age (Cortopassi, Shibata et al. 1992). Skeletal muscle fibers have been shown to accumulate multiple deletions in mtDNA with age (Kopsidas, Kovalenko et al. 1998) and focal respiratory chain deficiency has been associated with the accumulation of clonally expand mtDNA deletions in skeletal muscle fibers and neurons of the substantia nigra (SN) in humans, where single cell analysis has revealed the clonal expansion of different mtDNA deletions in different cells of the same tissue (Brierley, Johnson et al. 1998; Bender, Krishnan et al. 2006; Kraytsberg, Kudryavtseva et al. 2006). Focal COX deficiency has also been identified in skeletal muscle of rhesus monkeys and rats, where it was associated with muscle fiber degeneration (Herbst, Pak et al. 2007). As such mtDNA deletions are believed to be the root of COX deficiency in ageing post-mitotic tissues; however direct experimental evidence demonstrating a direct causal role for mtDNA deletions in age-related tissue dysfunction is still lacking.

The involvement of mtDNA point mutations in ageing was initially investigated by looking for levels of the m.8344A>G (Munscher, Rieger et al. 1993) and m.3243A>G mutations (Zhang, Linnane et al. 1993), that cause MERRF and MELAS respectively. Levels of these mutations in ageing tissues were found to be fairly low, reaching only ~2% in aged subjects (Munscher, Rieger et al. 1993; Zhang, Linnane et al. 1993). The use of more sensitive polymerase chain reaction (PCR) techniques, interestingly showed that the m.3243A>G mutation was actually present in skeletal muscle, brain, heart, liver and kidney of young children as well as adult tissues (Liu, Zhang et al. 1997). However, levels of the mutation were 10 fold higher in adult tissues and so this suggested that

mtDNA mutagenesis actually occurs during early life, most likely due to the high rates of replication during embryogenesis, and mutations subsequently clonally expand throughout adulthood. Early studies looking for mtDNA point mutation in ageing tissues also found that ~50% of human fibroblasts in elderly subjects harbour a m.414T>G mutation in mtDNA, that was indeed found to be absent from younger individuals (Michikawa, Mazzucchelli et al. 1999), and aged subjects have also been shown to possess ~2-3 point mutations per mitochondrial genome (Simon, Lin et al. 2004).

Age-related clonally expanded mtDNA point mutations were first documented in cardiomyocytes and buccal epithelium of individuals over the age of 75 (Nekhaeva, Bodyak et al. 2002). Interestingly, a very different spectrum of mtDNA mutations was documented in the two tissues, suggesting a different mechanism for the clonal expansion of mtDNA mutations in different tissues, potentially influenced by the mitotic activity of the tissue (Nekhaeva, Bodyak et al. 2002). Indeed the presence of clonally expanded mtDNA point mutations in COX deficient skeletal muscle fibers has not been reported very often (Fayet, Jansson et al. 2002; Durham, Samuels et al. 2006), suggesting that the type of mtDNA mutation and the clonal expansion that occurs in ageing is tissue specific. A causal role for mtDNA point mutations in the ageing process, however, only emerged when Taylor and colleagues discovered an age-related accumulation of COX deficient crypts in the ageing human colon, which was associated with the clonal expansion of somatic mtDNA point mutations (Taylor, Barron et al. 2003). Here the use of laser micro-dissection and whole mtDNA genome sequencing of individual cells, enabled the co-localization of a mitochondrial dysfunction phenotype with a genotypic defect. Furthermore, single cell analysis revealed that different cells of the same tissue contained different clonally expanded mtDNA point mutations, in which mtDNA deletions were found to be absent (Taylor, Barron et al. 2003). Clonally expanded mtDNA point mutations leading to the accumulation of COX deficient cells with age, have since been identified in a number of ageing human replicative tissues including the stomach, small intestine, liver and prostate, (McDonald, Greaves et al. 2008; Fellous, Islam et al. 2009; Blackwood, Williamson et al. 2011), indicating a potential causal role for clonally expanded mtDNA point mutations in ageing mitotic tissues.

Clonally expanded mtDNA point mutations are predominantly seen in mitotically active tissues that rely on stem cells for self-renewal, whereas mtDNA deletions prevail in ageing post-mitotic tissues. This further supports the finding by Nekhaeva and colleagues that different tissues exhibit different mechanisms for both the origin of mtDNA mutations and their clonal expansion, with the rate of tissue turnover and cell division being a key factor. Given that mtDNA point mutations are believed to primarily arise from mtDNA replication errors (Zheng, Khrapko et al. 2006), it is unsurprising that mtDNA point mutations predominate in dividing cells, for which random intracellular drift can explain their clonal expansion with age (Elson, Samuels et al. 2001). However, given the absence of cell division and the low rate of mtDNA replication in post-mitotic cells (Wang, Nutter et al. 1997), it remains controversial as to whether random intracellular drift could account for the clonal expansion of mtDNA deletions in post-mitotic tissues, especially the clonally high levels observed in the SN (Krishnan, Reeve et al. 2008).

Despite the documentation of clonally expanded somatic mtDNA mutations in a number of ageing human tissues, a causal role for mtDNA mutations in the ageing process still remains controversial, with many arguing that the overall level of mtDNA defects in ageing tissues is too low to cause tissue dysfunction. COX deficient cells in ageing human tissues, however frequently present in an intracellular and intercellular mosaic pattern. As such, the random distribution of mitochondrial dysfunction could indeed cause age-related tissue decline if critical cells, such as stem cells, are lost, by either apoptosis or senescence, as a result (Kukat and Trifunovic 2009). Respiratory chain deficiency results in clear pathological changes and tissue dysfunction in patients with mitochondrial disease and so understanding the consequences of clonally expanded mtDNA mutations and COX deficiency at the cellular level in ageing tissues will be critical for determining the role of mitochondria in the ageing process.

1.5 Mouse models of mitochondrial dysfunction

A number of mouse models, exhibiting mitochondrial dysfunction, have been developed that establish a significant causal role for mtDNA defects and respiratory chain dysfunction in age-related phenotypes and disease.

1.5.1 *TFAM* knockout mice

Mouse models of mitochondrial dysfunction began with the elimination of TFAM in tissue specific knockouts, which results in a drastic reduction in mtDNA copy number

and respiratory chain dysfunction. In pancreatic β -cells, an absence of TFAM in mice resulted in mitochondrial respiratory chain dysfunction directly associated with attenuated insulin secretion and an age associated loss of β -cells, closely resembling age-associated diabetes (Silva, Köhler et al. 2000). Disruption to the mitochondrial membrane potential, attributable to the reduced activity of ETC complexes, and defective Ca^{2+} homeostasis were also observed in the pancreatic β -cell mutant mice (Silva, Köhler et al. 2000). Tissue specific disruption of TFAM in dopaminergic (DA) neurons of mice, resulted in severe respiratory chain deficiency associated with reduced locomotion, tremors and limb rigidity, characteristic of a slow progressive movement disorder and age-associated Parkinson's disease (Ekstrand, Terzioglu et al. 2007). Such studies suggested that mitochondrial respiratory chain dysfunction has profound effects upon tissue function and can induce features characteristic of the ageing process and age-related disease. However, respiratory chain deficiency does not always induce age-related phenotypes, as TFAM depletion and respiratory chain deficiency in mouse skeletal muscle unexpectedly does not result in insulin resistance and diabetes (Wredenberg, Freyer et al. 2006). Furthermore, the tissue specific depletion of TFAM in adipose tissue, does not result in obesity or diabetes but actually enhances mitochondrial oxidation (Vernochet, Mourier et al. 2012). As such a causal role between respiratory chain dysfunction and age-related phenotypes still remains controversial.

1.5.2 *The MtDNA mutator mouse*

A direct causal relationship between the accumulation of mtDNA mutations and age-related phenotypes in mammals was established with the development of the mtDNA mutator mouse. Homozygous mtDNA mutator mice (*PolgA^{mut/mut}*) have a knock-in missense mutation that causes a critical amino acid change from aspartic acid to alanine (D257A) in the PolgA catalytic domain of mitochondrial Poly (Trifunovic, Wredenberg et al. 2004; Kujoth, Hiona et al. 2005). This mutation significantly reduces the proofreading activity of Poly and causes the accelerated, random accumulation of mtDNA mutations. A 3 to 5 fold increase in the level of mtDNA point mutations is observed in *PolgA^{mut/mut}* mice as well as increased levels of mtDNA deletions and severe respiratory chain deficiency. From 25 weeks old mice begin to display premature ageing phenotypes, which closely resemble signs of normal human ageing and include kyphosis, reduced subcutaneous fat, hair loss, weight loss, anaemia, osteoporosis, reduced fertility and enlargement of the heart as well as a reduced lifespan, <61 weeks old (Trifunovic, Wredenberg et al. 2004; Kujoth, Hiona et al. 2005). Two versions of

this mouse exist, which essentially differ in their WT mouse nuclear backgrounds and the gene excision system used. The model developed by Trifunovic and colleagues is on C57Bl/6N background and utilises an Flp-recombinase system, leaving the POLG gene flanked by two loxP sites (Trifunovic, Wredenberg et al. 2004), whereas the model developed by Kujoth and colleagues is on C57Bl/6J background and uses a Cre-recombinase system leaving behind only loxP site (Kujoth, Hiona et al. 2005).

Despite the significant respiratory chain dysfunction, *PolgA^{mut/mut}* mice do not experience increased ROS production or oxidative damage to macromolecules at the tissue level, providing evidence against the ‘vicious cycle’ hypothesis (Kujoth, Hiona et al. 2005; Trifunovic, Hansson et al. 2005). Furthermore the random, accumulation of mtDNA point mutations was found to be linear and constant across all tissues of the *PolgA^{mut/mut}* mouse, lending further support to the phenomenon that mtDNA mutagenesis is initiated early in development and does not involve the progressive accumulation of new mutations (Trifunovic, Hansson et al. 2005). Although there is an absence of evidence for the ‘vicious cycle’ hypothesis more recent studies have provided evidence for a relationship between mtDNA point mutations, ROS and oxidative damage in the mtDNA mutator mice. Oxidative damage has recently been documented in muscle (Kolesar 2014) and in vivo studies have demonstrated elevated levels of hydrogen peroxide in aged *PolgA^{mut/mut}* mice, where changes in redox signalling were proposed to have a pro-apoptotic and pro-inflammatory role (Logan, Shabalina et al. 2014). Multiple tissue of *PolgA^{mut/mut}* mice have been shown to display increased levels of caspase-3, suggesting that the progressive accumulation of mtDNA mutations could indeed cause enhanced apoptosis, giving rise to tissue dysfunction (Kujoth, Hiona et al. 2005). Alternatively, it has been proposed that tissue dysfunction may ensue from the induction of replicative senescence/ an energy defect in cells, caused directly by the respiratory chain deficiency (Trifunovic, Hansson et al. 2005).

Substantial levels of linear mtDNA molecules, spanning 12kb of the mtDNA genome have been detected in multiple tissues of *PolgA^{mut/mut}* mice (Trifunovic, Wredenberg et al. 2004). Linear mtDNA molecules are believed to be a consequence of stalled replication; however detection of these molecules at early stages of embryogenesis, a lack of accumulation in tissues and an absence of replication and transcription of these molecules, argues against a causal role for them in the premature ageing of *PolgA^{mut/mut}* mice (Kukat and Trifunovic 2009).

The causal role of mtDNA point mutations in the premature ageing of *PolgA^{mut/mut}* mice, was brought into question with the discovery that mice heterozygous for the D257A (*PolgA^{+/mut}*) mutation tolerate a 500 fold increase in the frequency of mtDNA point mutations compared to WT mice, and yet show no signs of premature ageing or a reduced lifespan (Vermulst, Bielas et al. 2007). Meanwhile the frequency of mtDNA deletions was shown to be 7 to 11 fold higher in *PolgA^{mut/mut}* mice compared to WT and *PolgA^{+/mut}* mice (Vermulst, Wanagat et al. 2008). As such it was argued that mtDNA deletions, rather than point mutations, drive the premature ageing in *PolgA^{mut/mut}* mice (Vermulst, Wanagat et al. 2008). However, other studies have failed to detect such deletions when using the same methods (Edgar, Shabalina et al. 2009), and groups that have detected mtDNA deletions only identify fairly low levels, ~1 mtDNA deletion: 1000 mtDNA point mutations in *PolgA^{mut/mut}* mice (Kraytsberg, Simon et al. 2009). Moreover mtDNA deletions do not progressively accumulate in tissues of *PolgA^{mut/mut}* mice but levels remain constant and mitochondrial translation and protein synthesis remain unimpaired, which would not be the case with large scale mtDNA deletions that generally cause a loss of protein encoding genes and multiple tRNAs (Edgar, Shabalina et al. 2009). Additional evidence against a role for mtDNA deletions in causing the premature ageing phenotypes of *PolgA^{mut/mut}* mice comes from other transgenic mouse models, such as the ‘deletor mouse’, where a mutation in mtDNA TWINKLE causes the progressive accumulation of multiple deletions in mtDNA and respiratory chain deficiency, without causing signs of premature ageing or a reduced lifespan (Tynismaa, Mjosund et al. 2005). The genetically engineered ‘mito-mouse’, that possess ~30% mtDNA deletions and focal COX deficiency in multiple tissues, also display an absence of premature ageing phenotypes (Inoue, Nakada et al. 2000). MtDNA point mutations that accumulate in *PolgA^{mut/mut}* mice, however have been shown to result in amino acid substitutions in protein encoding genes, disrupting the assembly and stability of respiratory chain complexes (Edgar, Shabalina et al. 2009). Indeed a recent study has documented that protein levels of respiratory chain complexes are decreased in the *PolgA^{mut/mut}* mice; however this was not accompanied by a reduction in mRNA levels, suggesting that somatic mtDNA mutations actually exhibit post-translational effects, leading to the respiratory chain deficiency (Hauser, Dillman et al. 2014). As such, it remains that point mutations in mtDNA, which accumulate progressively, in a linear fashion over the life course of the *PolgA^{mut/mut}* mouse

(Trifunovic, Wredenberg et al. 2004), are the primary cause of respiratory chain deficiency and tissue dysfunction that drive the premature ageing phenotypes.

1.5.3 *Mouse models of mtDNA disease*

Generating mouse models of mtDNA disease that carry specific mtDNA point mutations has proved very challenging, given that we cannot directly manipulate and engineer the mouse mtDNA genome in a living animal model. As such attempts to produce mouse models have relied on indirect methods to introduce mtDNA mutations into mice. Mice that were heterozygous for two different mtDNA haplogroups were the first heterozygous mouse models developed (Jenuth, Peterson et al. 1996; Jenuth, Peterson et al. 1997). Whilst these mice provided useful insights into mitotic segregation and tissue specific differences in the distribution of mtDNA they only possessed neutral mtDNA variants and not pathogenic disease causing mtDNA mutations.

1.5.3.1 *Mice harbouring mtDNA deletions*

The generation of mice carrying mtDNA deletions resulting in mitochondrial dysfunction and phenotypes characteristic of mtDNA disease have been reasonably successful. The first of these models was the ‘mito-mouse’, where mtDNA deletions were indirectly induced by introducing a respiratory chain deficient cybrid that carried a somatic mtDNA deletion, into fertilized mouse eggs (Inoue, Nakada et al. 2000). Successful germline transmission of the mtDNA deletion was achieved, producing progeny with fairly high levels of the deletion that displayed a mosaic distribution of COX deficient fibers in the heart and skeletal muscle as well as signs of cardiomyopathy and myopathy (Inoue, Nakada et al. 2000). Mice also presented with anemia, renal dysfunction and elevated levels of blood lactate, suggesting that they may serve as a model of mtDNA disease. However, certain features of the ‘mito mouse’ differed significantly to those seen in mtDNA disease, namely in terms of tissue distribution of the deletion, as high levels were detected in mitotic tissues, which is rarely reported in humans (Larsson and Clayton 1995; Fayet, Jansson et al. 2002; Yu-Wai-Man, Lai-Cheong et al. 2010). Furthermore questions remain surrounding the transmission of the mtDNA deletion to progeny, which indeed is rarely seen with human pathogenic deletions (Larsson 1995). It has however been suggested that this was due to transmission of a duplication, which later rearranged to form the deleted mtDNA molecule.

The alteration of nuclear encoded genes, resulting in the generation of mtDNA deletions has also been used to create mouse models, as seen in the 'deletor mouse'. In this mouse a DNA construct carrying a dominant mutation (A360T) in the mouse mtDNA helicase TWINKLE, corresponding to the m.359A>T mutation that causes Progressive External Ophthalmoplegia (PEO) in humans, was injected into mouse fertilised oocytes and used to propagate a mouse lineage (Tyynismaa, Mjosund et al. 2005). Resulting mice displayed the progressive accumulation of multiple mtDNA deletions in brain and skeletal muscle leading to a progressive respiratory chain deficiency with increasing age (Tyynismaa, Mjosund et al. 2005). Such features were absent from the 'deletor mice' until 12 months of age, which is in fact characteristic of chronic late-onset PEO, with mouse muscle also displaying several histological features of PEO such as abnormally large mitochondria with cristae inclusions (Tyynismaa, Mjosund et al. 2005). Despite the morphological homology to PEO, the 'deletor mice' did not however show any phenotypic evidence of myopathy: displaying normal grip strength, running ability and an absence of muscle weakness (Tyynismaa, Mjosund et al. 2005), questioning the validity of this mouse as a model of mtDNA disease.

Mice harbouring multiple mtDNA deletions and large scale rearrangements have also been created through the use of a restriction endonuclease targeted to mitochondria in mouse skeletal muscle, which resulted in double strand breaks (Srivastava and Moraes 2005). By 6 months old transgenic mice displayed features of mitochondrial myopathy characterised by restricted movement, respiratory chain deficiency and mitochondrial morphological abnormalities in skeletal muscle fibers, associated with a significant reduction in the levels of mtDNA (Srivastava and Moraes 2005). Such features closely resemble those of patients that harbour multiple mtDNA deletions in muscle, suggesting that this mouse was a useful model of disease. The accumulation of deletions from double strand breaks also provided useful insights into the mechanisms of deletion formation.

1.5.3.2 *Mice harbouring mtDNA point mutations*

The generation of mice carrying mtDNA point mutations has however proved more challenging. To date mtDNA point mutations have only been introduced into mice and stably transmitted through the germline through the use of mouse cell lines that carry naturally occurring pathogenic mtDNA point mutations (Kasahara, Ishikawa et al. 2006; Fan, Waymire et al. 2008; Yokota, Shitara et al. 2010; Lin, Sharpley et al. 2012).

The first of these studies used a respiratory chain deficient mouse cell line carrying a homoplasmic mtDNA point mutation in mt-*COI* (T6589C) to transfect embryonic stem cells, that were subsequently injected into mouse blastocysts to produce chimeric mice (Kasahara, Ishikawa et al. 2006). Chimeric mice were subsequently employed in a breeding strategy with WT B6 male mice and this successfully produced 6 generations of homoplasmic mutant mice, demonstrating maternal germline transmission of the mutation (Kasahara, Ishikawa et al. 2006). Homoplasmic mutant mice displayed COX deficiency in the heart and reduced complex IV activity in the liver, skeletal muscle and brain (Kasahara, Ishikawa et al. 2006). Mutant mice also displayed elevated blood lactate, a typical feature of pathogenic mt-*CO* mutations in patients (Rahman, Taanman et al. 1999; Varlamov, Kudin et al. 2002) and signs of reduced growth. However, other characteristic features of mt-*COI* mutations, such as epilepsy and muscle fatigue, were not observed (Rahman, Taanman et al. 1999; Varlamov, Kudin et al. 2002), thus questioning the potential of this mouse as a model of disease caused by mtDNA point mutations in structural genes.

Similarly in a study by Fan and colleagues two respiratory chain deficient mouse cell lines carrying the m.6589T>C mutation and a more severe mt-*ND6*-13885insC mutation, were used to transfect embryonic stem cells and generate two different chimeric mice that were used to propagate mouse lineages in a similar strategy to that above. Again this study showed successful germline transmission of the mt-*COI* T6589C mutation and a loss of COX activity in multiple tissues. Homoplasmic mice also showed histological features of mitochondrial myopathy including abnormal mitochondria and ragged red fibers in muscle, as well as predominant evidence of cardiomyopathy, including cardiomyocyte hypertrophy and fibrosis, suggesting that this mouse may serve as a good model of disease (Fan, Waymire et al. 2008). In contrast, the severe mt-*ND6* mutation was rapidly and selectively eradicated from the mouse maternal germline, within 4 generations, with experiments suggesting that selection occurred prior to ovulation, through apoptosis caused by increased oxidative stress (Fan, Waymire et al. 2008). Given the different severity of the two mutations, this study provided useful insights into the transmission of pathogenic mtDNA point mutations, helping to explain why more severe pathogenic point mutations tend to remain heteroplasmic in the population and milder mutations can reach homoplasmy (Wallace 2007).

A metastatic cancer cell line has also been used to generate transmitochondrial homoplasmic mice, similarly through the transfection of ES cells and generation of chimeric mice, to introduce a mutation in mt-*ND6*-G13997A that causes a complex I defect (Yokota, Shitara et al. 2010; Lin, Sharpley et al. 2012). Young mutant mice displayed evidence of complex I dysfunction as well as lactic acidosis in the blood; however typical features of LHON, which is commonly associated with complex I defects (Larsson and Clayton 1995; Wallace 1999), were not observed in these mice, which displayed evidence of normal vision and an absence of optic nerve atrophy (Yokota, Shitara et al. 2010; Lin, Sharpley et al. 2012). A second study that introduced the mt-*ND6*-G13997A mutation via an alternative cell line, however revealed that aged mutant mice (> 14 months old) did display typical signs of LHON, including reduced retinal function, loss of certain types of optic nerve fibers and neuronal abnormalities in the optic nerve, (Yokota, Shitara et al. 2010; Lin, Sharpley et al. 2012). Furthermore, the complex I defect in this mouse was associated with elevated ROS production, suggesting that LHON phenotypes may arise through oxidative stress rather than ATP deficiency (Yokota, Shitara et al. 2010; Lin, Sharpley et al. 2012). Such studies highlighted the importance of studying mutant mice at different ages to determine the onset of disease phenotypes, which is indeed a common feature of human mtDNA disease where patients present with clinical symptoms at a variety of different ages of onset (McFarland, Taylor et al. 2007).

More recently a transmitochondrial mouse was developed using a polymerase chain reaction (PCR) based cloning and sequencing technique to generate a respiratory chain deficient cell line carrying a m.7731G>A mutation in tRNA^{Lys}, that again was used to transfect ES cells and generate chimeric mice (Shimizu, Mito et al. 2014). Germline transmission of the mutation was achieved, producing five generations of mito-mice^{Lys7731}, with offspring demonstrating substantial variation in heteroplasmy. Heteroplasmy in offspring did not exceed 85%, which was due to lethality of oocytes carrying higher levels of the mutation (Shimizu, Mito et al. 2014). Mito-mice^{Lys7731} with high heteroplasmy demonstrated evidence of muscle phenotypes typically associated with pathogenic mutations in human mt-tRNA^{Lys} (Houshmand, Lindberg et al. 1999; Blakely, Swalwell et al. 2007), including a smaller body size and muscle weakness, as well as respiratory chain defects in the muscle and kidney (Shimizu, Mito et al. 2014). Mice did not however demonstrate evidence of ragged red fibers or renal failure (Shimizu, Mito et al. 2014), which are characteristic metabolic features of human

mtDNA disease caused by mutations in tRNA^{Lys} (MERRF) (Wallace 1999). Therefore whilst this mouse provided useful insights into the germline transmission and pathogenesis of a heteroplasmic mtDNA point mutation, it may serve as a more general model of a pathogenic mtDNA point mutation than a model of mtDNA disease and the associated clinical phenotypes.

1.6 The colon

A central focus of this thesis involves using the colon as a model replicative tissue to study the clonal expansion of mtDNA mutations and their consequences in mouse models of both ageing and disease. The structure and hierarchical arrangement of the colon is therefore examined below along with a brief account of different functions of the colon.

1.6.1 *Structure of the colon*

The colon is the terminal component of the gastrointestinal tract, beginning at the ileocecal junction at the small intestine and ending at the anus. The colon comprises four main parts: the ascending, transverse, descending and sigmoid colon, all made up of four discrete layers: the mucosa, the submucosa (a thin layer of smooth muscle), the muscularis externa (a double layer of smooth muscle and longitudinal muscle) and the submucosa.

The colonic epithelium is arranged as colonic crypts (tubular glands) that serve to create a large surface area for the absorption of water, the primary function of the colon. Columnar enterocytes, otherwise known as transporting/absorptive colonocytes and mucus-secreting goblet cells are the primary differentiated cell lineages contained within colonic crypts, along with a moderate number of hormone secreting cells known as enteroendocrine cells (Figure 1-7) (McKay 2005). The colonic epithelium is a high turnover, replicative tissue that is constantly developing. Pluripotent stem cells are located at the crypt base and as such all cell lineages within the crypts are derived from the stem cells (Figure 1-7) (Schmidt, Winton et al. 1988; Potten 1998). Indeed any genetic defect present in the stem cells will be inherited by the progeny cells and differentiated cells within the crypt and as such the genotype of the whole crypt will be equivalent to that of the stem cells. The hierarchical arrangement of the colonic crypt therefore enables the study of genetic defects in stem cell populations by studying the whole crypt. The exact number of stem cells within colonic crypts remains to be elucidated in humans due to a lack of appropriate stem cell markers; however studies in

mice suggest there are between 5 and 7 stem cells located at the base of intestinal crypts (Kozar, Morrissey et al. 2013), which is also believed to be the case for humans (Taylor, Barron et al. 2003). Differentiated cells of the crypt migrate towards the top of the crypt and are shed into the gut lumen, with the mean lifespan of an absorptive colonocyte estimated to be between 3-5 days (Karam 1999).

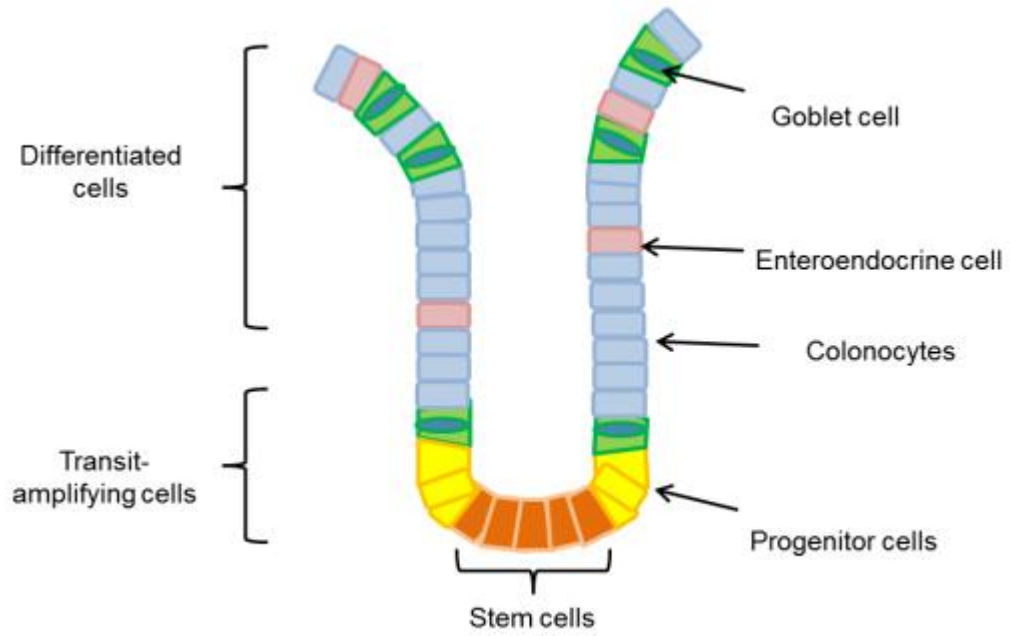


Figure 1-7: Structural arrangement of the colonic crypt.

Colonic stem cells are located at the base of colonic crypts and give rise to daughter/ progenitor cells, which move up the crypt dividing until they leave the cell cycle and become committed to one of the differentiated cell types (colonocyte/ goblet cell/ enteroendocrine cell), before being shed into the gut lumen. The colonic epithelium is therefore constantly replaced and all cells within colonic crypts can clearly be seen to be derived from the stem cells.

1.6.2 Functions of the colon

The primary function of the colon is to serve as a store of faecal material. As such the colon is involved in the absorption of water and salts from waste food material, to make faeces more solid and compact, facilitating its passage and release through the colon. This is further facilitated by the secretion of mucus by goblet cells in the colonic crypts. In addition to water absorption, certain electrolytes, vitamins and components of undigested food, such as fibre, are broken down in the colon and absorbed, which is mediated by the normal gut flora (bacteria). The colon is the largest reserve of normal micro flora in the human body, which is estimated to weigh between 1-2kg (Shanahan 2002). Hundreds of different species have been identified; of which 95% are anaerobic bacteria. Gut bacteria are responsible for the production of vitamin K, B12, riboflavin and thiamine as well as bile acid metabolism and the production of ammonia (Baron

1996). However, the principle role of the normal gut flora is the development of a mucosal barrier between the host and external pathogens. Immune homeostasis in the gut relies on a constant dialogue and interdependent relationship between the normal gut flora, colonic epithelial cells and mucosal immune cells. Normal gut flora prevents colonisation of the colon by external, harmful pathogens and plays a fundamental role in stimulating the innate and adaptive immune responses (Berg 1996). The secretion of mucins by goblet cells helps form the mucosal barrier and the primary mechanism of defence against microbes (Johansson, Phillipson et al. 2008) and normal gut flora stimulates the production of antimicrobial proteins (AMPs) by goblet cells and colonocytes (Peterson and Artis 2014), forming an essential second line of defence that directly targets bacterial structures. Colonic epithelial cells also contribute to the mucosal immune system, as they are involved in: the primary detection of pathogens through the expression of surface pattern recognition receptors; the secretion of immunoglobulin A (IgA) and the transfer of immune signals to phagocytes and antigen presenting cells (Peterson and Artis 2014). Indeed, the colon plays a significant role in the mucosal immune response, with its functions very much extending beyond the simple storage and release of faecal material.

1.7 The colon: a model stem cell tissue for studying mtDNA mutations

Given the hierarchical arrangement of colonic crypts and the fact that all cells within the crypt will have the same genotype as the stem cells in the crypt base, the colon is an ideal tissue in which to study genetic defects present within stem cells. As such many studies examining respiratory chain deficiency and the incidence and spectrum of clonally expanded somatic mtDNA point mutations in ageing stem cell populations have been performed in the human colon.

1.7.1 *Clonally expanded somatic mtDNA point mutations in the human colon*

In the ageing human colon COX deficient crypts accumulate in an exponential fashion with age, with COX deficiency rarely detected below the age of 30 and aged individuals display ~15% COX deficient colonic crypts over the age of 70 (Taylor, Barron et al. 2003). Indeed single cell analysis revealed that COX deficiency in the human colon was associated with the clonal expansion of a somatic mtDNA point mutation (Taylor, Barron et al. 2003). Over 50% of colonic crypts with respiratory chain deficiency display defects in multiple complexes of the respiratory chain, most notably complexes I, III and IV, with mtDNA mutations shown to clonally expand within these crypts (Greaves, Barron et al. 2010). Indeed, in some cases crypts displaying defects in

multiple complexes of the respiratory chain were found to contain a single clonally expanded mtDNA point mutation, demonstrating that a single mtDNA point mutation is capable of disturbing the whole respiratory chain (Greaves, Barron et al. 2010). Extensive mutational analysis of mtDNA from aged human colonic crypts has revealed that 90% of clonally expanded somatic mtDNA mutations are base transitions, of which the majority are C-T and G-A mutations, with very few C-A and G-T mutations detected (Greaves, Elson et al. 2012). As such it appears that mtDNA replication errors mediated by Poly are the dominant cause of clonally expanded somatic mtDNA mutations in the ageing colon, with very little evidence suggesting a causal role for oxidative damage, mediated by 8-oxo-deoxyguanine mutagenesis. The point at which mtDNA point mutations occur and the mtDNA mutation rate has recently been investigated in the human colonic epithelium using three different mtDNA mutation assays (Greaves 2014). Interestingly this study revealed that there was no significant increase in the number of low level mtDNA point mutations with age (detected by the random mutation capture method); however there was a significant increase (~10 fold higher) in the frequency of clonally expanded mtDNA point mutations in older individuals compared to those in the younger age groups (measured by next generation sequencing (NGS)) (Greaves 2014). Furthermore the same types of mtDNA point mutations were detected in young individuals as those previously detected in aged subjects (Greaves, Elson et al. 2012; Greaves 2014) and mutational analysis, by NGS of buccal and colonic epithelium, matched from the same individuals, revealed the presence of the same low level mtDNA point mutations in both tissues (Greaves 2014). Given that buccal and colonic epithelium are both derived from the endoderm, becoming distinct tissues at 3-4 weeks gestation (Noah, Donahue et al. 2011), this data, along with the finding that similar mutation types are present in both young and aged subjects, provides further evidence that mtDNA point mutations occur during early development/ embryogenesis (Elson, Samuels et al. 2001). Remarkably this study revealed that whilst there was no change in the rate of mtDNA mutagenesis with age there did appear to be an increase in the incidence of clonal expansions (Greaves 2014). Taken together these studies provide further evidence against the 'vicious cycle' hypothesis and strongly support the early life hypothesis, whereby age-related mitochondrial dysfunction is driven principally by mtDNA point mutations that arise during early life, most likely due to the high rates of mtDNA replication during development, and clonally expand throughout adulthood by random intracellular drift (Coller, Khrapko et al. 2001; Elson, Samuels et al. 2001).

1.7.2 *Random mtDNA mutagenesis and selective constraints*

The clonal expansion of mtDNA point mutations by random genetic drift relies on neutral evolution and the unbiased replication and amplification of a mutant mtDNA genome. It has been proposed however that mtDNA may be subject to selective constraints leading to the preferential amplification of a specific mtDNA genome, such that different mtDNA genomes within a cell may directly compete with each other or a mutant mtDNA genome may be lost or selected against if it affects cell survival. It is known that mtDNA is subject to selective constraints in the mammalian germline via the 'genetic bottleneck, affecting the transmission of certain pathogenic mtDNA mutations (see section 1.2.3). Indeed studies in mice have demonstrated strong purifying selection on mtDNA in the mammalian germline causing the elimination of severe pathogenic mtDNA point mutations. In 2008 Fan and colleagues demonstrated that a mild mutation in mt-*COI* could be successfully transmitted through the mouse female germline to multiple generations; however a severe mutation in was rapidly and selectively eliminated from the mouse female germline within four successive generations (Fan, Waymire et al. 2008). Furthermore studies examining the transmission of a random set of mtDNA point mutations in the *PolgA^{mut/mut}* mouse germline, have revealed strong purifying selection against non-synonymous mutations in protein encoding genes, with a mutational bias towards synonymous mutations and mutations occurring in mt-tRNA and mt-rRNA genes (Stewart, Freyer et al. 2008). Neutral evolution of mtDNA has also been contested by studies showing certain selection pressures on mtDNA in humans (Elson, Turnbull et al. 2004).

Extensive mutational analysis of the spectrum of age-related somatic mtDNA point mutations in the ageing colon have been performed to determine whether any selection pressures act on clonally expanded somatic mtDNA mutations with age (Greaves, Elson et al. 2012). However, it was found that such selective constraints were absent in ageing human colonic epithelial tissue, where a random spectrum of clonally expanded somatic mtDNA point mutations was shown to accumulate (Greaves, Elson et al. 2012).

Moreover somatic mtDNA point mutations were frequently non-synonymous or frameshift mutations and occurred within protein encoding genes, which were indeed shown to be significantly more pathogenic than normal population variants (Greaves, Elson et al. 2012). As such there was an absence of evidence for the selective clonal expansion of somatic mtDNA point mutations in ageing human somatic tissues. A recent study, confirmed an absence of selective constraints on somatic mtDNA point

mutations but provided evidence for purifying selection on mtDNA in the human germline (Greaves 2014). This was because no significant difference in the ratio of non-synonymous: synonymous changes was seen between young and aged individuals and 95% of mutations detected in both the buccal and colonic epithelium (originating from the same endoderm) from the same individual were non-pathogenic polymorphic variants (Greaves, Elson et al. 2012), suggesting that pathogenic mtDNA point mutations were selected against in the human germline. As such it would appear that mtDNA is subject to different selection pressures in the germline and in somatic tissues, which will undoubtedly have significant implications for the clonal expansion of mtDNA point mutations in both ageing and disease.

1.8 Aims and objectives

What can we learn about the clonal expansion of mtDNA point mutations and respiratory chain deficiency in the ageing process and mechanisms involved in disease, using mouse models?

To understand the role of mtDNA point mutations and respiratory chain deficiency in ageing and the mechanisms involved in mtDNA disease heterogeneity, it is vital to establish animal models that can be used to dissect these mechanisms. Transgenic mouse models carrying mtDNA point mutations will be used in this thesis to answer the following questions:

- Is the *PolgA*^{+/*mut*} mouse a good model of clonally expanded somatic mtDNA mutations and respiratory chain deficiency that we see in the ageing human colon?
- What are the functional consequences of age-related respiratory chain deficiency upon cellular processes in the colonic stem cell system?
- Can an in vivo mitochondrial dysfunction assay be used in the colonic epithelium as an early experimental screening tool to identify potentially pathogenic mtDNA point mutations in breeding mouse models of mtDNA disease?
- Is a C>T mutation at position m.5024 of the mouse mtDNA genome a candidate allele for modelling mitochondrial DNA disease in mice?

Chapter 2

Chapter 2. Materials and Methods

2.1 Equipment and consumables

2.1.1 Equipment

2511 Dry vacuum pump/compress	Welch
ABI 3130xl genetic analyzer	Applied Biosystems
ABI Veriti 96 well Thermal Cycler	Applied Biosystems
Agilent 2100 bioanalyzer	Agilent Technologies
Axioplan 2 Imagining 2 microscope	Zeiss
Axiovision sotware 3.1	Zeiss (imaging associates)
ChemDoc MP Imaging system	BIORAD
Electrophoresis power supply model 250EX	Life Technologies
Horizontal Agarose Gel Electrophoresis Systems	Amersham
Leica Laser-microdissection system	Leica
Nanodrop ND-1000 Spectrophotometer	Labtech International
ND-1000 Software	Labtech International
OFT 5000 Cryostat	Bright
PALM MicroBeam	Zeiss
PALMRobo software 4.6	Zeiss
PyroMark assay design software v2.0	Qiagen
Pyromark Q24 Platform	Qiagen
Pyromark Q24 Workstation	Qiagen
Pyromark's proprietary Q24 software	Qiagen
Seqscape software v 2.6	Applied Biosystems

2.1.2 Consumables

96 well semi-skirted Plate, with Raised Rim	Starlabs
24 well PCR plate, elevated wells	Starlabs
Agilent RNA 6000 picochip kit	Agilent Technologies
Coverslips (20x20mm and 22x50mm)	VWR International
Microtubes ultra clear, RNase free (1.7ml)	Axygen Scientific
Microscope colourcoat adhesion slides (76x26x1.0-1.2mm)	CellPath
Polyethylenephthalate (PEN) slides	Leica
PALM Membrane slides (1mm)	PALM microlaser technologies
Rneasy Micro kit (50)	Qiagen

2.2 Solutions and chemicals

2.2.1 Solutions

All solutions and buffers were prepared in Nanopure (18 Mega Ohms activity) water and subsequently autoclaved.

DNA Loading Buffer	0.25% (w/v) Bromophenol Blue 0.25% (w/v) Xylene Cyanol 30% (v/v) Glycerol
Electrophoresis Buffer (1l)	100ml 10x TAE 900ml Nanopure water
Formal Calcium	3.6% (v/v) Formaldehyde 1.1% (w/v) Calcium Chloride
Formaldehyde solution	100ml Formaldehyde (37-40%)

	900ml dH ₂ O
	4.0g NaH ₂ PO ₄
	6.5g Na ₂ HPO ₄
Gel Buffer (1l)	100ml 10x TAE
	900ml Nanopure water
Genotyping Lysis Buffer	2.5ml 1M Tris
	5ml 0.5M EDTA
	1.25ml 10% SDS
	41.25 ml dH ₂ O
50μl 0.5M TrisHCL pH 8.5	30.275g Trisma base in 500ml dH ₂ O
Phosphate Buffer, pH7.4	95ml 0.2M Disodium
	Hydrogen Phosphate
	405ml 0.2M Sodium
	Dihydrogen Phosphate
	500ml Water
Phosphate Buffered Saline	Prepared from tablets: 1 tablet in
	100ml dH ₂ O
Single cell Lysis Buffer (500μl)	250μl 1% Tween 20
	50μl 0.5M TrisHCL pH 8.5
	195μl dH ₂ O
	5μl proteinase K

2.2.2 Chemicals

2.2.2.1 Tissue preparation

Iso-pentane	Merck
Liquid Nitrogen	BOC
OCT cryoembedding matrix	Raymond Lamb

2.2.2.2 Histological and histochemical reagents

Acetic acid	VWR
Catalase	Sigma
Chromotrope 2R	Sigma-Aldrich
Cresyl violet acetate	Sigma
Cytochrome <i>c</i>	Sigma
3,3'Diaminobenzidine Tetrahydrochloride	Sigma
DPX™	Merck
Eosin “yellowish”	Merck
Fast Green FCF	Sigma-Aldrich
Formaldehyde (37-40%)	Sigma-Aldrich
Harris Haematoxylin	Sigma-Aldrich
Mayers Haematoxylin	TCS Biosciences Ltd
Histoclear™	National Diagnostics
Nitro Blue Tetrazolium	Sigma
Phenazine Methosulphate	Sigma
Phosphate Buffered Saline Tablets	Sigma
Phosphotungstic acid	Sigma-Aldrich

Sodium Dodecyl Sulfate (SDS)	BDH
Sodium Azide	Sigma
Sodium Succinate	Sigma
Trisma base	Sigma

2.2.2.3 *Molecular Biology Reagents*

Agarose MP	Roche
BigDye® Terminator v3.1 cycle sequencing kit	Applied Biosystems
Bromophenol Blue	Sigma
β-mercaptoethanol	Sigma
Deoxynucleotide Triphosphates	Rovalab
DEPC treated water	Ambion
Ethidium Bromide	Merck
Ethylenediaminetetraacetic acid disodium salt solution	Sigma
Exonuclease-1	Thermo Scientific
Ex Taq DNA polymerase	Takara
Exo-Sap IT	GE Healthcare
GelRed nucleic acid stain	Biotium
GO Taq Hot Start DNA Polymerase	Promega
Hyperladder IV	Bioline
Hi-Di Formamide	Life Technologies
La Taq DNA polymerase	Takara

Proteinase K	Invitrogen
PyroMark Annealing buffer	Qiagen
PyroMark Binding buffer	Qiagen
PyroMark Gold Q24 Reagents (5 x 24)	Qiagen
PyroMark Wash buffer (x10)	Qiagen
Quick-load 1kb DNA ladder	BioLabs
RNase Zap	Ambion
Sodium acetate buffer	Sigma
Streptavidin sepharose TM high performance beads (GE Healthcare)	GE Healthcare
Tris acetate EDTA (TAE x10)	Sigma
Tris HCl	Sigma
TSAP	Promega

2.3 Animals

2.3.1 Heterozygous (*PolgA*^{+/*mut*}) mice

Mitochondrial DNA mutator mice (*PolgA*^{*mut/mut*}) were generated with a knock-in missense mutation (D257A) that changes the amino acid from aspartic acid to alanine in the second endonuclease proofreading domain of the *PolgA* catalytic subunit of the mtDNA polymerase gamma (Trifunovic, Wredenberg et al. 2004). Four mice that were heterozygous for this mutation (*PolgA*^{+/*mut*}), aged 59 (n=1) and 81 (n=3) weeks old, were sacrificed and colon samples collected, provided by James Stewart and Nils-Göran Larsson, Max Planck Institute for Biology of Ageing, Cologne, Germany.

2.3.2 M.5024C>T tRNA^{Ala} mice

All mouse breeding was performed by James Stewart and Nils-Göran Larsson, Max Planck Institute for Biology of Ageing, Cologne, Germany. Female mice, heterozygous for the D257A mutation (*PolgA*^{+/*mut*}) were employed as the founders in a breeding

strategy to generate mice that would carry and transmit mtDNA point mutations. Female *PolgA*^{+/*mut*} mice were used in the breeding strategy as their moderate mtDNA mutation rate (Kraytsberg, Simon et al. 2009) produces only 1-3 mutations per mtDNA molecule, compared to 16-20 mtDNA mutations produced per molecule by *PolgA*^{mut/*mut*} mothers (Freyer, Cree et al. 2012). A lower number of mutations per mtDNA molecule make it easier to associate certain phenotypes with specific mutations, and mtDNA mutations of interest can be segregated much more rapidly into specific lineages. Female *PolgA*^{+/*mut*} mice were backcross mated with pure wild-type (WT) male mice, to produce female progeny that expressed wild-type mtDNA polymerase, but transmitted mutated mtDNA (*PolgA*^{+/*+*} mice) (Figure 2-1). A standard sequencing approach was used on mouse lineages to detect and identify candidate mtDNA point mutations for modelling disease. Female progeny harbouring an mtDNA mutation of interest were subsequently used to propagate the mouse lineages.

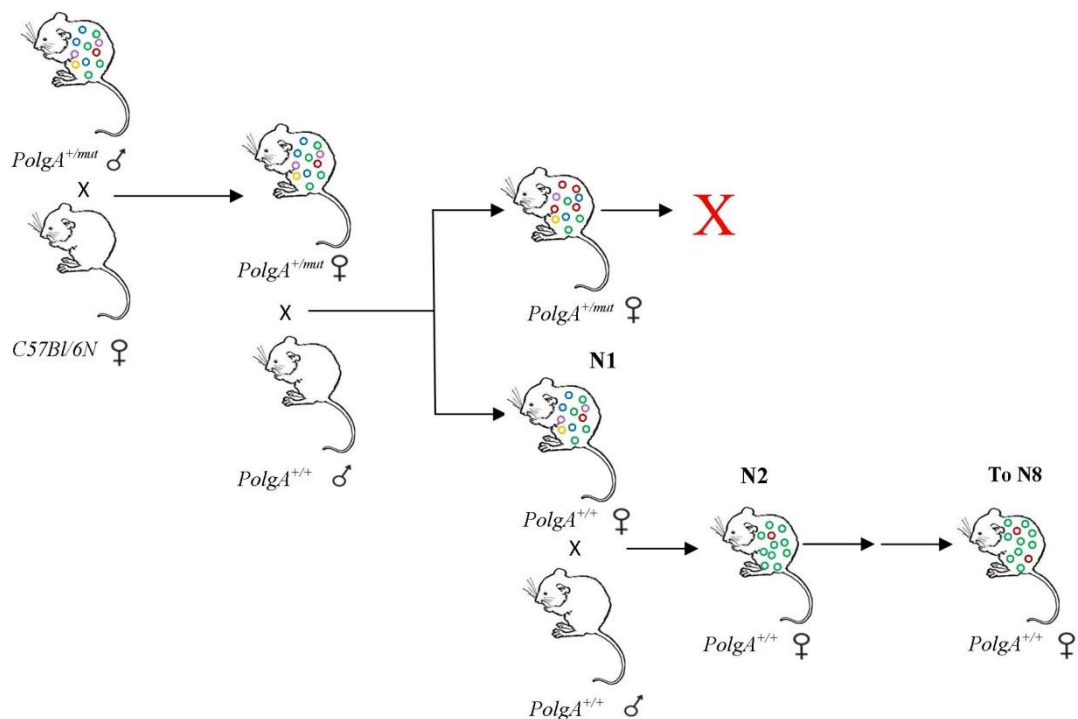


Figure 2-1: Germline mtDNA mutagenesis and breeding strategy using *PolgA*^{+/*mut*} female mice to segregate specific mtDNA mutations into mouse lineages.

MtDNA mutagenesis was initiated by mating C56Bl/6N female mice with *PolgA*^{+/*mut*} males to generate *PolgA*^{+/*mut*} females. Resulting *PolgA*^{+/*mut*} females were backcross mated with C57Bl/6N male mice, to produce female progeny that expressed wild-type mtDNA polymerase, but transmitted mutated mtDNA (*PolgA*^{+/*+*} mice). Female progeny were subsequently mated with WT (*PolgA*^{+/*+*}) male mice to propagate the mouse lineages and segregate specific mutations into specific mouse lineages.

Sequencing revealed a C>T mutation at position m.5024 of the mouse mtDNA genome, which was identified as a candidate allele for potentially modelling mitochondrial DNA disease in mice and was segregated into an independent mouse lineage using the above

strategy, until strong transmission of the allele was achieved (>6th generation) (see chapter 5 for further details). Standard tail biopsies were taken from mice at weaning (3 weeks old) to measure the m.5024C>T mutation load in each animal, using fluorescent restriction fragment length polymorphism (RFLP), completed by James Stewart, Max Planck Institute for Biology of Ageing, Cologne, Germany. This mouse lineage is currently producing the 14th backcross generation.

Colon samples were collected from 33 mutant mice across different generations (N1-N9) aged 10-83 weeks olds, displaying varied m.5024C>T mutation loads (see appendix A for details of mice used) and muscle and heart samples were provided for 11 of these animals. Colon, muscle and heart samples were also collected from 6 control animals with low levels of the m.5024C>T mutation, 4 WT control mice with no detectable levels of the m.5024C>T mutation and a colon sample from 1 negative control (TN139) with 16 known polymorphic variants in mtDNA (see appendix A for details of mice used). All tissue samples were provided by James Stewart and Nils-Göran Larsson, Max Planck Institute for Biology of Ageing, Cologne, Germany.

2.3.3 Breeding of homozygous (*PolgA^{mut/mut}*) and heterozygous (*PolgA^{+mut}*) mice
PolgA^{mut/mut} male mice (n=4) were originally obtained from a well-established colony kindly donated by Tomas Prolla, Departments of Genetics and Medical Genetics, University of Wisconsin, Madison, USA. *PolgA^{mut/mut}* male mice were mated with C57Bl/6J female pure, clean wild-type mice (Charles River Laboratories). Resulting *PolgA^{+mut}* female and *PolgA^{+mut}* male mice were mated to propagate our own colony of *PolgA^{mut/mut}* and *PolgA^{+mut}* mice (Figure 2-2). All mice were maintained in an ageing mouse unit at Newcastle University, UK, where they were kept in individually ventilated cages with unrestricted access RM3 expanded chow made by special diet services. Mice were kept at a constant temperature of 25°C and a 12 hour light/dark cycle was provided. Colon samples were collected from female *PolgA^{mut/mut}* and *PolgA^{+mut}* at 3 (n=5), 6 (n=5), 9 (n=≥5) and 12 (n=≥5) months of age (see appendix A for details of mice used).

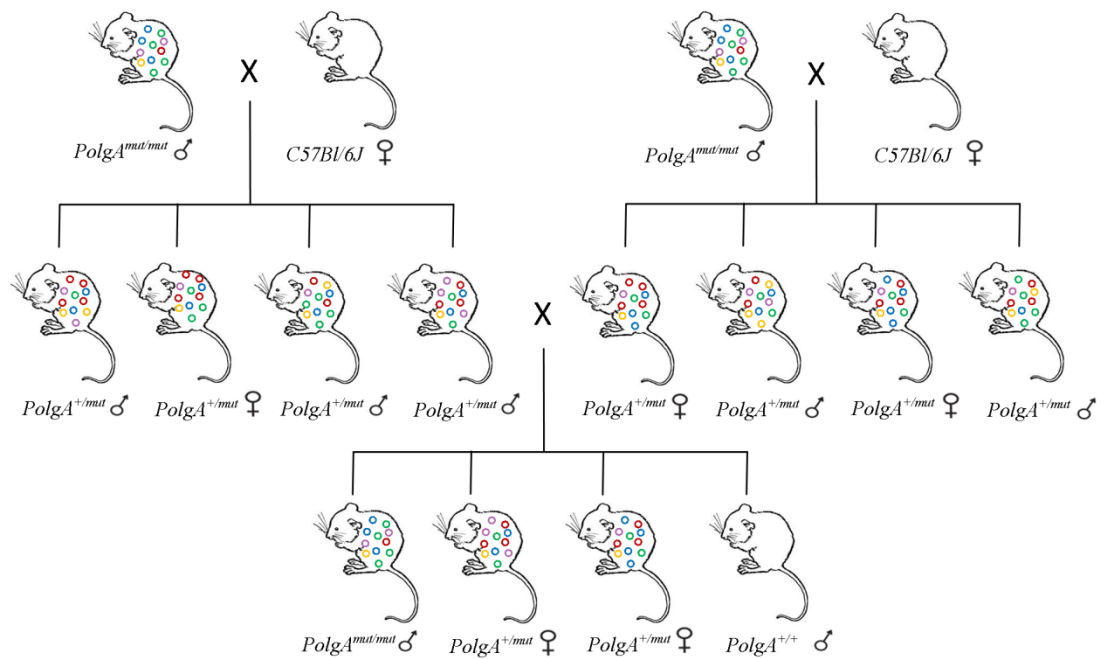


Figure 2-2: Breeding strategy to establish an ageing colony of *PolgA^{mut/mut}*, *PolgA^{+/mut}* and *PolgA^{+/+}* mice.

PolgA^{mut/mut} male mice were mated with C57Bl/6J female WT mice. Resulting *PolgA^{+/mut}* female and *PolgA^{+/mut}* male mice were mated to propagate our own colony of *PolgA^{mut/mut}*, *PolgA^{+/mut}* and *PolgA^{+/+}* (WT) mice.

2.4 Tissue preparation

PolgA^{mut/mut}, *PolgA^{+/mut}* and WT control mice were killed by cervical dislocation. Mouse colons were removed immediately and flushed with phosphate buffered saline (PBS), pH7.4, to remove any faeces and pellets.

2.4.1 Frozen Tissue

Colon tissue was mounted on Whatman filter paper and rapidly frozen in isopentane previously cooled to -160°C in liquid nitrogen for 15 seconds. Tissue was transferred to liquid nitrogen and stored at -80°C . For sectioning, colon tissue was mounted upright, longitudinally on Whatman filter paper using a small amount of OCT™ medium, previously cooled in an OFT 5000 Cryostat (Bright) at -30°C for 15 minutes, using forceps and a scalpel previously cooled in liquid nitrogen at -160°C . For histological staining procedures sections were cut at $10\mu\text{m}$ using the OFT 5000 Cryostat (Bright) on to glass colourcoat adhesion slides (CellPath) and air-dried at room temperature for one hour. For laser micro-dissection used for DNA extraction, frozen colon tissue was cut at $15\mu\text{m}$ on to polyethylenephthalate (PEN) slides (Leica Microsystems) and air-dried at room temperature for one hour. Slides were stored in sealed slide mailers at -80°C until use.

2.4.1.1 *Frozen tissue used for RNA extraction*

Colon samples were collected from 12 month *PolgA^{+/-mut}* mice from our own breeding colony (n=5), frozen in liquid nitrogen and were mounted in OCT medium as described above. Using the cryostat serial longitudinal colon sections (10µm) were cut on to PEN slides previously exposed to UV light for 30 minutes to remove any RNAses. Tissue sections cut on to PEN slides were immediately placed on dry ice and stored at -80°C until LCM was completed. At 20µm intervals, 10µm sections were cut on to glass slides and air-dried for 1 hour.

2.5 **Histological and Histochemical staining procedures**

2.5.1 *Haematoxylin and Eosin staining procedure*

Colon tissue sections (10µm) were air dried for 15 minutes following cutting and fixed in formal calcium solution (3.6% (v/v) Formaldehyde, 1.1% (w/v) Calcium Chloride) for 15 minutes. Sections were washed in running tap water for one minute and submerged in Mayer's haematoxylin (TCS biosciences Ltd) for 10 minutes. Sections were subsequently washed in running tap water and then submerged in eosin solution (1% (w/v) Eosin 'yellowish', 0.4% (w/v) Erythrosin B, 0.2% (w/v) Phloxin B) for 30 seconds. Sections were washed in running tap water and dehydrated through a graded ethanol series (70%, 95% and 2x 100%) and two concentrations of HistoClear™ (National Diagnostics, Atlanta, USA) and mounted in DPX using a glass coverslip.

2.5.2 *Dual cytochrome c oxidase (COX)/ succinate dehydrogenase (SDH) histochemistry*

Colon (10µm), heart (8µm) and muscle (10µm) tissue sections were cut using the cryostat on to glass slides and dried at room temperature for one hour. COX medium was prepared by adding 200µl of cytochrome *c* stock solution (500µM cytochrome *c* in 0.2M phosphate buffer, pH 7.0) to 800µl of 3,3'-diaminobenzidine tetrahydrochloride (DAB) stock solution (5mM DAB in 0.2M phosphate buffer, pH 7.0) with 20µg.ml⁻¹ catalase. 50µl of COX solution was applied to each tissue section and incubated at 37°C. Sections were washed in phosphate buffered saline (PBS) (3 x 5 minutes). SDH medium was prepared by adding 800µl NitroBlue tetrazolium (NBT) stock solution (1.5mM NBT in 0.2M phosphate buffer pH 7.0) to 100µl sodium succinate stock solution (1.3M sodium succinate in 0.2M phosphate buffer pH 7.0), 100µl phenazine methosulphate (PMS) stock solution (2mM PMS in 0.2M phosphate buffer pH 7.0) and 10µl sodium azide stock solution (100mM sodium azide in 0.2M phosphate buffer pH

7.0). 50µl of SDH medium was applied to tissue sections and incubated at 37°C. Tissue sections were washed in PBS (3 x 5 minutes) and dehydrated through graded ethanol (70%, 95% and 2x 100%) and two concentrations of HistoClear™ (National Diagnostics, Atlanta, USA) and mounted in DPX. Incubation times for the COX and SDH medium on the different mouse tissue types are detailed in the table below.

Tissue	COX medium	SDH medium
Colon	25 minutes	35 minutes
Heart	40 minutes	10 minutes
Skeletal muscle	35 minutes	30 minutes

The percentage of COX deficient colonic crypts and skeletal muscle fibers were identified in transverse and longitudinal tissue sections at multiple different levels and approximately 500 cells were examined per sample using Axiovision software 3.1 on an AxioPlan 2 Imaging 2 microscope (Zeiss). Given the small size and overlapping nature of colonic smooth muscle fibers and heart muscle fibers a colour detection algorithm was designed and constructed within MATLAB (version 8.0 MathWorks, Massachusetts, United States) to accurately detect and quantify the percentage of COX deficiency present within the tissue sections, courtesy of Craig Stamp. The Hue Saturation Value (HSV) colour space model was employed for automated detection of COX deficient (blue) fibers and COX positive (brown) fibers. Given that individual samples displayed slight variability in the intensity of blue and brown staining, variable colour space Hue tolerances of 0.025, 0.05 and 0.10 were employed for each image, and I subjectively chose the appropriate tolerance to ensure that all colour variations in COX deficiency and COX activity were correctly identified and quantified. A minimum of 15 images across various sections were analysed for each tissue type using the HSV colour space model and an average percentage of COX deficiency calculated for each tissue.

For laser micro-dissection colon tissue sections (15µm) mounted on PEN slides (Leica Microsystems) were exposed to dual colour histochemistry, as described above, and sections were air-dried for 90 minutes after dehydration through graded ethanol.

2.5.3 Cresol violet acetate alcoholic staining procedure

Slides were removed from the -80°C freezer and were placed directly on to dry ice. Without allowing the tissue sections to defrost slides were fixed directly with ice cold 75% EtOH for 3 minutes to reduce RNAses activity by dehydration. Sections were incubated in a solution of 1% cresol violet acetate (w/v) made in 50% EtOH for 1 minute, followed by rinsing in ice cold 75% EtOH and 95% EtOH for 30 seconds each. Finally sections were dehydrated in 100% EtOH for 1 minute, air dried for 5-10 minutes and used immediately for laser capture micro-dissection. All solutions were made with DEPC treated water and fresh solutions were used for each staining procedure. Fixing and staining using alcoholic solutions dehydrates the tissue sections and prevents RNAses activity, preserving RNA integrity for up to 90 minutes for micro-dissection (Clément-Ziza, Munnich et al. 2008).

2.6 Molecular Biology Techniques

2.6.1 Isolation of total DNA from mouse tissue

2.6.1.1 Mouse ear notches

For genotyping of *PolgA*^{mut/mut}, *PolgA*^{+/mut} and *PolgA*^{wt} mice, pups were weaned at 3 weeks old and ear-notches were taken. Ear-notches were lysed overnight at 55°C in 48.7µl lyses buffer (1m Tris, 0.5m EDTA, 10% SDS and dH₂O) and 1.3µl proteinase K.

2.6.1.2 Homogenate tissue

Frozen colon, heart and skeletal muscle tissue was mounted as above and 20µm tissue sections were cut using the OFT 5000 Cryostat (Bright) into sterile 1.5ml eppendorf tubes (Bio gene). Samples were centrifuged at 14 000rpm for 15 minutes and DNA was extracted using the DNeasy Blood and Tissue kit (Qiegen) according to the manufacturer's protocol.

2.6.1.3 Laser micro-dissected colonic crypts and colon smooth muscle fibers

Single COX positive and COX deficient colonic crypts were cut using Zeiss PALM micro-dissection system into sterile 0.5ml PCR tubes into 15µl of cell lysis buffer (50mM Tris-HCl pH8.5, 1% Tween-20, 20mg/ml proteinase K and dH₂O). Given the small size of the fibers, ≥25 colonic smooth muscle fibers were collected into lysis buffer per individual tube, to give enough DNA for pyrosequencing. Samples were centrifuged at 14 000rpm for 15 minutes and lysed at 55°C for 2 hours and then 95°C for 10 minutes to denature the proteinase K.

2.6.2 Isolation of total RNA from colonic crypts

Dual colour COX/SDH histochemistry was performed on 10µm colon sections on glass slides cut at 20µm intervals, as described above. This enabled identification of COX deficient and COX positive crypts during laser micro-dissection on colon sections (10µM) mounted on PEN slides that had been exposed to the cresyl violet acetate alcoholic staining procedure. A total of 250 COX positive and 250 COX deficient colonic crypts were cut for each 12 month old *PolgA^{+mut}* mouse using the Zeiss PALM micro-dissection system into sterile 0.5ml PCR tubes containing 65µl buffer RLT (Qiagen RNeasy Micro Kit) with β-mercaptoethanol (Sigma-Aldrich). Colonic crypts were lifted using a cut energy of 48, focus of 75 and LPC energy of 63, focus of 71. RNA integrity is only preserved for up to 90 minutes during micro-dissection following the cresyl violet acetate alcoholic staining procedure (Clément-Ziza, Munnich et al. 2008) and so the above method was repeated until a total of 250 COX positive and 250 COX deficient crypts were collected from each mouse. Samples were vortexed upside down for 30 seconds and centrifuged at 14 000rpm for 5 minutes and stored at -80°C. Lysates were subsequently pooled together to give samples of 250 COX positive and 250 COX deficient colonic crypts for each 12-month-old animal. The sample volume was adjusted to 350µl with buffer RLT containing β-mercaptoethanol, vortexed for 30 seconds and centrifuged at 14 000rpm for 1 minute. Samples were then incubated at room temperature for 30 minutes to ensure thorough lysis and a good RNA yield. RNA was extracted using the RNeasy Micro Kit (Qiagen) according to the manufacturer's protocol, including on-column DNase digestion.

2.6.3 Polymerase Chain Reaction (PCR) for *PolgA^{mut/mut}* genotyping

The DNA lysate from mouse ear notches was taken to a 1:10 dilution and PCR reactions were implemented in 25µl volumes using a mastermix comprising 1x LA PCR buffer (Mg²⁺) (Takara Bio Inc), 0.25mM dNTPs, 10.0µM primers, 5 U LA Taq DNA Polymerase (Takara Bio Inc) and 2µl of tissue lysate (1:10 dilution). See Appendix B for primer positions and sequences.

The PCR programme was as follows:

Cycles	Process	Temperature	Time
1	Initial Denaturation	94°C	1 minute
35	Denaturation	94°C	20 seconds
	Primer annealing	64°C	20 seconds
	Extension	68°C	45 seconds
1	Final Extension	72°C	5 minutes

The size of the PCR products was used to determine the correct genotype of the mice (Figure 2-3).

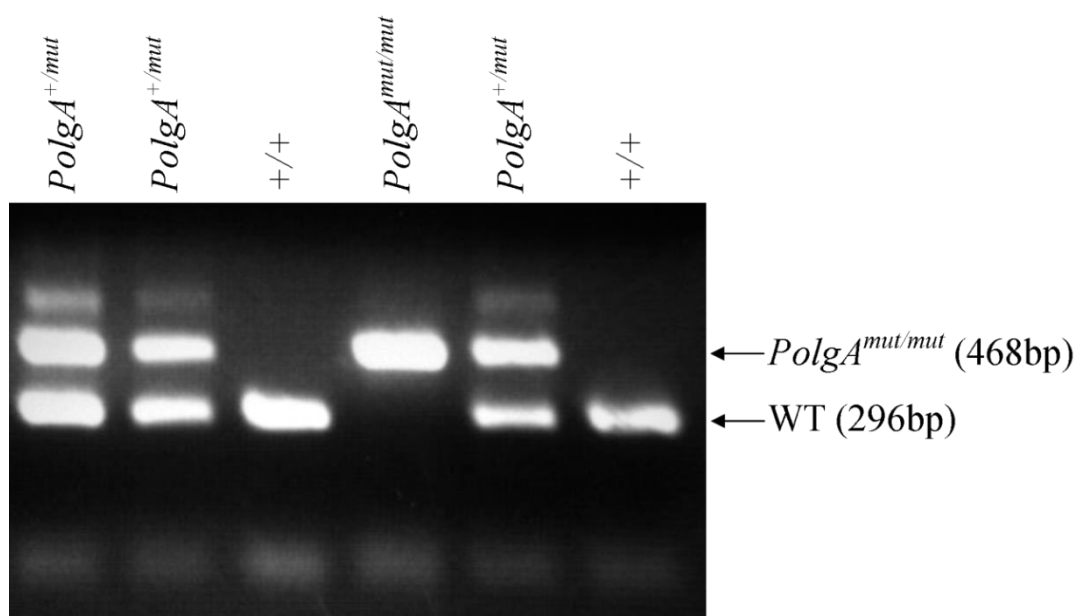


Figure 2-3: Example gel electrophoresis image gel following Polg PCR for genotyping.

Gel electrophoresis image showing the different sized DNA products produced in the presence or absence of the D257A mutation. Mice homozygous for the D257A mutation ($PolgA^{mut/mut}$) produce a 468bp DNA product, WT ($PolgA^{+/+}$) mice produce a 296bp DNA product and mice heterozygous for the D257A mutation ($PolgA^{+/mut}$) produce both the 468bp and 296bp fragments.

2.6.4 PCR amplification of the entire mitochondrial genome

The single cell lysate (see above) was employed as the DNA template to establish the complete mtDNA sequence from the single micro-dissected colonic crypts. The mitochondrial genome was amplified in a single PCR reaction using 30 pairs of forward and reverse primers to generate overlapping fragments of 1-1.2kb covering the entire mouse mtDNA genome (see appendix B for primer positions and sequences). The primer pairs were tagged with M13 sequence (Forward - 5'-tgtaaacgacggccagt-3',

Reverse - 5'-caggaacagctatgacc) to enable sequencing of the PCR products with a universal M13 primer, designed to anneal at 58°C. The DNA lysate was taken to a 1:10 dilution and PCR reactions were implemented in 37.5µl volumes using a mastermix comprising 1x LA PCR buffer (Mg²⁺) (Takara Bio Inc), 0.2mM dNTPs, 0.9µM primers, 5 U LA Taq DNA Polymerase (Takara Bio Inc) and 3.75µl of single cell lysate (1:10 dilution). The PCR programme was as follows:

Cycles	Process	Temperature	Time
1	Initial Denaturation	94°C	1 minute
35	Denaturation	94°C	20 seconds
	Primer annealing	58°C	20 seconds
	Extension	72°C	2 minutes
1	Final Extension	72°C	2 minutes

2.6.5 PCR amplification of the m.5024 region of the mouse mtDNA genome for sequencing

The cell lysate (see above) was used as the DNA template to establish the mtDNA genome sequence spanning ~1.3 kb around the m.5024 region from the single micro-dissected crypts and colon smooth muscle fibers using a two-stage PCR amplification protocol. The primary PCR reaction involved amplification of the mitochondrial genome with forward and reverse primers to generate a ~4.5kb fragment spanning the m.5024 region of the mouse mtDNA genome. PCR reactions were performed in 37.5µl volumes using a mastermix comprising 1x LA PCR buffer (Mg²⁺) (Takara Bio Inc), 0.2mM dNTPs, 0.6µM primers, 5 U LA Taq DNA Polymerase (Takara Bio Inc) and 3µl single cell lysate. PCR reaction conditions were as follows:

Cycles	Process	Temperature	Time
1	Initial Denaturation	94°C	1 minute
35	Denaturation	94°C	20 seconds
	Primer annealing	58°C	20 seconds
	Extension	72°C	8 minutes
1	Final Extension	72°C	2 minutes

The secondary PCR reaction used the DNA product from the first round PCR reaction as a template to amplify a ~1.3kb region encompassing the m.5024 region of the mouse mtDNA genome (see appendix B for primer positions and sequences). The PCR reactions employed 1µl of the primary PCR product as the DNA template with 24µl of mastermix using the same mastermix components as described above. The PCR reaction conditions were as follows:

Cycles	Process	Temperature	Time
1	Initial Denaturation	94°C	1 minute
35	Denaturation	94°C	20 seconds
	Primer annealing	58°C	20 seconds
	Extension	72°C	2 minutes
1	Final Extension	72°C	2 minutes

2.6.6 PCR amplification of the m.5024 region of the mouse mtDNA genome for pyrosequencing

The single cell lysate (see above) was used as the DNA template to establish the m.5024C>T mutation load from the single micro-dissected colonic crypts and colon smooth muscle fibers from mice harboring the m.5024C>T tRNA^{Ala} mutation. PyroMark assay design software v2.0 (Qiagen, Hilden, Germany) was used to design the trio of pyrosequencing (PSQ) primers in the reverse direction, comprising a forward biotinylated primer, reverse primer (see appendix B for primer positions and sequences) and pyrosequencing primer. A single PCR reaction was employed to amplify a 178bp PCR fragment spanning the m.5024 mutation site, using the forward biotinylated and reverse primers. The PCR reaction was implemented in 25µl volumes using a mastermix consisting of 5µl, 5 x reaction buffer (promega, UK), 3µl MgCl₂, 0.2mM dNTPs, 1.25ng primers (100µM), 5U Go Taq DNA polymerase (promega, UK) and 1µl DNA lysate for colonic crypts and 3µl for colonic smooth muscle fibers. The PCR programme was as follows, using 35 cycles for colonic crypts and 40 cycles for colonic smooth muscle fibers:

Cycles	Process	Temperature	Time
1	Initial Denaturation	95°C	10 minute
35/40	Denaturation	95°C	30 seconds
	Primer annealing	62°C	30 seconds
	Extension	72°C	30 seconds
1	Final Extension	72°C	10 minutes

2.6.7 Long-range PCR of single colonic crypts

The single crypt lysate (see above) was used as the DNA template for long-range PCR to establish whether large-scale circular mtDNA deletions were present in individual colonic crypts. This was completed using a two-stage PCR amplification protocol, performed by Dr Laura Greaves, Mitochondrial Research Group, Newcastle University. The initial PCR was performed using primers L272 and H16 283 to create a ~16kb product (see appendix B for primer positions and sequences). The PCR reaction was implemented in 25µl volumes using a mastermix comprising 1X LA PCR buffer (Mg²⁺) (Takara Bio Inc.), 0.2mM dNTPs, 10mM primers, 5 U LA Taq DNA Polymerase (Takara Bio Inc) and 2µl single cell lysate. The PCR cycle conditions were as follows:

Cycles	Process	Temperature	Time
1	Initial Denaturation	94°C	10 minute
30	Denaturation	94°C	20 seconds
	Primer annealing	68°C	16 minutes
1	Final Extension	72°C	5 minutes

The secondary PCR reaction used 2µl of the first round product as the DNA template to give an expected product size of ~14.5kb, using primers L1275 and H15833 (see appendix B for primer positions and sequences). The secondary PCR reaction employed the same mastermix constituents as above with the same PCR cycle conditions, but for 20 cycles instead of 30.

2.6.8 Agarose Gel electrophoresis

5µl of each PCR product was mixed with 1µl of loading dye (0.25% (w/v) bromophenol blue, 0.25% (w/v) xylene cyanol, 30% (v/v) glycerol) and then loaded on to a 1.0%

(W/V) agarose gel for mtDNA PCR sequencing and pyrosequencing products, 1.5% (W/V) agarose gel for genotyping PCR products and a 0.8% (W/V) agarose gel for long range PCR products. Gels contained GelRed for DNA visualisation and were loaded with either Quick-load 1kb DNA ladder (BioLabs) or 100bp Hyperladder IV (Bioline) depending on the size of the PCR product generated. Gels were electrophoresed at 75 volts for 45 minutes in 1x TAE (0.8mM Tris acetate, 0.02mM EDTA, 0.4µg/ml Ethidium Bromide) and the PCR products were visualised on an AlphaImager 2200 and a digital image of the gel obtained.

2.6.9 PCR clean up, cycle sequencing and DNA precipitation for mtDNA sequencing

PCR products were taken to a 1:2 dilution and purified using TSAP (Promega). Purification of DNA to remove excess primers was achieved by adding 1.5µl of TSAP, previously combined with 50µl Exonuclease 1 (Thermo Scientific), to 5µl of diluted DNA product, which was subsequently heated at 37°C for 15 minutes, followed by 80°C for 15 minutes. PCR products were then cycle sequenced using BigDye v3.1 terminator cycle sequencing chemistries (Applied Biosystems) and M13 universal primer for sequencing of the entire mitochondrial genome. To enable direct sequencing of the m.5024 region of the mouse mtDNA genome specific sequencing primers were employed during the cycle sequencing stage: forward 5'-cactcatagcaataatagctc-3' and reverse 5'-caggaacagctatgaccacagtttcgtaggttaattcctgcc3-', that are designed to anneal at 58°C.

The PCR programme was as follows:

Cycles	Process	Temperature	Time
1	Initial Denaturation	96°C	1 minute
25	Denaturation	9°C	10 seconds
	Primer annealing	50°C	5 seconds
	Extension	60°C	4 minutes

The DNA was precipitated by adding 2µl 125mM EDTA, 2µl 3M sodium acetate and 70µl 100% EtOH, before sealing the samples, inverting and leaving at room temperature for 15 minutes. Samples were then spun down at 2000g for 30 minutes and inverted to leave the remaining pellet. The pellet was washed in 70% (v/v) EtOH, spun

at 1650g for 15 minutes and inverted, prior to being air-dried in the dark for a minimum of 20 minutes. 10µl of HiDi® Formamide (Applied Biosystems) was added to each DNA pellet; samples were then denatured at 95°C for 2 minutes and were sequenced on an ABI3130xl Genetic Analyser (Applied Biosystems). The mtDNA sequence for each cell was aligned to the C57Bl/6J mouse reference sequence (GenBank Accession number NC_005089) and additionally to the consensus DNA sequence from homogenate colon tissue for each mouse for single *PolgA*^{+/mut} colonic crypts using SeqScape software (Applied Biosystems) to determine the somatic mtDNA point mutations present in the colonic crypts. This was repeated and DNA products resequenced to confirm the somatic mtDNA mutations detected. Heteroplasmy levels were estimated based upon the relative peak height of electropherograms.

2.6.10 *M.5024C>T* mutation quantification using pyrosequencing

PCR products (20µl) were combined with dH₂O, PyroMark binding buffer (Qiagen) and Streptavidin sepharose™ high performance beads (GE Healthcare) to give an 80µl volume and samples were agitated for 10 minutes, to assist DNA binding to the beads. Samples were transferred to the Pyromark Q24 workstation (Qiagen), where a hedgehog (Qiagen) attached to a 2511 Dry vacuum pump/compress (Welch) was used to pass samples through a series of reservoirs containing: 70% EtOH (5 seconds), denaturation solution (0.2M NaOH, 5 seconds) and 1 x PyroMark wash buffer (x10, Qiagen) (10 seconds). Beads were released by immersing the hedgehog probes into 25µl aliquots of PyroMark annealing buffer (Qiagen) containing the m.5024C>T pyrosequencing primer (5'tgtaggatgaagtcttaca3', m.5001-5020) in a shallow 24 well pyrosequencing plate. Samples were heated at 80°C for 2 minutes to denature the DNA and the plate was transferred to the Pyromark Q24 machine (Qiagen), where it was left to cool at room temperature for a minimum of 5 minutes to ensure annealing of the pyrosequencing primer to the DNA amplicon strand. PyroMark Gold Q24 Reagents (5 x 24, Qiagen), were used to load the PyroMark Q25 Cartridge (Qiagen) with the appropriate volumes of enzyme mix (DNA polymerase, ATP sulfurylase, luciferase and apyrase), substrate mix (adenosine 5' phosphosulfate and luciferin) and dNTPs. Pyrosequencing was completed on the Pyromark Q24 platform (Qiagen) using the specific m.5024C>T assay and each run employed a WT mouse DNA sample as a control, with no detectable or low level m.5024C>T heteroplasmy (≤4%) and a cloned fragment with high heteroplasmy (m.5024C>T >98%). The m.5024C>T mutation load was quantified using the allele quantification application of Pyromark's proprietary Q24 software

(Qiagen) and statistical analysis employed Prism v.5 software. All samples were performed in triplicate and an average mutation load calculated.

2.6.11 RNA quantification and quality control

The RNA concentration, quality of total RNA and the RIN algorithm for micro-dissected COX positive and COX deficient colonic crypt samples was assessed using an Agilent 2100 bioanalyzer, using a 1:2 dilution of the lysate (Agilent RNA 6000 PicoChip). A RIN score of ≥ 7 was classified as good quality RNA and a total mass of 10ng RNA (1ng/ μ l RNA) was optimum for gene expression analysis by RNA sequencing. RNA lysates were stored at -80°C before shipment to BGI Tech Solutions (Honkong) CO., Limited for RNA sequencing. cDNA libraries were prepared from $>10\text{ng}$ of total RNA using the SMARTer Library construction and sequencing (11 Gb per sample) method. Illumina HiSeq 2000 sequencers were used for sequencing of RNA and generation of paired-end libraries, with two technical replicates generated for each sample (BGI Tech Solutions).

2.7 Bioinformatic analysis

2.7.1 RNA sequencing data

All bioinformatic analysis of RNA sequencing data was performed by Dr Graham Smith, Bioinformatics support unit, Newcastle University. This was successfully completed for 6 biological samples (a COX deficient and COX positive sample from 3 *PolgA*^{+/*mut*} animals), with RNA sequencing data from the other two animals still remaining to be produced at the time this thesis was completed.

Quality control analysis of paired-end reads was performed using FastQC software (<http://www.bioinformatics.bbsrc.ac.uk/projects/fastqc>) to check that samples were of adequate quality and there was an absence of any bias that could have been caused by RNA degradation. Paired-end reads were subsequently aligned to the mouse genome *Mus_musculus.GRCm38.75.dna.toplevel.fa* and gene set annotation *Mus_musculus.GRCm38.75.gtf* (<http://www.ensembl.org/info/data/ftp/index.html>) using STAR (Dobin, Davis et al. 2013). The technical replicates for each sample were summed and the number of reads that mapped to the mouse genome (*Mus_musculus.GRCm38.75.gtf*) was determined using Ht-seq count, a component of HTSeq (Anders, Pyl et al. 2014) to quantify the level of expression for each gene in each sample. To examine gene expression levels a criterion was used, such that at least

20 reads were required to map to a gene in at least two out of the six biological samples, for a gene to be used in downstream pathway analysis. Differential gene expression between COX positive and COX deficient colonic crypt samples was assessed using the DESeq2 Bioconductor package version 1.2 and the Wald test (Love, Huber et al. 2014) with a Benjamini-Hochberg (BH) adjusted p value of <0.05 . Differential gene expression was further filtered on the basis of a measurable log₂ fold change of <-1 or >1 . Differentially expressed (DE) genes were mapped to biological pathways using KEGG pathways (Kanehisa and Goto 2000; Kanehisa, Goto et al. 2006) and Reactome (Joshi-Tope, Gillespie et al. 2005; Croft, Mundo et al. 2014). The over-representation of DE genes was evaluated in KEGG using KEGG.db and GOstats Bioconductor packages (Falcon and Gentleman 2007) and for Reactome using the reactome.db and reactomePA Bioconductor package Yu G. *ReactomePA: Reactome Pathway Analysis*. R package version 1.8.1). Mapping of DE genes to biological pathways was filtered further through the use of an absolute expression criterion for pathway completeness, such that $>50\%$ of genes had to be expressed basally in a pathway mapped to KEGG and Reactome. Annotation of gene function was performed using Uniprot, GO Terms and Pubmed for all significantly DE genes mapped to both KEGG and Reactome.

Gene Set Enrichment Analysis (GSEA) (Subramanian, Tamayo et al. 2005) was also performed using KEGG and Reactome to identify those pathways that demonstrated a general up or down regulation in gene expression of several genes, which individually may not have reached significance but in combination could potentially cause a general up or down regulation in activity of a given biological pathway. GSEA analysis of gene expression was measured by calculating the average log₂ fold-change of all genes that were differentially expressed, with a false discovery rate (FDR) q value of 0.05. An absolute criterion for GSEA pathway analysis was employed such that a pathway had to contain a minimum of 15 genes and a maximum of 750 genes and 50% of genes had to be basally expressed for pathway completeness.

2.8 In silico modelling

In silico modelling was used to determine how the incidence of mtDNA mutations observed in *PolgA*^{+/*mut*} mouse colonic crypt stem cells was influenced by the mtDNA mutation rate. The model was designed and developed using MATLAB (version 8.0 MathWorks, Massachusetts, United States) by Craig Stamp, Mitochondrial Research Group, Newcastle University. The replication and segregation of both mutant and wild-type mtDNA molecules to daughter cells during stem cell division was based upon

certain assumptions documented within the literature (Coller, Khrapko et al. 2001; Elson, Samuels et al. 2001; Taylor, Barron et al. 2003). The model assumes that each stem cell contains a constant number of 200 mtDNA molecules (Coller, Khrapko et al. 2001) and that COX deficiency occurs when more than 75% of mtDNA molecules are mutant. During each stem cell division there is a given probability that a mutated mtDNA molecule will be replicated (equivalent to the mtDNA mutation rate) and will be retained by the stem cell pool during asymmetric division. If a mutant mtDNA molecule is retained in the stem cell pool, it can clonally expand to become the dominant species within a stem cell and give rise to COX deficiency. To determine the mechanism by which mtDNA mutations clonally expand within *PolgA*^{+/*mut*} mouse colonic crypts a parameter scan of the mtDNA mutation rate required to match the experimental calculations of COX deficiency observed in an ageing series of WT (Greaves, Barron et al. 2011), *PolgA*^{+/*mut*} and *PolgA*^{*mut*/*mut*} mice, was completed. A total of 1000 stem cells undergoing 1080 cell divisions, during the life course of a mouse (36 months), were simulated for each mtDNA mutation rate and an average was taken to determine the mtDNA mutation rate and the mechanism for mtDNA point mutation accumulation in ageing *PolgA*^{+/*mut*} mouse colonic crypts.

Chapter 3

Chapter 3. Results: Age-related clonally expanded somatic mtDNA mutations are similar in the colon of *PolgA*^{+/*mut*} mice and humans

3.1 Introduction

3.1.1 *Somatic mtDNA point mutations in ageing mitotic tissues*

The identification that clonally expanded mtDNA point mutations result in focal respiratory chain deficiency in a number of ageing human replicative tissues (Taylor, Barron et al. 2003; McDonald, Greaves et al. 2008; Fellous, Islam et al. 2009; Gutierrez-Gonzalez, Deheragoda et al. 2009), has suggested that mtDNA point mutations could play a role in tissue dysfunction the ageing process. In the ageing human colon, respiratory chain deficiency has been associated with a mild phenotype characterised by a decrease in cell proliferation and a mild decrease in crypt cell number (Nooteboom, Johnson et al. 2010). However, this is the only study to examine the functional consequences of age-related somatic mtDNA point mutations in a human mitotic tissue, with evidence for a causal role of somatic mtDNA point mutations in human stem cell ageing still lacking.

Performing functional studies in human mitotic tissues is very challenging, not only due to the limited availability of human replicative tissues and the static nature of samples only being available at one time point, but also due to a lack of robust human stem cell markers and the difficulty of performing functional interventions. As such there is the need to establish an animal model that demonstrates a similar age-related mitochondrial dysfunction phenotype to that observed in humans, to enable detailed phenotyping of the functional effects of somatic mtDNA point mutations and focal respiratory chain deficiency in ageing replicative tissues. Robust stem cell markers are available for mouse tissue (Barker, Van Es et al. 2007; Itzkovitz, Lyubimova et al. 2012) and the use of mice enables the routine collection of replicative tissues at multiple stages throughout lifespan, ideal for an ageing study.

3.1.2 *Overview of animal models*

Normal- ageing WT mice accumulate very low levels of mtDNA point mutations (Vermulst, Bielas et al. 2007) and demonstrate a significantly lower incidence of COX deficient colonic crypts, reaching a maximum of only ~1.5% in 36 month old mice (Greaves, Barron et al. 2011), compared to aged humans (~15%) (Taylor, Barron et al. 2003). As such WT mice are not a suitable model for the investigation of clonally

expanded somatic mtDNA point mutations in ageing mitotic tissues. Given that somatic mtDNA mutations are believed to clonally expand by random genetic drift in ageing mitotic tissues, it may simply be that the short lifespan of a mouse is too minimal to facilitate the clonal expansion of a mutation to high enough levels to reach the threshold level necessary to give a mutant phenotype. Indeed, this has been supported by modelling studies examining the incidence of COX deficiency in post-mitotic tissues of rats, where it was hypothesised that random genetic drift could not explain the clonal expansion of mtDNA deletions in post-mitotic tissues of short lived mammals and could only apply to much longer lived mammals (~100 years old) (Kowald and Kirkwood 2013).

The original modelling studies that proposed random intracellular drift as the mechanism by which mtDNA mutations clonally expand, suggested that this mechanism was likely to be affected by the rate of mtDNA mutagenesis (Elson, Samuels et al. 2001). As such an increase in the rate of mtDNA mutagenesis could lead to the accelerated accumulation of cells containing clonally expanded mtDNA mutations and result in an age-related mitochondrial dysfunction phenotype, even in animals with a shorter lifespan. Evidence from the *PolgA^{mut/mut}* mouse, which shows an accelerated accumulation of mtDNA point mutations (x3-5 fold) leading to respiratory chain deficiency and a premature ageing, supports this phenomenon (Trifunovic, Wredenberg et al. 2004). Indeed multiple studies have been performed that demonstrate early onset stem cell dysfunction in response to the accumulation of mtDNA point mutations in *PolgA^{mut/mut}* mice, with effects seen on: downstream differentiation events resulting in the production of abnormal progeny; decreased stem cell self-renewal capacity and the number of quiescent stem cells and altered proliferative capacity of stem cells (Norrdahl, Pronk et al. 2011; Ahlqvist, Hämäläinen et al. 2012; Fox, Magness et al. 2012). Seemingly the accumulation of mtDNA point mutations has a profound effect upon stem cell function. *PolgA^{mut/mut}* mice, however display a disease-like phenotype and accumulate a much higher degree of mtDNA point mutations than seen in normal human ageing (Khrapko, Kraytsberg et al. 2006). Furthermore mtDNA mutations occur during embryogenesis in these mice and are evenly distributed across tissues, unlike in humans where mutations are heterogeneous and occur sporadically over time (Khrapko, Kraytsberg et al. 2006). Moreover ageing phenotypes in the *PolgA^{mut/mut}* mice are caused solely by mtDNA mutations, an exaggerated molecular defect, whereas normal human ageing is a multi-factorial process driven by interactions

between multiple molecular mechanisms, such as ROS, protein damage and DNA damage. Significant interactions between different forms of molecular damage in the ageing process are therefore absent and as such the *PolgA^{mut/mut}* mouse is not a suitable model for determining the effects of clonally expanded somatic mtDNA point mutations in the context of normal human ageing.

Mice that are heterozygous (*PolgA^{+/mut}*) for the D257A mutation also accumulate mtDNA point mutations but to a lesser extent than the *PolgA^{mut/mut}* mice, displaying ~4 point mutations per molecule of mtDNA (Kraytsberg, Simon et al. 2009). These mice do not display signs of premature ageing or a reduced lifespan (Vermulst, Bielas et al. 2007) but have been found to show evidence of respiratory chain deficiency in the heart and duodenum, reaching ~20% COX deficiency in the duodenum of 15 month old mice (Vermulst, Wanagat et al. 2008). It could therefore be expected that the enhanced rate of mtDNA mutagenesis in *PolgA^{+/mut}* mice would increase the pool of available mutations for clonal expansion, thereby increasing the probability that an mtDNA mutation would clonally expand to reach the critical threshold level during the short lifespan of a mouse. As such the frequency of respiratory chain deficiency in *PolgA^{+/mut}* mice would increase and could result in a similar mitochondrial dysfunction phenotype to that which is seen in normal human ageing.

An age-related accumulation of respiratory chain deficient cells has been detected in the colon of 18-48 week old *PolgA^{+/mut}* mice, with 48 week old animals displaying ~10% COX deficient colonic crypts (Holly Baines, MRes project). Colonic crypts were detected with both full and partial COX deficiency in *PolgA^{+/mut}* mice, demonstrating a mosaic, intracellular pattern of respiratory chain deficiency, which is a hallmark of normal human ageing (Taylor, Barron et al. 2003). Whole mtDNA genome sequencing of 6 COX deficient colonic crypts from two 48 week old animals, revealed the presence of 18 clonally expanded somatic mtDNA mutations. Base transitions accounted for the majority of the point mutations, which predominantly occurred within protein-encoding genes, specifically subunits of complexes I and IV (Holly Baines, MRes project). The prevalence of base transitions and mutations in protein encoding genes was similar to that observed in the ageing human colon (Taylor, Barron et al. 2003; Greaves, Barron et al. 2010). Though the incidence of respiratory chain deficiency in 48 week old *PolgA^{+/mut}* mice was lower than that seen in the normal ageing human colon (~15%), this preliminary data suggested that the *PolgA^{+/mut}* mouse had the potential to be a good

animal model of clonally expanded somatic mtDNA point mutations and the resulting respiratory chain deficiency.

3.2 Aims

The aim of this study was to perform detailed characterisation of the magnitude of focal respiratory chain deficiency and the spectrum of somatic mtDNA point mutations in colonic crypts of aged *PolgA*^{+/*mut*} mice. Colonic epithelial tissue was studied in the *PolgA*^{+/*mut*} mouse, given that the majority of studies investigating somatic mtDNA point mutations in ageing human mitotic tissues have been performed in the human colon, and would therefore allow for more extensive comparisons when establishing a potential model.

I aimed to determine whether the incidence of COX deficiency in aged *PolgA*^{+/*mut*} mice reached a level more comparable to that observed in the ageing human colon, and to perform extensive mutational analysis of the mtDNA defects responsible for the COX deficiency, through whole mtDNA genome sequencing of single COX positive and COX deficient colonic crypts. I aimed to determine whether the spectrum of somatic mtDNA point mutations was comparable between the *PolgA*^{+/*mut*} mouse and the ageing human colon with respect to mutation type, location and pathogenicity as well as investigating the clonal expansion of these mutations with respect to the action of any selective constraints and the plausibility of random genetic drift.

3.3 Results

3.3.1 *Respiratory chain deficiency in PolgA*^{+/*mut*} *mouse colonic crypts*

PolgA^{+/*mut*} mice have previously been shown to accumulate COX deficient colonic crypts with age, reaching ~10% by 48 weeks old (Holly Baines, MRes project). This is only half the natural lifespan of a *PolgA*^{+/*mut*} mouse and so these mice cannot be considered to be aged and indeed would not be representative of aged human colonic epithelial tissue. As such colon sections (10µm) were subject to dual COX/SDH histochemistry on colon samples from 59 (n=1) and 81 (n=3) week old *PolgA*^{+/*mut*} mice, to determine whether the level of COX deficiency accumulated further with age and reached a level more comparable to the ageing human colon. Aged *PolgA*^{+/*mut*} mice were provided by James Stewart and Nils-Göran Larsson, Max Planck Institute for Biology of Ageing, Cologne, Germany, which were derived from the *PolgA*^{*mut/mut*} mouse model generated by Trifunovic and colleagues (Trifunovic, Wredenberg et al. 2004). The incidence of COX deficient colonic crypts was calculated in longitudinal

and transverse colon sections, across multiple different levels, with > 500 colonic crypts analysed per colon sample. A Haematoxylin and Eosin stain was also performed on colonic epithelial tissue to demonstrate normal crypt morphology.

Aged *PolgA*^{+/*mut*} mice continued to display colonic crypts with both full and partial COX deficiency, distributed in a random, mosaic pattern throughout the tissue; a hallmark of normal human ageing (Taylor, Barron et al. 2003) (Figure 3-1a,b). Analysis of longitudinal colonic crypts revealed that COX deficiency extended from the crypt base (the stem cell compartment) along the whole length of the crypt to the apex, which is similar to the observations in the ageing human colon (Taylor, Barron et al. 2003) (Figure 3-1b). In aged *PolgA*^{+/*mut*} mice the magnitude of fully COX deficient colonic crypts increased further with age, with 81-week-old mice displaying an average of 14% COX deficient colonic crypts (Figure 3-1c). The number of crypts displaying partial COX deficiency also increased with age, from 0% in 18 week old animals to 8% in 81 week old *PolgA*^{+/*mut*} mice. Upon comparing the magnitude of focal respiratory chain deficiency between *PolgA*^{+/*mut*} mice (~14%) and ageing human colon (15%) (Taylor, Barron et al. 2003), there was no significant difference between the two ($p = 0.854$, unpaired t test). As such, both the level and patterns of COX deficient colonic crypts were considered similar between 81 week old *PolgA*^{+/*mut*} mice and aged humans, >70 years old.

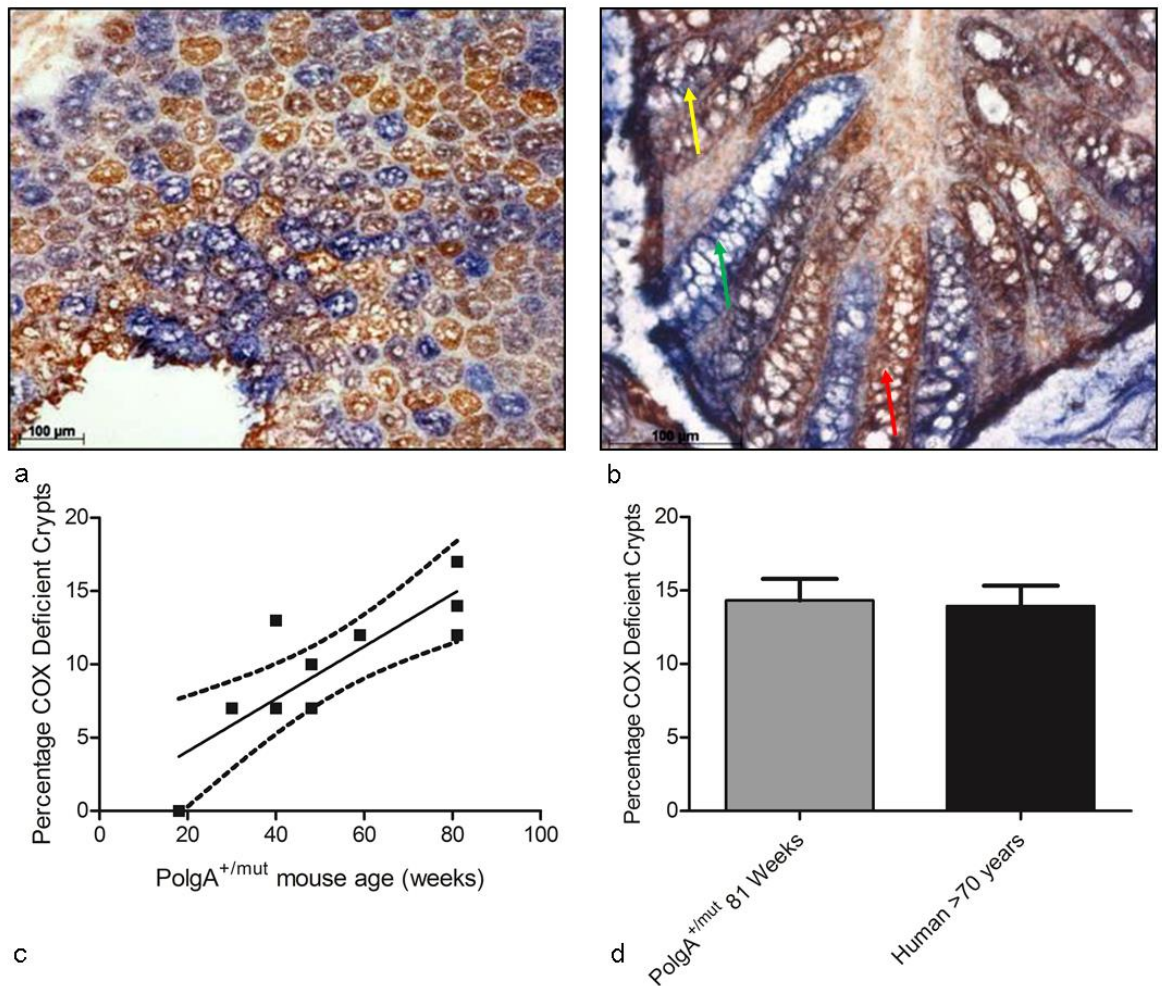


Figure 3-1: Respiratory chain deficiency in colonic crypts of ageing *PolgA*^{+/*mut*} mice.

COX/SDH histochemistry on 81 week old *PolgA*^{+/*mut*} colon sections showing (a) a transverse section through the crypts and (b) a longitudinal section through the crypts. Scale bars: 100μm. Crypts stained brown are positive for COX activity (red arrow), those stained blue are COX deficient (green arrow), and crypts stained purple/grey display partial COX deficiency (yellow arrow). (c) Magnitude of COX deficient colonic crypts in *PolgA*^{+/*mut*} mice aged 18-48 weeks old (Holly Baines, MRes project) and 59-81 week old mice. Linear regression analysis, $p = 0.0028$. (d) Mean incidence (\pm SEM) of COX deficient colonic crypts in 81 week old *PolgA*^{+/*mut*} mice and aged humans >70 years old (Taylor, Barron et al. 2003), $p = 0.854$ (unpaired t test). Image taken from (Baines, Stewart et al. 2014).

3.3.2 MtDNA genome analysis of *PolgA*^{+/*mut*} mouse colonic crypts

Single cell analysis and whole mtDNA genome sequencing of 6 COX deficient colonic crypts from two 48 week old *PolgA*^{+/*mut*} mice, had previously revealed the presence of somatic mtDNA point mutations (Holly Baines, MRes project). Preliminary mutational analysis revealed that the majority of these point mutations were base transitions and occurred within protein encoding genes, similar to what is seen in the ageing human colon (Taylor, Barron et al. 2003). To further characterise the mtDNA defects underlying COX deficiency in the *PolgA*^{+/*mut*} mouse colon, single COX positive (>4 per mouse) and COX deficient (>8 per mouse) colonic crypts were laser micro-dissected from three 81 week old *PolgA*^{+/*mut*} mice and lysed in a standard lysis buffer. To identify

the presence of somatic mtDNA point mutations in colonic crypts PCR amplification of the whole mtDNA genome was performed in a single stage PCR reaction using 30 overlapping pairs of forward and reverse primers. Samples were sequenced on an ABI3130xl Genetic Analyser (Applied Biosystems) and the mtDNA sequence for each cell was analysed using SeqScape software (Applied Biosystems). Long range PCR was performed, courtesy of Dr Laura Greaves, to identify whether large-scale mtDNA deletions were present in *PolgA*^{+/*mut*} mouse colonic crypts.

In human colonic crypts, previous studies have revealed an absence of clonally expanded mtDNA deletions (Taylor, Barron et al. 2003). To confirm that mtDNA deletions were not present and could not contribute to the COX deficiency in colonic crypts from *PolgA*^{+/*mut*} mice, long range PCR was performed on the single COX deficient and COX positive colonic crypts, courtesy of Dr Laura Greaves. Long-range PCR confirmed an absence of large scale mtDNA deletions in colonic crypts from *PolgA*^{+/*mut*} mice, with both COX deficient and COX positive colonic crypts displaying only the WT ~14.5kb mtDNA molecule, and an absence of any smaller deleted mtDNA molecules (Figure 3-2)

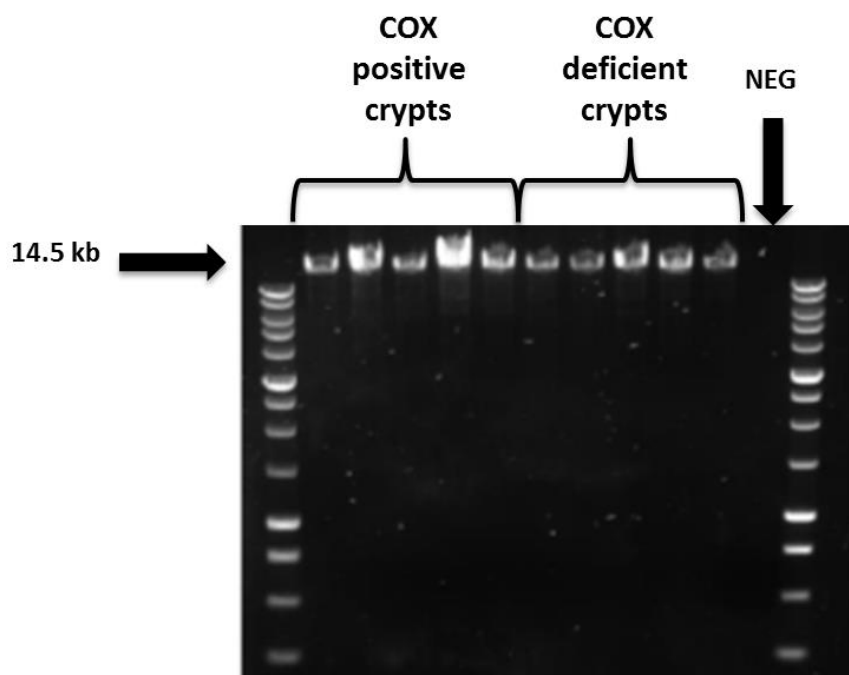


Figure 3-2: Absence of large scale mtDNA deletions in *PolgA*^{+/*mut*} mouse single colonic crypts.

Agarose gel electrophoresis image showing long range-PCR products in single COX positive and COX deficient colonic crypts, courtesy of Dr Laura Greaves. The WT mtDNA band (~14.5kb) was present in all COX positive and COX deficient colonic crypts, with no smaller deleted mtDNA molecules detected. Image taken from (Baines, Stewart et al. 2014).

3.3.2.1 *Respiratory chain deficiency is caused by random somatic mtDNA point mutations in $PolgA^{+/mut}$ mouse colonic crypts.*

Whole mtDNA genome sequencing was performed on the single cell lysate from COX positive and COX deficient colonic crypts from $PolgA^{+/mut}$ mice for the detection of somatic mtDNA point mutations. The sequence for each crypt was aligned to the C57Bl/6J mouse reference sequence (NC_005089) and the consensus DNA sequence from homogenate colon DNA for that mouse to determine the somatic mtDNA point mutations that accumulated in the crypts over time. Heteroplasmy levels were estimated based upon the relative peak height of electropherograms.

In addition to the 18 point mutations previously detected in COX deficient crypts of 48 week old animals (Holly Baines, MRes project), a further 223 mtDNA point mutations were detected in colonic crypts of 81 week old $PolgA^{+/mut}$ mice (see Appendix C), with point mutations detected in both the homoplasmic and heteroplasmic form (Figure 3-3). Some colonic crypts contained only one clonally expanded somatic point mutation, while many contained multiple somatic mtDNA point mutations (see Appendix C). Example electropherograms, illustrating the presence of homoplasmic and heteroplasmic point mutations affecting protein encoding genes and an mt-rRNA gene present in COX deficient crypts are shown in Figure 3-3.

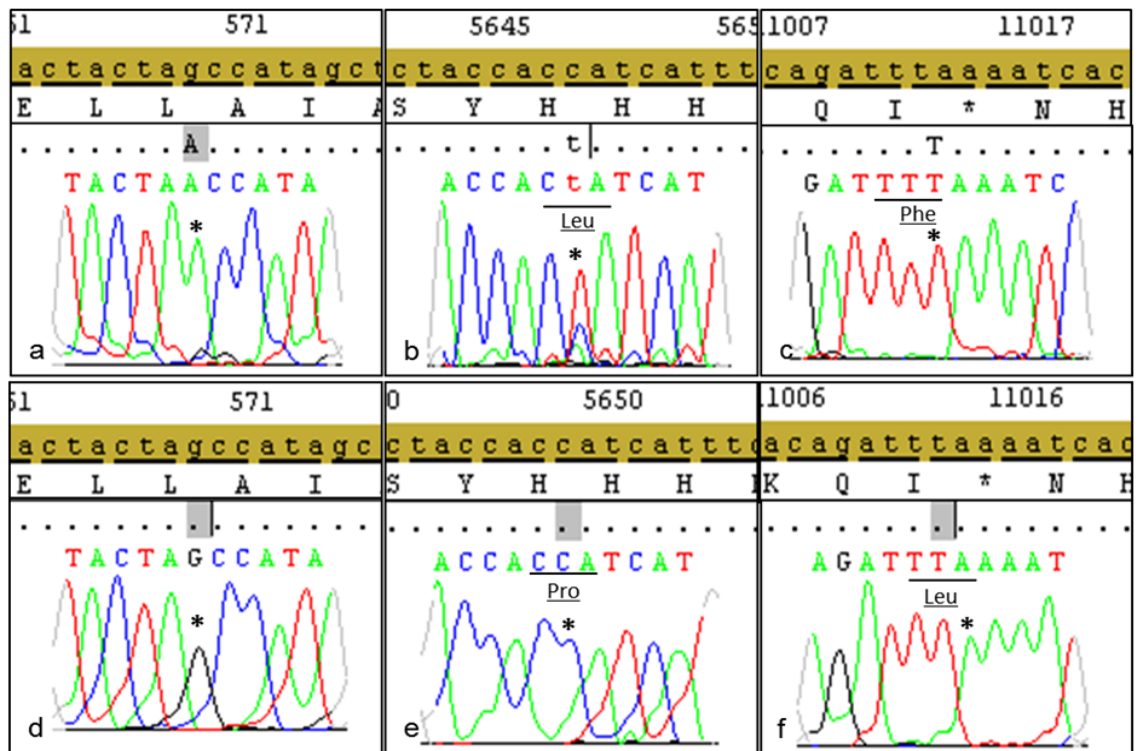


Figure 3-3: Detection of somatic mtDNA mutations in *PolgA*^{+/*mut*} colonic crypts.

Example sequencing electropherograms showing the presence of mtDNA point mutations in COX deficient crypts from *PolgA*^{+/*mut*} mice. (a) Electropherogram showing a homoplasmic m. 568 G>A transition in mt-srRNA. (b) Electropherogram showing the heteroplasmic (75%) m.5647 C>T transition. This change predicts a proline to leucine amino acid change in mt-*CO1*. (c) Electropherogram showing the homoplasmic m.11012 A>T transversion. This change predicts a leucine to phenylalanine amino acid change in mt-*ND4*. Wild-type homogenate sequences are shown in panels (d-f). Image taken from (Baines, Stewart et al. 2014).

Somatic mtDNA point mutations (n=55) were detected in COX positive colonic crypts, of which a substantial proportion (67%) were present at a low heteroplasmy ($\leq 50\%$), and were therefore unlikely to affect mitochondrial protein function (Figure 3-4a). No homoplasmic point mutations were detected in COX positive colonic crypts. The overwhelming majority of point mutations were base transitions (80%) (Figure 3-4b) and 49% of the base changes occurred within subunits of complex I (Figure 3-4c), which was unsurprising given the large portion of the mtDNA genome occupied by genes encoding subunits of complex I. In COX deficient colonic crypts, again ~80% of changes were base transitions, of which 49% were C>T changes and 17% were G>A changes (Figure 3-4b). Mutations predominantly occurred within protein encoding genes, of which 34% of changes affected complex I subunits and 27% affected subunits of complex IV (Figure 3-4c). In COX deficient colonic crypts 73% of mutations were present at high heteroplasmy ($\geq 50\%$) (Figure 3-4a) and were non-synonymous mutations, predicted to cause amino acid changes. Homoplasmic and heteroplasmic point mutations ($\geq 75\%$) were frequently detected in mt-rRNA and mt-tRNA genes, accounting for 25% of the total number of point mutations (Figure 3-4c).

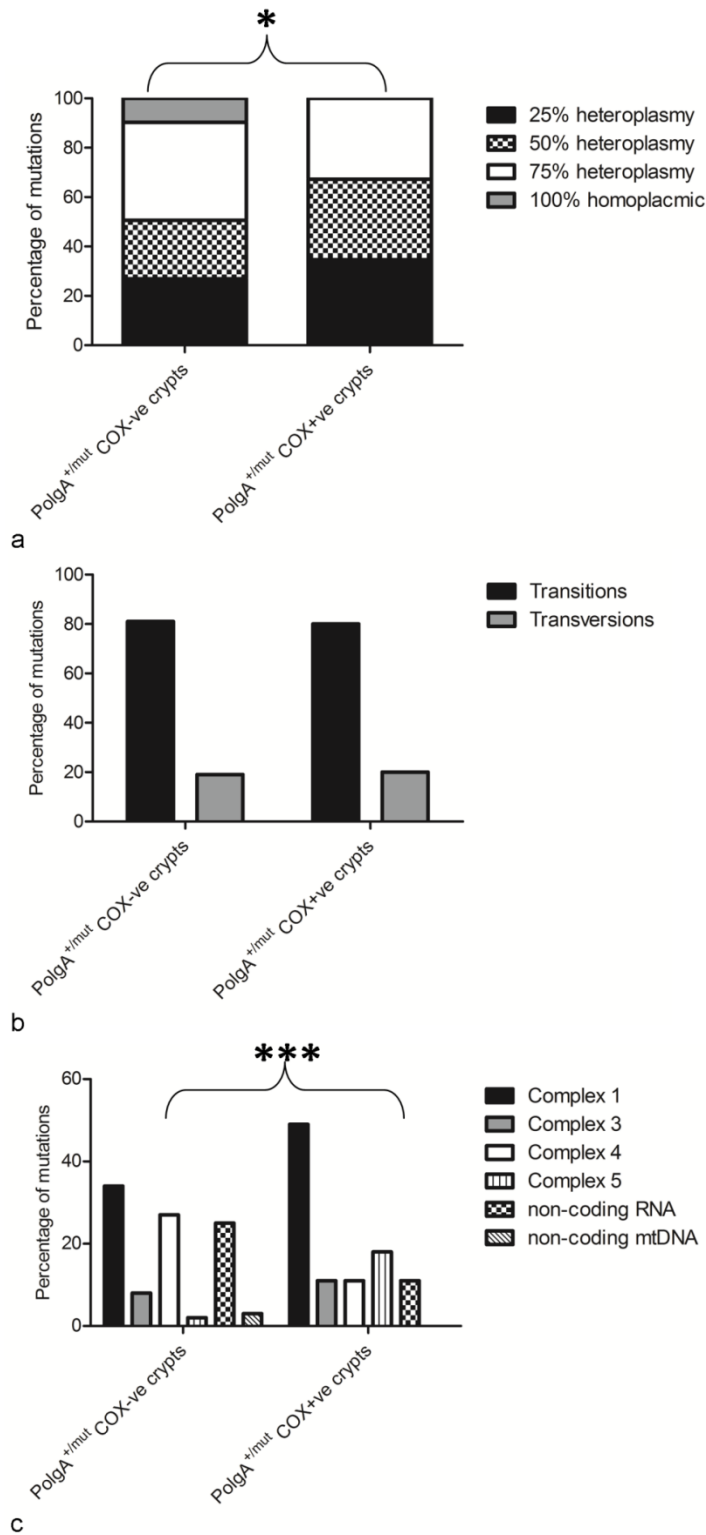


Figure 3-4: The frequency, type and location of somatic mtDNA point mutations in *PolgA*^{+mut} mouse COX positive and COX deficient colonic crypts.

(a) The frequency of mtDNA point mutations present within the different heteroplasmy classes from *PolgA*^{+mut} mouse COX deficient and COX positive colonic crypts. There was a significantly higher frequency of mtDNA point mutations in the higher heteroplasmy classes in the COX deficient crypts ($p = 0.0439$, χ^2 analysis). (b) Types of changes observed in COX deficient and COX positive colonic crypts. There was no significant difference in the types of changes between the two datasets ($p = 1.000$, χ^2 test). (c) Gene location of point mutations in individual mtDNA encoded genes in COX deficient and COX positive colonic crypts. There was a significant difference between the location of the mtDNA point mutations detected in COX positive and COX deficient crypts ($p < 0.0001$, χ^2 test). Image taken from (Baines, Stewart et al. 2014).

In the ageing human colon somatic mtDNA point mutations have been shown to accumulate randomly throughout the genome, with an absence of any mutational hotspots (Greaves, Elson et al. 2012). To determine whether random mutagenesis was also observed in colonic crypts of *PolgA^{+/-mut}* mice the frequency of mtDNA point mutations were grouped according to gene location. Taking into account the relative portion of the genome occupied by each gene, there was no significant difference found between the frequency of mtDNA point mutations observed in each gene type and that which would be expected if the mutations were falling randomly on the genome ($p=0.139$, X^2) (Figure 3-5a). To determine whether there was a bias towards the clonal expansion of more deleterious mtDNA point mutations and a higher frequency of non-synonymous changes in the higher heteroplasmy classes the relative frequency of point mutations in each heteroplasmy class was examined. No significant difference in the frequency of synonymous: non-synonymous changes was identified in the different heteroplasmy classes ($p=0.6765$, X^2 test) (Figure 3-5b), supporting that the clonal expansion of somatic mtDNA point mutations appears to be random in *PolgA^{+/-mut}* colonic crypts.

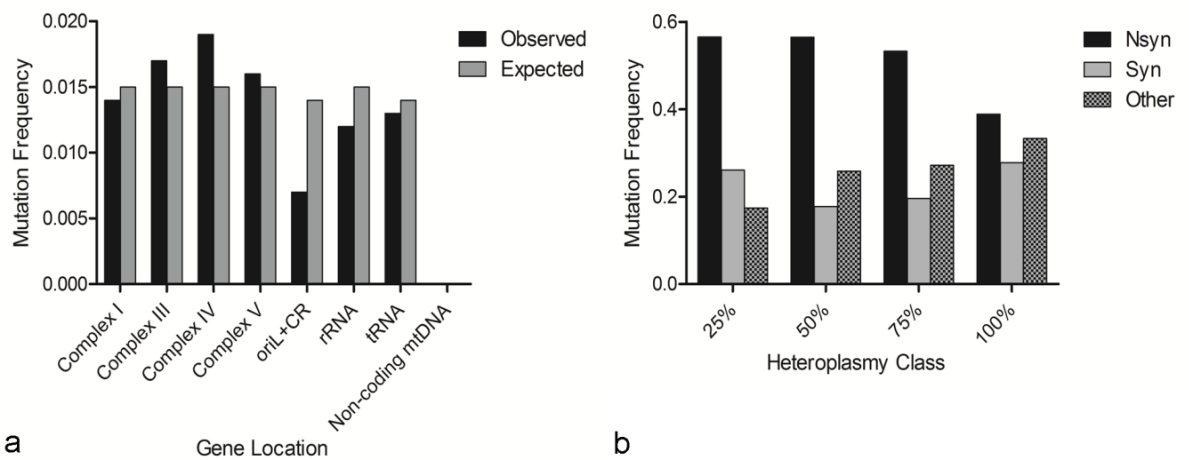


Figure 3-5: MtDNA mutations occur randomly in *PolgA^{+/-mut}* mouse colonic crypts.

(a) Positional mutation frequency of observed vs expected (number of mutations/base pairs) somatic mtDNA mutations in the different mtDNA encoded genes detected in *PolgA^{+/-mut}* colonic crypts ($p=0.0139$, X^2 test) Abbreviations: oriL, origin of light strand replication; CR, control region. Non-coding mtDNA refers to the 25bp in between genes that do not code for anything within the mtDNA genome. Only 0.322 mutations are expected in non-coding mtDNA, hence the absence of a mutation frequency bar here. (b) The mutation frequency of non-synonymous, synonymous and “other” changes across the different heteroplasmy classes in the *PolgA^{+/-mut}* mouse colonic crypts. Contingency analysis using X^2 test where a p value of <0.05 is statistically significant ($p=0.6765$). Abbreviations: Nsyn, non-synonymous and syn, synonymous changes. Image taken from (Baines, Stewart et al. 2014).

3.3.2.2 *The levels of clonally expanded somatic mtDNA point mutations in the PolgA^{+mut} mouse colon are comparable to the ageing human colon.*

To determine whether the *PolgA^{+mut}* mouse is a representative model of age-related mitochondrial dysfunction, the nature and spectrum of clonally expanded somatic mtDNA point mutations observed in *PolgA^{+mut}* mouse colonic crypts was compared to the data available for the human colon (Table 3-1) (Taylor, Barron et al. 2003; Greaves, Preston et al. 2006; Greaves, Barron et al. 2010; Greaves, Elson et al. 2012), to identify whether the mtDNA point mutations responsible for age related respiratory chain deficiency were consistent between the two species.

	Mutation frequency in COX +ve crypts		Mutation frequency in COX -ve crypts	
	<i>PolgA^{+mut}</i> mice	Humans	<i>PolgA^{+mut}</i> mice	Humans
Transitions	44 (80%)	28 (85%)	150 (81%)	82 (86%)
Transversions	11 (20%)	2 (6%)	36 (19%)	5 (5%)
Ins/Dels	0	3 (9%)	0	9 (9%)
Complex 1	27 (49%)	8 (24%)	64 (34%)	23 (24%)
Complex 3	6 (11%)	1 (3%)	14 (8%)	7 (7%)
Complex 4	6 (11%)	9 (27%)	51 (27%)	29 (30%)
Complex 5	10 (18%)	0	4 (2%)	2 (2%)
non-coding RNA	6 (11%)	9 (27%)	47 (25%)	26 (27%)
non-coding mtDNA	0	6 (18%)	6 (3%)	9 (9%)

Table 3-1: A comparison of the location, types and frequency of mtDNA point mutations in COX positive and COX deficient colonic crypts from *PolgA^{+mut}* mice and aged humans (Greaves, Elson et al. 2012).

Abbreviations: Ins/Dels, insertions and deletions. Table taken from (Baines, Stewart et al. 2014).

The gene location of mtDNA point mutations in COX deficient colonic crypts was not significantly different between the *PolgA^{+mut}* mouse and human colon, with the majority of changes occurring in protein-encoding genes (~60%), specifically subunits of complexes I and IV as well as 25% of changes occurring within mt-tRNA and mt-rRNA (non-coding RNA) genes in both datasets ($p = 0.2204$, X^2 test) (Figure 3-6a). A comparison of the types of changes (transitions, transversions, insertions/deletions) detected in COX deficient colonic crypts did however reveal a significant difference between the *PolgA^{+mut}* mouse and ageing human colon ($p < 0.0001$, X^2) (Figure 3-6b). Approximately 10% of changes in the ageing human colon are caused by insertion/deletion mutations (Greaves, Elson et al. 2012); however there was an absence of insertions/deletions detected in colonic crypts of the *PolgA^{+mut}* mice. Transversion mutations have also been detected at a higher frequency in the ageing human colon (19%) than in the *PolgA^{+mut}* mouse colon (5%). Nevertheless the majority of changes in both datasets were indeed base transitions (~80%). Given that the aim of this study was to determine whether the *PolgA^{+mut}* mouse was a good model of age-related focal respiratory chain deficiency caused by clonally expanded somatic mtDNA mutations

seen in the human colon, the pathogenicity of somatic mtDNA point mutations was determined to identify the mechanism responsible for COX deficiency in the colonic crypts. Somatic mtDNA point mutations were assigned pathogenicity according to the following criteria: changed an amino acid or occurred in an mt-tRNA or mt-rRNA gene; present at >50% heteroplasmy; associated with decreased activity of a respiratory chain complex (COX deficiency) (Taylor, Barron et al. 2003; Greaves, Barron et al. 2010); and not previously identified as a polymorphic variant. Point mutations detected in *PolgA*^{+/*mut*} colonic crypts were compared to mutations previously reported in *Mus musculus* mtDNA sequences deposited in Genbank and to mutations transmitted through the *PolgA*^{*mut/mut*} germline (Stewart, Freyer et al. 2008) to eliminate previously identified variants in mouse mtDNA. The percentage of COX deficient colonic crypts that contained at least one pathogenic mtDNA point mutation was 62% in the *PolgA*^{+/*mut*} colon and 59% in the human colon, with no significant difference between the two ($p=0.8194$, X^2 test) (Figure 3-6c). This suggests that the clonal expansion of at least one pathogenic mtDNA point mutation is causal in the COX deficiency observed in ~60% of colonic crypts in both *PolgA*^{+/*mut*} mice and humans with age.

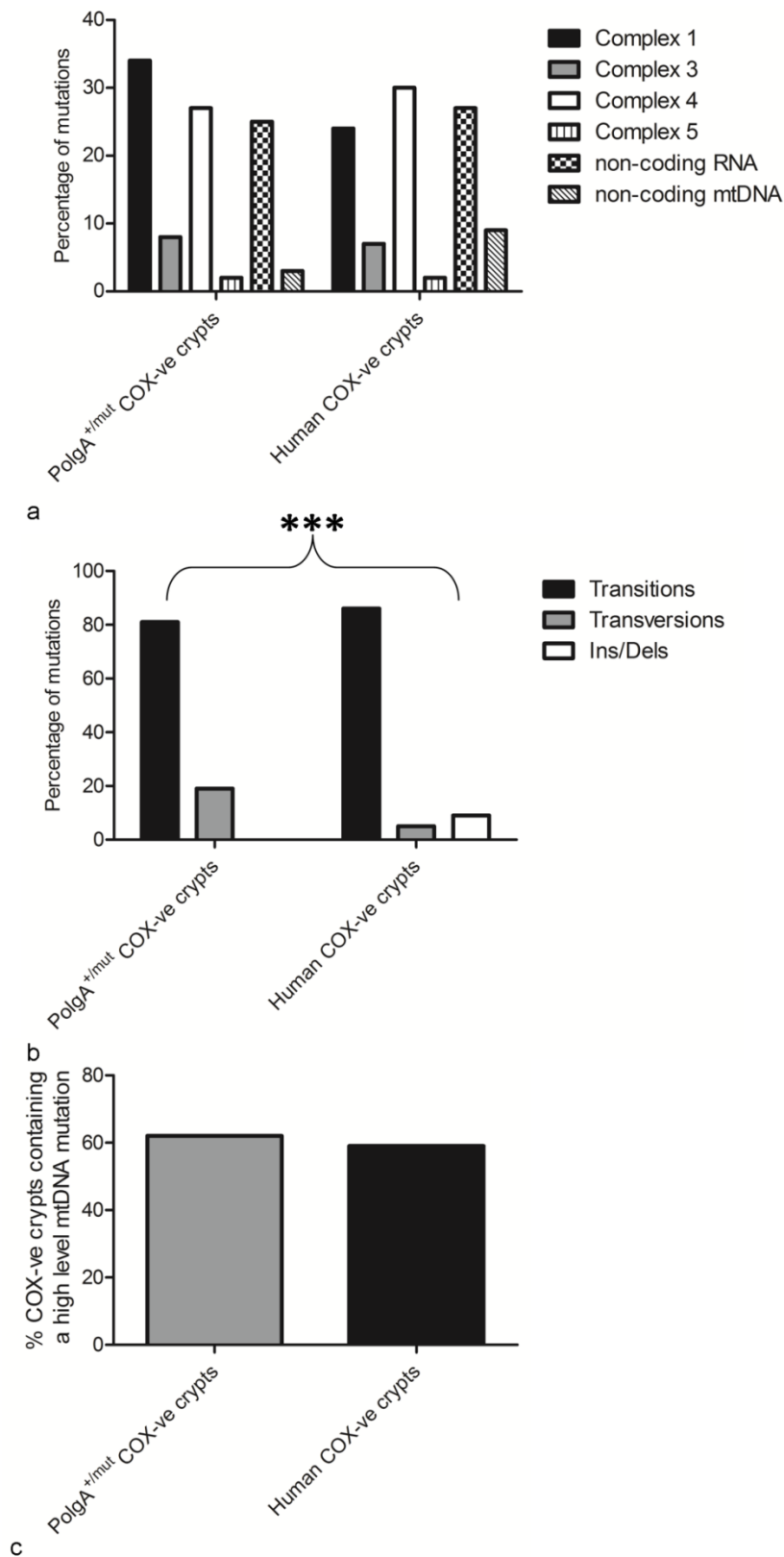


Figure 3-6: Gene type, location and pathogenicity of somatic mtDNA point mutations in COX deficient colonic crypts in the ageing *PolgA^{+mut}* mouse and human colon.

(a) Gene location of point mutations in individual mtDNA encoded genes in COX deficient colonic crypts $p = 0.2204$, χ^2 test. (b) Types of changes observed in COX deficient colonic crypts. There was a significantly higher frequency of insertion/deletion mutations in the human crypts ($p < 0.001$, χ^2 test). (c) Percentage of COX deficient colonic crypts containing at least one pathogenic mtDNA point mutation in the *PolgA^{+mut}* mouse and human colon ($p = 0.8194$, χ^2 test). Image taken from (Baines, Stewart et al. 2014).

3.3.2.3 Absence of evidence for purifying selection on the clonal expansion of somatic mtDNA point mutations in *PolgA*^{+/*mut*} mouse colonic crypts

In the ageing human colon the accumulation of somatic mtDNA point mutations is random and their expansion is not subject to selective constraints (Greaves, Elson et al. 2012). To determine whether somatic mtDNA point mutations in the ageing *PolgA*^{+/*mut*} mouse colon were subject to selective constraints the *PolgA*^{+/*mut*} mouse mutation dataset was compared to: mtDNA variants reported in *Mus musculus* mtDNA sequences downloaded from Genbank and to mtDNA point mutations transmitted through the *PolgA*^{*mut/mut*} germline (Stewart, Freyer et al. 2008). Comparison to *Mus musculus* sequences gives an estimate of the natural mutation/ selection balance in mice and comparison to the *PolgA*^{*mut/mut*} germline mutations ensures that selective constraints are only examined in the context of somatic mtDNA point mutations. Each mutation transmitted through the *PolgA*^{*mut/mut*} germline was scored once, and only mutations observed in 2 or more related animals were counted to filter out false positives.

Somatic mtDNA point mutations in *PolgA*^{+/*mut*} mouse colonic crypts were frequently non-synonymous mutations, where the ratio of non-synonymous substitutions per site (dN) to synonymous substitutions per site (dS) gave a value of 0.783, providing little evidence of purifying selection against amino acid changes in protein encoding genes (values approaching 1 signify an absence of purifying selection) (Figure 3-7). A Fischer's exact test failed to reject the null hypothesis that observed mtDNA mutations evolve neutrally in *PolgA*^{+/*mut*} mouse colonic crypts (dN/dS=1 null) ($p= 0.3402$). This was significantly different to mutations observed in the *PolgA*^{*mut/mut*} mouse germline (dN:dS= 0.0310) and normal mouse strains (dN:dS= 0.0640), where mutations were more frequently synonymous changes (Figure 3-7). Furthermore a Fischer's exact test rejected the neutral null hypothesis (dN/dS=1) for observed mtDNA point mutations in both the *PolgA*^{*mut/mut*} mouse germline ($p=<0.0001$) and normal mouse strains ($p=<0.0001$). This data therefore suggests that somatic mtDNA point mutations evolve neutrally in the *PolgA*^{+/*mut*} mouse colon and indicates there is no evidence for purifying selection.

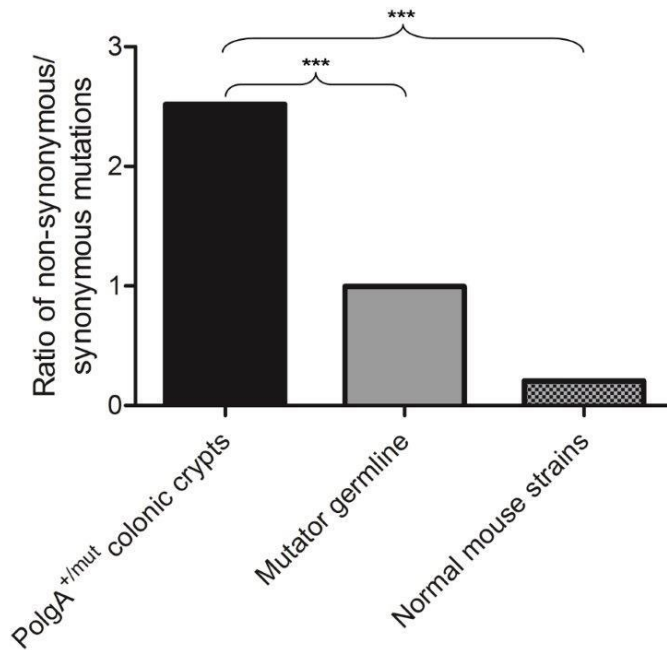


Figure 3-7: Genetic consequences of somatic mtDNA point mutations in the *PolgA*^{+/*mut*} mouse colon.

The ratio of non-synonymous mutations: synonymous mutations in *PolgA*^{+/*mut*} mouse colonic crypts, the *PolgA*^{*mut/mut*} mouse germline and normal mouse strains. The ratio of non-synonymous to synonymous mutations is significantly higher in *PolgA*^{+/*mut*} mouse colonic crypts compared to the *PolgA*^{*mut/mut*} germline and normal mouse strains ($p < 0.0001$, Fisher's exact test). Image taken from (Baines, Stewart et al. 2014).

In *PolgA*^{+/*mut*} mouse colonic crypts a considerably higher number of point mutations were also detected in the first and second codon positions of protein encoding genes, of which many were non-synonymous changes (Figure 3-7a) compared to the *PolgA*^{*mut/mut*} germline (Figure 3-7b) and normal mouse strains (Figure 3-7c). This further supports that somatic mtDNA point mutations in the ageing *PolgA*^{+/*mut*} mouse colon are not subject to selective constraints, as changes in the first and second codon positions frequently cause amino acid substitutions. Furthermore a significantly higher number of point mutations were also detected in mt-tRNA and mt-rRNA genes in the *PolgA*^{+/*mut*} mouse colon than the *PolgA*^{*mut/mut*} germline and normal mouse strains ($p < 0.0001$, X^2 test) (Figure 3-7a-c). Too few somatic mtDNA mutations were detected in the control region of *PolgA*^{+/*mut*} colonic crypts and so appropriate comparisons could not be made here. The random mutagenesis observed in *PolgA*^{+/*mut*} colonic crypts (Figure 3-5a) was also significantly different to the genome distribution of mtDNA point mutations observed in the *PolgA*^{*mut/mut*} germline ($p = 0.0005$, X^2 test) and normal mouse strains ($p < 0.0001$, X^2 test), where there was a mutation bias towards mt-tRNA and non-coding mutations, with purifying selection against mutations in protein-encoding genes (Figure 3-7d, e). As such it appears that somatic mtDNA point mutations in the ageing

PolgA^{+/*mut*} colon are indistinguishable from random and that their clonal expansion is not subject to selective constraints.

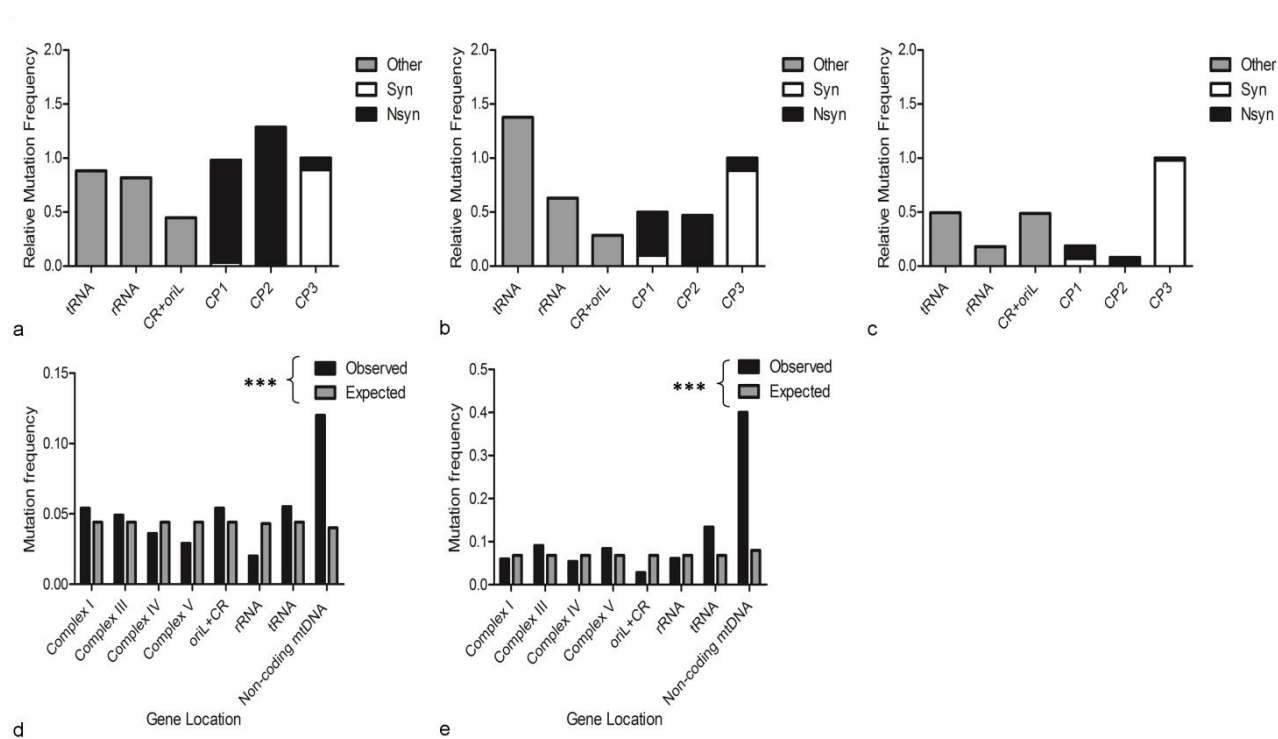


Figure 3-8: Positional mutation frequency and mutation distribution by codon position and gene reveals an absence of evidence for purifying selection on somatic mtDNA point mutations in *PolgA*^{+/*mut*} colonic crypts

(a) Positional mutation frequency (observed mutations per base pair) of somatic mtDNA point mutations observed in *PolgA*^{+/*mut*} colonic crypts compared to (b) mtDNA mutations observed, transmitted through the *PolgA*^{mut/mut} mouse germline (Stewart, Freyer et al. 2008) and (c) mtDNA sequences of mouse strains from Genbank, *Mus musculus*. To compare between the classes the sum of the 3rd codon position was taken and standardized as 1 (value/ 3rd codon sum). Abbreviations: CP1-3, codon positions 1-3. (d) Positional mutation frequency (number of mutations/base pairs) of observed vs expected (based on a random distribution) mtDNA point mutations transmitted through the *PolgA*^{mut/mut} mouse germline (Stewart, Freyer et al. 2008) ($p < 0.0001$, X^2 test) and (e) mtDNA sequences of mouse strains from Genbank, *Mus musculus* ($p < 0.0001$, X^2 test). Contingency analysis using X^2 test with Bonferroni correction for multiple testing was carried out on the frequency of changes in each gene type category where $p < 0.025$ was statistically significant. Non-coding mutations were excluded from the contingency analysis as values were frequently below 5. Image taken from (Baines, Stewart et al. 2014).

3.3.2.4 The clonal expansion of somatic mtDNA point mutations in the ageing colon of *PolgA*^{+/*mut*} mice can be explained by random genetic drift.

Somatic mtDNA mutations have been proposed to clonally expand by random genetic drift, causing age-related focal respiratory chain deficiency in both post-mitotic and mitotic human tissues (Coller, Khrapko et al. 2001; Elson, Samuels et al. 2001). Recent experimental data from the human colon and buccal epithelium strongly supports the early life hypothesis for the origin of mtDNA point mutations and that clonal expansion occurs throughout adulthood (Greaves 2014). A study in short lived animals, hypothesised that random genetic drift cannot explain the clonal expansion of mtDNA deletions and the incidence of COX deficiency observed in post-mitotic tissues of rats

(Kowald and Kirkwood 2013). This study, however did not examine the clonal expansion of mtDNA point mutations in mitotic tissues of short-lived animals, and so it remains unknown whether the high cell division in replicating tissues could influence clonal expansion and whether random genetic drift would indeed be sufficient to explain the incidence of COX deficiency in mitotic tissues of short-lived animals.

The original modelling studies in humans suggested that the rate of mtDNA mutagenesis could influence the clonal expansion of mtDNA mutations by random genetic drift (Elson, Samuels et al. 2001). A computational model, based upon previously published models and experimental data (Coller, Khrapko et al. 2001; Elson, Samuels et al. 2001; Taylor, Barron et al. 2003; Vermulst, Bielas et al. 2007), was therefore developed, courtesy of Craig Stamp, to determine whether changing only the mtDNA mutation rate could lead to accelerated clonal expansion of somatic mtDNA point mutations and the levels of COX deficiency observed experimentally in short-lived animals. The model involved the simulation of 1000 cells, assuming that each cell contained 200mtDNA molecules (Coller, Khrapko et al. 2001) and underwent cell division once a day every day for 3 years. The mean of 1000 simulation runs of 1080 divisions during the 36 month lifespan of mice was performed to determine the mtDNA mutation frequency. Parameter scans for different mtDNA mutation rates were performed to simulate the level of COX deficiency produced at each rate, assuming that >75% mutated mtDNA was required to confer COX deficiency (Taylor, Barron et al. 2003), and this was subsequently matched to experimental data for the WT (Greaves, Barron et al. 2011), *PolgA*^{+/*mut*} and *PolgA*^{*mut/mut*} mice, given that these mice exhibit different rates of mtDNA mutagenesis.

Dual COX/SDH histochemistry was performed on 3 (n=5), 6 (n=5), 9 (n=7) and 12 (n=6) month old *PolgA*^{*mut/mut*} mouse colon tissue to determine the incidence of age-related COX deficiency (Figure 3-9) at a high rate of mtDNA mutagenesis, to be included in the simulations. The computer modelling (Figure 3-10) demonstrated that changing only the mtDNA mutation rate could lead to enhanced clonal expansion of somatic mtDNA point mutations and the incidence of COX deficiency observed experimentally in WT (Greaves, Barron et al. 2011), *PolgA*^{+/*mut*} (Figure 3-1) and *PolgA*^{*mut/mut*} (Figure 3-9) mouse colon tissue. As such random genetic drift was sufficient to explain the clonal expansion of somatic mtDNA point mutations in colonic epithelial tissue of ageing mice, which parallels what we see in the ageing human colon (Taylor, Barron et al. 2003; Greaves, Elson et al. 2012).

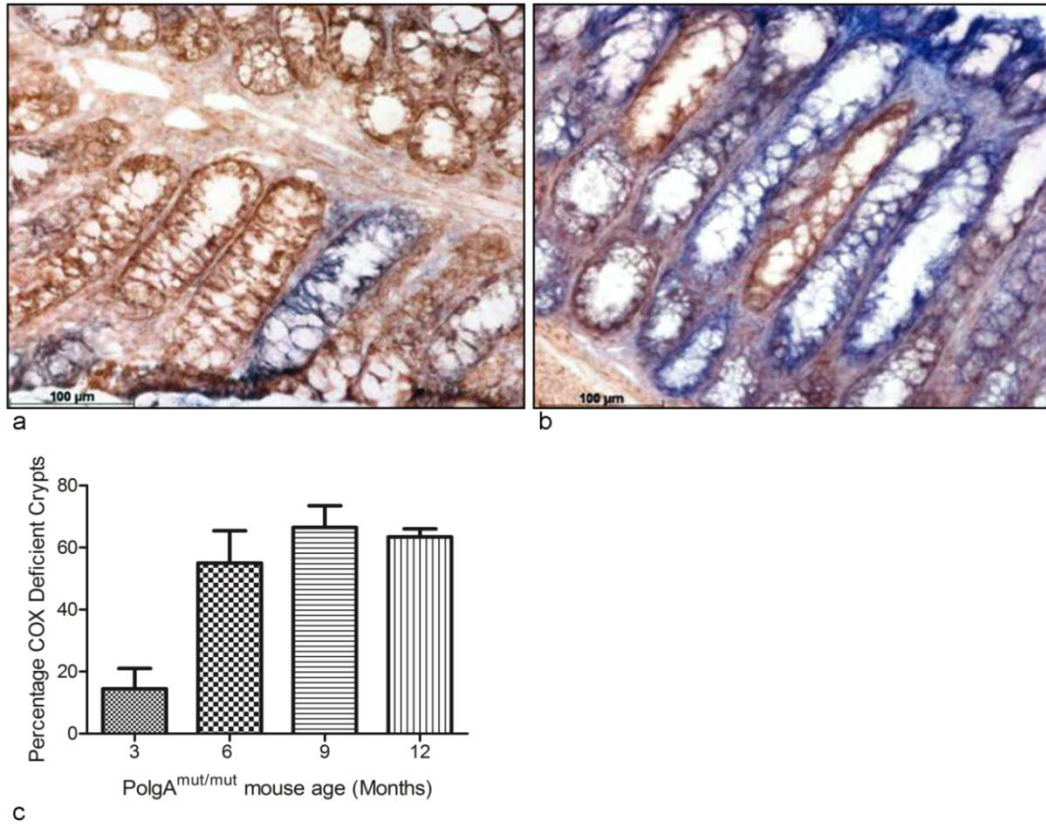


Figure 3-9: Respiratory chain deficiency in ageing *PolgA^{mut/mut}* mouse colon.

COX/SDH histochemistry on (a) 3 month old and (b) 12 month old *PolgA^{mut/mut}* mouse colon tissue. Crypts stained brown are positive for COX activity, those stained blue are COX deficient and those stained purple/grey display intermediate COX deficiency. (c): Mean incidence (± SEM) of COX deficient colonic crypts in 3, 6, 9 and 12 month old *PolgA^{mut/mut}* mice. Image taken from (Baines, Stewart et al. 2014).

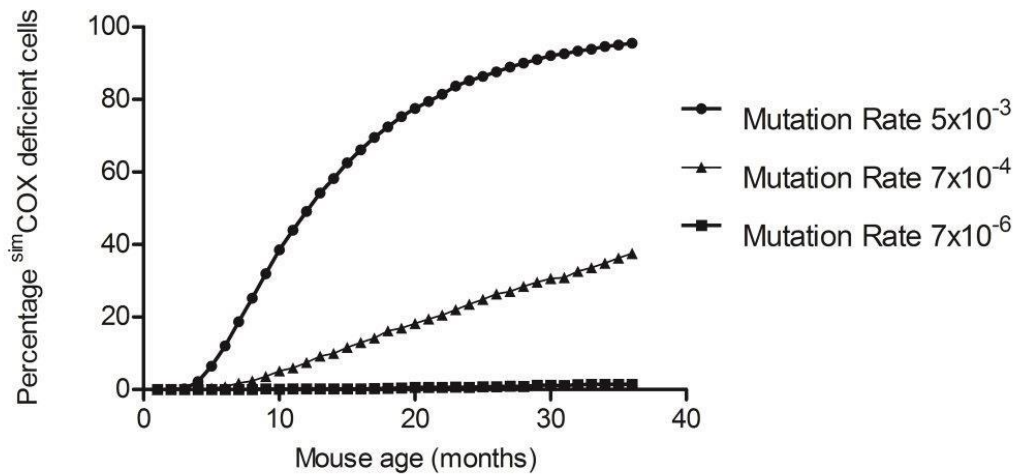


Figure 3-10: Random genetic drift can explain the clonal expansion of mtDNA point mutations and the incidence of COX deficiency in colonic crypt stem cells of ageing mice.

In silico modelling demonstrates that the percentage of simulated cells containing >75% mutant mtDNA molecules (^{sim}COXdeficient cells) at the different indicated mtDNA mutation rates, closely matches the incidence of COX deficiency observed experimentally in WT (Greaves, Barron et al. 2011) *PolgA^{+/mut}* (Figure 3.1) and *PolgA^{mut/mut}* mice (Figure 3-9). Image taken from (Baines, Stewart et al. 2014).

3.4 Discussion

Clonally expanded somatic mtDNA point mutations, leading to respiratory chain deficiency are frequently observed in ageing human stem cell populations, yet the functional significance of such mutations remains largely unknown. As such there is the need to establish a good animal model that displays a similar age-related mitochondrial dysfunction phenotype so that more detailed phenotyping can be performed of the functional consequences of clonally expanded somatic mtDNA point mutations in ageing mitotic tissues.

I have previously shown that *PolgA*^{+/*mut*} mice accumulate COX deficient colonic crypts with age and that such COX deficiency was associated with somatic mtDNA point mutations (Holly Baines, MRes project). The aim of this study was to determine whether the incidence of COX deficiency in aged *PolgA*^{+/*mut*} mice reaches a level more comparable to that observed in the ageing human colon and to determine whether the nature, spectrum and clonal expansion of somatic mtDNA point mutations underlying the COX deficiency was similar between the two species. Results from this study revealed that by 81 weeks of age, *PolgA*^{+/*mut*} display a similar level and pattern of COX deficiency in colonic crypts as ageing humans (>70 years old) (Taylor, Barron et al. 2003) and confirm that the mtDNA defects underlying the COX deficiency are clonally expanded somatic mtDNA point mutations. Point mutations were found to occur randomly within the genome, and paralleled those observed in the ageing human colon in terms of gene location and pathogenicity (Greaves, Elson et al. 2012). Moreover somatic mtDNA mutations were not subject to purifying selection, confirming that their clonal expansion was indeed random. Computer modelling also demonstrated that random genetic drift can explain the clonal expansion of somatic mtDNA point mutations in the ageing *PolgA*^{+/*mut*} mouse colon, suggesting a similar mechanism for the clonal expansion of somatic mtDNA point mutations in the colon between mice and humans.

Differences in the types of mtDNA point mutations were observed between the *PolgA*^{+/*mut*} mouse and ageing human colon, which was principally due to a lack of frameshift mutations in the *PolgA*^{+/*mut*} colon. This was not unexpected, given that *PolgA*^{+/*mut*} mice are heterozygous for an allele that disrupts the proof-reading function of mtDNA Pol γ , which induces mutations in mtDNA during replication through the misincorporation and miscopying of bases (Zheng, Khrapko et al. 2006). Indeed, a recent study involving extensive mutational analysis of 442 mutations in the *PolgA*^{*mut/mut*}

mice revealed that <1% of mutations were frameshift mutations (Ross, Stewart et al. 2013), with strong purifying selection observed on the transmission of insertion/deletion mutations in transgenic mouse models that carry mtDNA mutations (Fan, Waymire et al. 2008; Stewart, Freyer et al. 2008; Ross, Stewart et al. 2013). Furthermore, the rare mtDNA deletions that are observed in *PolgA^{mut/mut}* mice only persist in mt-tRNA genes and the oriL (Stewart, Freyer et al. 2008; Ross, Stewart et al. 2013). As such it was unlikely that any frameshift mutations would be detected in the *PolgA^{+/mut}* mutation dataset, given the modest size of 241 mutations coupled with the low frequency of insertion/deletion mutations observed in these mouse strains. A lower incidence of transversion mutations was also observed in the *PolgA^{+/mut}* mouse colon, which again is likely to be due to the defective mtDNA Poly. Nevertheless the frequency of transversion mutations in the *PolgA^{+/mut}* mouse and human colon was only moderate, highly suggesting that few age-related somatic mtDNA mutations are induced by 8-oxo-deoxyguanine mediated mutagenesis and oxidative damage. In both datasets the overwhelming majority of changes were base transitions, confirming that age-related somatic mtDNA point mutations appear to occur during early development from Poly mediated replication errors and/or spontaneous cytosine deamination (Zheng, Khrapko et al. 2006; Vermulst, Bielas et al. 2007), with somatic mtDNA mutations clonally expanding throughout the lifespan (Coller, Khrapko et al. 2001; Elson, Samuels et al. 2001).

In this study COX deficient colonic crypts, frequently presented with clonally expanded mtDNA point mutations in genes other than mtDNA encoded subunits of Complex IV, confirming that mutations in other genes can result in COX deficiency. Point mutations in mt-tRNA and mt-rRNA genes accounted for the majority of these mutations, which are likely to precipitate COX deficiency through translational defects that cause a reduction in protein levels and therefore activity of respiratory chain subunits. However, occasionally a *PolgA^{+/mut}* COX deficient colonic crypt presented with just one pathogenic mutation in a complex I gene. A definitive explanation for this observation still remains to be elucidated, however complex I defects are frequently associated with complex IV defects in the ageing human colon (Greaves, Barron et al. 2010) and multiple respiratory chain defects have been observed in mitochondrial DNA disease patients that harbour pathogenic mutations in a mt-ND genes (Hinttala, Smeets et al. 2006). Furthermore respiratory chain complexes are believed to exist as ‘respirasomes’, where complexes I, III and IV associate to form supercomplexes (Schägger and Pfeiffer

2000). Complex I is believed to be fundamental in the assembly and activation of such supercomplexes (Moreno-Lastres, Fontanesi et al. 2012; Winge 2012) and indeed a respirasome will not form in the absence of one of the respiratory chain complexes (Acín-Pérez, Fernández-Silva et al. 2008). As such it is not surprising that a single pathogenic point mutation in a complex I gene could affect the structural support and activity of complex IV, thus leading to COX deficiency. Colonic crypts were observed that did not contain a single pathogenic mtDNA point mutation. Such crypts, however frequently contained multiple heteroplasmic point mutations, which in combination, could potentially precipitate COX deficiency.

Mutational analysis of mtDNA point mutations in the *PolgA^{mut/mut}* mouse germline has previously revealed strong purifying selection against mutations in the first and second codon positions of protein encoding genes (Stewart, Freyer et al. 2008). In contrast, this study revealed that somatic mtDNA point mutations in the *PolgA^{+/mut}* mouse were subject to random mutagenesis and showed an absence of evidence for purifying selection. In ageing humans an absence of selective constraints acting on somatic mtDNA point mutations was not restricted to the ageing human colon, but was also considered to be true for other human somatic tissues (Greaves, Elson et al. 2012). As such, although this study primarily focused on the colonic epithelium of the *PolgA^{+/mut}* mouse, it is expected that these findings would be replicated in other mitotic tissues. This study therefore supports that mtDNA mutations are subject to different selective constraints in germ cells and somatic cells (Greaves, Elson et al. 2012; Greaves 2014). A hypothesis derived from the Disposable Soma theory of ageing (Kirkwood 1977) has been postulated as an explanation for this phenomenon. This implies that the existence of selective constraints in germ cells may be due to selection for mitochondrial fitness during oocyte development (Cummins 1998), preventing the transmission of pathogenic mtDNA mutations to offspring via the genetic bottleneck (Stewart, Freyer et al. 2008). Pooling all available resources into reproduction to maintain species fitness would result in a lack of resources later in life and as such an absence of selective mechanisms in somatic tissues. Even in the presence of such selective mechanisms, low level heteroplasmic mtDNA point mutations are still frequently inherited through the germline (Li, Schönberg et al. 2010; Payne, Wilson et al. 2013) and data looking at the transmission of mutations in *PolgA^{mut/mut}* suggests that pre-existing germline mtDNA point mutations can exacerbate somatic mutagenesis during ageing (Ross, Stewart et al. 2013). Given that *PolgA^{+/mut}* mice display a higher frequency of inherited mtDNA point

mutations than WT mice (Vermulst, Bielas et al. 2007) the higher incidence of respiratory chain deficiency and somatic mtDNA point mutations observed in the colon of ageing *PolgA*^{+/*mut*} mice compared to normal ageing WT mice, (Greaves, Barron et al. 2011) further supports this phenomenon.

In silico modelling revealed that random genetic drift was sufficient to explain the clonal expansion of somatic mtDNA point mutations in colonic epithelial tissue from ageing *PolgA*^{+/*mut*} mice, providing evidence for a similar mechanism for clonal expansion in the ageing mouse and ageing human colon. Given that a recent study hypothesised that random genetic drift cannot explain the clonal expansion of mtDNA deletions in post-mitotic tissues of short-lived animals (Kowald and Kirkwood 2013), this study can be said to lend further support to the fact that the clonal expansion of somatic mtDNA mutations appears to be governed by the type of defect (point mutation/ deletion) and the tissue type (post-mitotic/ mitotic) (Nekhaeva, Bodyak et al. 2002; Krishnan, Reeve et al. 2008), with cell division and mitotic activity playing a fundamental role. Different tissue segregation of mtDNA in mice, has previously been shown in a mouse heterozygous for two different mtDNA genotypes (Jenuth, Peterson et al. 1997). In this study it was shown that colonic crypts in young mice displayed a mixture of the two mtDNA genotypes, later forming two diverse populations of crypts, each containing a different genotype in aged animals (Jenuth, Peterson et al. 1997). This differed somewhat to the distribution of mtDNA in the liver, kidney, spleen and blood of these mice, where a bias towards one mtDNA genotype over the other was observed (Jenuth, Peterson et al. 1997). It would therefore appear that evolution of mtDNA in colonic crypts is subject to neutral drift, whereas post-mitotic tissues appear to exhibit different selection pressures. A study examining clonally expanded somatic mtDNA mutations in different human mitotic tissues, has also revealed different mutation frequencies in the intestine, liver, pancreas and skin with the colon displaying the highest frequency of clonal expansions (Fellous, McDonald et al. 2009). Taken together these studies highly suggest that the clonal expansion of somatic mtDNA point mutations with age is strongly influenced by tissue specific differences. Therefore, whilst somatic mtDNA point mutations appear to clonally expand by random genetic drift in colonic crypts of both *PolgA*^{+/*mut*} mice and humans; this may not be a suitable mechanism for other tissues.

3.4.1 *Future work*

Given the normal lifespan and absence of premature ageing phenotypes seen in *PolgA*^{+/*mut*} mice, this mouse model would enable the investigation of clonally expanded somatic mtDNA point mutations in the context of normal ageing. This mouse model could therefore be useful for studying the interaction between mtDNA mutations and other forms of molecular damage that drive the ageing process together. A fundamental relationship between mtDNA damage, ROS and senescence is beginning to emerge within ageing (Passos, Saretzki et al. 2007) and so it would be beneficial to determine whether replicative tissues such as the colon demonstrate co-localization of mtDNA defects, such as complex IV deficiency, with senescent markers such as SA- β -GAL staining; YH2A.X staining and DNA damage foci (Hewitt, Jurk et al. 2012).

Future work would indeed involve using the *PolgA*^{+/*mut*} mouse to investigate the functional consequences of clonally expanded somatic mtDNA point mutations and respiratory chain deficiency in ageing mitotic tissues to help identify how mtDNA mutations may contribute to age related tissue dysfunction. This will be addressed further in chapter 4.

3.5 **Conclusion**

In this study I have presented evidence for a conserved mechanism for the clonal expansion of somatic mtDNA point mutations by random genetic drift, with an absence of any selective constraints, resulting in age-related respiratory chain deficiency in colonic epithelial tissue of both *PolgA*^{+/*mut*} mice and ageing humans. This suggests that the *PolgA*^{+/*mut*} mouse will be a valuable tool for studying the cellular consequences caused by the random intracellular pattern of mitochondrial dysfunction that occurs with age. Given that stem cell markers are much more robust in mouse tissues (Barker, Van Es et al. 2007) functional studies using the *PolgA*^{+/*mut*} mouse could provide valuable insights into the role of clonally expanded somatic mtDNA point mutations in human stem cell ageing, age-related tissue dysfunction and disease.

Chapter 4

Chapter 4. Results: How does age-related mitochondrial respiratory chain dysfunction affect the gene expression profile of colonic crypts and what are the potential functional effects of this upon cellular processes?

4.1 Introduction

4.1.1 *Stem cell ageing*

A decline in the replicative and regenerative function of adult stem cell populations plays a major role in age related frailty and disease (Sharpless and DePinho 2007). Typical features of ageing such as decreased wound repair in the skin, diminished immunity, hair greying and hair loss, suggest that there is deregulation of the homeostatic and regenerative properties of these tissues, due to altered stem cell function with age (Sharpless and DePinho 2007). The unique self-renewing properties of stem cells means that they accumulate age-related damage due to both chronological and replicative ageing (Liu and Rando 2011). As such genomic damage is likely to be at the forefront of age-related stem cell dysfunction, particularly in stem cells that reside in rapidly replicating tissues, such as the gut, skin and blood (Liu and Rando 2011). The age-related accumulation of molecular damage in stem cells has been hypothesised to cause changes in their normal fate or that of their progeny by three possible mechanisms (Liu and Rando 2011):

1. A decline in the stem cell pool, arising either due to replicative senescence or reduced self-renewal capacity (Maslov, Barone et al. 2004; Nishimura, Granter et al. 2005)
2. Malignant transformation and a predisposition to cancer (Liu and Rando 2011)
3. Altered differentiation and the production of abnormal progeny cells (Rossi, Bryder et al. 2005).

Dissecting and understanding the molecular mechanisms responsible for age-related changes in stem cells is vital if we want to try and maintain normal tissue homeostasis and prolong tissue repair/ regeneration in order to improve health and quality of later life.

4.1.2 *Mitochondria and stem cell ageing*

The age-related accumulation of somatic mtDNA point mutations resulting in focal respiratory chain deficiency has been reported in a number of mitotic, replicative tissues that rely on stem cells for self-renewal (Taylor, Barron et al. 2003; McDonald, Greaves et al. 2008; Fellous, McDonald et al. 2009). Stem cells are the only constant, surviving cells in mitotic tissues and so it is believed that somatic mtDNA mutations must occur and clonally expand within the stem cells (Kirkwood 2008), suggesting a potential role for mtDNA point mutations in stem cell ageing. Given the specific structural architecture of colonic crypts (see Chapter 1, section 1.6.1), the colon is an ideal tissue in which to study stem cell populations. Indeed the only functional study looking at the effects of somatic mtDNA point mutations has been performed in ageing human colonic colon crypts (Nooteboom, Johnson et al. 2010). As such the effects of mtDNA point mutations upon stem cell fate and function still remains largely unknown, with it still possible that these defects may simply be a biomarker or consequence of the ageing process.

4.1.2.1 *MtDNA mutations and colorectal cancer*

Colorectal cancer is one of the most prevailing types of cancer in both the United States and Europe, for which ageing is a dominant risk factor (Ferlay 2001; Health 2006). Given that cancer cells typically demonstrate a decrease in OXPHOS and a dramatic increase in glycolytic activity, a phenomenon known as the Warburg effect (Warburg 1930) it has long been considered that mitochondrial (respiratory chain) dysfunction plays a role in tumorigenesis and carcinogenesis. The role of mitochondria in apoptosis further supports that mitochondria become dysfunctional during cancer development, given that mutant, neoplastic cells persist and continue to proliferate, escaping cell death (Cavalli and Liang 1998). Elevated oxidative stress (Toyokuni 1995), a raised mitochondrial membrane potential (Chen 1988) and reduced expression and activity of respiratory chain complexes (Carew and Huang 2002) are also well documented features of cancer cells, supporting a potential role for mitochondrial dysfunction in cancer development.

MtDNA point mutations have been reported in a number of different cancers including gastric, lung, liver, colorectal, breast, prostate, kidney and haematological malignancies (Ivanova, Lepage et al. 1998) (Jerónimo, Nomoto et al. 2001; Nomoto, Yamashita et al. 2002; Tan, Bai et al. 2002; Lee, Yin et al. 2005). In colorectal cancer mtDNA point mutations have been reported in the D-loop of mtDNA (Lee, Yin et al. 2005; Lièvre,

Chapusot et al. 2005) and throughout the mtDNA genome (Polyak, Li et al. 1998; Nishikawa, Oshitani et al. 2005; Sui, Zhou et al. 2006). Both homoplasmic and heteroplasmic mtDNA point mutations have been detected in colorectal cancers (Polyak, Li et al. 1998; Coller, Khrapko et al. 2001; Sui, Zhou et al. 2006), with heteroplasmic mutations associated with increased tumour growth (Park, Sharma et al. 2009). A study examining an mt-*ND5* mutation in colorectal cancer suggested that mtDNA mutagenesis actually contributed to early carcinogenesis through changes in ROS production/ signaling and apoptosis (Park, Sharma et al. 2009). Other studies have also demonstrated the presence of mtDNA point mutations in precancerous lesions of gastrointestinal epithelial tissue as well as invasive tumors, suggesting that damage to the mtDNA genome occurs during early cell transformation and tumorigenesis (Sui, Zhou et al. 2006). As such it has been suggested that mtDNA point mutations can serve as an early diagnostic biomarker in colorectal cancer. Mutations in the mtDNA genome may also be an important prognostic indicator for cancer progression and survival (Lièvre, Chapusot et al. 2005), as studies have shown that a functional mitochondrial respiratory chain and intact mtDNA genome are necessary for effective treatment with anti-cancer therapies (Joshi, Li et al. 1999; Singh, Russell et al. 1999).

Whether mtDNA mutations have a causal role in early tumorigenesis and cancer development or are a result of the enhanced oxidative stress and instability of cancer cells, still remains to be elucidated. Given the stem cell hypothesis of cancer and the fact that somatic mtDNA mutations accumulate in stem cells with age, it is however plausible that the age-related accumulation of somatic mtDNA point mutations could render stem cells selectively vulnerable to malignant transformation and contribute to early tumorigenesis, giving a predisposition to cancer (Liu and Rando 2011).

Understanding the cellular changes that occur in response to the accumulation of somatic mtDNA point mutations in stem cells is therefore fundamental for both normal tissue ageing and the development of age-related diseases, such as cancer.

4.1.3 Mouse models

Given the inherent limitations of studies using human replicative tissues (as outlined in chapter 3) it is difficult to study the impact of somatic mtDNA point mutations upon stem cell function and the potential role in age-related disease and cancer development. The progressive accumulation of mtDNA point mutations has been shown to induce a profound early-onset stem cell dysfunction in *PolgA^{mut/mut}* mice, driving the ageing phenotypes seen in these animals (Norrdahl, Pronk et al. 2011; Ahlqvist, Hämäläinen et

al. 2012; Fox, Magness et al. 2012) (see Chapter 3, section 3.1.2 for more detail or (Baines, Turnbull et al. 2014)). Whilst the mitochondrial dysfunction phenotype observed in *PolgA^{mut/mut}* mice is not representative of normal human ageing, these studies demonstrated that mtDNA mutations do have a direct effect upon stem cell function, which could contribute to age-related stem cell dysfunction in humans in a similar manner, but to a reduced extent (Baines, Turnbull et al. 2014). Given that *PolgA^{+mut}* mice display a similar age-related mitochondrial dysfunction phenotype to that seen in the normal ageing human colon (see chapter 3 and (Baines, Stewart et al. 2014)), the *PolgA^{+mut}* mouse appears to be a sensible model in which to study the functional effects of somatic mtDNA mutations and respiratory chain deficiency in a stem cell population in the context of normal human ageing and disease.

4.2 Aim of the study

To identify any changes in gene expression and the potential impact this could have upon cellular processes, caused by respiratory chain deficiency and clonally expanded somatic mtDNA point mutations in colonic crypts, using the *PolgA^{+mut}* mouse as a representative model of the normal ageing human colon. I aimed to use RNA sequencing of laser-microdissected COX positive and COX deficient colonic crypts to examine their gene expression profiles and provide preliminary insights into the potential cellular responses invoked by age-related respiratory chain dysfunction and the implications this may have for disease development.

Prior to the submission of this thesis no validation experiments were performed to confirm the changes in gene expression observed in the RNA sequencing dataset. All results presented in this chapter are therefore preliminary and all discussions about the potential functional effects upon cellular processes and disease associations are hypothesis driven, indicating potentially interesting avenues to follow up on.

4.3 Experimental procedures

The transcriptome of a cell comprises the whole set of mRNAs expressed from all genes within the cell. As such transcriptomic analysis can be used to determine differences in gene expression between cells and any potential alterations in cellular and physiological processes that may result. RNA sequencing is an innovative tool that can be used to accurately determine the gene signature and level of transcripts within a cell, which can detect low level changes in gene expression and can be used on relatively small quantities of RNA (Wang, Gerstein et al. 2009).

To determine differences in the transcriptome conferred by respiratory chain deficiency in a stem cell population, RNA was extracted from laser microdissected COX deficient and COX positive colonic crypts from *PolgA*^{+/*mut*} mice and was subjected to RNA sequencing, to examine the crypt specific gene expression profiles. RNA degradation and a reduction in RNA quality has a significant impact on gene signature profiles, and can result in a false bias towards the downregulation of a number of mRNAs. To overcome RNA degradation during laser microdissection, histological identification of COX deficient crypts was combined with cresyl violet acetate alcoholic staining on colon sections cut at 20µm intervals on PEN slides, from which colonic crypts were then laser microdissected (Figure 4-1). Fixing and staining using alcoholic solutions dehydrates the tissue sections and prevents RNase activity, preserving RNA integrity for up to 90 minutes during microdissection (Clément-Ziza, Munnich et al. 2008). Laser microdissection was used to cut a population of COX positive (n=250) and COX deficient (n=250) colonic crypts from five 12 month old *PolgA*^{+/*mut*} animals. Colonic crypts were collected into buffer RLT (Qiagen RNeasy Micro Kit) containing β-mercaptoethanol, to prevent RNA degradation by RNases during collection and storage of the samples and RNA was extracted using the RNeasy Micro Kit (Qiagen).

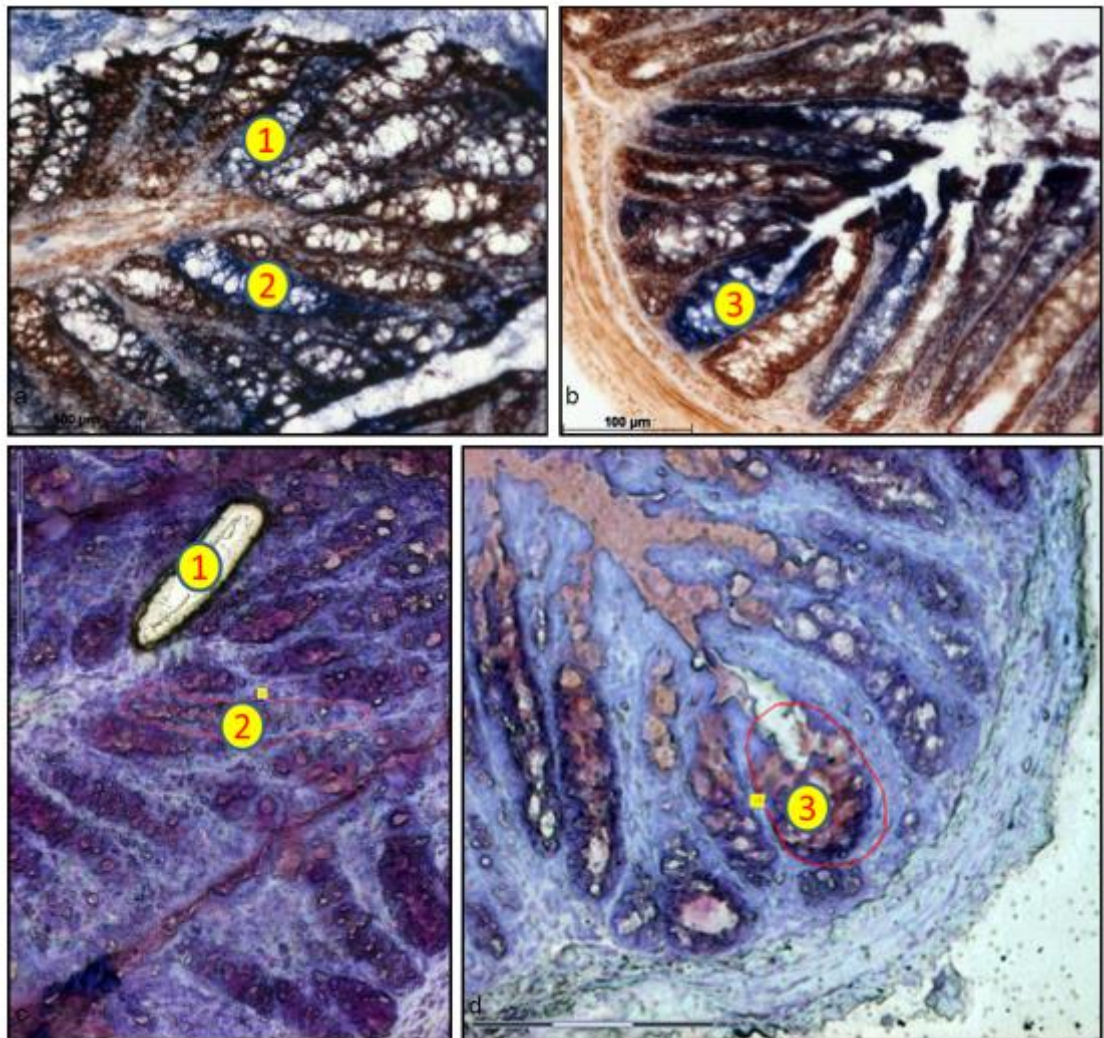


Figure 4-1: Combined COX/SDH histochemistry and Cresyl violet acetate alcoholic staining on colon sections for the identification of COX deficient and COX positive colonic crypts during laser microdissection.

COX/SDH histochemistry on colon sections from (a) *PolgA*^{+/*mut*} mouse 23 and (b) *PolgA*^{+/*mut*} mouse 45. Cresyl violet acetate alcoholic staining on sequential colon sections from (c) *PolgA*^{+/*mut*} mouse 23 and (d) *PolgA*^{+/*mut*} mouse 45 that were then used during laser- microdissection. Crypts that correspond between the two staining procedures are indicated by the numbers.

The RNA integrity number (RIN) gives a quantitative value for the relative proportion of 28S:18S rRNA within a sample, acting as a measure of the amount of RNA degradation within a sample and thus indicates the quality of the RNA (Schroeder, Mueller et al. 2006). The RIN score (RNA quality) and RNA concentration for the COX positive and COX deficient samples from each of the 5 *PolgA*^{+/*mut*} mice was determined using an Agilent 2100 bioanalyzer. Example RIN image outputs generated from the bioanalyzer are shown in Figure 4-2 and the RNA concentration and integrity for each of the ten samples is described in Table 4-1. BGI Tech solutions required a RIN score >7 and 10ng of RNA per sample for RNA sequencing. Samples were shipped to BGI Tech Solutions, China and RNA sequencing was performed using the SMARTer Library construction and sequencing (11Gb per sample) method.

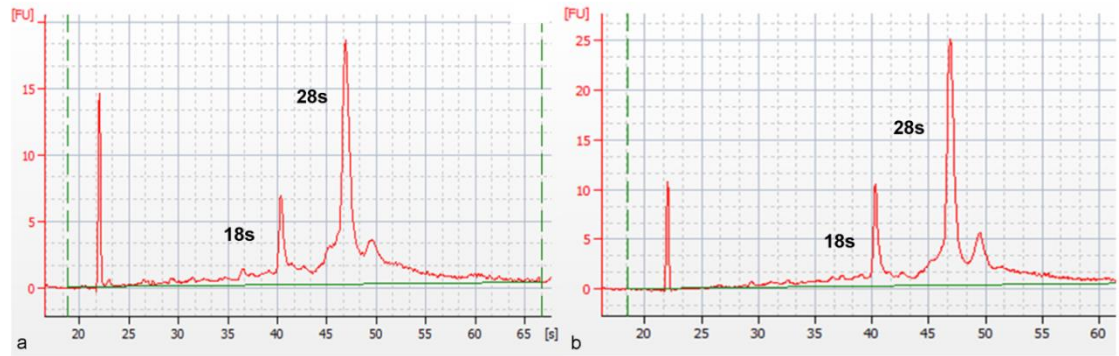


Figure 4-2: RIN output images showing the relative proportion of 28S:18S in a sample.

RIN output for (a) *PolgA*^{+/*mut*} mouse 42 COX +ve crypt sample (RIN 8.5) and (b) *PolgA*^{+/*mut*} mouse 44 COX-ve crypt sample (RIN 8.7).

Sample	RNA Conc (pg/μl)	RIN
<i>PolgA</i> ^{+/<i>mut</i>} 23 COX +ve crypts	1410	7.8
<i>PolgA</i> ^{+/<i>mut</i>} 25 COX +ve crypts	1919	8.1
<i>PolgA</i> ^{+/<i>mut</i>} 42 COX +ve crypts	1298	8.5
<i>PolgA</i> ^{+/<i>mut</i>} 44 COX +ve crypts	685	9.1
<i>PolgA</i> ^{+/<i>mut</i>} 45 COX +ve crypts	3130	8.5
<i>PolgA</i> ^{+/<i>mut</i>} 23 COX –ve crypts	574	7.3
<i>PolgA</i> ^{+/<i>mut</i>} 25 COX –ve crypts	856	7.8
<i>PolgA</i> ^{+/<i>mut</i>} 42 COX –ve crypts	454	7.9
<i>PolgA</i> ^{+/<i>mut</i>} 44 COX –ve crypts	997	8.7
<i>PolgA</i> ^{+/<i>mut</i>} 45 COX –ve crypts	673	7.9

Table 4-1: RNA concentration and RIN scores for each COX positive and COX deficient sample from the 5 *PolgA*^{+/*mut*} mouse samples.

4.4 Results

Six RNA samples, a COX positive and COX deficient sample from 3 of the *PolgA*^{+/*mut*} mice (animals 25, 44 and 45) were successfully sequenced and bioinformatic analysis performed on RNA reads, prior to completion of this thesis. Quality control analysis, statistical analysis and mapping to biological pathways, was completed by Dr Graham Smith, Bioinformatics support unit, Newcastle University.

To determine the quality of the RNA sequencing reads and identify whether any bias had resulted from RNA degradation, quality control analysis was performed using FastQC software (<http://www.bioinformatics.bbsrc.ac.uk/projects/fastqc>). This software determines the integrity of RNA based upon a number of parameters including the: sequence content and whether all the correct bases were identified in the reads; GC base

content; the length of RNA sequencing reads; sequence duplication and whether certain sequences were overrepresented in the dataset. All 6 biological samples satisfied the quality control checks and sequencing reads were subsequently mapped to the mouse genome (*Mus_musculus.GRCm38.75.fa*) using STAR (Dobin, Davis et al. 2013). RNA sequencing of each COX positive and COX deficient sample generated two technical replicates, which were individually mapped to the genome. The number of reads mapping to each gene was calculated using Ht-seq count for each replicate (Anders, Pyl et al. 2014) and replicate counts were then summed for each sample, giving a mean read count for each sample. The mean read count therefore acted as a direct measure of gene expression for each sample, giving a measure of gene expression for each gene in each of the three COX deficient samples and the three COX positive crypt samples. For a gene to be considered to be expressed in a sample an absolute gene expression criterion was used, such that at least 20 reads had to map to a gene in at least two out of the six biological samples, which was similar to the approach taken in (McLoughlin KE 2014). This revealed that 13943 genes out of a possible 39144 Ensembl mouse genes were expressed in the RNA sequencing dataset.

4.4.1 *Significant differentially expressed genes in *PolgA*^{+mut} COX deficient colonic crypts*

To identify any significant changes in gene expression between COX positive and COX deficient colonic crypts statistical analysis was performed using the DESeq2 Bioconductor package version 1.2 (Love, Huber et al. 2014). This used a Wald test to estimate the difference in the mean read counts (expression level) for each gene in the COX deficient crypts (all three samples combined) compared to the mean read counts (expression level) for each gene in the COX positive crypts (all 3 samples combined). This therefore estimated the difference in mean expression level for each gene between the two sample populations (similar to a paired t test) for normally distributed data. When comparing the mean read counts (expression level) for each gene between the COX deficient and COX positive crypts the Wald test also takes into account the variation (standard deviation) in the difference between the read counts for each mouse. In simple terms the difference in gene expression (read counts) is calculated between the COX deficient and COX positive sample from the first mouse and then the same for the second mouse and the third mouse, and the difference between these is averaged across the three mice and used to calculate the standard deviation, which is corrected for the effect of the baseline variability between the animals. The estimate of the standard

deviation is then stabilised for each gene using an Empirical Bayes correction (Smyth 2004), which incorporates evidence from the variability of other genes with similar expression levels in the dataset i.e. it assumes that genes with more or less the same expression level will tend to have more or less the same variability. A p value of <0.05 , adjusted using a Benjamini-Hochberg (BH) correction, was used to identify those genes that were significantly differentially expressed (DE) between the COX deficient crypts and the COX positive. The BH correction was used to correct for the expected number of false positives within the dataset, based on the assumption that 5% of the total number of genes (13947) would be expected to be false positives (697 genes) if an unadjusted p value of <0.05 was used. Throughout this chapter COX deficient crypts refers to all three samples combined and COX positive crypts refers to the three COX positive crypt samples combined.

Using the above criteria, COX deficient colonic crypts displayed 280 genes that were significantly differentially expressed compared to COX positive colonic crypts, of which 126 were significantly upregulated and 154 were significantly downregulated. When the BH correction was applied 14 of these genes were expected to be false positives, and as such this is taken into consideration when the test determines the statistical significance for each gene. Given the large number of genes that were significantly different between the two populations, a log₂ fold change (FC) (<1 or >1) was also applied, such that the expression level had to have increased by more than double in COX deficient crypts compared to COX positive (>1) or the expression level had to have decreased by more than half in the COX deficient crypts (<1). This identified 63 genes that were significantly upregulated and 58 genes that were significantly downregulated in the COX deficient colonic crypts compared to COX positive crypts (Figure 4-3).

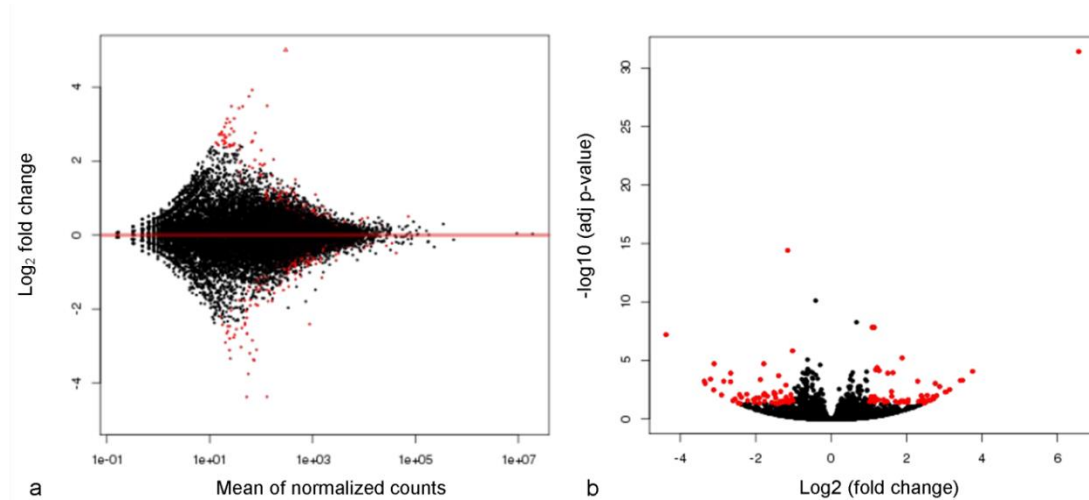


Figure 4-3: Genes that were significantly differentially expressed, with the highest log fold change in the COX deficient crypts versus the COX positive crypts.

(a) DESeq2 MA plot (log₂ FC versus the number of reads mapped for each gene) representing the mean expression level of genes. Note that genes are shown here (to the left of the plot) that only have 1 read mapping to them. (b) A volcano plot (log₂FC versus the log of the adjusted *p* value) showing all DE genes in COX deficient colonic crypts (all 3 samples combined) compared to COX positive crypts (all three samples combined). Red dots represent those significant DE genes (BH adjusted *p* <0.05) with the highest log₂FC (<1 or >1) and black dots represent those DE genes that were filtered out based on either: a lack of statistical significance or did not meet the fold change criteria. Figures courtesy of Dr Graham Smith.

Genes that were significantly differentially expressed (BH adjusted *p* value <0.05) and had more than doubled/ halved in their expression levels (log₂FC of <1 or >1) in COX deficient crypts compared to COX positive crypts (n=120) were subsequently mapped to biological pathways using both KEGG (Kanehisa and Goto 2000; Kanehisa, Goto et al. 2006) and Reactome (Joshi-Tope, Gillespie et al. 2005; Croft, Mundo et al. 2014), to identify the cellular processes these genes were involved in and develop potential hypotheses for the functional consequences these changes could have. Two biological pathway mapping packages were used as they differ in the number of genes they contain and the gene annotation to biological pathways, which is mainly due to differences in the modification and updates of the two systems, with Reactome being updated much more recently than KEGG. Pathways in Reactome also show a hierarchical arrangement of the genes, whereas those in KEGG do not, such that sometimes only genes that are crucial to the function of a pathway will be described, and other genes, such as those that facilitate cross-talk between pathways, may be missed out. Furthermore many pathways in KEGG relate to disease processes and in Reactome they are predominantly cellular processes. As such both biological pathway packages were used in the analysis to enable the mapping of a greater number of genes to a greater number of cellular processes, with certain significant DE genes in COX deficient crypts only mapping to cellular processes in KEGG pathways and others only mapping to pathways in

Reactome. Out of the 39144 Ensembl mouse genes identified, 6660 of these map to 225 biological pathways in KEGG and 6422 genes map to 1402 pathways in Reactome.

Upon mapping of significant DE genes to biological pathways in both KEGG and Reactome a further filter was applied, such that >50% of genes had to be normally expressed in a given pathway, to act as a further control on the data. This criterion was used given that a local minimum of 0.5 for the fraction of genes expressed in both KEGG and Reactome was observed (Figure 4-4). Given the difference in gene number and annotation to cellular processes in KEGG and Reactome (see above), when this criteria was applied 13 significant DE genes were mapped to the same biological pathway in both KEGG and Reactome (Table 4-2), 11 significant DE genes mapped to pathways in KEGG alone (Table 4-3) and 11 genes mapped to Reactome pathways alone (Table 4-4). Note that the pathway completeness criterion only eliminates ~10% of pathways mapped to both KEGG and Reactome (Figure 4-4), and the substantial reduction in the number of DE genes mapped to pathways (from 121 to 55) is primarily due to the fact that only a sixth of all possible mouse Ensembl genes have been annotated to biological pathways in KEGG and Reactome (see above).

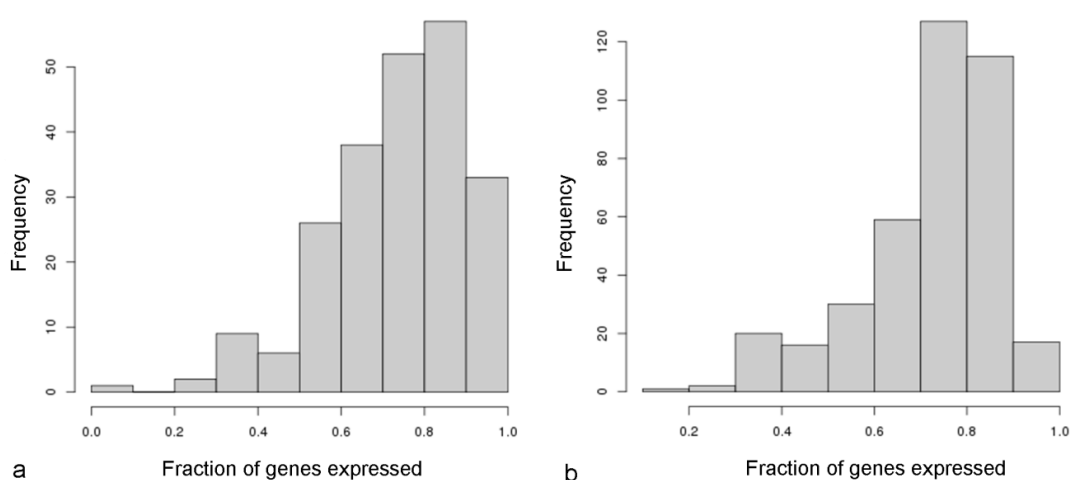


Figure 4-4: The fraction of genes expressed in biological pathways at different pathway completeness's for (a) KEGG pathways and (b) Reactome pathways.

A local minimum of 0.5 is observed in both cases and so a pathway completeness of >50% was chosen for basal gene expression in biological pathways using both pathway packages. Figures courtesy of Dr Graham Smith.

The function of each gene and the role within cellular processes was determined using Uniprot, Gene ontology (GO) Terms and Pubmed for all significant DE genes mapped to biological pathways in both KEGG and Reactome to form potential hypotheses for how the change in gene expression may affect cellular processes. Functional analysis of genes revealed a significant difference in the gene expression profiles of COX deficient

colonic crypts compared to COX positive crypts, namely genes associated with: the cell cycle, proliferation and differentiation; cell adhesion and epithelial permeability; DNA maintenance and repair and the immune response (Figure 4-5). I will therefore predominantly discuss those genes associated with these cellular processes, the potential effects this may have upon function of a pathway and any potential associations this may have with disease.

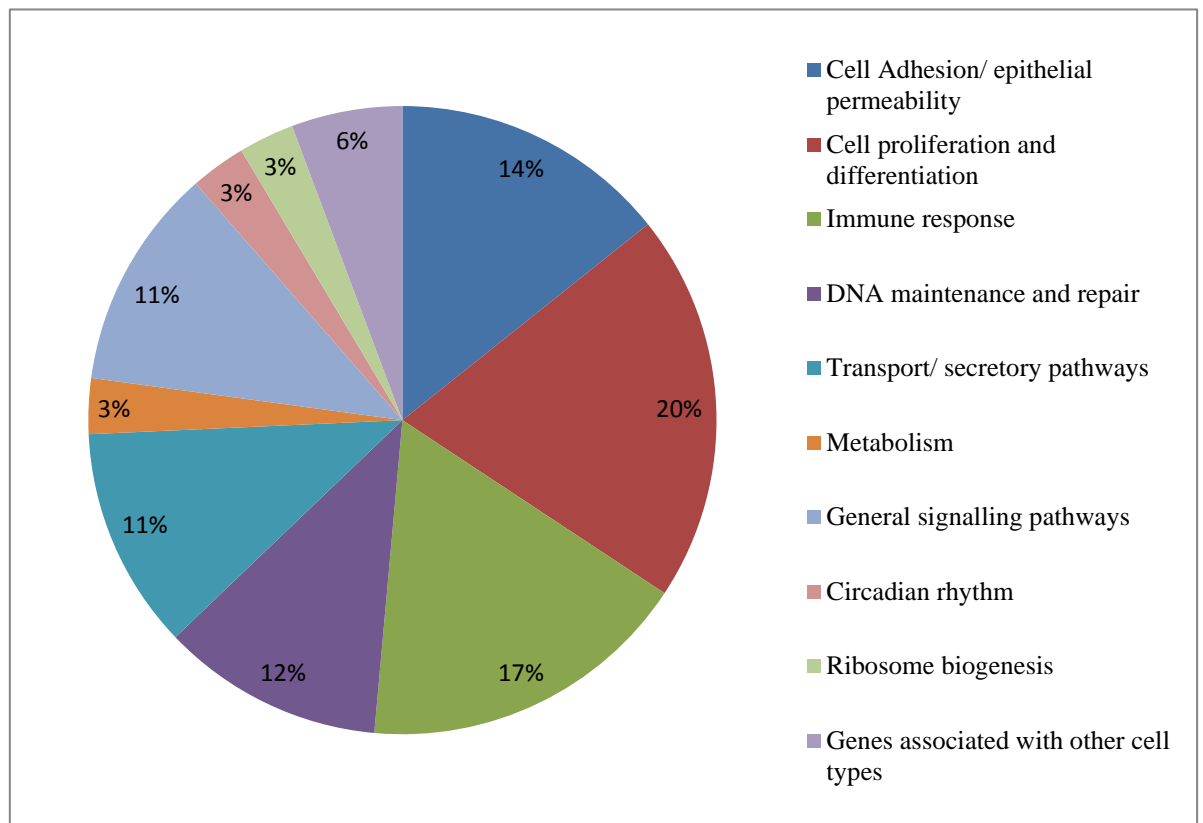


Figure 4-5: Gene ontology categories of the significant DE genes in COX deficient colonic crypts compared to COX positive colonic crypts.

Those genes expressed on other cell types are likely to be irrelevant to changes in colonic crypts as their function only concerns immune or neuronal cells. This may be a result of contamination in the samples.

4.4.1.1 *KEGG and Reactome combined*

Thirteen significant DE genes mapped to the same cellular pathway in both KEGG and Reactome, which are described in Table 4-2.

Gene Name	Description	Pathway/ Function	<i>p</i> value	BH Adj <i>p</i> value	Log2 FC
Upregulated					
Erc4	DNA repair endonuclease XPF	DNA maintenance. Nucleotide excision repair	0.000279	0.0224	+1.39
Esp11	Extra spindle pole bodies 1 (separin)	Cell cycle. Chromosome segregation.	0.0000283	0.00458	+1.6
Ippk	Inositol pentakiphosphate kinase	Phosphatidylinositol signalling. Role in mRNA export, DNA repair, focal adhesions, tight junctions.	0.000612	0.036	+1.15
Zbtb17	Zinc finger and BTB domain-containing protein 17 (MIZ-1)	Transcription factor that regulates genes involved in the cell cycle	0.0000000 414	0.0000406	+1.22
Downregulated					
Adcy1	Adenyl cyclase 1	Synthesis of cAMP in a number of cell signalling pathways	0.0000738	0.0089	-2.91
Fgf7	Fibroblast growth factor 7 (keratinocyte growth factor)	Cell proliferation and differentiation	0.0000548	0.0076	-1.5
H2-DMb2	Histocompatibility complex 2 beta 2	Immunity and antigen presentation.	0.0000010 3	0.000392	-3.198
Il1rap	Interleukin 1 receptor associated protein 1	Il-1 signalling. Role in apoptosis.	0.000362	0.0264	-1.09
Itgb7	Integrin beta-7	Focal cell adhesion	0.0000000 149	0.0000193	-3.103
Pard6g	Partitioning defective homolog gamma	Asymmetric cell division and cell polarisation	0.0000673	0.00841	-1.75
Per2	Period circadian protein homolog 2	Circadian rhythm. Regulates vast number of physiological functions	0.000569	0.0343	-1.16
Plod2	Procollagen-lysine,2-oxoglutarate 5-dioxygenase 2	Stability of collagen cross links	0.000139	0.0141	-2.38
Rdh10	Retinol dehydrogenase	Embryonic development and visual pathways	0.0000000 0087	0.0000015 1	-1.02

Table 4-2: Significant DE genes mapped to biological pathways in both KEGG and Reactome.

BH: Benjamini-Hochberg adjusted *p* value. FC: fold change.

Three significant DE genes, *Esp11*, *Zbtb17* and *Fgf7*, in COX deficient crypts were associated with the cell cycle and cell proliferation. *Esp11* is responsible for chromosome segregation during the cell cycle and was upregulated in COX deficient crypts. Studies have suggested that *Esp11* is an oncogene as overexpression is associated with premature separation of chromosomes and aneuploidy in tumours (Zhang, Ge et al. 2008), and it is upregulated in a number of malignancies, where it is associated with an increased risk of metastasis and a poor prognosis (Meyer, Fofanov et al. 2009). *Zbtb17*, suppresses negative regulators of the cell cycle that cause growth arrest, namely p21

(Vousden 2002) and prevents cell death by inducing expression of the anti-apoptotic factor BCL2 (Patel and McMahon 2007) and suppressing tumour necrotic factor (TNF) induced apoptosis (Liu, Yan et al. 2012). It could be hypothesised therefore that overexpression of Zbtb17 in COX deficient crypts could prevent cell cycle arrest/ cell death and cause progression through the cell cycle, potentially leading to aberrant proliferation and growth. Fgf7, which was significantly downregulated in COX deficient crypts, positively regulates cell proliferation and growth, particularly cells in the intestinal epithelium. Expression of Fgf7 prolongs the survival of intestinal crypts, particularly in response to cancer therapies (Booth and Potten 2001; Potten, O'Shea et al. 2001). As such decreased expression of Fgf7 in COX deficient crypts could be associated with reduced crypt survival, which has previously been documented in the ageing human colon (Nooteboom, Johnson et al. 2010) and a poor response to anti-cancer therapies. Changes in these three transcripts associated with the cell cycle could therefore be associated with aberrant cell growth, potentially playing a role in early tumorigenesis, as well as cancer progression, given the association with a poorer prognosis.

Significant DE genes were also identified in COX deficient colonic crypts with functions in focal cell adhesion, polarisation and epithelial permeability (Itgb7 and Pard6g). Itgb7 is principally involved in cell-cell adhesion and cell-matrix adhesion and decreased expression is associated with reduced cellular adhesion (Neri, Ren et al. 2011). Itgb7 is also involved in the recruitment of lymphocytes to intestinal tissues (Gorfu, Rivera-Nieves et al. 2010). As such decreased expression of Itgb7 in COX deficient crypts could lead to diminished cell adhesions and have implications for immune responses. Pard6g forms part of the centriole and is important for asymmetric cell division, cell polarisation and the formation of epithelial tight junctions. Decreased expression of Pard6g has been associated with disturbed cell adhesion and cell migration due to disorganization of microtubules within the cytoskeleton (Dormoy, Tormanen et al. 2013). As such depletion of Pard6g in COX deficient crypts could result in decreased cell adhesion, along with Itgb7, and potentially decrease the formation of epithelial tight junctions. This could have implications for inflammatory bowel diseases (IBD) as increased epithelial cell permeability, caused by decreased maintenance of epithelial tight junctions, is implicated in the pathogenesis of IBD (Hollander 1992; McKay 2005; Mankertz and Schulzke 2007). Moreover this could also

indicate a potential increase in cell migration, which could also have implications for the invasion and metastasis of neoplastic cells.

The gene expression profile of COX deficient crypts was also different in terms of genes concerning DNA maintenance and repair (*Ercc4* and *Ippk*), which showed a general upregulation in activity. *Ercc4* was upregulated in COX deficient crypts. This is the catalytic element of a DNA repair endonuclease enzyme that protects against genome instability and is involved in telomere maintenance (McDaniel and Schultz 2008). Genes involved in the nucleotide excision repair pathway and telomere maintenance, such as *Ercc4*, are thought to predispose to cancer and contribute to aberrant growth of damaged cells; however studies have failed to find a correlation between abnormal *Ercc4* and an increased risk of cancer (Shi, He et al. 2012; Gong, He et al. 2013). *Ippk*, involved in phosphatidylinositol signalling, is also involved in DNA repair pathways, principally non-homologous end joining and this gene was significantly upregulated in COX deficient crypts. The upregulation of genes involved in DNA repair pathways in COX deficient colonic crypts could indicate a response to the instability of the mtDNA genome caused by somatic point mutations. Alternatively, it could be hypothesised that this could also enable damaged, mutagenic cells to persist by preventing cell cycle arrest/death, as with *Ippk*, where studies have shown that *Ippk* induced production of inositol hexakisphosphate 6 can prevent TNF induced apoptosis (Verbsky and Majerus 2005).

Two genes concerned with the immune response were also significantly differentially expressed in COX deficient colonic crypts. *H2-DMb2* forms part of the major histocompatibility complex, involved in antigen presentation in immune responses, and is required for intestinal IgA production against bacteria. *Il1rap* is essential for interleukin 1 signalling, which is involved in immune and inflammatory responses. Given that both of these genes were downregulated, along with *Itgb7* (see above) in COX deficient crypts, this could indicate that immune responses are decreased. However, IL-1 signalling also plays a role in apoptosis, for which there are two different forms of the *Il1rap* co-receptor, one which promotes and one which prevents apoptosis (Jensen and Whitehead 2003). It is unknown which form of this receptor was downregulated in COX deficient colonic crypts, however if it is the pro-apoptotic co-receptor, this could also play a role in the persistence of damaged, unstable cells. IL-1 receptor signalling is also important for NF κ B activation of transcription and DNA

repair pathways, and so downregulation of this co-receptor could impact upon genome stability in COX deficient crypts.

Interestingly, Per2, a core component of the circadian clock, was also significantly downregulated in COX deficient crypts, possibly suggesting that COX deficient crypts have become unsynchronised from COX positive crypts in their circadian cycle. Disturbance of this rhythm is known to play a role in ageing, cancer and metabolic syndromes. Per2 functions as a transcriptional repressor and is thought to be an important tumour suppressor gene through the regulation of several cell cycle checkpoints. A number of human malignancies display a depletion in Per2 (Mazzoccoli, Piepoli et al. 2012; Hwang-Verslues, Chang et al. 2013) and loss of Per2 is associated with abnormal growths and colon tumours in mice (Fu, Pelicano et al. 2002; Wood, Yang et al. 2008; Soták, Polidarová et al. 2013; Kelleher, Rao et al. 2014). A loss of Per2 is associated with enhanced cell proliferation, and this has been shown to be associated with overexpression of the ‘cancer causing genes’ c-MYC and β -catenin (Kelleher, Rao et al. 2014). Furthermore depleted Per2 also suspends the onset of DNA damage responses (Yang, He et al. 2012). As such the downregulation of Per2, coupled with the significant alterations in cell cycle and proliferation genes mentioned above, could suggest a potential link between mtDNA genome instability and respiratory chain deficiency with malignant transformation and carcinogenesis in colonic crypts.

4.4.1.2 *KEGG only*

As mentioned previously the fact that KEGG and Reactome contain a different number of genes annotated to different biological pathways, the hierarchical arrangement of genes is different and the different packages have been updated at different time points, some significant DE genes were only mapped to cellular pathways using KEGG. This identified an additional 11 significant DE genes in COX deficient crypts that mapped to cellular processes (Table 4-3).

Gene Name	Description	Pathway/ Function	<i>p</i> value	BH Adj <i>p</i> value	Log2 FC
Upregulated					
Cd37	Leukocyte antigen CD37	Positive regulator of Ig production. Negative regulator of cell proliferation	0.00000774	0.00172	+2.88
Epha2	Ephrin type A-receptor 2	Bidirectional signalling in cell adhesion, differentiation and cell proliferation	0.000427	0.0287	+1.92
Reln	Reelin protein	Focal cell adhesion	0.0000318	0.00499	+3.03
Llg1	Lethal giant larvae protein homolog 1	Cell polarity and epithelial integrity	0.000211	0.0186	+1.11
Pwp2	Periodic tryptophan protein 2	G ₁ phase of cell cycle and cell cycle progression	0.00000354	0.000925	+2.76
Sema4b	Semaphorin 4B	Cell differentiation (neuronal)	0.000115	0.0125	+1.09
Abcc4	ATP-binding cassette, sub-family C member 4	ATPase activity coupled to Drug transmembrane transport	0.0000000991	0.000074	+1.27
Downregulated					
Calcr1	Calcitonin receptor	Activates adeny cyclase and positively regulates Ca ²⁺ homeostasis	0.00000128	0.000434	-1.88
Mus81	Crossover junction endonuclease Mus 81	DNA repair and DNA recombination	0.000508	0.0326	-1.36
Vamp1	Vesicle associated membrane protein 1	Vesicular transport	0.000171	0.0163	-1.47
Heatr1	HEAT repeat containing protein	Ribosome biogenesis	0.0000676	0.00841	-1.49

Table 4-3: Significant DE genes mapped to KEGG pathways alone.

BH: Benjamini-Hochberg adjusted *p* value. FC: fold change.

Three of the DE genes were associated with cellular proliferation and differentiation. CD37 and Sema4b were both upregulated in COX deficient crypts; however they are unlikely to convey any changes to the colonic crypts themselves, given that all known functions of CD37 concern B and T lymphocytes and Sema4b is a signalling peptide that governs axonal extension and is therefore only concerned with neuronal differentiation. An explanation as to why somatic mtDNA mutations in the COX deficient colonic crypts could be associated with gene expression changes concerning other cell types is unknown; however the potential disturbance in the circadian rhythm could be a plausible explanation. Pwp2 was significantly upregulated in COX deficient crypts and this gene is involved in the G₁ phase of the cell cycle and determines cell cycle progression, predominantly in highly proliferative tissues (Jayasena, Trinh et al. 2011). Pwp2 regulates entry into the cell cycle through ribosome biogenesis, such that if ribosome biogenesis is reduced, entry into the cell cycle is delayed (Jayasena, Trinh et

al. 2011). Thus an overexpression of pwp2 in COX deficient colonic crypts could potentially increase entry into the cell cycle and enhance cell proliferation.

Epha2 is expressed in stem cells (Funk and Orr 2013) and is involved in cell proliferation, differentiation and cell adhesion through bidirectional signalling. Epha2 was significantly upregulated in COX deficient colonic crypts and an upregulation of Epha2 has been shown to have an oncogenic effect (Funk and Orr 2013).

Overexpression of Epha2 has been reported in a number of human cancers, where it correlates with enhanced tumour invasion and metastasis, due to a lack of cell-cell adhesion and increased cell migration (Biao-Xue, Xi-Guang et al. 2011). Epha2 is commonly overexpressed in early stage colorectal cancer (Kataoka, Igarashi et al. 2004) and is associated with an increased prevalence of liver metastases (Saito, Masuda et al. 2004), a common site of metastasis from colorectal malignancies. Increased expression of Epha2 in COX deficient colonic crypts could therefore have implications for carcinogenesis and increase the risk of metastasis, given the increased potential for cell migration. Overexpression of Epha2 has also been documented in patients with IBD and Crohn's disease (Hafner, Meyer et al. 2005). Reln, associated with focal cell adhesions, was also significantly upregulated in COX deficient crypts. Expression of this gene is reported in the colon; however most of the literature is concerned with neuronal cell adhesion and migration. As such it is unclear whether upregulation of Reln could also affect cell migration in the colon. Llg1 was also overexpressed in COX deficient crypts, which is involved in cell polarity and maintaining epithelial cell integrity. The potential association of this gene with tumorigenesis is unclear given that the human homolog is downregulated in certain end-stage, progressive malignancies, but it is expressed in other cancers (Schimanski, Schmitz et al. 2005). Overexpression of this gene is, however associated with reduced formation of epithelial cell junctions and so overexpression could potentially contribute to enhanced cell migration in COX deficient crypts. Alternatively reduced formation of epithelial cell junctions, could also have implications for the development of IBD due to increased epithelial permeability (Hollander 1992; Mankertz and Schulzke 2007), as mentioned previously.

Mus81 was also identified in KEGG pathways, which is a crossover junction endonuclease with a role in DNA damage responses. Downregulation of this gene in COX deficient colonic crypts could therefore have implications for DNA repair and enhance genome instability, which could have implications for early cell transformation during carcinogenesis. Interestingly an ABC transporter gene, Abcc4, was also

significantly upregulated in COX deficient colonic crypts. This is a multidrug resistance protein, known to suppress the action of certain anti-cancer drugs (Tian, Zhang et al. 2005). Indeed the expression of Abcc4 has been reported in a number of cancer cell lines (Szakács, Annereau et al. 2004) and is associated with poor prognosis in certain malignancies (Steinbach, Lengemann et al. 2003; Norris, Smith et al. 2005). As such overexpression of this protein in COX deficient colonic crypts could hold implications for responses to anti-cancer therapies and contribute to enhanced tumour progression.

4.4.1.3 *Reactome Only*

Mapping of significant DE genes to Reactome pathways revealed a further 11 genes and cellular processes, not identified in Reactome due to reasons mentioned previously, that could also be affected by COX deficiency in colonic crypts Table 4-4).

Gene Name	Description	Pathway/ Function	<i>p</i> value	BH Adj <i>p</i> value	Log2 FC
Upregulated					
Cyp4b1	Cytochrome P450 4B1	Fatty acid and biological oxidations	0.000118	0.0127	+2.71
Itgax	Integrin alpha x receptor	Receptor for fibrinogen expressed on dendritic cells. Mediates cell-cell interaction during inflammatory responses	0.000234	0.0197	+2.43
Pcsk1	Neuroendocrine convertase 1	Secretory pathways	0.000000202	0.000113	+1.64
Slc29a1	Equilibrative nucleoside transporter 1	Vitamin and nucleoside transport	0.0000000000012	0.0000000148	+1.09
Stard8	StAR-related lipid transfer protein 1	Rho-GTPase pathway	0.000690	0.0391	+2.03
Terf2	Telomeric repeat-binding factor 2	Telomere maintenance and DNA damage response	0.000541	0.0328	+1.02
Downregulated					
2310003H01Rik (Faap100)	Fanconi anemia associated protein of 100 kDa	DNA maintenance and repair	0.000747	0.0413	-1.11
Btla	B and T lymphocyte attenuator	Inhibits lymphocytes during immune response	0.00000361	0.000928	-3.34
Cadml	Cell adhesion molecule 1	Cell-cell adhesion in a Ca ²⁺ dependent manner	0.000828	0.0447	-1.39
Lyz1	Lysozyme C1	Bacteriolytic immune response	0.0000000000277	0.000000062	-4.38
Pfn2	Profilin 2	Regulates structure of the cytoskeleton and negatively regulates epithelial cell migration	0.000271	0.0220	-2.06

Table 4-4: Significant DE genes mapped to Reactome pathways alone.

BH: Benjamini-Hochberg adjusted *p* value. FC: fold change.

Two of these, Faap100 and Terf2 are associated with DNA maintenance and repair and hold potential links with cancer development. Faap100 is a core component of the Fanconi anemia complex, involved in DNA repair, and this was significantly downregulated in COX deficient colonic crypts. Decreased expression of this gene is associated with a high frequency of mutations, chromosomal abnormalities and DNA cross-linking in cells (Ling, Ishiai et al. 2007). As such a downregulation of this gene in COX deficient crypts could suggest reduced DNA repair and enhanced genome instability, which could hold implications for cellular transformation. Terf2 is responsible for maintaining telomere length and is therefore thought to prevent activation of cell cycle checkpoints that lead to cell arrest and senescence (Takai, Smogorzewska et al. 2003), thus promoting cell proliferation and aberrant growth. Terf2 was significantly upregulated in COX deficient colonic crypts and elevated expression of Terf2 has been documented in a number of malignancies in epithelial tissues, including gastric carcinomas, where overexpression was associated with a reduced response to anti-cancer therapies (Matsutani N 2001; Cookson 2009). Terf2 tends to be overexpressed during the invasive stage of carcinogenesis and is also associated with a reduced stimulation of natural killer (NK) cells that are involved in immune responses mounted against malignant cells (Biroccio A 2013). As such overexpression of Terf2 in COX deficient colonic crypts could prevent cell cycle arrest facilitating aberrant growth that could have a tumorigenic effect.

DE genes associated with immune responses were also identified in Reactome pathways. Btla, a negative regulator of B and T lymphocytes, was downregulated in COX deficient crypts, potentially indicating that proliferation of B and T lymphocytes may be elevated in the gut, potentially leading to an overactive immune response. However, btla is proinflammatory when it is overexpressed, as it interacts with the HVEM receptor in the gut, which has been shown to play a role in IBD pathogenesis (Shui, Steinberg et al. 2011). Downregulation of btla is therefore unlikely to be associated with an inflammatory response in COX deficient colonic crypts. The downregulation of LyZ1 in COX deficient crypts was the largest downregulation in the whole dataset. LyZ1 encodes a lysozyme involved in the destruction of bacteria, and so reduced expression of this gene could suggest a decreased immune response against bacteria in the COX deficient crypts and potentially increase susceptibility to infection. Cadm1 also has a role in the immune response through the activation of NK cells, and is believed to be a tumour suppressor. Cadm1 was significantly downregulated in COX

deficient colonic crypts and this gene has been reported to be downregulated in a number of malignancies, predominantly those of epithelial origin, where it has been associated with metastasis and a poor prognosis (Nakahata and Morishita 2012). Similarly to *Terf2*, it could therefore be hypothesised that Downregulation of *Cadm1* in COX deficient colonic crypts could enhance carcinogenesis by potentially suppressing an immune response against malignant cells. Most notably, however *Cadm1* is known for its function in cell-cell adhesions and the organization of cell junctions. As such a downregulation of this gene may also affect cell organization and disrupt epithelial permeability, with possible implications for the pathogenesis of IBD (Hollander 1992; Mankertz and Schulzke 2007).

Itgax and *Pfn2* are two other genes that were differentially expressed in the COX deficient crypts and are associated with cell-cell interactions. *Itgax* is a dendritic cell receptor that was overexpressed in COX deficient crypts. Overexpression of this gene is associated with reduced cellular interactions and has been reported in certain malignancies (Venyo 2014) and as such one could hypothesise that it could be associated with enhanced cell migration and metastasis, due to disturbed cellular adhesion in COX deficient colonic crypts. *Pfn2* suppresses epithelial cell migration, and as such the decreased expression in COX deficient crypts could again contribute to enhanced cell migration. This gene is predominantly associated with neuronal responses, however reduced expression has been reported in oral squamous cell carcinomas and was associated with worse disease progression (Ma, Zhang et al. 2011). Therefore whilst these cell-adhesion genes are associated with other cell types that are independent of colonic crypts, their abnormal expression has been associated with tumorigenesis in other tissues and could therefore indicate that such changes in COX deficient crypts could potentially be associated with tumour development.

The transporter gene, *Slc29a1*, was also significantly upregulated in COX deficient colonic crypts compared to COX positive crypts. High expression of this nucleoside transporter has been associated with a low response to 5- fluorouracil, a common anti-cancer treatment used in patients with colorectal cancer (Phua, Mal et al. 2013). As such it would appear that COX deficiency in colonic crypts could be associated with enhanced expression of transporters that convey resistance to anti-cancer therapies (see also *Abcc4* above), which could have important implications for the progression of colorectal cancer. Finally of interest was the upregulated expression of *Cyp41b* in COX deficient colonic crypts. This enzyme is involved in fatty acid (β) oxidation, and as such

could suggest that COX deficient crypts are attempting to compensate for the dysfunctional respiratory chain by boosting processes that would increase the substrates available for OXPHOS and ATP production.

4.4.2 Gene set enrichment analysis

The gene expression profile of COX deficient colonic crypts was also compared to COX positive crypts using Gene Set Enrichment Analysis (GSEA) (Subramanian, Tamayo et al. 2005) to further identify the potential functional consequences that COX deficiency may have on colonic crypts. GSEA identifies pathways that contain a number of genes that were up or down regulated, that individually did not reach statistical significance, but in combination could affect the activity of that cellular process. Again given the difference in genes, their annotation and updates of the two biological software packages GSEA analysis was performed separately for both KEGG and Reactome, to identify potential differences that may occur in cellular processes in COX deficient colonic crypts. GSEA analysis of gene expression was measured on the basis of log₂ fold-change, the unadjusted nominal *p* value (<0.05) and the false discovery rate (FDR) *q* value, which was used to correct for false positives, given the small sample sizes of only n=3 for the two populations. Again a pathway completeness criterion was applied, such that >50% of genes had to be expressed basally in a given pathway, and a pathway was required to contain a minimum of 15 genes and a maximum of 750 genes to further filter the results and identify those cellular processes that could be different in COX deficient colonic crypts compared to COX positive crypts. All pathways identified showed a combination of both up and down regulated genes, which were combined to give an average logFC for that pathway. Thus a broadly upregulated pathway would, and did contain genes that were downregulated, giving a fairly minimal average logFC, as seen in Table 4-5 and Table 4-6.

The GSEA analysis of pathways broadly affected in COX deficient colonic crypts gave complementary results to those genes and pathways identified with significant differential expression, showing potential alterations in pathways predominantly concerning: DNA maintenance and repair; cell adhesion; immune responses and energy metabolism.

4.4.2.1 GSEA analysis of Reactome pathways

GSEA analysis with Reactome pathways revealed a general upregulation of genes in 8 pathways and a general downregulation of genes in 9 pathways in COX deficient colonic crypts compared to COX positive crypts (Table 4-5).

Pathway	<i>p</i> value	FDR <i>q</i> value	Average Log ₂ FC	Pway size	NSeen
Upregulated					
Meiosis	0.00631	1	+0.095	141	85
Meiotic recombination	0.00851	1	+0.105	108	61
Retinoid metabolism and transport	0.02394	0.826	+0.122	49	31
Extension of telomeres	0.02804	1	+0.271	25	21
Telomere C-strand (lagging strand) synthesis	0.03501	0.979	+0.271	23	20
Chromosome maintenance	0.03528	1	+0.075	173	113
Meiotic synapsis	0.04077	1	+0.059	122	71
Gluconeogenesis	0.04539	1	+0.167	57	30
Downregulated					
Respiratory electron transport	0.000209	0.332	-0.145	105	80
Respiratory electron transport, ATP synthesis by chemiosmotic coupling and heat production	0.000644	0.561	-0.132	132	97
Immunoregulatory interactions between a lymphoid and non-lymphoid cell	0.000841	0.234	-0.214	96	49
Activated TAK1 mediates p38 MAPK activation	0.037128	1	-0.162	24	18
Interferon gamma signalling	0.038324	0.614	-0.132	75	57
Glutamate binding, activation of AMPA receptors and synaptic plasticity	0.038359	0.903	-0.159	32	17
Trafficking of AMPA receptors	0.040657	0.781	-0.159	32	17
Molecules associated with elastic fibres	0.042201	0.816	-0.275	37	27
MHC Class II presentation	0.048418	0.928	-0.0822	103	82

Table 4-5: Cellular pathways identified in Reactome that are broadly upregulated and broadly downregulated in COX deficient colonic crypts compared to COX positive.

FDR *q* value: the adjusted *p* value. P way size: the number of genes that belong to the pathway, Nseen: the number of genes in the pathway that were expressed in the RNA sequencing dataset.

Reactome pathways in which DE genes were broadly upregulated, indicating that activity of these processes could be increased in COX deficient crypts, were principally involved in chromosome/telomere maintenance (Extension of telomeres, Telomere C strand synthesis and chromosome maintenance). Given that telomere shortening is a dominant trigger of replicative senescence and cell cycle arrest, it is well established that factors which maintain/ elongate telomeres play a fundamental role in aberrant cell growth, transformation and carcinogenesis (Meyerson, Counter et al. 1997; Cech 2004; Reddel 2014). As such the upregulation of these pathways acting to maintain chromosomes and telomeres in COX deficient crypts could indicate that growth arrest of damaged cells was suppressed, promoting aberrant cell growth and transformation. A number of genes involved in biological pathways concerning meiosis were also broadly upregulated in COX deficient crypts; however these are largely irrelevant in the colon, given that meiosis only occurs in germ cells. A broad upregulation in gluconeogenesis, the pathway responsible for metabolising non-carbohydrate carbon molecules into glucose, was also observed in COX deficient crypts. Gluconeogenesis predominately occurs in the liver; however it has been reported in the intestine (Mithieux, Rajas et al. 2004). As glucose is the primary substrate for glycolysis, a potential increase in glucose production in COX deficient crypts could indicate a switch in energy metabolism from OXPHOS to glycolysis, which is a hallmark of malignant cells (Warburg 1930).

Unsurprisingly pathways that were broadly downregulated in COX deficient crypts did indeed concern the respiratory electron transport chain and associated ATP production. This was to be expected given that these crypts show reduced/ absent activity of complex IV, suggesting a potential reduction in ATP production via OXPHOS. A number of pathways involved in immune responses, also negatively correlated with the COX deficient phenotype in crypts. Interferon gamma signalling and MHC class II presentation are important in the adaptive immune response, and as such a potential downregulation in their activity could indicate decreased mucosal immune responses to bacteria in COX deficient crypts. Interferon gamma signalling is also important for activation of NK cells, and downregulated activity of this pathway could therefore imply a reduction in NK cell responses (Gattoni, Parlato et al. 2006), which could have implications for immune responses against tumour cells (Moretta 1994).

4.4.2.2 GSEA analysis of KEGG pathways

GSEA analysis with KEGG revealed 4 pathways that showed a general upregulation in gene expression and 13 pathways with a general downregulation in gene expression in COX deficient colonic crypts (Table 4-6).

Pathway	<i>p</i> value	FDR <i>q</i> value	Average Log ₂ FC	Pway size	NSeen
Upregulated					
Fructose and Mannose metabolism	0.0319	1	+0.186	37	33
Pentose and glucuronate interconversions	0.0368	1	+0.212	31	21
Amino acid and nucleotide sugar metabolism	0.0471	0.789	+0.154	48	40
Galactose metabolism	0.0475	0.754	+0.145	27	21
Downregulated					
Cell adhesion molecules	0	0.021	-0.210	149	87
Staphylococcus aureus infection	0.000206	0.003	-0.452	50	31
Leishmaniasis	0.003308	0.156	-0.238	64	52
Leukocyte transendothelial migration	0.005534	0.215	-0.129	120	89
Salivary secretion	0.006281	0.125	-0.199	77	51
Intestinal immune network for IgA production	0.010084	0.142	-0.381	43	25
Rheumatoid arthritis	0.01513	0.287	-0.206	81	55
Parkinson's disease	0.026598	0.434	-0.103	148	116
Oxidative phosphorylation	0.033646	0.417	-0.097	147	118
Gap junction	0.034847	0.411	-0.109	88	66
Chemokine signalling pathway	0.03798	0.445	-0.106	185	132
Fc gamma R-mediated phagocytosis	0.039572	0.436	-0.124	90	78
Renal cell carcinoma	0.040151	0.420	-0.155	71	63

Table 4-6: Cellular pathways mapped to KEGG that are broadly upregulated and broadly downregulated in COX deficient colonic crypts compared to COX positive.

FDR *q* value: the adjusted *p* value. P way size: the number of genes that belong to the pathway, Nseen: the number of genes in the pathway that were expressed in the RNA sequencing dataset.

Interestingly the broadly upregulated pathways in COX deficient colonic crypts were all involved in sugar metabolism, that function to produce glucose, the primary substrate for glycolysis, from the catabolism of complex sugars, amino acids and nucleotides. Fructose and mannose metabolism, which were upregulated in COX deficient crypts, can also directly feed into and drive glycolysis. As such a potential upregulation in activity of these pathways could suggest that COX deficient crypts show enhanced glycolysis, again indicating that there is switch in energy metabolism from OXPHOS to glycolysis, a well-established feature of malignant cells, which have a high glucose demand (Warburg 1930; Carew and Huang 2002).

Broadly downregulated pathways in KEGG again revealed DE genes involved in OXPHOS, with a substantial number of DE genes in both Complexes I and IV of which many were downregulated, suggesting a possible decrease in activity of these complexes. All components of complex III were also differentially expressed and as such altered activity of these three complexes lends support to the fact that they associate to form respirasomes (Schägger and Pfeiffer 2000). The general downregulation of a number of genes involved in OXPHOS again supports a switch in energy metabolism from OXPHOS to glycolysis in COX deficient crypts, which may have a potential role in priming cells for early transformation and increasing sensitivity to carcinogenesis (Warburg 1930).

A number of KEGG pathways containing DE genes that were negatively correlated with COX deficiency in colonic crypts were involved in specific disease development and are irrelevant in the colon, such as Leishmaniasis, Parkinson's disease and Rheumatoid arthritis. However, a change in gene expression in these pathways could indicate a potential role for somatic mtDNA mutations and respiratory chain deficiency in the disease pathogenesis of these disorders. Pathways involving cell adhesion molecules again contained DE genes, which were broadly downregulated and included *Cadm1* and *Itgb7* which are mentioned above. Downregulated expression of cell adhesion molecules could affect cell adhesion and epithelial permeability, lending support to a potential role in IBD pathogenesis (Hollander 1992; Mankertz and Schulzke 2007). Alternatively it could indicate that there would be disturbances in cellular organization that may encourage cell migration, playing a role in metastasis (Nakahata and Morishita 2012). Furthermore the intestinal production of IgA, a critical component of mucosal immunity (Peterson and Artis 2014) was also broadly downregulated in COX deficient crypts,

which could hold implications for the mucosal immune response and the epithelial barrier function in COX deficient crypts.

Given that a number of biological pathways in KEGG are associated with disease processes, GSEA analysis using KEGG also revealed that a substantial number of genes were differentially expressed in pathways involved in cancer and colorectal cancer in COX deficient crypts compared to COX positive crypts. These pathways were not listed in the above tables due to filtering based on the absolute basal gene expression criterion used for GSEA analysis. Nevertheless such a high number of DE genes in these pathways is very interesting and indicates that they could be affected in COX deficient crypts, providing further evidence for a potential link between age-related respiratory chain deficiency in colonic crypts, a selective vulnerability to malignant transformation and a predisposition to cancer.

4.5 Discussion

Clonally expanded somatic mtDNA point mutations and respiratory chain deficiency have been reported in a number of ageing mitotic tissues (Taylor, Barron et al. 2003; McDonald, Greaves et al. 2008; Fellous, Islam et al. 2009; Gutierrez-Gonzalez, Deheragoda et al. 2009); however the effects of these mutations upon stem cell fate and function still remain to be elucidated. To begin to address this problem I employed RNA sequencing of COX deficient and COX positive colonic crypts from *PolgA*^{+/*mut*} mice, previously shown to be a good model of age related mitochondrial dysfunction in the ageing human colon, (see Chapter 3 and (Baines, Stewart et al. 2014)) to examine the gene expression profiles and uncover any possible changes in cellular processes that might be associated with age-related respiratory chain deficiency. Given that no validation experiments were performed prior to the completion of this thesis it is important to emphasize that all changes in cellular processes and the potential disease associations discussed here are all based on hypotheses that simply highlight potentially interesting relationships. Preliminary data from the RNA sequencing results in this study indicated that COX deficient crypts show a differential gene expression profile, largely with respect to: the cell cycle, proliferation and differentiation; DNA maintenance and repair; immunity; cell adhesion and epithelial permeability and energy metabolism. Furthermore these observations indicated a potential association of age-related COX deficiency in colonic crypts with tumorigenesis and a predisposition to colorectal cancer as well as the disease pathogenesis of IBD.

4.5.1 *Potential implications for aberrant cell growth and tumorigenesis in colonic crypts*

It has been proposed that the clonal expansion of somatic mtDNA mutations in ageing human colonic crypts could contribute to genome instability and potentially prime stem cells for early transformation playing a role in cancer initiation and development (Taylor, Barron et al. 2003; Greaves, Preston et al. 2006). Preliminary results from this study suggested that age-related COX deficiency could be associated with cancer initiation and development in colonic crypts through potential changes in the cell cycle, proliferation, DNA repair and cell migration. The altered gene expression profile between COX deficient crypts and COX positive crypts revealed 5 potential mechanisms by which such changes could play a role in tumorigenesis:

1. Enhanced progression through the cell cycle and aberrant cell proliferation by: increasing entry into the cell cycle (Pwp2); suppressing negative regulators of the cell cycle (Zbtb17) and enhancing genes/pathways that maintain DNA and telomeres (Ercc4, Ippk, Terf2 and upregulation of pathways concerning chromosome maintenance and the extension/synthesis of telomeres) that could enable cells to bypass cell cycle checkpoints and prevent cell cycle arrest, potentially leading to aberrant cell growth and the persistence of damaged cells.
2. Reduced cell adhesion and enhanced cell migration, potentially promoting invasion and metastasis of malignant cells (Epha2, Pfn2, Llg11 and downregulation in pathways concerning cell adhesion molecules).
3. Genome instability and chromosomal aberrations (Esp11, Faap100 and Mus81).
4. Increased expression of transporters associated with resistance to anticancer therapies (Abcc4 and Slc29a1).
5. Switch in energy metabolism from OXPHOS to glycolysis (downregulated gene expression in the ETC and OXPHOS pathways and enhanced expression of genes involved in pathways that produce glucose that could enhance glycolysis).

As such there are a number of potential mechanisms by which the differential gene expression profile of COX deficient colonic crypts could be associated with cancer initiation and development lending support to a potential association between age-related mitochondrial dysfunction in colonic crypts, an increased vulnerability to malignant transformation and a predisposition to the development of age-related colorectal cancer (Taylor, Barron et al. 2003; Greaves, Preston et al. 2006). Indeed previous studies do support similar changes in gene expression associated with

mitochondrial respiratory chain defects as cells with mitochondrial dysfunction have been shown to harbour altered expression of genes that regulate cell cycle progression and growth (Crimi 2005; Cortopassi, Danielson et al. 2006; Compton, Kim et al. 2011) as well as the “cancer causing gene” c-Myc (Miceli and Jazwinski 2005; Cortopassi, Danielson et al. 2006). Alterations in genome stability have also been reported (Elstner and Turnbull 2012) and metabolic defects have been directly associated with COX deficiency in rat skeletal muscle fibers (Herbst, Johnson et al. 2013).

The mechanism by which somatic mtDNA point mutations and respiratory chain deficiency could predispose to the development of cancer is unknown. However, a simple explanation could simply be the reduced OXPHOS capacity of respiratory chain deficient cells, which could promote a switch in energy metabolism and prime stem cells for early transformation contributing to tumour initiation and development (Warburg 1930). Alternatively it could be hypothesised that mitochondrial respiratory chain dysfunction could affect the sensitivity of cells to transformation by affecting pathways in which Ca^{2+} is a key signalling molecule i.e. pathways implicated in cancer in which *Per2* and *Fgf7* were downregulated. Calcium sequestration in mitochondria is dependent upon the negative mitochondrial membrane potential, maintained by the ETC and defects in the ETC have been shown to affect Ca^{2+} homeostasis, as seen in the TFAM knockout mouse with mitochondrial diabetes (Silva, Köhler et al. 2000). Alterations in Ca^{2+} homeostasis, caused by the defective respiratory chain in COX deficient crypts, could therefore affect the above signalling pathways, providing a potential link between COX deficiency and the alterations seen in pathways concerning cellular proliferation.

An alternative hypothesis could be that somatic mtDNA point mutations may drive cellular changes that increase sensitivity to tumorigenesis through altering ROS production. Enhanced ROS production was observed in a human colorectal cancer cell line carrying a mtDNA point mutation, and this was shown to promote tumour development (Park, Sharma et al. 2009). Furthermore studies in the *PolgA^{mut/mut}* mouse have recently shown that mtDNA mutations are associated with an increase in ROS production with age (Logan, Shabalina et al. 2014) and studies in replicative tissues of these mice have shown that stem cell function is sensitive to slight changes in redox status (Ahlqvist, Hämäläinen et al. 2012). Moreover ROS are critical signalling molecules in stem cell proliferation and differentiation events (Hamanaka and Chandel 2010; Shao, Li et al. 2011) and the accumulation of mtDNA mutations in the intestine

of *PolgA^{mut/mut}* has been directly associated with enhanced proliferation and cell growth (Fox, Magness et al. 2012). Microarray analysis of cells with mitochondrial dysfunction representative of that which occurs in mitochondrial disease, has also revealed gene expression changes in genes associated with ROS (Van der Westhuizen, Van den Heuvel et al. 2003). Thus it could be hypothesised that somatic mtDNA point mutations in colonic crypt stem cells could cause slight alterations in ROS production, affecting pathways involved in the cell cycle and proliferation, which could render stem cells more sensitive to early cell transformation and predispose to the development of age-related colorectal cancer (Baines, Turnbull et al. 2014).

Given that cell transformation and cancer initiation is dependent upon a number of cellular insults (Grizzi, Di Ieva et al. 2006) if mtDNA mutations do contribute to tumorigenesis it could be that mtDNA mutations are associated with cellular changes in colonic crypts through a combination of the above mechanisms. The differential gene expression analysis in this study revealed a potential association between age-related respiratory chain deficiency and events that are typical in early cell transformation as well as events involved in cancer development/ progression. However, whether or not somatic mtDNA point mutations are predominantly involved in the early development of colorectal cancer by priming stem cells for transformation or are more of a prognostic biomarker playing a role in cancer progression and response to anti-cancer therapies, still remains to be elucidated. Nevertheless this potential association remains a very interesting avenue of research to follow up on, for which validating changes in gene expression and any functional effect on protein expression will be crucial.

4.5.2 Potential implications for epithelial permeability and the pathogenesis of inflammatory bowel disease in the colon

An up and downregulation of cell adhesion genes (Itgb7, Pard6g, Epha2, Cadm1 and Llg1 and cell adhesion molecule pathways) was also associated with COX deficiency in colonic crypts, with functional analysis suggesting that this could negatively impact upon cellular interactions, organization and the formation of epithelial tight junctions. A lack of tight junction formation, could increase epithelial permeability, which has in fact been proposed as an early event in the pathogenesis of IBD (Hollander 1992; Mankertz and Schulzke 2007). The formation and preservation of tight junctions is energy dependent, and so it would be unsurprising that respiratory chain deficient crypts, with a decreased capacity to produce ATP via OXPHOS, could show defects in tight junction formation and increased epithelial permeability (McKay 2005). It is therefore possible

that mitochondrial dysfunction, through alterations in epithelial permeability, could be associated with a predisposition to the development of IBD. Given that Ca^{2+} is a key signalling molecule involved in the formation of intercellular junctions, for example through *Adcy1* signalling (KEGG pathways), it could also be hypothesised that respiratory chain deficiency could influence intercellular junctions and epithelial permeability through changes in Ca^{2+} ion homeostasis due to disturbances in the mitochondrial membrane potential. Patients with ulcerative colitis, a form of IBD have been shown to harbour significantly more mtDNA point mutations than controls (Nishikawa, Oshitani et al. 2005) and histochemical analysis of colonic biopsies from patients with colitis has previously revealed clusters of respiratory chain deficient crypts (unpublished data from this lab), indicating a significant level of mitochondrial dysfunction in these patients. As such age-related mitochondrial respiratory chain dysfunction could have implications for inflammatory problems and abnormal bowel movements in aged individuals.

4.5.3 Potential implications for the immune response and sensitivity to bacterial infection in colonic crypts

Differential gene expression concerning immune responses (*LyZ1*, *Il1rap*, *H2-DMb2*, *Itgb7*, *Cadm1*, interferon signalling and intestinal production of IgA) appeared to be predominantly downregulated in COX deficient colonic crypts, suggesting that immune responses could have been diminished. This could be deemed surprising given the potential association between COX deficient crypts and the pathogenesis of IBD, as you would expect there to be an overactive immune response, given that inflammation is a hallmark of inflammatory bowel disease (Fiocchi 1998). Functional analysis implied that adaptive immune responses, particularly those against bacteria could be reduced, which could hold implications for sensitivity to bacterial infections in aged individuals. Ca^{2+} is a fundamental signalling molecule in the adaptive immune response and the activation of lymphocytes, especially T cells, which are highly sensitive to intracellular Ca^{2+} levels (Cahalan and Chandy 2009). Therefore if mitochondrial respiratory chain dysfunction could affect the sequestration of Ca^{2+} ions and Ca^{2+} homeostasis this could affect signalling pathways involved in the adaptive immune response, providing a potential explanation for the changes observed in COX deficient colonic crypts. Interestingly a number of changes in COX deficient crypts were associated with decreased activation of NK cells, which hold an important role in immune defence

against malignant cells (Moretta 1994), again lending support to a potential association between mitochondrial dysfunction and a predisposition to colorectal cancer with age.

Whilst a lot of interesting observations, that have important implications for disease processes, have come to light from the RNA sequencing of COX positive and COX deficient colonic crypts of *PolgA*^{+/*mut*} mice, all results discussed in this chapter are preliminary and hypothesis based. As such these results simply highlight potentially interesting changes and give initial insights into how somatic mtDNA point mutations and respiratory chain deficiency could affect cellular processes. Validation of differential gene expression via either real-time PCR to look at mRNA levels or immunohistochemistry/ immunofluorescence to look at protein expression, will therefore be vital to confirm gene expression changes, determine whether this has a functional effect on proteins and as such whether activity of a particular cellular process is likely to be affected. Furthermore at the time this thesis was completed successful RNA sequencing and bioinformatics analysis had only been completed on COX deficient and COX positive crypts from 3 *PolgA*^{+/*mut*} mice. Successful sequencing of the laser microdissected samples I collected from the other 2 *PolgA*^{+/*mut*} animals, which is currently underway, will be important to confirm whether the differences in gene expression observed are consistent across more samples, making the statistics more robust. This would also enable better selection of genes that should be targeted for validation experiments

4.5.4 Future work

Given that all results presented in this chapter were preliminary and all potential associations are based on hypotheses, validation experiments looking at mRNA and protein expression levels need to be performed to confirm changes in gene expression and that this elicits a functional effect in COX deficient colonic crypts. It would be particularly interesting to develop antibodies against several of the cell cycle and cell adhesion genes, with implications in carcinogenesis, and look at protein expression levels via immunohistochemistry/ immunofluorescence on *PolgA*^{+/*mut*} colon sections. This could be done for genes such as *Per2*, *Esp11* and *Pfn2*, all of which showed a fairly high log₂FC, and may be more likely to convey a significant difference in protein expression. Looking at expression of *Per2* in combination with β -catenin and complex IV protein expression, could also prove very interesting, given that a depletion in *Per2* is thought to cause enhanced expression of β -catenin, driving tumorigenesis (Kelleher, Rao et al. 2014). Furthermore looking for changes in markers of nuclear DNA damage,

telomere length and senescence (Hewitt, Jurk et al. 2012) could also help uncover the potential relationship between somatic mtDNA mutations and other forms of molecular damage that occur with age.

Whilst studies have indicated that the *PolgA*^{+/*mut*} is a good representative model of mitochondrial dysfunction in the ageing human colon (see chapter 3 and (Baines, Stewart et al. 2014), and this study has provided useful insights into some potential functional effects that somatic mtDNA point mutations may have in ageing replicative tissues, ultimately similar experiments would want to be performed on ageing human colonic crypts. This would determine whether respiratory chain deficiency and somatic mtDNA point mutations do elicit similar functional effects in the two species and would help to determine whether mtDNA defects are causal in age-related tissue dysfunction and disease development.

4.6 Conclusion

In this study I have provided preliminary data suggesting that somatic mtDNA point mutations and age-related COX deficiency in colonic crypts could be associated with alterations in: the cell cycle and proliferation; DNA maintenance and repair; cell adhesion and tight junction formation; the adaptive immune response and energy metabolism. Such changes hold a number of potential implications and associations between mitochondrial respiratory chain dysfunction and the initiation and development of cancer as well as the pathogenesis of inflammatory bowel disease. The data suggests that age-related mitochondrial dysfunction could be associated with the development of age-related colorectal cancer, indicating that mtDNA defects may cause an alteration in colonic stem cell fate and function, through potentially priming stem cells for malignant transformation. Examining protein expression of a number of genes highlighted in this study will therefore be key to establish a suitable relationship between age-related COX deficiency, changes in the above cellular processes and the potential implications this may have for disease. Only then will we be able to determine the consequences of somatic mtDNA point mutations upon normal tissue homeostasis and begin to understand their potential contribution to stem cell ageing and disease development.

Chapter 5

Chapter 5. Results: M.5024 C>T tRNA^{Ala} mutation: a candidate allele for modelling mitochondrial disease in mice.

5.1 Introduction

MtDNA diseases are an extremely heterogeneous group of disorders that present with a variety of different clinical symptoms and different ages of onset, even in patients with the same mutation and functional deficit (Jacobs 2003; McFarland, Taylor et al. 2007). Heteroplasmy and the threshold effect, clonal expansion, the genetic bottleneck, mitotic segregation and tissue specificity are just a few of the factors believed to influence the heterogeneity amongst patients (Taylor and Turnbull 2005); however the functional consequences of specific point mutations and the molecular mechanisms that govern disease diversity remain largely unknown. Understandably there is a keen interest to develop models of mitochondrial DNA disease to begin to uncover such molecular mechanisms.

5.1.1 Models of mtDNA disease

Experimental models of mtDNA disease have proved challenging to develop given the difficulty/inability to directly manipulate the mtDNA genome due to: the high copy number of mtDNA within a cell, its enclosure within double-membraned mitochondria and the negligible recombination that mtDNA experiences.

Transmitochondrial cybrids, created through fusing rho⁰ cells that are depleted of mtDNA, with enucleated cytoplasts from patient cell lines containing a specific mtDNA mutation (King and Attardi 1989), have proved valuable tools for studying the relationship between specific mtDNA mutations and different nuclear backgrounds (Dunbar, Moonie et al. 1995), heteroplasmy and the consequences upon cellular function and physiology (Hayashi, Ohta et al. 1991; Chomyn, Martinuzzi et al. 1992). However, given that cybrids are developed from tumour cells it is unknown whether aneuploidy could affect mitochondrial function and the cellular transcriptome. Furthermore tumour cells are largely glycolytic and so any OXPHOS dysfunction caused by a mtDNA mutation is unlikely to precipitate the same functional effect in cybrids as would be encountered by patients (Swerdlow 2007).

Yeast models have also proved beneficial; given that it is possible to directly introduce mtDNA mutations into the mtDNA genome of *Saccharomyces cerevisiae* through biolistic transformation and homologous recombination (Bonney and Fox 2001). The sequence and structure of certain mt-tRNAs is comparable between *Saccharomyces cerevisiae* and humans and as such yeast models have been valuable for studying the pathogenicity of certain mt-tRNAs mutations (De Luca, Besagni et al. 2006; Montanari, Besagni et al. 2008) and serious mitochondrial dysfunction. However, similarities between yeast and human mt-tRNAs are indeed limited to a select few and mutations in *Saccharomyces cerevisiae* are characteristically homoplasmic, preventing the study of heteroplasmy and the threshold effect, which are significant factors that influence the diverse genotype: phenotype relationship observed in patients.

5.1.2 Mouse models of mtDNA disease

Whilst the above model systems have been useful for studying the pathogenicity of certain mtDNA mutations and the influence of nuclear backgrounds, the ultimate model of mtDNA disease would indeed be a living mammalian model, that would display characteristic features of mtDNA disease (Taylor and Turnbull 2005). Given the rapid life cycle, simple breeding and homology between the human and mouse mtDNA genome (Bibb, Van Etten et al. 1981), it is unsurprising that there is keen interest to create mice that carry pathogenic mtDNA mutations to model disease. Not only would mouse models enable the study of specific disease mechanisms and pathogenesis associated with a specific mtDNA mutation but they would also potentially enable research into: mitotic segregation and tissue specificity; disease progression, by looking at multiple stages of their lifespan; the transmission and inheritance of pathogenic mtDNA mutations through multiple generations and the development of potential treatments, through various interventions and follow-up studies.

Technologies that enable the direct recombinant modification of mouse mtDNA in a living animal model are however still very much lacking. As such, many studies have employed indirect methods to introduce mtDNA mutations into mouse models. Fruitful attempts have been achieved in creating mice that carry mtDNA deletions by using: a somatic mtDNA deletion that occurred in a cell line (Inoue, Nakada et al. 2000); manipulating nuclear encoded genes that caused the progressive accumulation of mtDNA deletions (Tyynismaa, Mjosund et al. 2005) and using mitochondrial targeted restriction endonucleases (Srivastava and Moraes 2005). Generating mice that carry mtDNA point mutations has however proved much more challenging. All successful

attempts have focused on using mouse cell lines that carry naturally occurring pathogenic mtDNA point mutations, which have resulted in the successful transmission and creation of mice harbouring the following point mutations: mt-*COI* (T6589C), mt-*ND6*-13885insC, mt-*ND6*-G13997A, mt-*tRNA*^{Lys} G7731A (Kasahara, Ishikawa et al. 2006; Fan, Waymire et al. 2008; Yokota, Shitara et al. 2010; Lin, Sharpley et al. 2012; Shimizu, Mito et al. 2014). These mouse models are described in more detail in chapter 1, section 1.5.3.

The above mouse models provided useful insights into the pathogenesis and germline transmission of specific mtDNA point mutations, of which some did indeed display characteristic features of mtDNA disease. However, generating mice carrying mtDNA point mutations through donor cell lines is very restricted, as only a few cell lines are available that carry pathogenic mtDNA point mutations, of which very few are equivalent to pathogenic mutations that cause human disease. Moreover, maintaining stable heteroplasmic cell lines has proved difficult and we are still lacking heteroplasmic mouse lineages, with all, except one of the above model systems (Shimizu, Mito et al. 2014) generating homoplasmic mutant mice. Heteroplasmy, the threshold effect and mitotic segregation are significant factors believed to contribute to the heterogeneity observed in mtDNA disease patients that harbour the same mutation, and as such there remains the need to generate different mice that carry and transmit pathogenic heteroplasmic mtDNA point mutations, in order to improve our understanding of different mtDNA diseases.

5.2 Breeding of mice harbouring specific mtDNA point mutations

All breeding experiments and the propagation of mouse lineages was performed by James Stewart and Nils-Göran Larsson, Max Planck Institute for Biology of Ageing, Cologne, Germany. The original purpose of the *PolgA*^{mut/mut} mouse was to generate mice that accumulated mtDNA point mutations to high levels, so that specific mutations could then be isolated and segregated into different mouse lineages, thus creating mouse models of specific pathogenic mtDNA point mutations. As such female *PolgA*^{mut/mut} mothers were employed in a breeding strategy to transmit heteroplasmic mtDNA point mutations into true-breeding female lineages of mice. This resulted in mouse lineages enriched for point mutations in tRNA and rRNA genes and a moderate number of amino acid substitutions in protein encoding genes, generating a profile of mutations comparable to those seen in human mtDNA disease (Stewart, Freyer et al. 2008). However, mouse lineages carried 16-20 mutations per mtDNA molecule (Freyer, Cree

et al. 2012), resulting in complications with attributing phenotypes to a specific mutation, compounded by the synergistic action of multiple point mutations acting together. Given that *PolgA*^{+/*mut*} mice harbour only 1-3 mutations per mtDNA genome (Kraytsberg, Simon et al. 2009), female *PolgA*^{+/*mut*} mice were instead employed as the founders in the breeding strategy. Female *PolgA*^{+/*mut*} mice were backcross mated with pure wild-type (WT) male mice, to produce female progeny that expressed wild-type mtDNA polymerase, but transmitted mutated mtDNA (*PolgA*^{+/*+*} mice) (Figure 5-1). This resulted in the successful transmission of mtDNA point mutations to offspring, which were subsequently segregated into independent mouse lineages using the breeding strategy outlined in below (Figure 5-1).

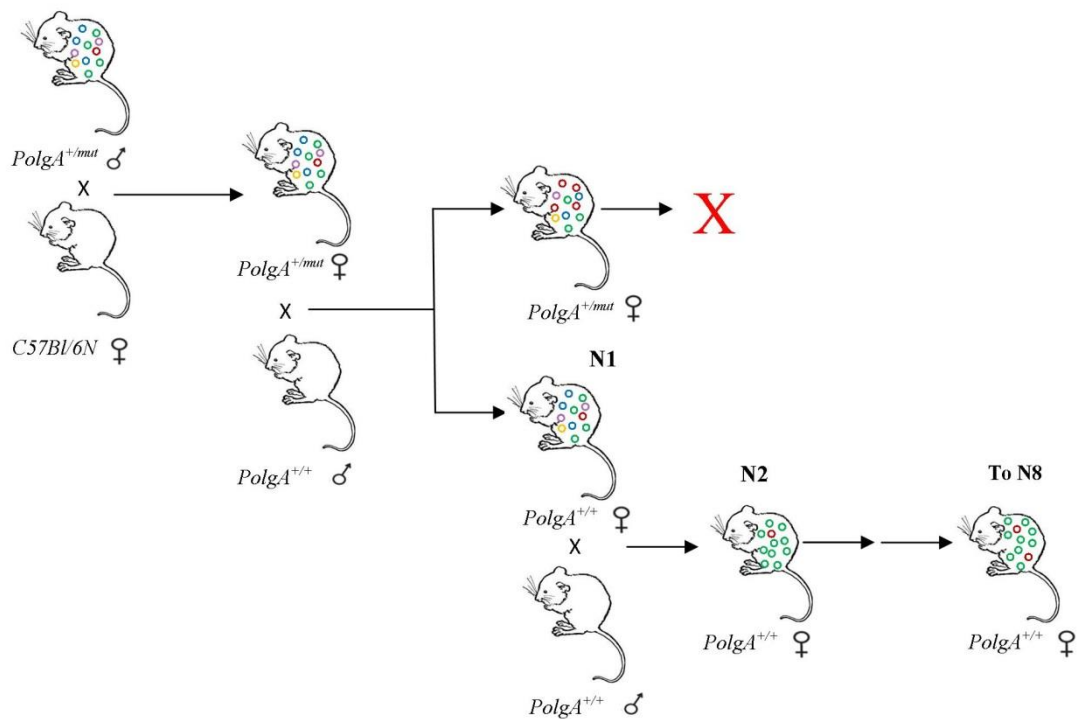


Figure 5-1: Germline mtDNA mutagenesis and breeding strategy using *PolgA*^{+/*mut*} female mice to segregate specific mtDNA mutations into mouse lineages.

MtDNA mutagenesis was initiated by mating C56Bl/6N female mice with *PolgA*^{+/*mut*} males to generate *PolgA*^{+/*mut*} females. Resulting *PolgA*^{+/*mut*} females were backcross mated with C57Bl/6N male mice, to produce female progeny that expressed wild-type mtDNA polymerase, but transmitted mutated mtDNA (*PolgA*^{+/*+*} mice). Female progeny were subsequently mated with WT (*PolgA*^{+/*+*}) male mice to propagate the mouse lineages and segregate specific mutations into specific mouse lineages.

5.3 Can dual COX/SDH histochemistry in the colonic epithelium be used as an early experimental screening tool for evidence of mitochondrial dysfunction and identifying potential pathogenic mtDNA point mutations in the breeding of mice harbouring specific mtDNA point mutations?

MtDNA point mutations transmitted to offspring in the above mouse lineages were identified through a standard sequencing procedure, performed by James Stewart, Max Planck Institute for Biology of Ageing, Cologne, Germany. Whilst sequencing can be used to identify point mutations in the mouse lineages, the initial selection of mice chosen for sequencing was blind and random, and as such sequencing multiple mouse lineages became extensive and expensive, especially given that not all mice would harbour a mutation of interest. There was therefore the need to develop an early, *in vivo* experimental screening tool in these animals that could be used to determine whether a point mutation caused any mitochondrial dysfunction and could be pathogenic. This would subsequently identify whether an mtDNA point mutation could serve as a candidate allele for modelling mtDNA disease and a specific mouse lineage was worth propagating.

It is well established that pathogenic mtDNA point mutations result in reduced function of the mitochondrial respiratory chain and cells harbouring clonally expanded mtDNA mutations can be readily identified by dual COX/SDH histochemistry (Sciacco M 1994; Kaido, Fujimura et al. 1995). The colonic epithelium is proposed to be a permissive environment, given that mtDNA point mutations clonally expand to high levels in colonic crypts and result in focal respiratory chain deficiency, undergoing higher rates of clonal expansion than other tissues (Taylor, Barron et al. 2003; McDonald, Preston et al. 2006; Fellous, McDonald et al. 2009). Studies in mouse small intestinal stem cells suggest that mtDNA copy number is quite low (Barker, Van Es et al. 2007) and as such this is also believed to be true of the colonic epithelium. The threshold level for precipitating a biochemical defect and mitochondrial dysfunction could therefore be expected to be lower in the colon, given that there would be less WT mtDNA molecules able to maintain normal mitochondrial function. As such it was hypothesised that if an mtDNA point mutation was pathogenic, that COX deficiency and mitochondrial dysfunction would ensue much earlier in the colonic epithelium of these mice and could be used as an early experimental screening tool for identifying candidate pathogenic alleles in the breeding of mouse lineages.

Given that my research has involved a long standing collaboration with James Stewart and Nils-Göran Larsson, colon samples from 2 mice were provided from a potential mouse lineage to perform the COX/SDH histochemistry on colonic epithelial tissue. This revealed the presence of colonic crypts with both full and partial COX deficiency (Figure 5-2) providing early evidence of mitochondrial dysfunction and an indication that this specific mouse lineage may be carrying a pathogenic mt-tRNA point mutation and was worth propagating as an interesting mouse lineage.

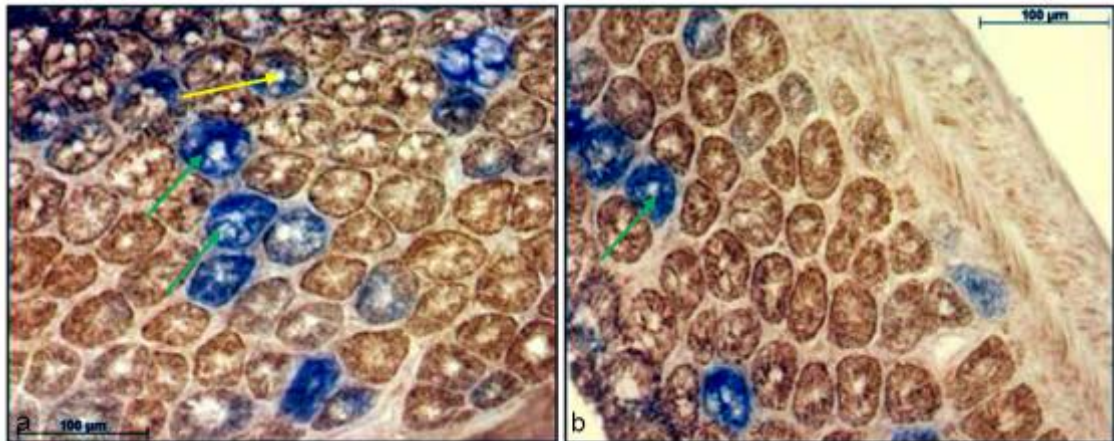


Figure 5-2: Dual COX/SDH histochemistry screen on colonic epithelium of a mouse lineage created via the *PolgA*^{+mut} breeding strategy.

Colon sections showing a transverse section through the colonic crypts. Crypts stained brown are positive for COX activity, crypts stained blue are COX deficient (green arrows) and crypts with partial COX deficiency are a mixture (yellow arrow).

5.3.1 Identification of a candidate allele and breeding of mice with a m.5024 C>T *tRNA*^{Ala} mutation

Following the discovery of COX deficiency in the above colonic epithelium, whole mtDNA genome sequencing was performed on tail biopsies, previously collected from these mice, by James Stewart, to identify any mtDNA point mutations. This revealed a C>T mutation at position m.5024 of the mouse mtDNA genome in the *tRNA*^{Ala} gene, in a region associated with two alleles that cause human mitochondrial disease (Finnilä, Tuisku et al. 2001; Swalwell, Deschauer et al. 2006; McFarland, Swalwell et al. 2008). Both the m.5650G>A and m.5591G>A mutations in human *tRNA*^{Ala} are associated with pure mitochondrial myopathies, where patients displayed profound muscle phenotypes, a combined respiratory chain defect and high levels of COX deficiency in muscle biopsies, with which the mutation segregated (Swalwell, Deschauer et al. 2006; McFarland, Swalwell et al. 2008). The m.5024C>T mutation is in fact on the opposite side of the amino acid stem to the human m.5650G > A *tRNA*^{Ala} allele, disrupting the same base pair within the acceptor stem of the *tRNA* (Figure 5-3) (Finnilä, Tuisku et al.

2001; McFarland, Swalwell et al. 2008). The m.5024 C>T mutation was therefore identified as a candidate allele to potentially model mtDNA disease in mice and this mouse lineage was propagated, with stable transmission of the m.5024C>T mutation achieved after the 6th generation. Earlier generations still transmitted the allele, however they also harboured additional mtDNA variants, which had been transmitted from the founder *PolgA*^{+/*mut*} mother and the *PolgA*^{+/*+*} mothers. Standard tail biopsies were taken from mice at weaning (3 weeks old) to measure the m.5024 C>T heteroplasmy in each animal by RFLP, completed by James Stewart. This mouse lineage is currently producing the 14th backcross generation and will be referred to from now on as tRNA^{Ala} mutant mice.

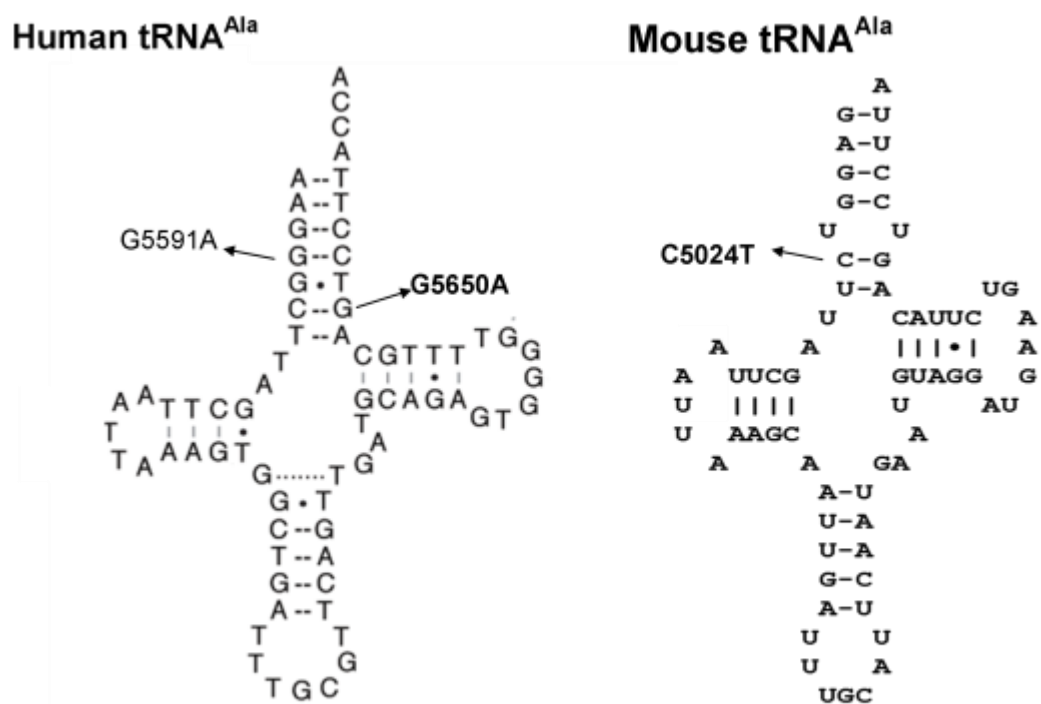


Figure 5-3: Clover leaf structure of the human and mouse mt-tRNA^{Ala}.

Mutations are displayed on the tRNA as the mutation in the DNA sequence. The m.5591G>A and the m.5650G>A mutations are indicated on the human tRNA^{Ala}, with the m.5024C>T mutation indicated on the mouse tRNA^{Ala}. The m.5024C>T mutation is on the opposite side of the amino acid stem to the human m.5650G>A mutation in the tRNA^{Ala} gene disrupting the same base pair. Image (adapted) courtesy of James Stewart.

5.3.2 Early molecular characterisation of m.5024C>T tRNA^{Ala} mutant mice

All initial experiments examining young mutant tRNA^{Ala} mice (<22 weeks old) were engineered around breeding, transmission of the allele and molecular characterization of the tRNA defect, all of which were performed by James Stewart. RFLP analysis of the

heteroplasmy in tail clippings revealed an apparent threshold level for transmission of the mutation, with an absence of any pups generated exceeding 77% m.5024 C>T (Figure 5-4a). Characterization studies revealed a defect in the tRNA in young mice with high m.5024 C>T heteroplasmy (>60%), which displayed decreased steady levels of tRNA^{Ala} and decreased in organello translation of mitochondrial proteins in heart mitochondria (Figure 5-4back).

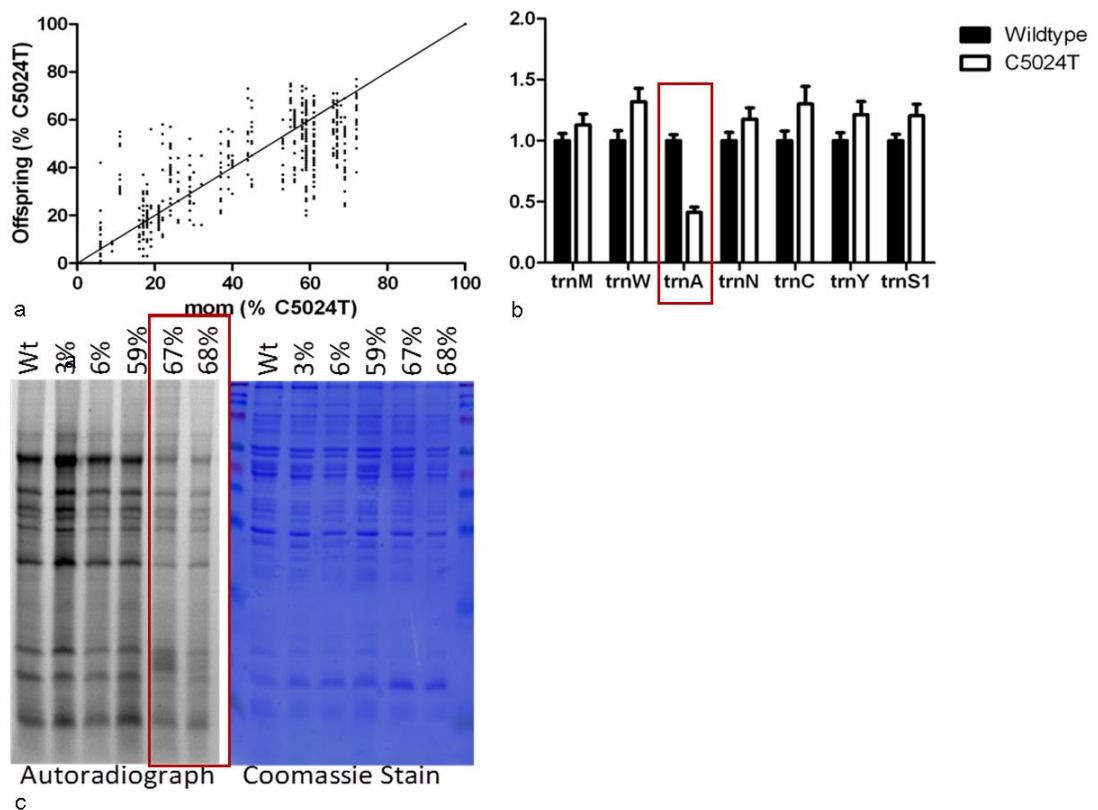


Figure 5-4: Molecular characterization of young tRNA^{Ala} mutant mice.

(a) Transmission of the m.5024C>T mutation from mother to offspring demonstrates non-random transmission of the m.5024C>T allele and an apparent threshold of 77% in offspring. (B) Northern blots reveal reduced steady state levels of tRNA^{Ala} in skeletal muscle in m.5024C>T tRNA^{Ala} mutant mice. (c) In organello translation in heart mitochondria for mitochondrial proteins: ND5, COXI, ND4, CytB, ND2, ND1, COXIII, COXII, ATP6, ND6, ND3and ATP8/ND4L, showing decreased efficiency and truncated protein products in mice with high levels of the mutation (>60%). Figures provided by James Stewart.

This data therefore suggested that the m.5024 C>T mutation was associated with a defect in the tRNA and a disruption in protein translation in the tRNA^{Ala} mutant mice; however evidence of phenotypic mitochondrial dysfunction and information regarding the pathogenicity of the mutation still remained to be elucidated.

5.4 Aims of the study

1. Perform detailed characterisation of the in vivo mitochondrial dysfunction observed in the colonic epithelium of young m.5024 C>T tRNA^{Ala} mutant mice. I aimed to use mtDNA genome analysis of m.5024 C>T heteroplasmy in single colonic crypts to determine the pathogenicity of the mutation and whether or not it segregated with the COX deficiency in the colonic epithelium. This would further confirm whether dual COX/SDH histochemistry in the colonic epithelium is a good early experimental screening tool for detecting in vivo mitochondrial dysfunction and identifying pathogenic mtDNA point mutations in mouse lineages that harbour point mutations.
2. Determine whether m.5024 C>T tRNA^{Ala} mutant mice are a good model of mtDNA disease caused by an mt-tRNA point mutation and could be used to uncover disease mechanisms associated with a heteroplasmic point mutation, using classical histochemical approaches?

5.5 Results

5.5.1 *Do young tRNA^{Ala} mutant mice routinely display phenotypic evidence of mitochondrial dysfunction in the colonic epithelium?*

All m.5024 C>T tRNA^{Ala} mutant mice were sacrificed and tissue samples provided by James Stewart, Max Planck Institute for Biology of Ageing, Cologne, Germany. Colon sections (10µm) from 23 mutant tRNA^{Ala} mice (16 of which were <22 weeks old and surpassed the 6th breeding generation) with variable m.5024 C>T tail heteroplasmy (see Appendix A), were subjected to dual COX/SDH histochemistry. Approximately ~500 colonic crypts, in both transverse and longitudinal tissue sections, were assessed for COX activity per sample, to characterise the level of respiratory chain deficiency and phenotypic mitochondrial dysfunction in mice harbouring the m.5024 C>T mutation. Colonic crypts were identified that displayed both full and partial COX deficiency (Figure 5-5), with partial COX deficiency detected in all mutant tRNA^{Ala} mice, even those with a fairly moderate level of the mutation, ~30% (see Appendix D).

In the first part of this study all animals beyond the 6th generation (where stable, strong transmission of the allele was achieved) were <22 weeks old (young mutants), as the initial aim was to identify early evidence of phenotypic mitochondrial dysfunction in mice harbouring the m.5024C>T tRNA^{Ala} mutation. For young mutant tRNA^{Ala} mice the incidence of full and partial COX deficient crypts were combined and compared to

the m.5024 C>T tail heteroplasmy, to determine whether the incidence of COX deficiency was associated with the m.5024C>T tail heteroplasmy in animals. Higher levels of COX deficiency (~17%) were observed in mutant tRNA^{Ala} mice with higher tail heteroplasmy (>60%) compared to those with moderate to low-level heteroplasmy (COX deficiency =<9%) ($p = <0.0001$, one way ANOVA) (Figure 5-6), confirming that levels m.5024 C>T tail heteroplasmy did correlate with the magnitude of COX deficiency detected in the colonic epithelium.

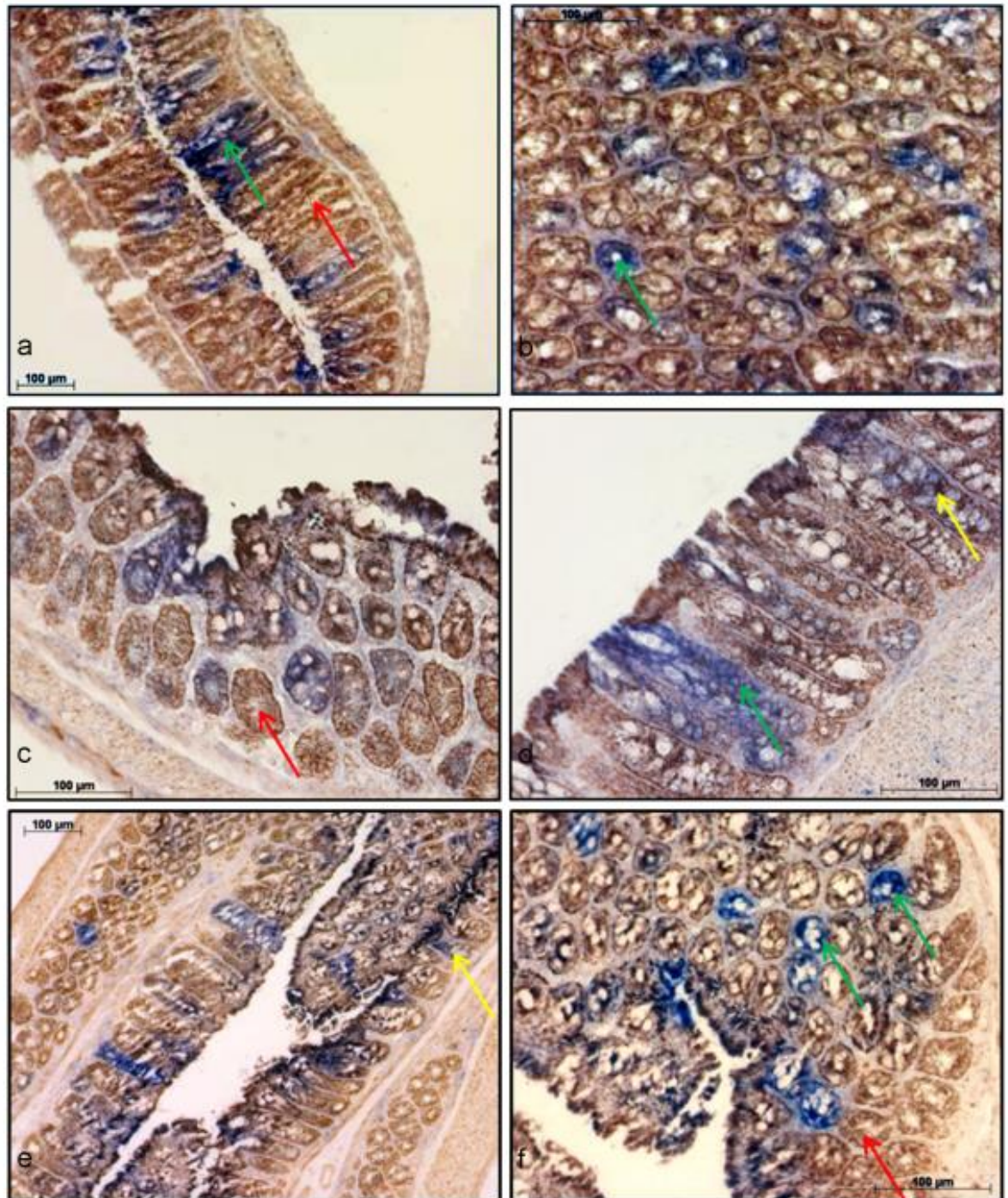


Figure 5-5: Respiratory chain deficiency in colonic epithelial tissue of young m.5024C>T tRNA^{Ala} mutant mice.

COX/SDH histochemistry on (a) + (b) Mouse 1623 (m.5024C>T75%) colon tissue, at x10 and x20 magnification respectively (c+d) Mouse 2267 (m.5024C>T77%) colon tissue, at x20 magnification. (e)+ (f) Mouse 1184 (m.5024C>T59%) colon tissue, at x10 and x20 magnification respectively. Scale bars: 100μm. COX positive crypts are brown (red arrow), COX deficient crypts are blue (green arrow) and crypts with partial COX deficiency are a mix of blue and brown (yellow arrow).

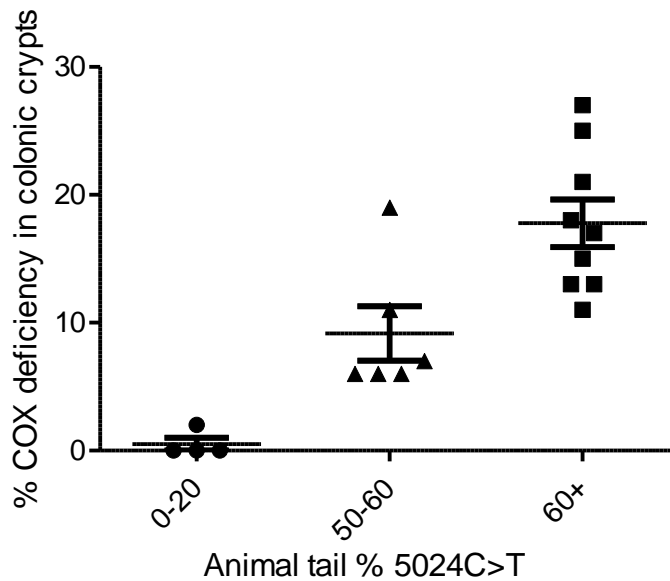


Figure 5-6: The magnitude of COX deficiency in the colon correlates with m.5024C>T tail heteroplasmy in young tRNA^{Ala} mutant mice.

The percentage of colonic crypts that lacked normal COX activity (COX deficient crypts + crypts with partial COX deficiency) was significantly higher in those mutant mice that possessed high m.5024C>T heteroplasmy in the tail, >60% (17.6 ± 1.668), than animals with moderate, 50-60% (9.167 ± 2.120) and low level heteroplasmy, <20% (0.400 ± 0.400), $p = < 0.0001$, one way ANOVA.

Given that pure WT littermates cannot be generated from the same *PolgA*^{+/+} mother that transmits the m.5024 C>T mutation to her offspring, young animals with low levels of the mutation (<25%) were used as controls. Dual COX/SDH histochemistry was completed on colon sections (10µm) from 6 low-level control animals (<22 weeks) and a negative control animal (TN139) carrying 16 known polymorphic variants in mtDNA (see Appendix A). All colonic crypts displayed normal COX activity, in all 6 low level control animals and the negative control (Figure 5-7). A lack of COX deficiency associated with any of the 16 alleles in animal TN139, further supported that the m.5024 C>T mutation was associated with phenotypic mitochondrial dysfunction in the colon and suggested that this mutation could be pathogenic.

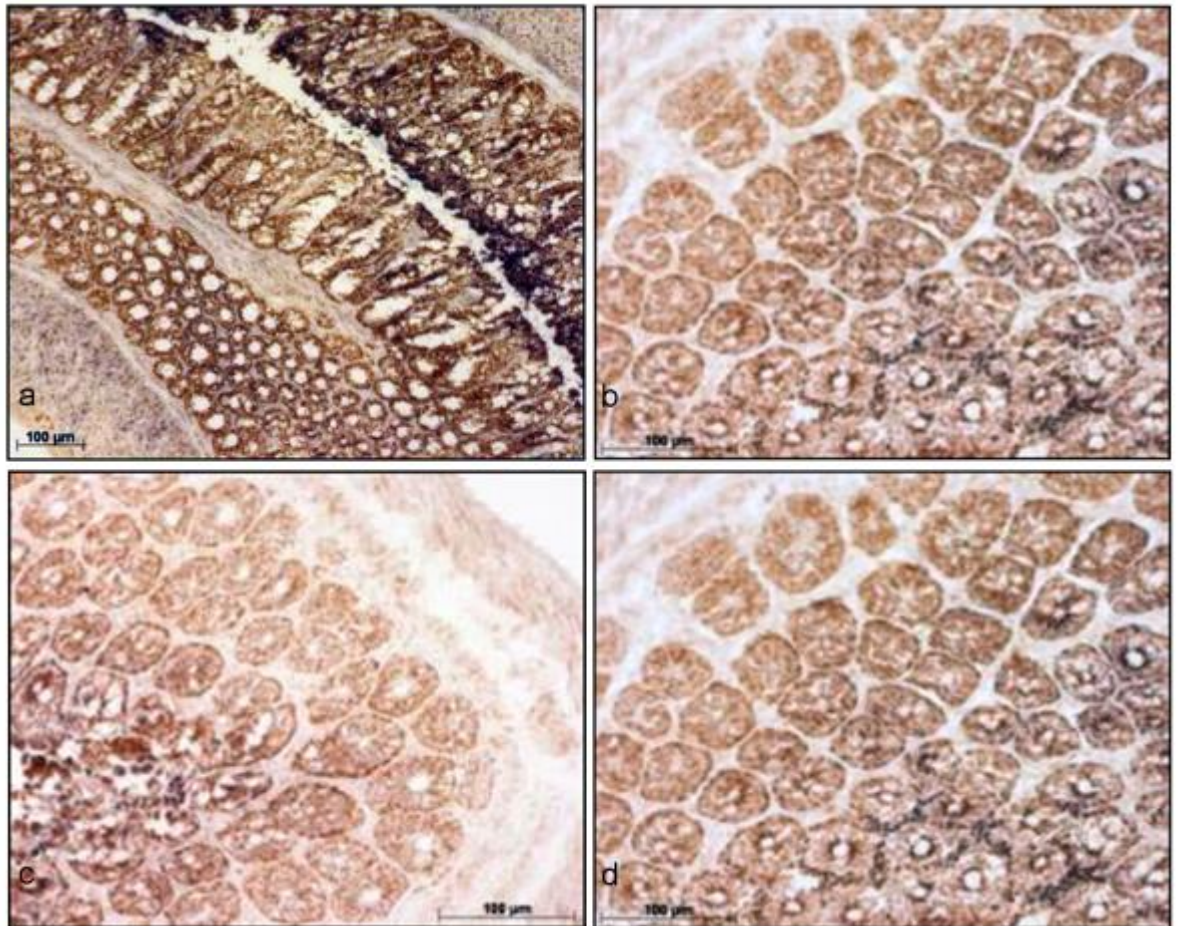


Figure 5-7: Normal COX activity in colonic epithelial tissue of young control mice.

COX/SDH histochemistry on (a) + (b) Mouse TN139 colon tissue, at x10 magnification. (b) Mouse 2430 (m.5024C>T24%) colon tissue, at x20 magnification. (c) Mouse 2432 (m.5024C>T13%) colon tissue, at x20 magnification. (d) Mouse 2489 (m.5025C>T7%) colon tissue at x20 magnification. Scale bars: 100μm.

5.5.2 *Is the m.5024C>T mutation pathogenic? Segregation of the m.5024C>T mutation with COX deficiency in colonic crypts of young mutant *tRNA^{Ala}* mice.*

To determine whether a mtDNA mutation is pathogenic, standard criteria states that the mutation has to segregate with the biochemical defect (DiMauro and Schon 2001) and the examination of single cells is considered to be the ‘gold-standard’ for determining pathogenicity of an mt-tRNA mutation (McFarland, Elson et al. 2004; Yarham, Al-Dosary et al. 2011). MtDNA genome analysis was therefore performed on single micro-dissected COX positive and COX deficient colonic crypts for the detection of the m.5024C>T mutation and correlation with the COX deficient phenotype.

5.5.2.1 *MtDNA genome analysis for the m.5024C>T mutation by Sanger sequencing*

Initial detection of the mutation involved mtDNA genome sequencing of a ~1.3kb region spanning the m.5024 site of the genome in COX positive (n=7) and COX

deficient (n=7) colonic crypts from two mice with moderate tail heteroplasmy from early breeding generations, <6th (471 and 472- see Appendix A) and two young (>6th breeding generation) tRNA^{Ala} mutant mice with high tail heteroplasmy (1622 and 1623- see Appendix A). The mtDNA sequence for each colonic crypt was aligned to the C57Bl/6J mouse reference sequence (GenBank Accession number NC_005089) and the consensus DNA sequence from homogenate colon tissue for a WT mouse. Heteroplasmy levels were estimated based upon the relative peak height of electropherograms.

The m.5024C>T mutation was detected in the heteroplasmic state in all COX positive and COX deficient colonic crypts, confirming the presence of the mutation in single colonic crypts (Figure 5-8). Sequencing electropherograms, most notably from animals 1622 and 1623, revealed an apparent segregation of the mutation with COX deficiency, with the m.5024C>T mutation presenting at high heteroplasmy (>75%) in COX deficient crypts and low heteroplasmy (<50%) in COX positive colonic crypts (Figure 5-8e-h). M.5024C>T heteroplasmy did not appear to segregate with the COX deficiency in colonic crypts sequenced from animal 471, with COX deficient crypts recurrently displaying low heteroplasmy.

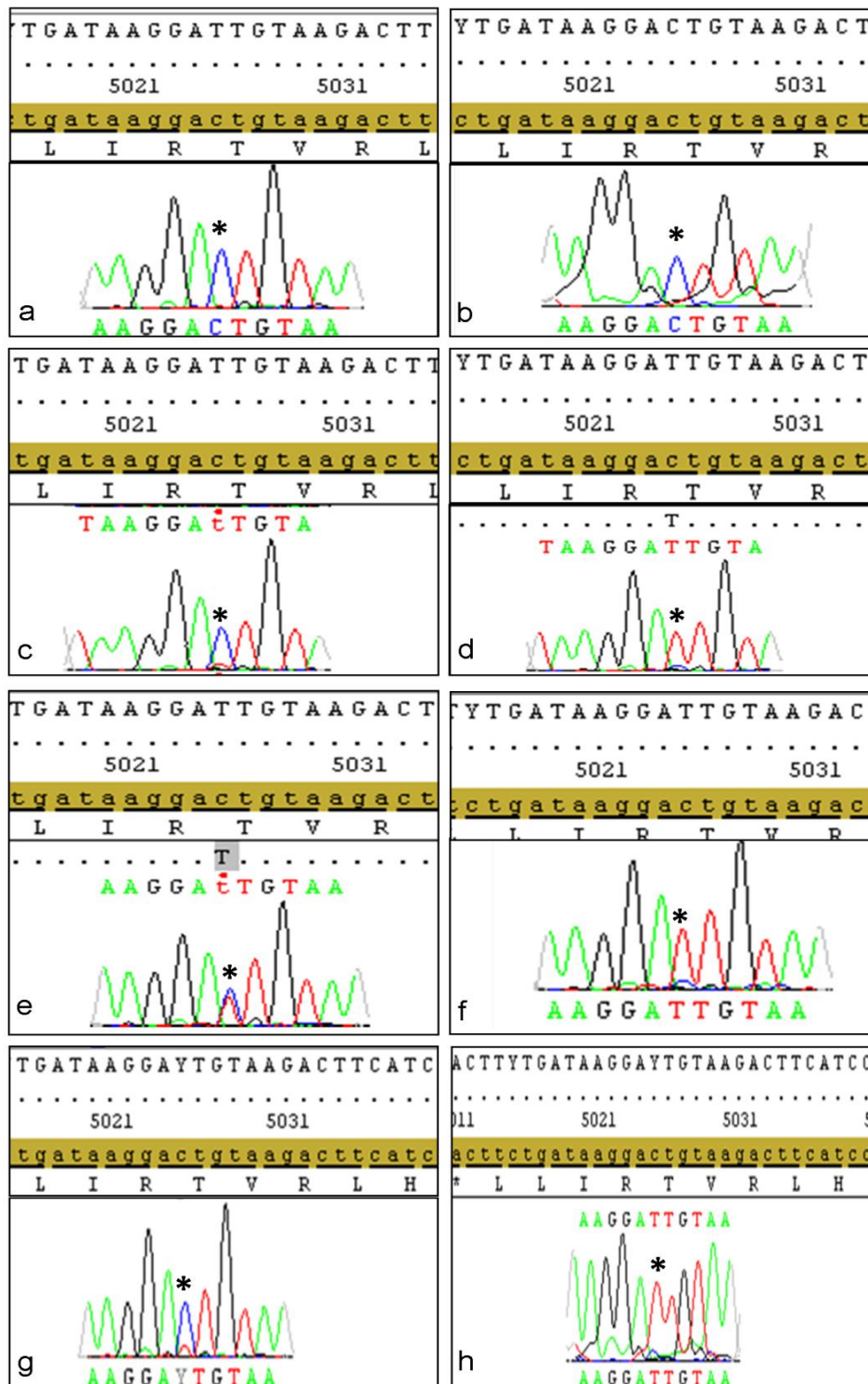


Figure 5-8: Sequencing electropherograms illustrating the presence of the m.5024C>T mutation in COX positive and deficient colonic crypts from mutant tRNA^{Ala} mice.

(a+b) Electropherograms showing the m.5024 region of the mtDNA genome from WT mouse DNA in the forward and reverse directions respectively, showing the presence of the WT C base. Sequencing of this region in a (c) COX positive crypt from mouse 472 (m.5024C>T18%) revealed the presence of the WT C base and (d) in a COX deficient crypt revealed the presence of the m.5024C>T mutation, ~80% heteroplasmy. Sequencing of this region in a (e) COX positive crypt from mouse 1622 (m.5024C>T74%) revealed a heteroplasmic C>T change (~50%) at position m.5024 and (f) in a COX deficient crypt revealed high heteroplasmy, ~80%. (g) Sequencing of this region in a COX positive crypt from mouse 1623 (m.5024C>T75%) revealed a heteroplasmic C>T change (~25%) at position m.5024 and (h) in a COX deficient crypt revealed high heteroplasmy, ~80%. The stars indicate the m.5024 position and the C>T base change in the mouse mtDNA sequence.

5.5.2.2 Quantification of the m.5024C>T mutation by pyrosequencing

Sanger sequencing is principally used for the detection of mtDNA point mutations and is not an accurate and precise method of mutation quantification. Pyrosequencing is a sequencing by synthesis method that can be used to give an exact measure of heteroplasmy by quantifying the amount of light emitted when a nucleotide is incorporated into the growing DNA strand. As such, PyroMark assay design software v2.0 (Qiagen, Hilden, Germany) was used to design a m.5024C>T mutation specific assay and a trio of pyrosequencing primers in the reverse direction, for the accurate quantification of the m.5024 C>T mutation (see chapter 2, section 2.6.9).

Pyrosequencing was performed on laser micro-dissected single COX positive (n=15) and COX deficient colonic (n=15) crypts, from the two animals with moderate tail heteroplasmy (471 and 472-see Appendix A) and four young animals (>6th generation) with high tail heteroplasmy (1622, 1623, 2267 and 2269- see Appendix A) to determine whether the m.5024 C>T mutation segregated with the COX deficiency in the colon and fulfilled the standard pathogenicity criteria. A WT DNA sample (m.5024C>T <2%) and a cloned fragment (m.5024C>T >98%) were employed in pyrosequencing runs as controls. All pyrosequencing was performed in triplicate and an average mutation load calculated for each sample.

Pyrosequencing revealed that the highest level of the m.5024C>T mutation segregated with the COX deficiency in colonic crypts from all mutant tRNA^{Ala} mice (p value= <0.0001, one way ANOVA), with COX deficient crypts displaying higher heteroplasmy (57.93 ± 2.814) than COX positive colonic crypts (43.39 ± 1.705) (p = <0.0001, unpaired t test). The young mutant tRNA^{Ala} mice with higher m.5024 C>T heteroplasmy (1622, 1623, 2267 and 2269) displayed a much clearer segregation of the m.5024 C>T mutation with the COX deficiency, with an absence of any segregation observed in animal 471, where COX deficient crypts actually displayed lower heteroplasmy ($18.0 \pm 18.0\%$) than COX positive crypts ($35.7 \pm 20.5\%$). Mice 471 and 472 were the original animals that underwent COX/SDH screening in this mouse lineage (Figure 5-2) and were from the very early breeding generations, in which the *PolgA*^{+/+} mother transmitting the m.5024 C>T mutation was also known to transmit other mtDNA alleles to her offspring (James Stewart, personal communication). Given that other mtDNA alleles could also have led to the COX deficiency and mutation segregation in the early breeding generations, animals 471 and 472 were excluded from the statistical analysis. This revealed a much clearer segregation of the m.5024C>T

mutation with COX deficiency in all young m.5024C>T tRNA^{Ala} mutant mice ($p = <0.0001$, one way ANOVA) (Figure 5-9a), with COX deficient colonic crypts displaying significantly higher m.5024 C>T heteroplasmy (71.18 ± 1.647) than COX positive colonic crypts (47.22 ± 1.614) ($p = <0.0001$, unpaired t test) (Figure 5-9b). A two way ANOVA test confirmed that COX activity significantly affected the m.5024 C>T heteroplasmy in colonic crypts ($p = <0.0001$), accounting for 39% of the variance in heteroplasmy; however variation between mice had no significant effect ($p = 0.3093$), accounting for only 1.36% variance (Figure 5-9c). This data provided evidence that the m.5024C>T mutation was pathogenic and could therefore serve as a candidate allele for modelling mitochondrial disease caused by mt-tRNA mutations in mice. From here onwards all mutant tRNA^{Ala} mice studied exceeded the 6th generation, where there was a lack of transmission of other mtDNA variants from mothers to offspring.

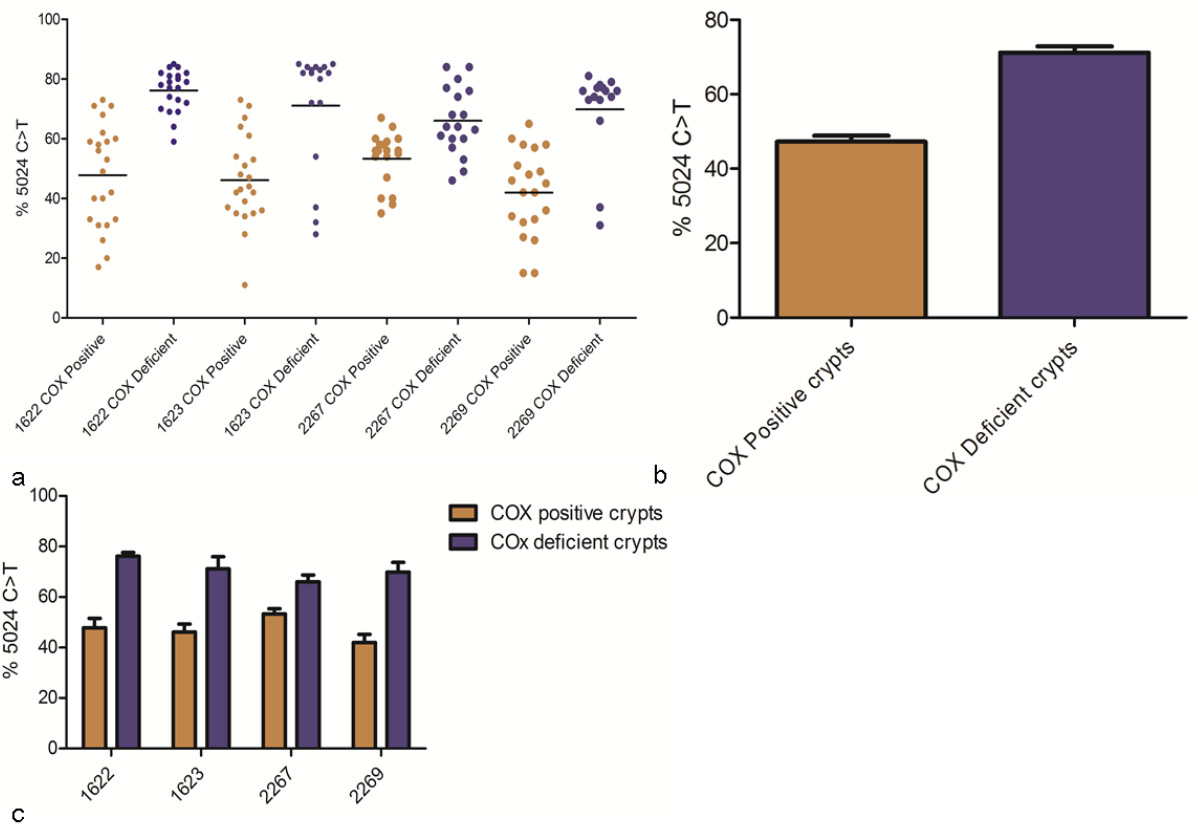


Figure 5-9: Pathogenicity and segregation of the m.5024C>T mutation with COX deficiency in single colonic crypts from young tRNA^{Ala} mutant mice.

M.5024C>T heteroplasmy in single COX positive and COX deficient colonic crypts from young tRNA^{Ala} mutant mice, excluding mice 471 and 472. M.5024C>T heteroplasmy is significantly higher in COX deficient colonic crypts of all mice compared to COX positive crypts ($p < 0.0001$, one way ANOVA test). (b) M.5024C>T heteroplasmy in all COX negative (71.18 ± 1.647 N=72) and positive crypts (47.22 ± 1.614 N=83) ($p < 0.0001$, unpaired t test). (c) The effect of COX activity and mouse variability on the m.5024C>T heteroplasmy in single colonic crypts. COX activity significantly affected the m.5024C>T heteroplasmy in single colonic crypts ($p < 0.0001$) but variability between mice had no significant effect ($p = 0.3093$), two way ANOVA test.

Pyrosequencing was also performed on single COX positive colonic crypts ($n > 10$) from three low level control animals (2431, 2432 and 2489), to confirm that the m.5024 C>T mutation was present at higher levels in the colonic crypts of tRNA^{Ala} mutant mice compared to controls (Figure 5-10a). This revealed that m.5024 C>T heteroplasmy was significantly lower in COX positive colonic crypts from control animals (10.82 ± 1.396) than COX positive colonic crypts from tRNA^{Ala} mutant animals (47.22 ± 1.614), ($p < 0.0001$, unpaired t test) (Figure 5-10b).

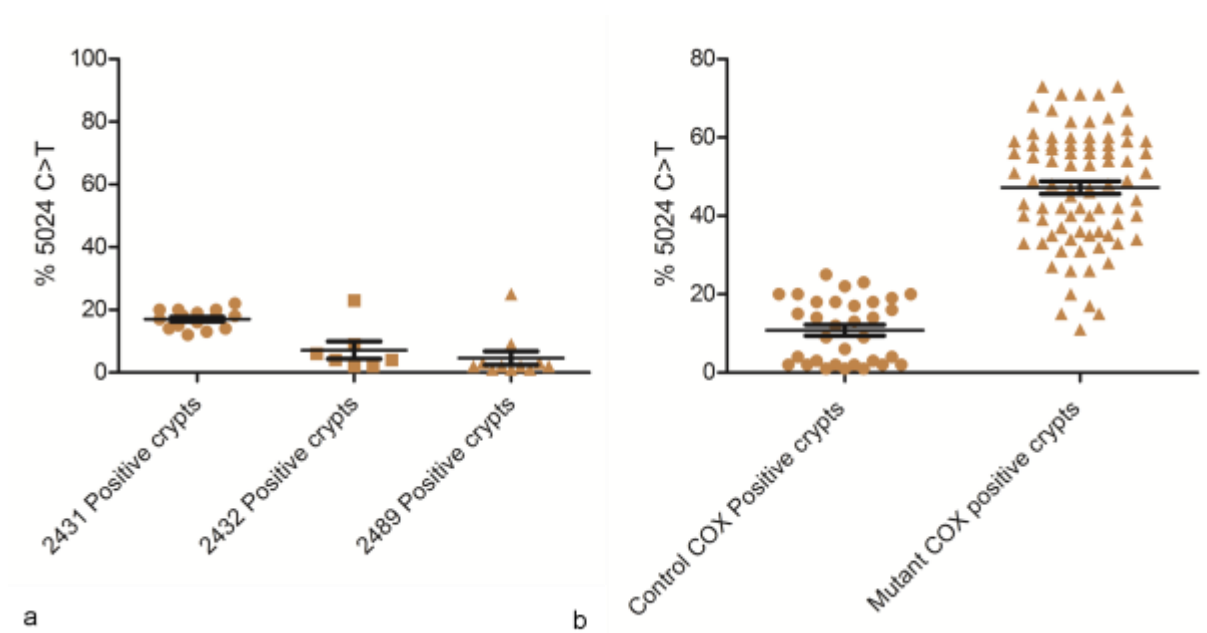


Figure 5-10: M.5024C>T heteroplasmy in single colonic crypts from young control animals.

(a) M.5024C>T heteroplasmy in single COX positive colonic crypts from low level control mice, 2431(m.5024C>T7%), 2432(m.5024C>T 13%) and 2489 (m.5024C>T 7%). (b) M.5024C>T heteroplasmy in COX positive colonic crypts from control animals (10.82 ± 1.396) is significantly lower than COX positive colonic crypts from tRNA^{Ala} mutant animals (47.22 ± 1.614), ($p = <0.0001$, unpaired t test).

5.5.3 *Is there evidence of respiratory chain deficiency in post-mitotic tissues of young m.5024C>T tRNA^{Ala} mutant mice?*

Given that the m.5024C>T mutation was shown to be pathogenic I then wanted to determine whether the mutant tRNA^{Ala} mice displayed signs of mitochondrial dysfunction and tissue phenotypes that typically present in patients affected by mtDNA disease. Cardiomyopathy and muscle myopathy are typical symptoms that present in mitochondrial disease patients with mt-tRNA point mutations, with heart and muscle biopsies frequently showing high levels of COX deficiency (Taniike, Fukushima et al. 1992; Taylor, Giordano et al. 2003; Swalwell, Deschauer et al. 2006; McFarland, Swalwell et al. 2008). I therefore performed dual COX/SDH histochemistry on heart (8µm) and skeletal muscle (thigh and/or calf) (10µm) tissue supplied from young (<22 weeks) mutant tRNA^{Ala} mice (n=8) and young (<22 weeks) low level control animals (n=6) to determine whether the mutant tRNA^{Ala} mice displayed typical signs of disease associated with an mt-tRNA mutation.

All low level control animals displayed normal COX activity in heart tissue (Figure 5-11a+b) and only 2 of the 8 young mutant tRNA^{Ala} mice displayed evidence of COX deficient heart fibers, reaching 2% in animal 1734 (Figure 5-11c+d) and 12% in animal 2307 (Figure 5-11e+f). All other mutant tRNA^{Ala} mice maintained normal COX activity

throughout the heart tissue, even those with the highest tail heteroplasmy (Figure 5-11g+h). It is worth noting at this point that animal 2307 had to be culled due to ill health at 12 weeks old and so additional complications or defects may have also led to the respiratory chain deficiency, accounting for the high incidence here.

Similarly in the skeletal muscle, all low level control animals displayed normal COX activity in the thigh and calf muscle (Figure 5-12a+b) and only 2 mutant tRNA^{Ala} (1764 and 2266), displayed evidence of COX deficient fibers in the thigh (Figure 5-12c-f), of which only a few were detected, amounting to 0.4% across the whole tissue section. Again, normal COX activity was preserved in the thigh and calf muscle of young mutant tRNA^{Ala} mice with the highest m.5024 C>T tail heteroplasmy (Figure 5-12g+h).

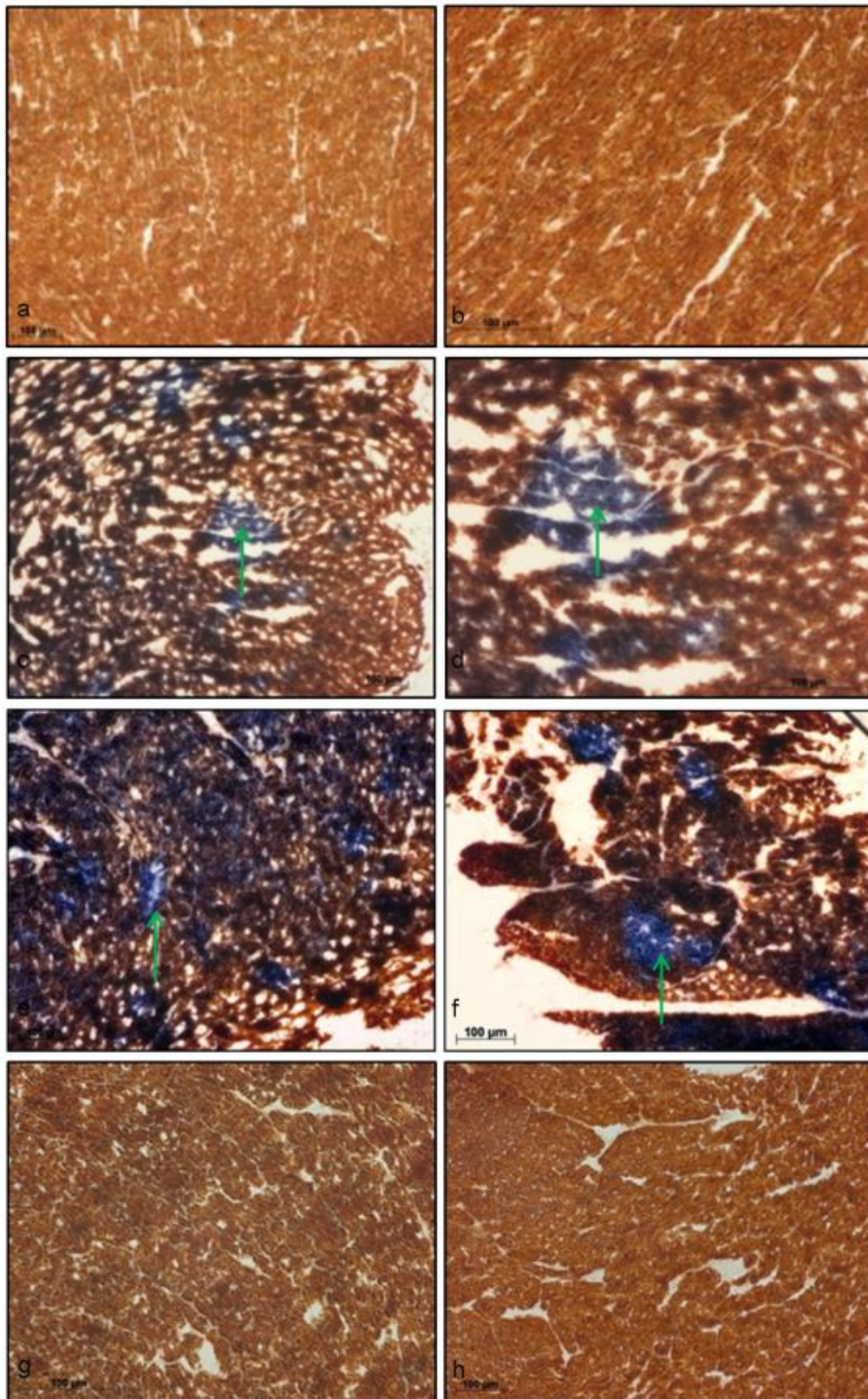


Figure 5-11: COX/SDH histochemistry on heart tissue from control and mutant m.5024C>T tRNA^{Ala} mutant mice.

COX/SDH histochemistry on: (a) Control mouse 2431 (m.5024C>T7%) heart tissue at x10 magnification. (b) Control mouse 2432 (m.5024C>T13%) heart tissue at x20 magnification. (c)+ (d) Mouse 1734 (m.5024C>T60%) heart tissue, at x10 and x20 magnification respectively (e)+ (f) Mouse 2307 (m.5024C>T 51%) heart tissue, at x10 and x20 magnification respectively. (g) Mouse 2267 (m.5024C>T77%) heart tissue at x20 magnification. (h) Mouse (2269 m.5024C>T74%) heart tissue at x10 magnification. Scale bars: 100μm. COX positive heart muscle fibers are brown and COX deficient fibers appear blue (green arrows).

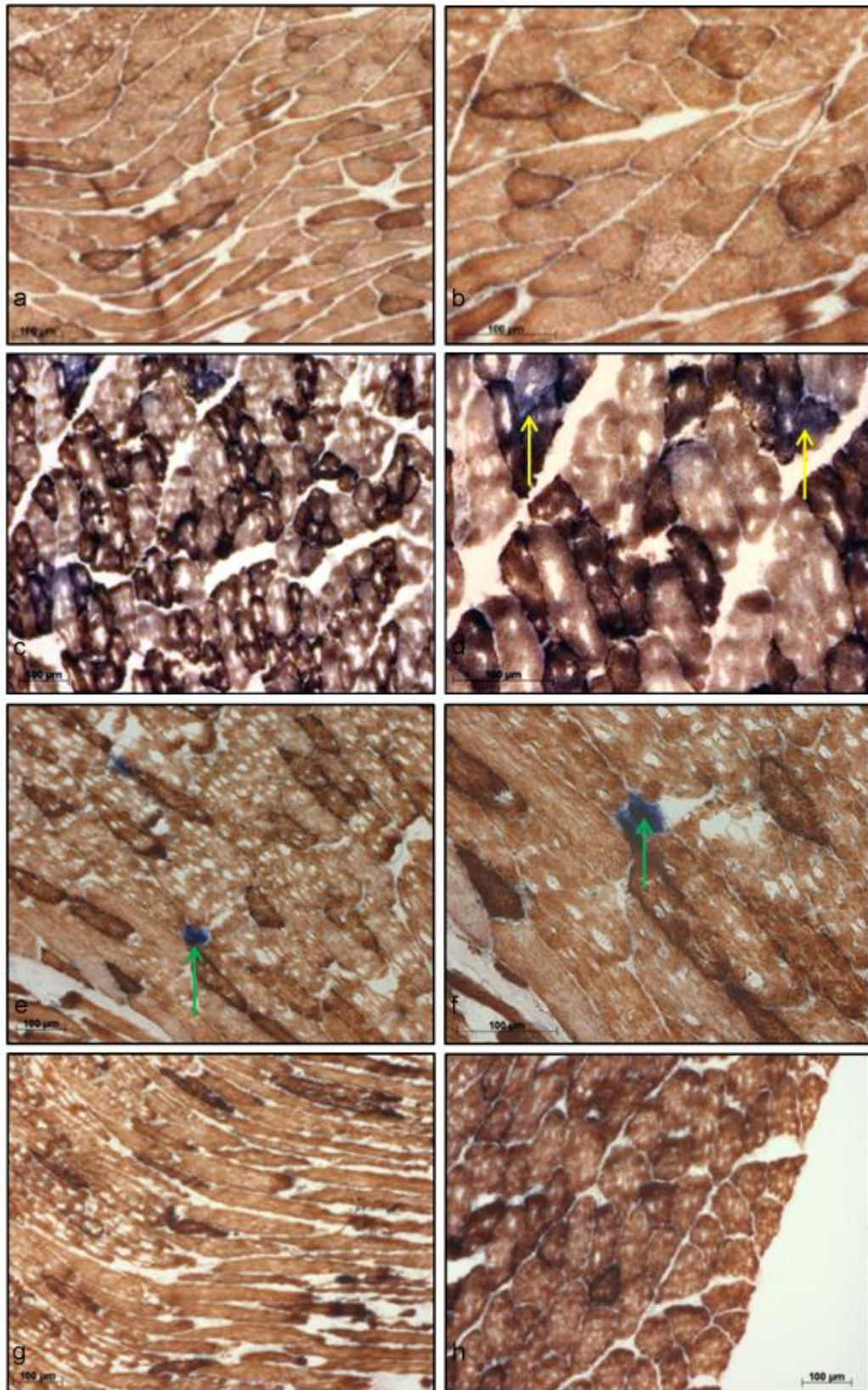


Figure 5-12: COX/SDH histochemistry on skeletal muscle from control and m.5024C>T tRNA^{Ala} mutant mice.

COX/SDH histochemistry on: (a)+ (b) Control mouse 2431 (m.5024C>T7%) calf and thigh muscle at x10 and x20 magnification. (c)+ (d) Mouse 1764 (m.5024C>T66%) thigh muscle at x10 and x20 magnification. (e)+ (f) Mouse 2266 (m.5024C>T53%) thigh muscle, at x10 and x20 magnification respectively. (g)+ (h) Mouse 2269 (m.5024C>T74%) calf and thigh muscle, at x10 and x20 magnification respectively. Scale bars: 100μm. COX positive fibers are brown, COX deficient fibers are blue (green arrows) and fibers with intermediate COX deficiency are purple (yellow arrows).

5.5.4 Does mitotic segregation affect m.5024C>T heteroplasmy across different tissues of young tRNA^{Ala} mutant mice?

Mitotic segregation of mtDNA results in considerable variation in heteroplasmy between different tissues and even different cell lineages of the same tissue (Macmillan, Lach et al. 1993), and is a principal factor involved in disease heterogeneity (Taylor and Turnbull 2005). To determine whether mitotic segregation influenced the m.5024 C>T heteroplasmy in different tissues of the mutant tRNA^{Ala} mice, and whether this may explain the different respiratory chain phenotypes observed, pyrosequencing was performed on homogenate DNA taken from the heart, thigh, calf and colon tissue supplied for young mutant tRNA^{Ala} mice (n=8). Note that all four tissues were not always supplied for each animal, with animals 1734 and 1764 lacking calf muscle and 1764 lacking a heart sample. Tail heteroplasmy was also taken into account, as recorded for each animal by RFLP, by James Stewart.

M.5024C>T heteroplasmy was not significantly different across the different tissues from young tRNA^{Ala} mutant mice ($p=0.1971$, One way ANOVA) (Figure 5-13a); however heteroplasmy in the colon was slightly lower compared to the other tissues, ($p=0.0180$, unpaired t test). This does however comply with the ~7% variation seen across multiple different tissues, including the blood and the skin, where even ~4% variation is seen in different skin patches (James Stewart, Personal communication). Nevertheless there was no segregation of the m.5024C>T mutation towards higher heteroplasmy in those tissues in which COX deficiency was observed (heart and skeletal muscle). Pyrosequencing of homogenate DNA from the different tissues from low level control animals also confirmed no significant difference in heteroplasmy across the tissues ($p=0.2835$, One way ANOVA) (Figure 5-13b).

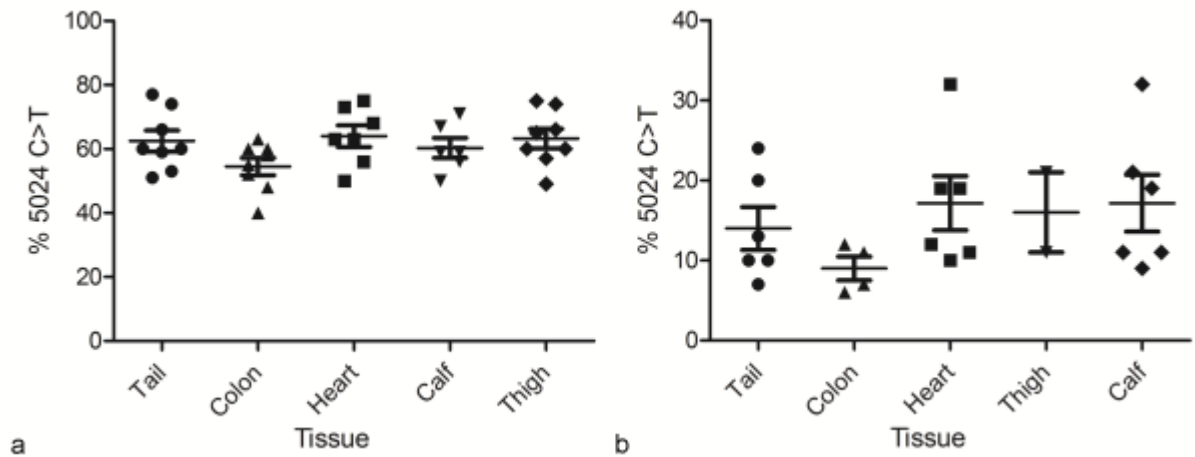


Figure 5-13: M.5024C>T heteroplasmy in different tissues of young mutant *tRNA^{Ala}* and control mice.

M.5024C>T heteroplasmy recorded in whole tissue from tail clippings, colon, heart, calf and thigh in (a) Young mutant *tRNA^{Ala}* mice 2307, 1734, 1764, 2265, 2266, 2267, 2268 and 2269. The m.5024C>T heteroplasmy was not significantly different across different tissues of mutant animals ($p=0.1971$, One way ANOVA). (b) Young low level control animals 2191, 2192, 2430, 2431, 2432 and 2489. The m.5024C>T heteroplasmy was not significantly different across different tissues of control animals ($p=0.2835$, One way ANOVA).

5.5.5 Do aged m.5024C>T *tRNA^{Ala}* mutant mice show evidence of enhanced mitochondrial dysfunction and a progressive mtDNA disease phenotype?

Prior to this point, mutant *tRNA^{Ala}* mice (>6th generation) were all young (<22 weeks old). MtDNA disease in humans can present at a variety of different ages of onset, with a substantial number of patients showing an absence of clinical phenotypes until adulthood (McFarland, Taylor et al. 2007). To determine whether aged animals displayed enhanced mitochondrial dysfunction and tissue phenotypes characteristic of human mitochondrial disease caused by an mt-tRNA mutation, m.5024 C>T *tRNA^{Ala}* mutant mice were aged to >65 weeks old.

5.5.5.1 Respiratory chain deficiency in mitotic and post-mitotic tissues of aged *tRNA^{Ala}* mutant mice

Dual COX/SDH histochemistry was performed on colon (10 μ m) samples from 65 week (n=7) and 70 week (n=3) old mutant *tRNA^{Ala}* mice. Fully COX deficient colonic crypts were rarely detected in aged animals (see Appendix D); however a substantial proportion of colonic crypts with partial COX deficiency (mix of blue and brown) were detected in all aged mice (Figure 5-14). The presence of partial COX deficient crypts indicates that only a few stem cells in a given crypt harbour high levels of the mutation and give rise to COX deficient progeny cells (the blue parts) and other stem cells carry low levels of the mutation and repopulate the majority of the crypt with progeny cells that have normal COX activity (Taylor, Barron et al. 2003). When the incidence of fully

and partial COX deficient colonic crypts was combined and compared to the m.5024 C>T tail heteroplasmy for each animal, there was an absence of correlation between the two ($p= 0.2752$, one way ANOVA) (Figure 5-15). In fact the two appeared to be more negatively correlated, with the highest percentage of combined COX deficiency detected at 50% (47% partial COX deficiency) in animal 2885 with the lowest m.5024 C>T tail heteroplasmy (26%) and animals with high tail heteroplasmy (m.5024 C>T, >60%) showing the lowest incidence of COX deficiency (23% partial COX deficiency). This could suggest that colonic crypts are being repopulated predominantly by stem cells with lower levels of the mutation, especially in the high heteroplasmy mutant mice, raising the possibility that high levels of the m.5024C>T mutation could be selected against at the level of colonic crypt stem cells.

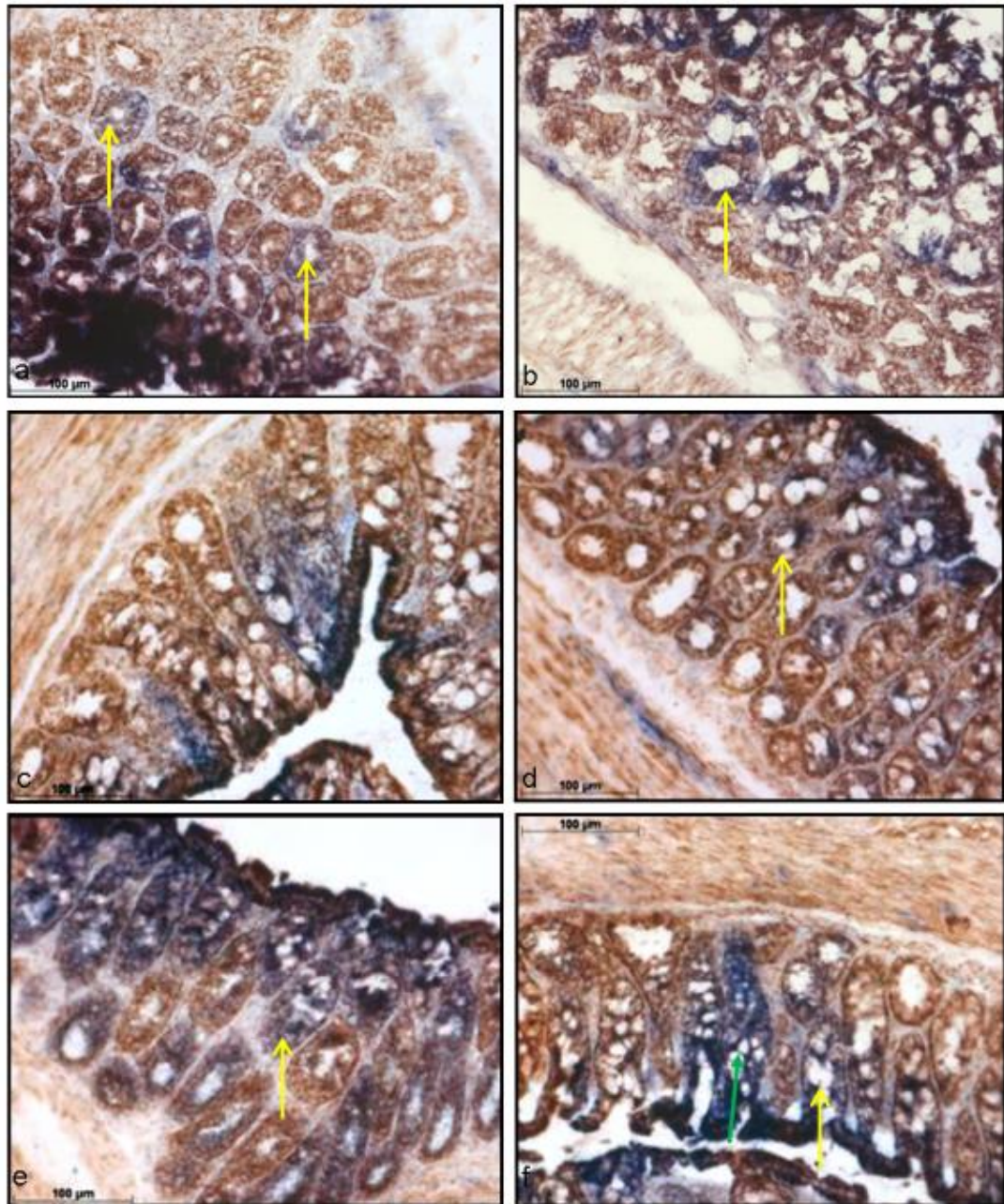


Figure 5-14: Respiratory chain deficiency in the colonic epithelium of 65 and 70 week old *m.5024C>T* *tRNA^{Ala}* mutant mice.

COX/SDH histochemistry on mouse: (a) 2241, 65 weeks old (*m.5024C>T*68%) (b) 2200, 65 weeks old (*m.5024C>T*58%) (c) +(d) 2884, 70 weeks old (*m.5024C>T*66%) (e) 2885, 70 weeks old (*m.5024C>T*26%). (e) 2887, 70 weeks old (*m.5024C>T*51%). All images were taken at x20 magnification. Scale bars: 100μm. COX positive crypts are brown, COX deficient crypts appear blue (green arrow) and those with partial COX deficiency are a mixture of brown and blue (yellow arrow).

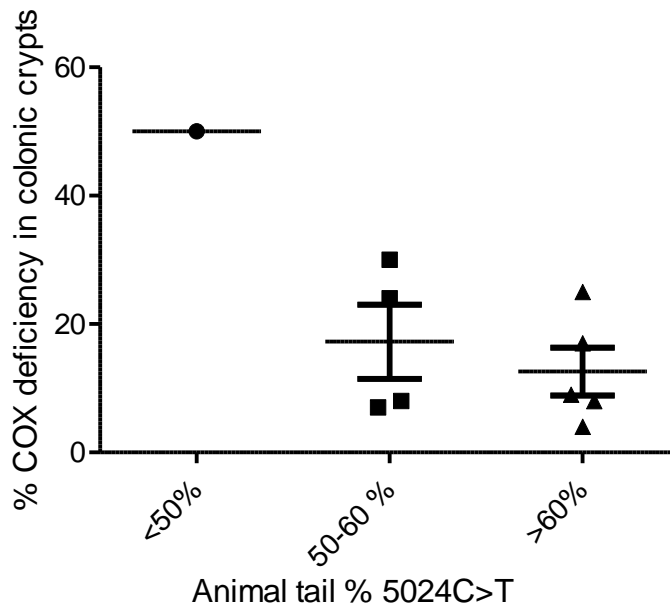


Figure 5-15: Absence of correlation between the magnitude of COX deficiency in the colon and the m.5024C>T tail heteroplasmy in aged (65 and 70 week old) mutant tRNA^{Ala} mice.

The percentage of colonic crypts that lacked normal COX activity (COX deficient crypts + crypts with partial COX deficiency) was not significantly different in mutant mice with high m.5024C>T tail heteroplasmy >60% (12.60 ± 3.750), than those with moderate levels of the mutation, 50-60% (17.25 ± 5.764) or the one animal with a low level of the mutation (50%), $p = 0.2752$, one way ANOVA.

Interestingly dual COX/SDH histochemistry on colon tissue from the aged mutant tRNA^{Ala} mice revealed the presence of COX deficient fibers in the colonic smooth muscle from 7 animals (Figure 5-16). Indeed COX deficiency in the colonic smooth muscle was never detected in the young (<22 week old) animals, indicating that muscle may just take longer to become afflicted by the m.5024 C>T mutation. Given the small size of the colonic smooth muscle fibers a Hue Saturation Value (HSV) colour space model was employed for automated detection of COX deficient (blue) fibers and COX positive (brown) fibers, courtesy of Craig Stamp (Figure 5-17a+b). A minimum of 15 images across various sections were analysed for each animal using the HSV colour space model and an average percentage of COX deficiency calculated. The highest level of COX deficiency in the colonic smooth muscle was recorded at 4% in two aged mutant animals (see Appendix D). The presence of COX deficiency in the colonic smooth muscle provided the first evidence of muscle phenotypes in the mutant tRNA^{Ala} mice.

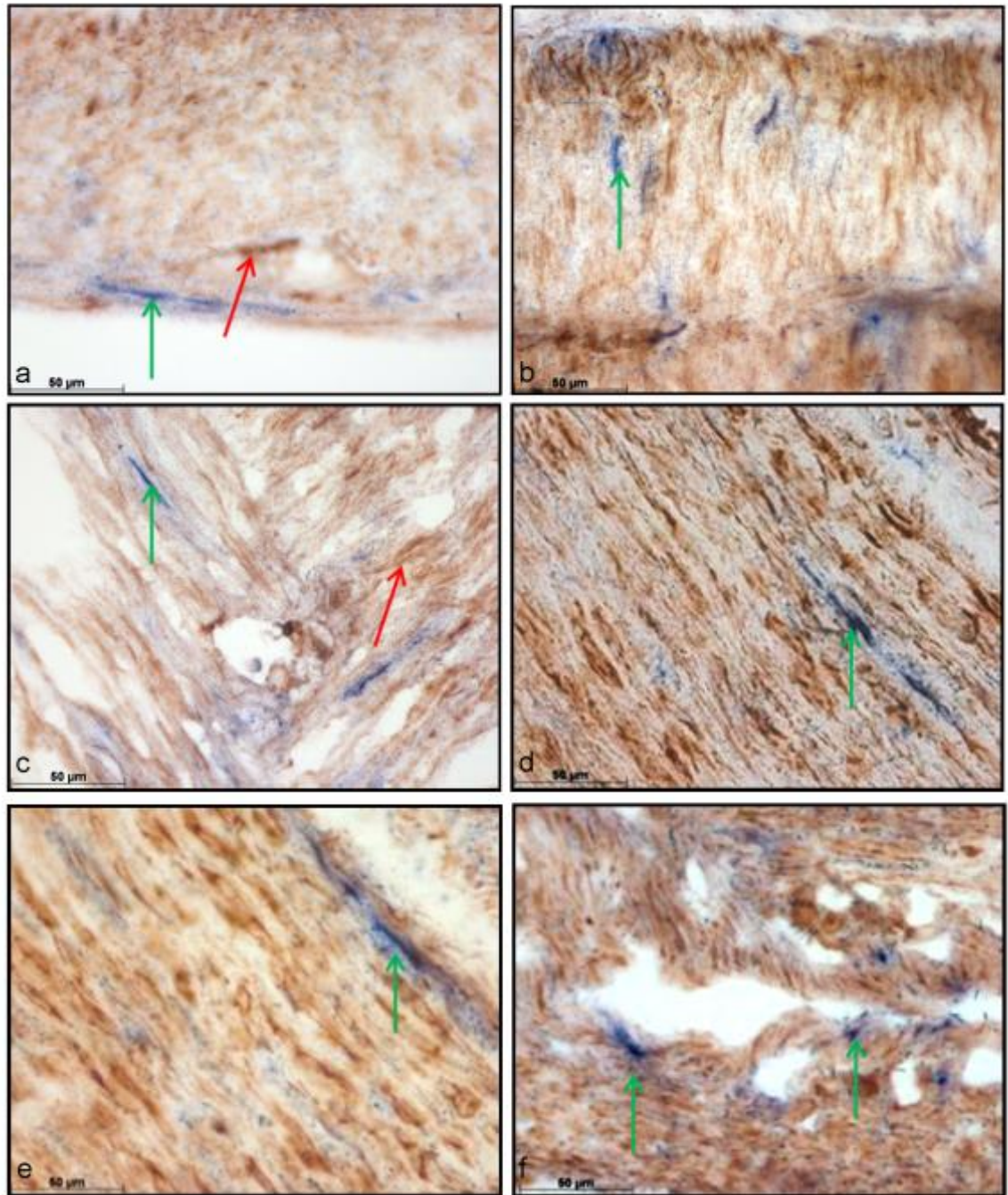


Figure 5-16: Respiratory chain deficiency in the colonic smooth muscle of 65 and 70 week old m.5024C>T tRNA^{Ala} mutant mice.

COX/SDH histochemistry on mouse: (a) 2241, 65 weeks old (m.5024C>T68%) (b) 2261, 65 weeks old (m.5024C>T64%) (c) 2200, 65 weeks old (m.5024C>T58%) (d)+ (e) 2884, 70 weeks old (m.5024C>T66%) (f) 2887, 70 weeks old (m.5024C>T51%) All images were taken at x40 magnification. Scale bars: 50μm. COX positive fibers are brown (red arrow) and COX deficient fibers appear blue (green arrow).

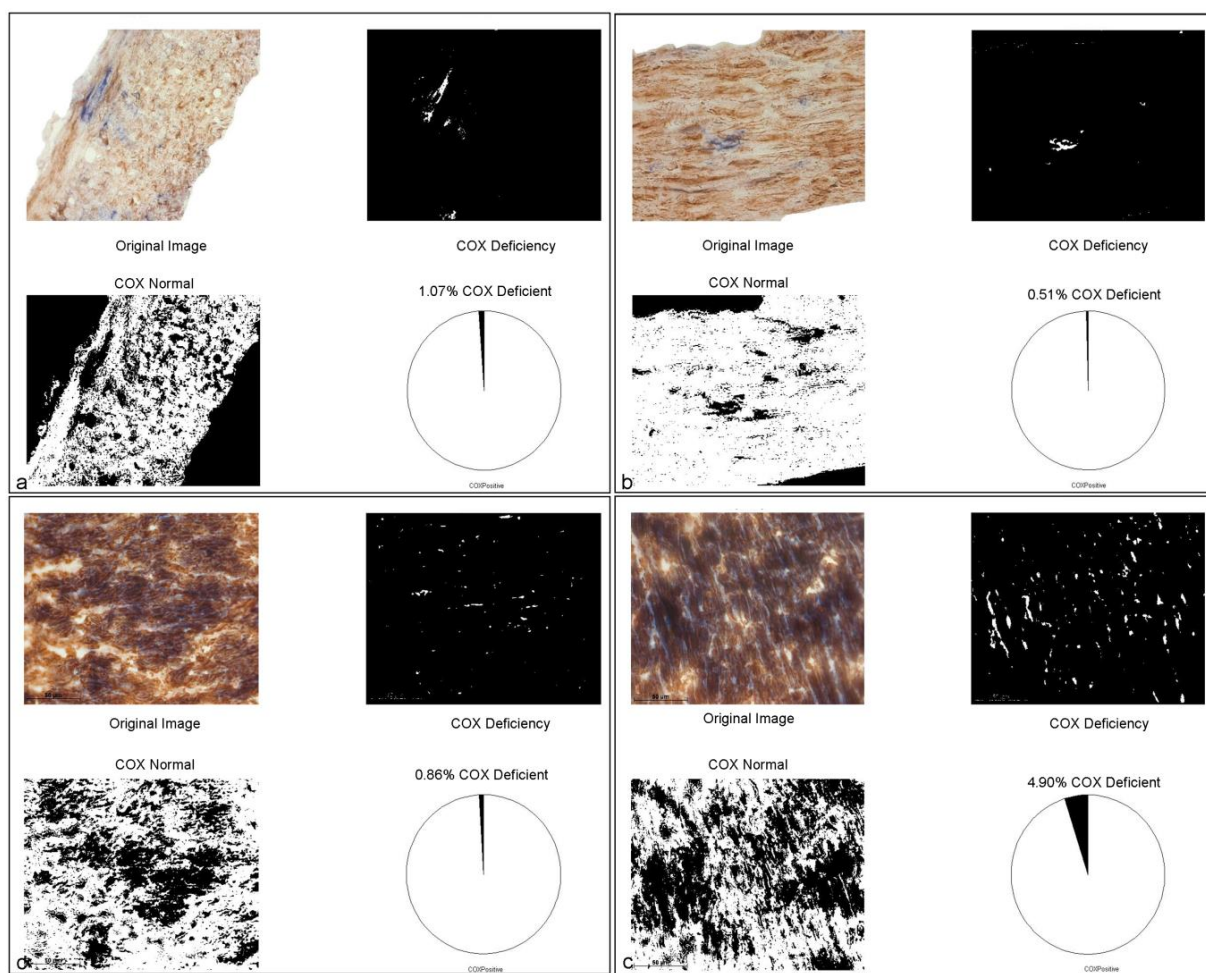


Figure 5-17: Example image outputs generated using the HSV colour space model for the accurate detection and quantification of COX deficiency in colonic smooth muscle and heart fibers of aged tRNA^{Ala} mutant mice.

Outputs show the original image, the image demonstrating the saturation for blue fibers (COX deficient), the image detecting brown fibers (COX positive) and a pie chart illustrating the percentage of COX deficiency for each image. Example outputs are shown for (a) Mouse 2200, 65 weeks old (m.5024TC>58%) colonic smooth muscle (b) Mouse 2884, 70 weeks old (m.5024C>T66%) colonic smooth muscle (c) Mouse 2884 (m.5024C>T66%) heart tissue and (d) Mouse 2885, 70 weeks old (m.5024C>T26%) heart tissue. Images courtesy of Craig Stamp.

To determine whether respiratory chain deficiency and a mitochondrial dysfunction phenotype were routinely observed in muscle tissues of aged tRNA^{Ala} mutant mice, COX/SDH histochemistry was performed on heart (8µm) and skeletal muscle (calf and thigh) (8µm) supplied for the three 70 week old animals (2884, 2885 and 2887). COX deficient heart fibers were detected in all three mice (Figure 5-18). Again, given the small size of the fibers coupled with their overlapping nature, the HSV colour space model was employed to determine the magnitude of COX deficiency in the heart (Figure 5-17c+d). This revealed a maximum of 9% COX deficiency in the heart of animal 2884 (m.5024 C>T 66%) (see Appendix D). Both the calf and thigh from all three aged mutant tRNA^{Ala} mice displayed fibers that lacked normal COX activity, presenting with intermediate COX deficient fibers (purple) and transitional COX deficient fibers (part brown and part blue) (Figure 5-19). The incidence of COX

deficiency was calculated subjectively, for ~500 muscle fibers across multiple different sections per tissue sample (see Appendix D). Fully COX deficient muscle fibers were only detected in the calf of animal 2884 (m.5024 C>T 66%), reaching a mere 1% across the whole tissue section. Nevertheless the percentage of fibers that lacked normal COX activity (intermediate and transitional fibers) frequently reached 5% in the calf and thigh of the three 70 week old mutant tRNA^{Ala} mice (see Appendix D). As such this data demonstrated that aged mutant tRNA^{Ala} mice displayed phenotypic evidence of mitochondrial dysfunction in muscle tissues, a common histological feature of disease caused by an mt-tRNA mutation (Taniike, Fukushima et al. 1992; Taylor, Giordano et al. 2003; Swalwell, Deschauer et al. 2006; McFarland, Swalwell et al. 2008)..

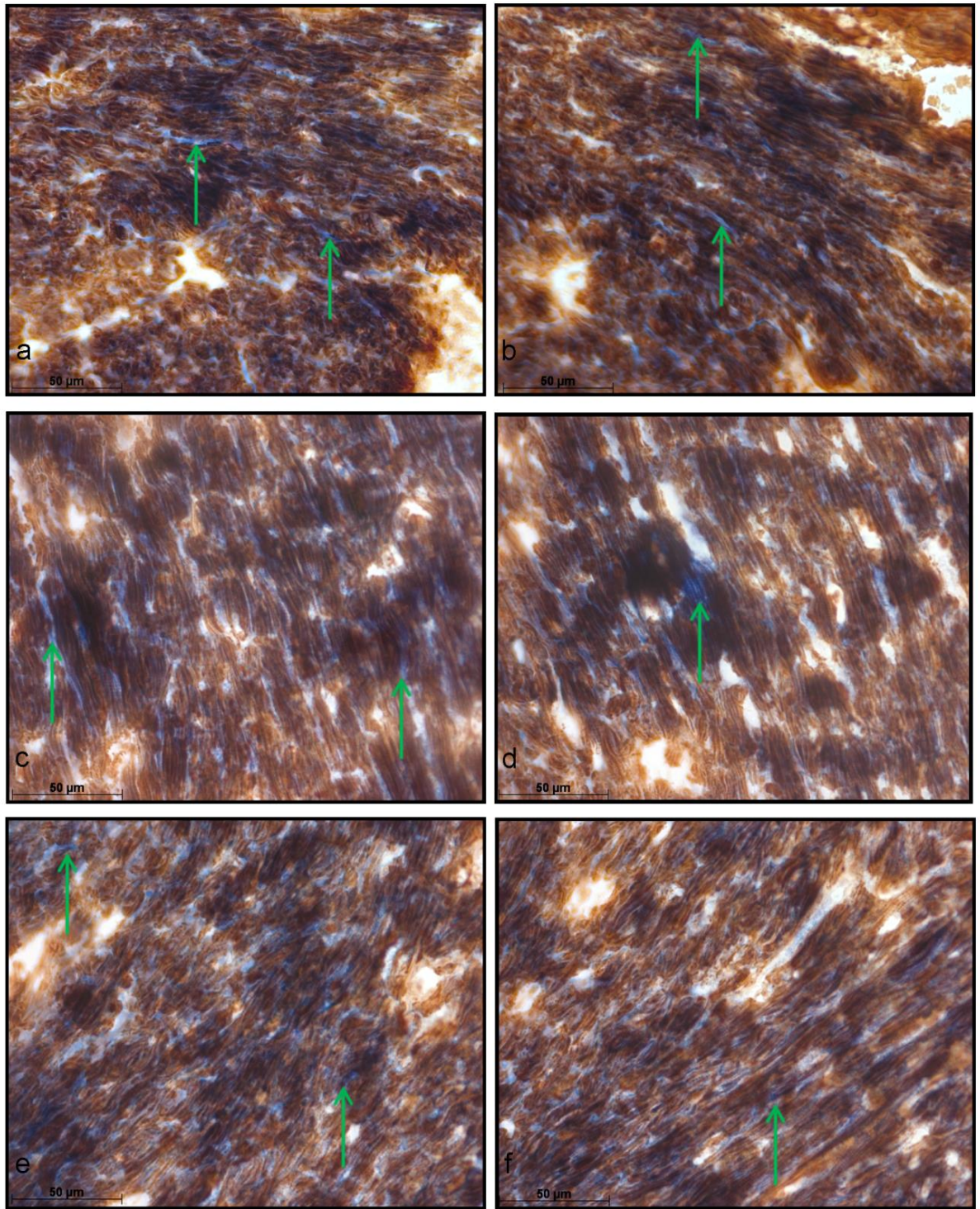


Figure 5-18: Respiratory chain deficiency in the heart of 70 week old m.5024C>T tRNA^{Ala} mutant mice.

COX/SDH histochemistry on: (a)+(b) Mouse 2884 (m.5024C>T66%) heart (c)+(d) Mouse 2885 (m.5024C>T26%) heart and (e)+(f) Mouse 2887 (m.5024C>T51%) heart. All images were taken at x40 magnification. Scale bars: 50μm. COX positive cardiac muscle fibers are brown and COX deficient fibers appear blue (green arrows).

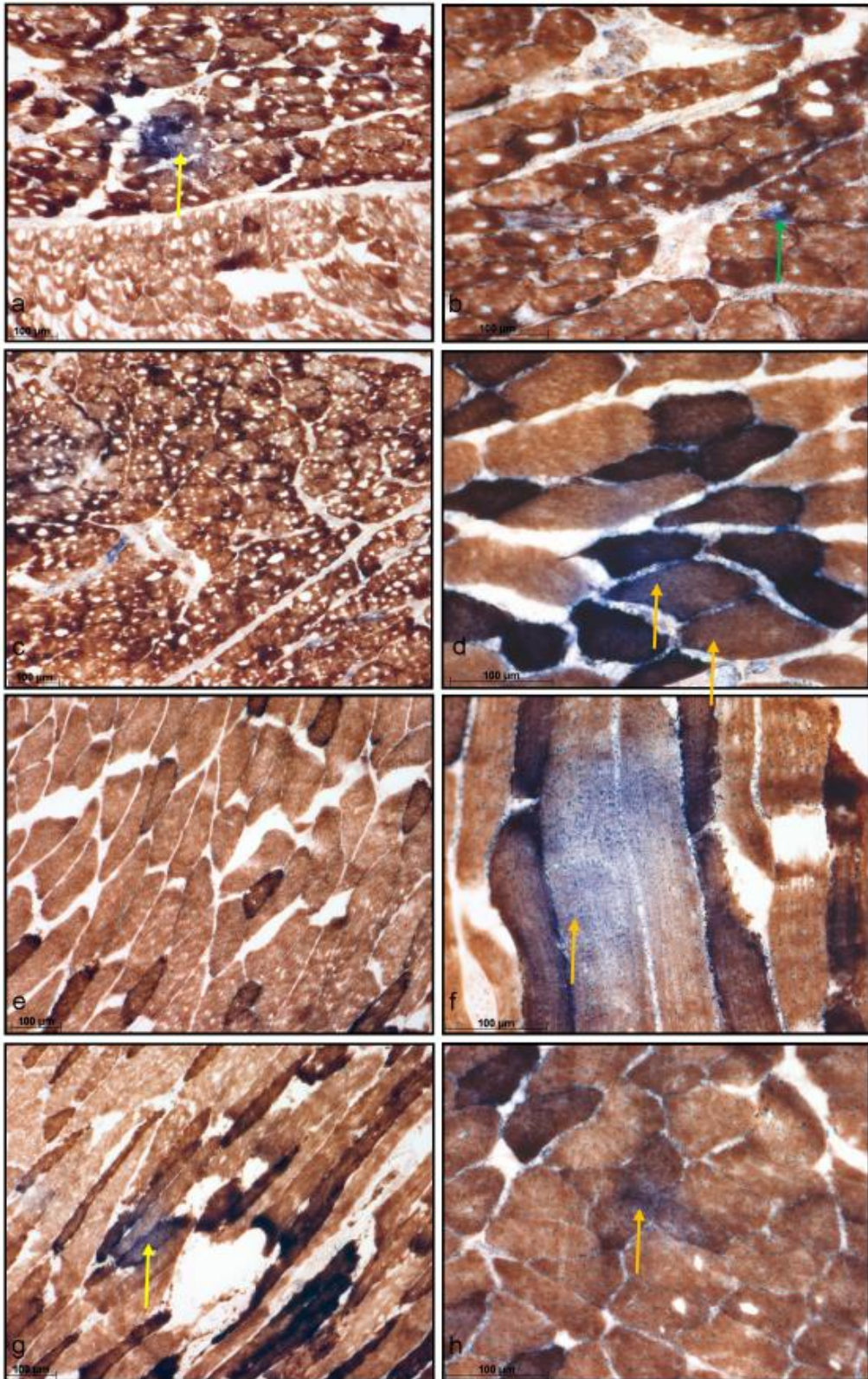


Figure 5-19: COX/SDH histochemistry on skeletal muscle tissue from 70 week old m.5024C>T tRNA^{Ala} mutant mice.

COX/SDH histochemistry on: (a+b) Mouse 2884, 70 weeks old (m.5024C>T66%) thigh and (c) calf at x10 and x20 magnification. (d+e) Mouse 2885 (m.5024C>T26%) thigh and (f) calf at x10 and x20 magnification. (g) Mouse 2887 (m.5024C>T51%) thigh and (h) calf at x10 and x20 magnification respectively. Scale bars: 100μm. COX positive fibers are brown, COX deficient fibers appear blue (green arrow), those with intermediate deficiency appear a purple colour (yellow arrow) and those fibers with transitional COX deficiency appear part blue and part brown (orange arrows).

To determine whether the magnitude of COX deficiency observed in the colon (crypts and smooth muscle) heart and skeletal muscle (thigh and calf) was influenced by the m.5024 C>T tail heteroplasmy of aged tRNA^{Ala} mutant mice, the percentage of total COX deficiency (cells that lacked normal COX activity) for each tissue was categorized according to low, moderate and high tail heteroplasmy for animals and a two way ANOVA performed. This revealed that COX activity was significantly affected by the tissue type ($p=0.0015$), accounting for 76% variance in the percentage of COX deficiency, but was not significantly affected by the m.5024 C>T tail heteroplasmy of the animal ($p=0.2860$), which only accounted for 4% variance in COX activity (Figure 5-20). One way ANOVA tests for each individual tissue type confirmed that m.5024 C>T heteroplasmy of aged tRNA^{Ala} mice had no significant effect on COX deficiency in the: colonic crypts (Figure 5-15); colonic smooth muscle ($p=0.2169$); heart ($p=0.3675$) and skeletal muscle ($p=0.6495$). However, the statistical analysis was only performed on 3 tissue samples for the post-mitotic tissues of aged animals and so appropriate and robust correlations cannot really be made here. In general, however the mice with higher m.5024C>T tail heteroplasmy did display the higher levels of COX deficiency, as seen in animal 2884 (m.5024C>T 66%), which presented with the highest COX deficiency in the heart (9%) and calf muscle (~5% of fibers lacked normal COX activity) (see Appendix D). As such I would expect this correlation to be more statically robust if more tissue samples were provided. Nevertheless, aged mutant tRNA^{Ala} mice did display evidence of respiratory chain deficiency and mitochondrial dysfunction in post-mitotic tissues, which are typical features of mt-tRNA disease (Taniike, Fukushima et al. 1992; Taylor, Giordano et al. 2003; Swalwell, Deschauer et al. 2006; McFarland, Swalwell et al. 2008).

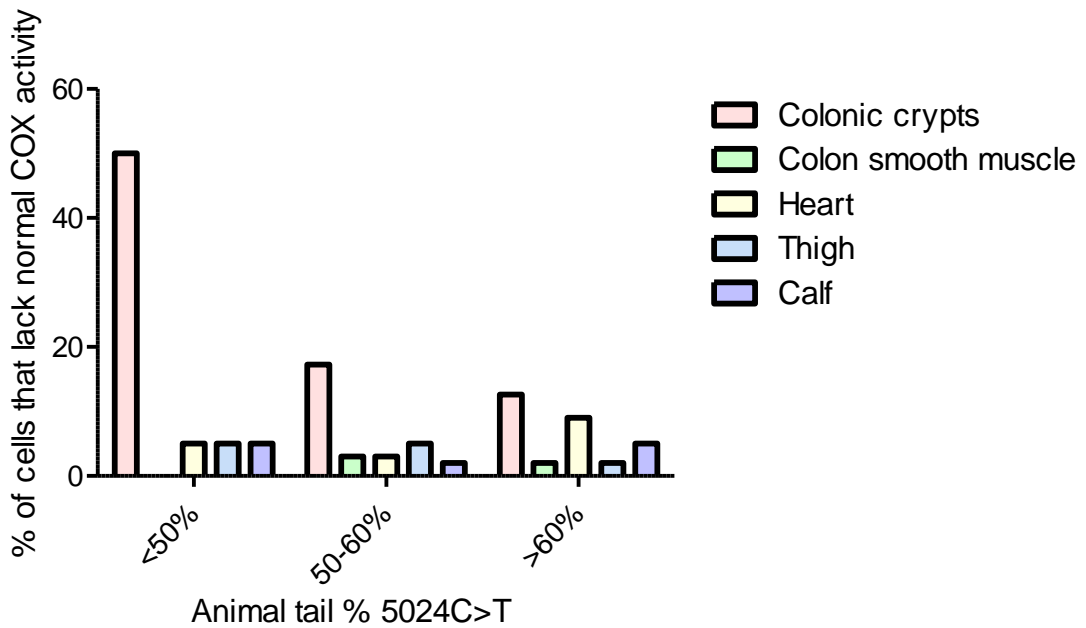


Figure 5-20: The effect of m.5024C>T tail heteroplasmy and tissue variability on the incidence of COX deficiency in aged mutant tRNA^{Ala} mice.

The percentage of cells that lacked normal COX activity comprised a combination of full COX deficient cells and those with partial/ intermediate and transitional COX deficiency. COX activity was significantly affected by the tissue type in aged tRNA^{Ala} mutant animals ($p=0.0015$) but m.5024C>T heteroplasmy had no significant effect on COX activity in colonic crypts, colonic smooth muscle, heart, thigh and calf muscle, $p=0.2860$, two way ANOVA test.

Dual COX/SDH histochemistry was also completed on colon ($n=4, 10\mu\text{m}$), heart ($n=2, 8\mu\text{m}$) and skeletal muscle (thigh and calf) ($n=2, 10\mu\text{m}$) of pure WT control animals, aged 65-69 weeks old, used to maintain the m.5024 C>T tRNA^{Ala} breeding colony. All tissues displayed normal COX activity, with only one COX deficient crypt detected in animal 17066 (Figure 5-21). This confirmed an absence of respiratory chain deficiency in normal ageing animals, supporting that the COX deficiency observed in the aged mutant tRNA^{Ala} mice was not associated with the normal ageing process but was due to the presence of the m.5024C>T mutation.

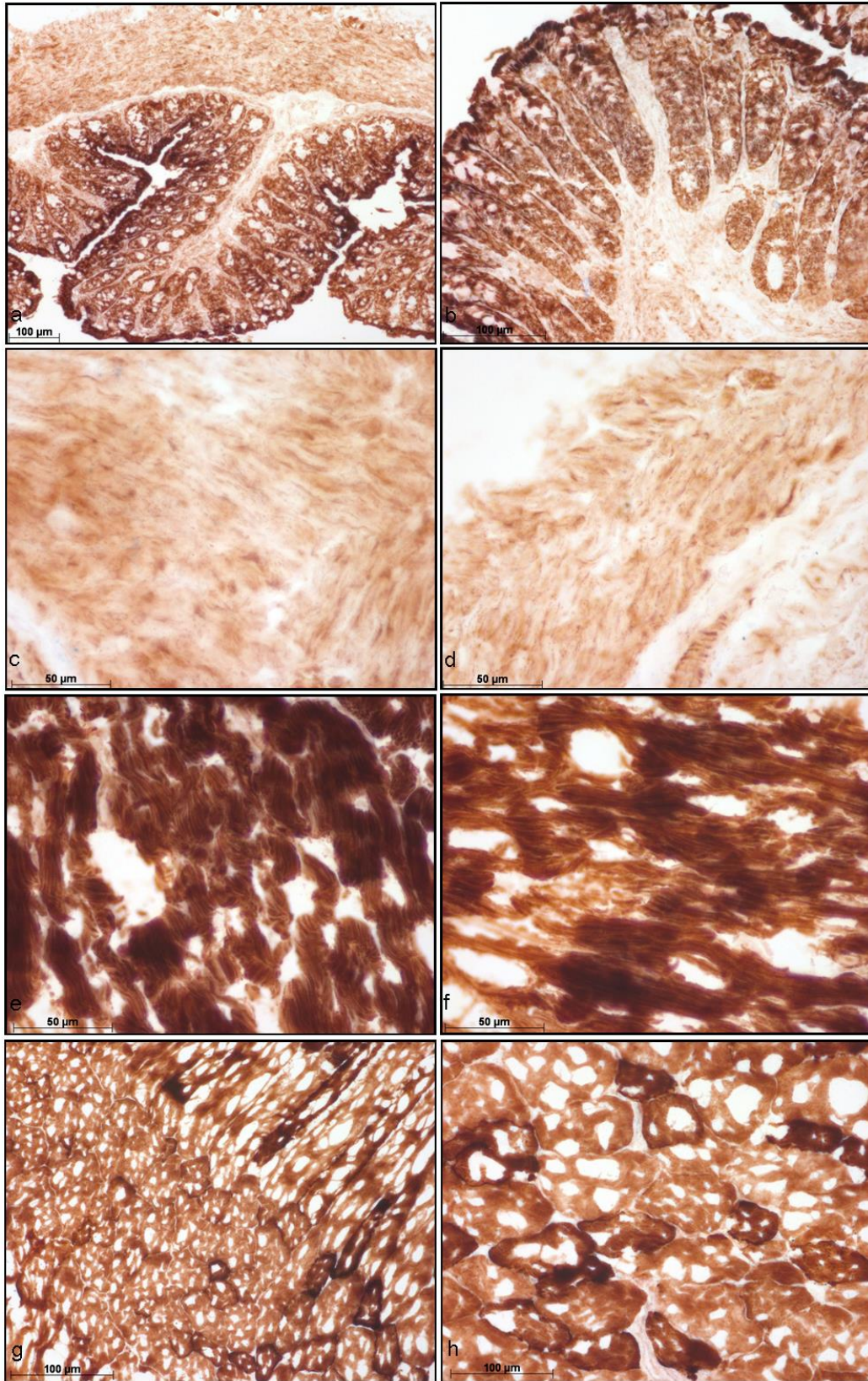


Figure 5-21:COX/SDH histochemistry on aged WT control mouse muscle tissues.

Colonic crypts of (a) Mouse 17066, x10 magnification and (b) Mouse 17369, x 20 magnification. Colonic smooth muscle of (c) Mouse 17066 and (d) Mouse 17369, both at x40 magnification. Heart tissue of (e) Mouse 17066 and (f) Mouse 17369, both at x40 magnification. (g) Mouse 17066 thigh at x 10 magnification. (h) Mouse 17369 calf at x20 magnification. Scale bars: 100μm.

5.5.5.2 *Is there a selective loss of the m.5024C>T mutation in the colon of aged mutant tRNA^{Ala} mice?*

Given that the incidence of combined COX deficiency was lower in aged tRNA^{Ala} mutant mice with high m.5024 C>T tail heteroplasmy, it appeared that the m.5024 C>T mutation may have been lost from the colonic epithelium over time. To determine whether the m.5024 C>T mutation was selected against in the colon of aged tRNA^{Ala} mutant mice pyrosequencing was performed on homogenate colon DNA for all 65 (n=7) and 70 (n=3) week old mice to quantify the m.5024 C>T heteroplasmy in the colon. This was subsequently compared to the tail the m.5024 C>T heteroplasmy, previously measured by RFLP by James Stewart. This revealed that m.5024 C>T heteroplasmy was significantly lower in the colon compared to the tail for each animal ($p = <0.0001$, paired t test), with all animals showing a reduction by more than half of m.5024 C>T heteroplasmy in the colon (mean difference= 27%) (Figure 5-22). The colon homogenate DNA would contain a small amount from the colonic smooth muscle; however, given that the overwhelming proportion of the colon consists of the colonic epithelium, this data suggests that the m.5024C>T mutation is being lost from the colonic epithelium.

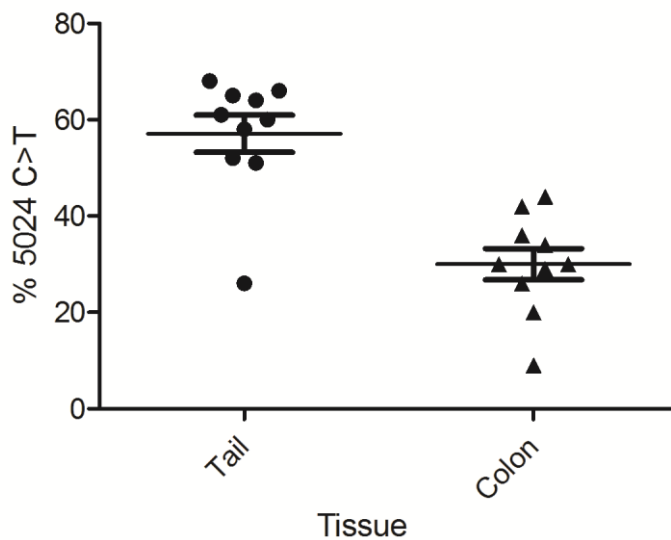


Figure 5-22: The m.5024C>T heteroplasmy in the colon compared to the tail in aged (65 and 70 week old) tRNA^{Ala} mutant mice.

The m.5024C>T heteroplasmy is significantly lower in the colon than in the tail clippings for each 65 and 70 week old tRNA^{Ala} mutant mouse, $p = <0.0001$, paired t test. Mean of differences= 27.10%. M.5024C>T heteroplasmy in the tail was measured by RFLP by James Stewart.

5.5.5.3 *Does mitotic segregation influence m.5024C>T heteroplasmy in different tissues in aged mutant tRNA^{Ala} mice?*

Given that the m.5024 C>T mutation appears to be selectively lost in the colonic epithelium of aged tRNA^{Ala} mutant mice (Figure 5-22), I wanted to determine whether mitotic segregation influenced the m.5024 C>T heteroplasmy in other tissues of these animals and whether the selective loss was limited to a mitotic tissue. Furthermore, when aged mutant tRNA^{Ala} mice were sacrificed they routinely showed an increased heart to body mass ratio (James Stewart, personal communication). As such I wanted to determine whether the heart displayed higher m.5024 C>T heteroplasmy and had become more afflicted over time. Heart, thigh and calf (calf was absent for animal 2885), in addition to colon tissue, were provided for the three 70 week old tRNA^{Ala} mutant mice, and so pyrosequencing of homogenate DNA from these tissues was completed to determine the m.5024 C>T heteroplasmy. This was also compared to the tail heteroplasmy, measured by RFLP by James Stewart. Heart and skeletal muscle were not provided for the 65 week old animals, and so this could not be performed.

Pyrosequencing of the different tissues of 70 week mutant tRNA^{Ala} mice confirmed that the m.5024 C>T heteroplasmy was significantly lower in the colon compared to all other tissues ($p=0.0202$, unpaired t test) (Figure 5-23). Furthermore heteroplasmy was not significantly different between the heart, skeletal muscle and tail ($p=0.8964$, one way ANOVA), demonstrating that the m.5024C>T mutation was maintained at constant levels in these tissues (Figure 5-23). Given that the colonic epithelium is mitotic and all other tissues examined were post-mitotic; this data suggests that the m.5024C>T mutation is selectively lost from actively dividing, mitotic cells. Furthermore this data does not indicate that the cardiomyopathy observed in aged animals was due to higher m.5024C>T heteroplasmy in the heart.

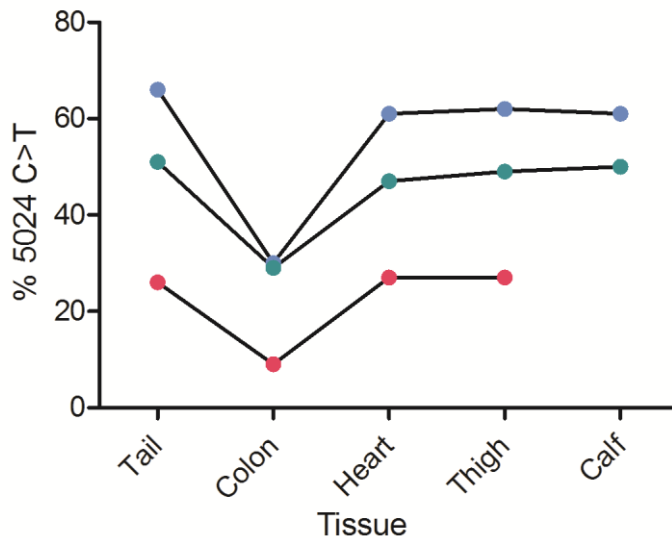


Figure 5-23: M.5024C>T heteroplasmy in different tissues of 70 week old mutant $tRNA^{Ala}$ mice.

M.5024C>T heteroplasmy recorded in whole tissue from tail clippings, colon, heart, calf and thigh in mice: 2884 (m.5024C>T66%), blue data points; 2885 (m.5024TC>26%), red data points and 2887 (m.5024C>T51%), green data points. The m.5024C>T heteroplasmy is significantly lower in the colon than in the other tissues of 70 week mutant mice, $p=0.0202$, unpaired t test.

5.5.5.4 *Is the m.5024C>T heteroplasmy lower in the colonic crypts of aged mutant $tRNA^{Ala}$ mice?*

To determine what was happening to the m.5024C>T heteroplasmy in the colonic crypts of aged mutant $tRNA^{Ala}$ mice, pyrosequencing was performed on single COX positive crypts (n=14) and crypts with partial COX deficiency (n=14). This was successfully achieved for the three 70 week old animals; however attempts in 65 week old animals failed. A freeze thaw issue upon shipment of the tissue provided for the 65 week old animals, resulted in problems with DNA degradation, with DNA smears observed on PCR gels and an absence of the single, clear 178bp fragment necessary for pyrosequencing of the m.5024 region (Figure 5-24).

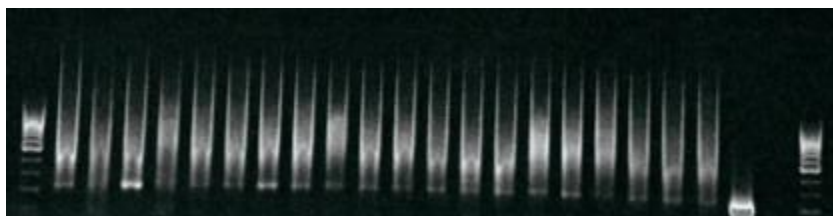


Figure 5-24: Example gel electrophoresis image following the pyrosequencing PCR of single colonic crypts from 65 week old $tRNA^{Ala}$ mutant mice.

Gel electrophoresis image showing the presence of DNA smears for single colonic crypts and an absence of a clear 178bp fragment necessary for pyrosequencing, indicating DNA degradation within the samples. The one defined band is a WT control.

Successful pyrosequencing of single COX positive and partial COX deficient colonic crypts from the three 70 week old tRNA^{Ala} mutant mice revealed only moderate m.5024C>T heteroplasmy in all colonic crypts (Figure 5-25a). COX positive crypts actually displayed higher heteroplasmy (18.66 ± 2.165) than those with partial COX deficiency (11.70 ± 2.411) ($p= 0.0367$, unpaired t test) (Figure 5-25b). A two way ANOVA revealed that m.5024 C>T heteroplasmy in colonic crypts was mildly affected by COX activity ($p= 0.0454$) accounting for only ~5% variance in heteroplasmy, but that variability between mice had no significant effect ($p=0.0686$), accounting for ~6% variance (Figure 5-25c). Low m.5024C>T heteroplasmy in the partial COX deficient crypts suggests that the majority of crypt progeny cells are generated from stem cells that harbour only low levels of the mutation, indicating that any stem cell with high levels of the mutation are potentially being lost from the stem cell pool. If I had more time it would have been beneficial to laser micro-dissect and pyrosequence the COX positive portion and COX deficient portions of the partial crypts to determine whether there was a difference in heteroplasmy. As such this could indicate whether the different progeny cells were arising from different stem cells harbouring different m.5024C>T heteroplasmy.

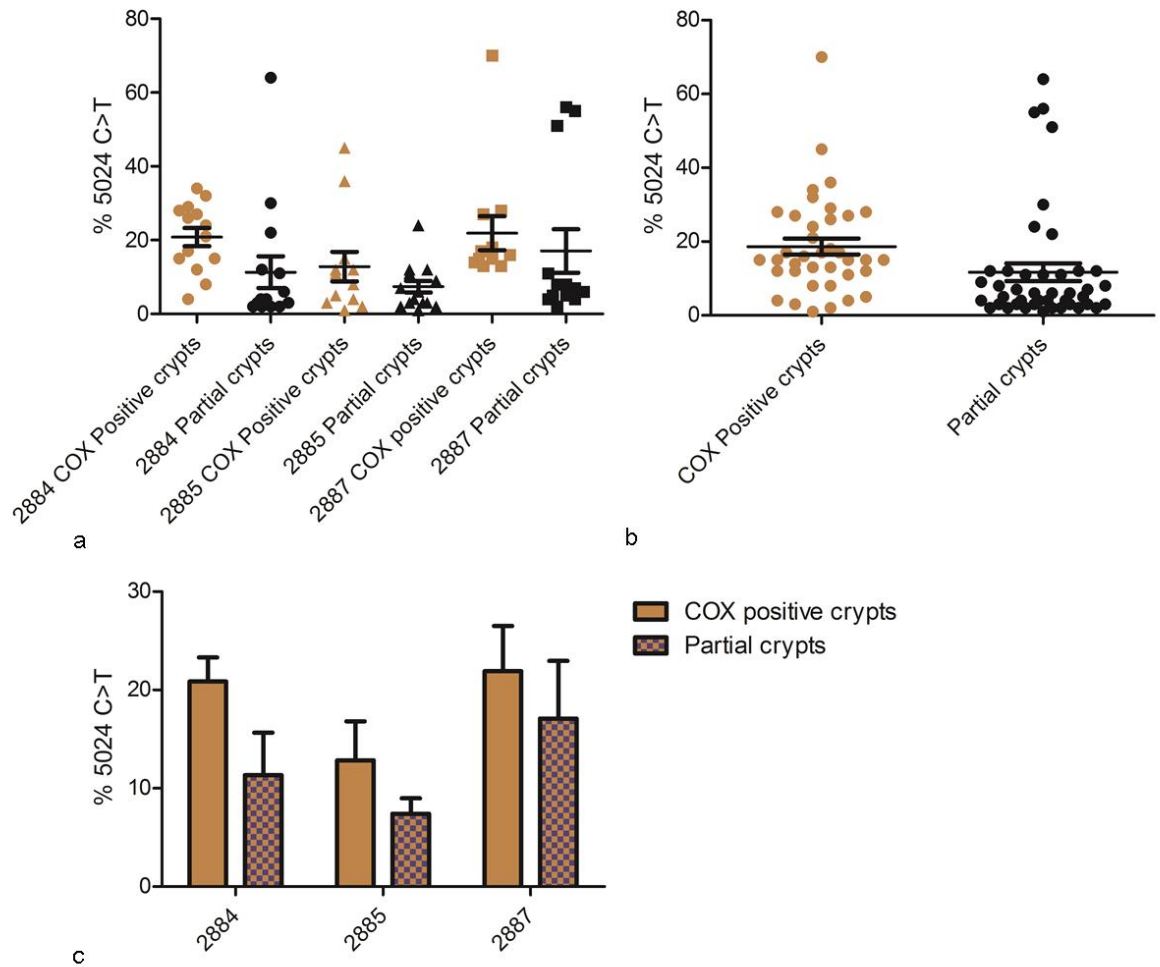


Figure 5-25: M.5024C>T heteroplasmy in single colonic crypts from 70 week old mutant tRNA^{Ala} mice.

(a) The m.5024C>T heteroplasmy is not significantly different in single COX positive colonic crypts and crypts with partial COX deficiency from tRNA^{Ala} mutant mice 2884 (m.5024C>T 66%), 2885 (m.5024C>T 26%) and 2887 (m.5024C>T 51%) ($p = 0.3046$, one way ANOVA test). (b) M.5024C>T heteroplasmy in all COX positive colonic crypts (18.66 ± 2.165) is significantly higher than in crypts with partial COX deficiency (11.70 ± 2.411) ($p = 0.0367$, unpaired t test). (c) The effect of COX activity and mouse variability on the m.5024C>T heteroplasmy in single colonic crypts. COX activity significantly affected the m.5024C>T heteroplasmy in single colonic crypts ($p = 0.0454$), but variability between mice had no significant effect ($p = 0.0686$), two way ANOVA test.

5.5.5.5 Does the m.5024C>T mutation segregate with the muscle phenotype observed in the colon of aged mutant tRNA^{Ala} mice?

To determine whether the m.5024 C>T mutation segregated with the COX deficiency in the colonic smooth muscle of aged tRNA^{Ala} mutant mice, mtDNA genome analysis of the m.5024 region was performed on COX positive and COX deficient colonic smooth muscle fibers. Again, given the DNA degradation issue in the colon of 65 week old animals this was only successfully completed for the 70 week old tRNA^{Ala} mutant mice. Given that there was an absence of COX deficiency (0%) detected in the colonic smooth muscle of animal 2885 (m.5024 C>T 26%), this could only be completed in animals 2884 and 2887. Due to the small size of the colonic smooth muscle fibers, successful

amplification of DNA fragments for mtDNA genome analysis was only achieved when >25 single muscle fibers were laser micro-dissected and pooled together for each sample.

Sequencing of the m.5024 region in COX positive (n=5) and COX deficient (n=5) smooth muscle fibers from animals 2884 and 2887, confirmed the presence of the m.5024 C>T mutation in colonic smooth muscle fibers, revealing very high heteroplasmy (Figure 5-26). Furthermore the m.5024 C>T mutation appeared to segregate with the COX deficiency, with COX deficient smooth muscle fibers presenting with very high heteroplasmy (>75%) /homoplasmy of the m.5024 C>T mutation and COX positive fibers presenting with moderate heteroplasmy (<75%) (Figure 5-26).

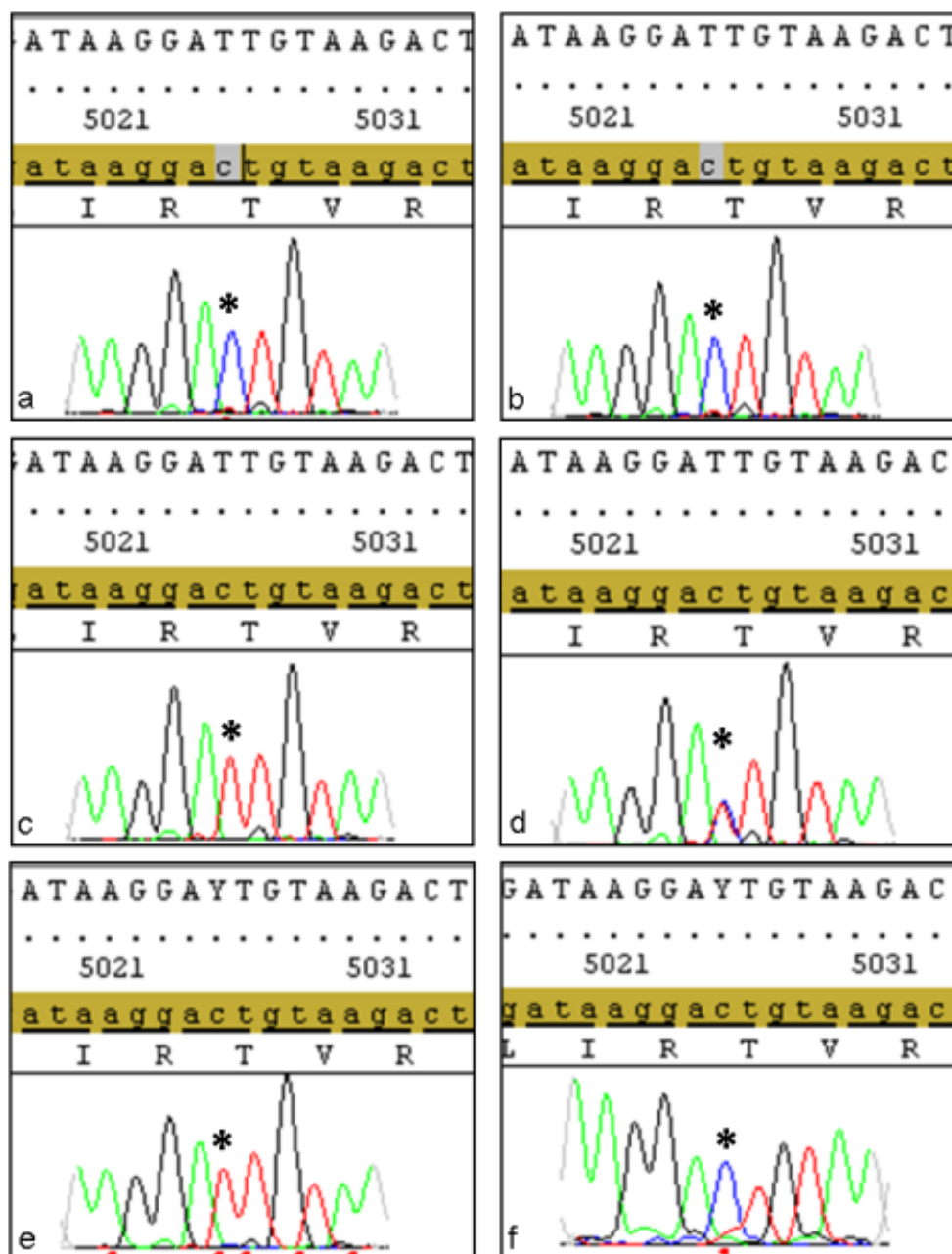


Figure 5-26: Example sequencing electropherograms demonstrating the presence of the m.5024C>T mutation in colonic smooth muscle fibers of aged mt5024C>T tRNA^{Ala} mutant mice.

(a)+(b) Electropherograms from control mice 9831 and 10045 respectively, illustrating the presence of the WT C base at position m.5024. (c) Sequencing of this region in a COX deficient smooth muscle fiber sample from mouse 2884, 70 weeks old (m.5024C>T66%) revealed the m.5024C>T mutation at 100% homoplasmy and (d) in a COX positive smooth muscle fiber sample m.5024C>T ~50% heteroplasmy. (e) Sequencing of this region in a COX deficient smooth muscle fiber sample from mouse 2887, 70 weeks old (m.5024C>T51%) revealed the m.5024C>T mutation at 100% homoplasmy and (f) in a COX positive smooth muscle fiber sample revealed m.5024C>T, ~15% heteroplasmy. The stars indicate the m.5024 position and the C>T base change in the mouse mtDNA sequence.

Pyrosequencing of COX positive (n=14) and COX deficient smooth muscle fibers

(n=14) from animals 2884 and 2887 was subsequently completed to accurately quantify the m.5024 C>T heteroplasmy, determine whether the mutation segregated with COX deficiency and identify the biochemical threshold in smooth muscle fibers. This revealed that the highest levels of the m.5024 C>T mutation segregated with the COX

deficiency in both 70 week old tRNA^{Ala} mice ($p = <0.0001$, one way ANOVA) (Figure 5-27a). COX deficient fibers presented with significantly higher heteroplasmy (84.31 ± 1.055) than COX positive fibers (54.85 ± 1.550) ($p = <0.0001$, unpaired t test), identifying a potential threshold of ~84% (Figure 5-27b). Note that the variation in heteroplasmy in COX positive versus COX deficient smooth muscle fibers is very tight, demonstrating a clear and precise segregation of the mutation with COX deficiency. A two way ANOVA revealed that m.5024C>T heteroplasmy in colonic smooth muscle fibers was significantly affected by COX activity ($p = <0.0001$), accounting for ~81% variance in heteroplasmy (Figure 5-27c). Variability between the two mice also had a significant effect on m.5024 C>T heteroplasmy ($p = <0.0001$), however this only accounted for ~6% variance (Figure 5-27c). This variability was unsurprising given that only two mice were used; however the m.5024C>T heteroplasmy was indeed higher in the COX deficient and COX positive colonic smooth muscle fibers of animal 2884 with the higher tail heteroplasmy (m.5024C>T 66%) than animal 2887 (m.5024C>T 51%) (Figure 5-27a). Segregation of the m.5024C>T mutation with the COX deficiency in the colonic smooth muscle fibers further demonstrates pathogenicity of the mutation, showing that it is causal in the muscle phenotypes observed in these mice, which is representative of disease caused by mt-tRNA mutations (Swalwell, Deschauer et al. 2006; McFarland, Swalwell et al. 2008). Given that the apparent threshold for COX deficiency in the colonic crypts was ~70%, the data from the colonic smooth muscle fibers also provides evidence that different cell types in the mutant tRNA^{Ala} mice have different biochemical thresholds.

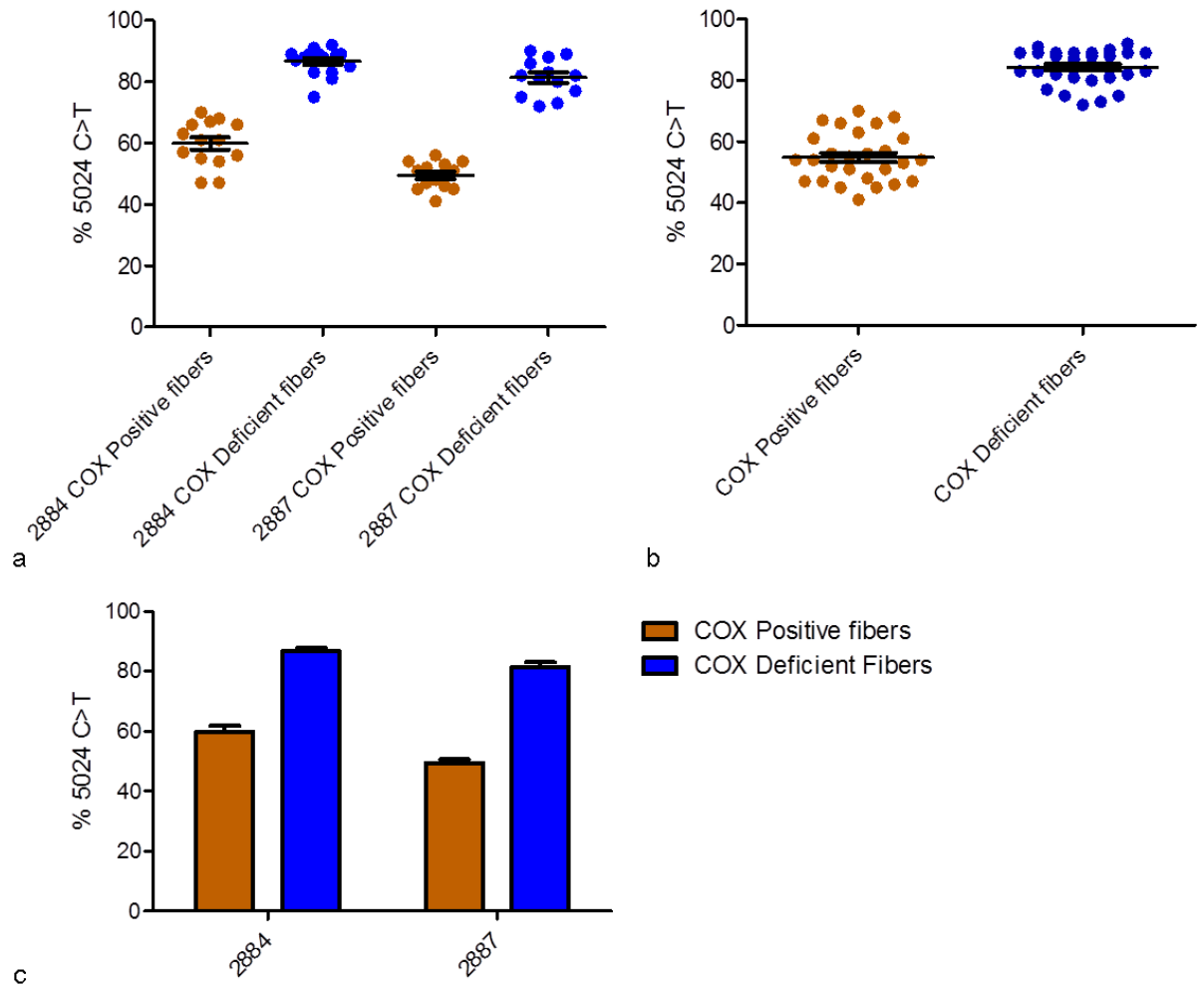


Figure 5-27: Segregation of the m.5024C>T mutation with COX deficiency in colonic smooth muscle fibers of 70 week old mutant tRNA^{Ala} mice.

(a) The m.5024C>T heteroplasmy is significantly higher in COX deficient colonic smooth muscle fibers than COX positive fibers from tRNA^{Ala} mutant mice 2884 (m.5024C>T 66%) and 2887 (m.5024C>T 51%) ($p < 0.0001$, one way ANOVA test). (b) M.5024C>T heteroplasmy in all COX positive colonic smooth muscle fibers (54.85 ± 1.550) is significantly lower than COX deficient fibers (84.31 ± 1.055) ($p < 0.0001$, unpaired t test). (c) The effect of COX activity and mouse variability on the m.5024C>T heteroplasmy in colonic smooth muscle fibers. The m.5024C>T heteroplasmy was significantly affected by COX activity ($p < 0.0001$) and variability between the two mice ($p < 0.0001$) two way ANOVA test.

5.6 Discussion

Establishing mouse models of mitochondrial DNA disease that harbour pathogenic heteroplasmic mtDNA point mutations is extremely desirable to enable further research into: disease mechanisms and pathogenicity; disease progression; transmission and the development of potential treatments. In this study I show that young mice harbouring a m.5024C>T mutation in mt-tRNA^{Ala} routinely display evidence of respiratory chain deficiency in the colonic epithelium, with which the mutation segregated, establishing that the m.5024 C>T mutation was pathogenic. This also suggests that dual COX/SDH histochemistry in the colon is a good early experimental screening tool for identifying in

vivo mitochondrial dysfunction and pathogenic mtDNA point mutations in the breeding of mouse lineages. Furthermore I show that aged m.5024C>T tRNA^{Ala} mutant mice show signs of progressive disease, displaying muscle phenotypes and respiratory chain deficiency, with different cell types showing different biochemical thresholds, which are typical features of mitochondrial disease caused by an mt-tRNA mutation (Jacobs 2003). Finally I also demonstrate a selective loss and elimination of the m.5024C>T mutation from the colonic epithelium of aged tRNA^{Ala} mutant mice, establishing a difference in m.5024C>T heteroplasmy between post-mitotic and mitotic tissues. This data therefore suggests that mice harbouring the m.5024C>T mutation would be a valuable model of mitochondrial disease caused by an mt-tRNA point mutation and could be extremely useful for studying disease progression, presentation, transmission and the development of treatments.

COX deficiency routinely presented in colonic crypts of young tRNA^{Ala} mutant mice, where the m.5024C>T mutation segregated with the COX deficiency and revealed an apparent threshold level of ~70%. Different point mutations have different critical threshold levels for precipitating a biochemical defect. Mt-tRNA point mutations are commonly quite recessive and have a high critical threshold level before a biochemical defect is observed as seen with: the A8344G mutation in tRNA^{Lys} in MERRF patients (>80%) (Boulet L 1992), the m.5591G>A mutation (~99%) and the m.5650G>A mutation (~95%) in tRNA^{Ala} in patients with isolated mitochondrial myopathies (Swalwell, Deschauer et al. 2006; McFarland, Swalwell et al. 2008). One potential reason for the lower threshold of the m.5024C>T mutation in the colonic crypts of tRNA^{Ala} mutant mice could be the hypothesised low mtDNA copy number in colonic crypt stem cells. As such there would be a decreased number of WT mtDNA molecules capable of maintaining normal mitochondrial function, resulting in much earlier segregation of the mutation and presentation of COX deficiency. Alternatively, or in combination with, another reason could be that the m.5024C>T mutation is more pathogenic. Highly recessive mt-tRNA mutations, presenting at very high heteroplasmy increases the transmissibility of a mutation to offspring, as seen with the m.5650G>A mutation in the three successive female generations (McFarland, Swalwell et al. 2008). If the m.5024C>T mutation is indeed more pathogenic this may explain why there is high variability in the transmission of the mutation to offspring, and why a threshold of 77% m.5024 C>T heteroplasmy is consistently observed, even still to date. Embryo reabsorption of the allele or early death of pups before or immediately after they are

born, due to the m.5024C>T mutation being more pathogenic could explain this apparent threshold seen in offspring.

It is widely accepted that mt-tRNA point mutations in the stem region of tRNAs are highly likely to be pathogenic (McFarland, Elson et al. 2004). The m.5024C>T mutation is predicted to cause a significant deformation in the acceptor stem of the tRNA^{Ala} and as such may render this mutation more pathogenic and contribute to the lower threshold level observed. The acceptor stem of a tRNA is critical for binding to the aminoacyl tRNA synthetase necessary for aminoacylation and binding to the specific amino acid (alanine) prior to protein translation (Park and Schimmel 1988). The m.5024C>T mutation occurs next to a U:U pairing in the acceptor stem of the mouse tRNA^{Ala} (Figure 5-3). U:U lacks a Watson-Crick base pair, which alone is very destabilizing to the tRNA acceptor stem. Thus the presence of the C>T mutation next to the U:U pairing, is expected to be highly destabilizing to the acceptor stem and is likely to cause a break down in the tertiary structure, leading to degradation of tRNA^{Ala}. Indeed reduced steady state levels of tRNA^{Ala} are observed on northern blots from both young (Figure 5-4b) and aged mutant tRNA^{Ala} mice with high m.5024C>T tail heteroplasmy, where there is an absence of any down regulation of other tRNAs, supporting that the m.5024 C>T mutation causes degradation of tRNA^{Ala}. This would be expected to have significant effect upon mitochondrial protein translation, which has indeed been detected by western blots from mutant tRNA^{Ala} mice with high (67/68%) tail heteroplasmy (Figure 5-4c). Such a significant deformation in the tRNA^{Ala} and impact upon protein translation in mice with 67% m.5024 C>T heteroplasmy therefore indicates high pathogenicity of the mutation, which would contribute to the low threshold for COX deficiency in the colonic crypts and threshold of 77% for producing offspring.

COX deficiency in the heart and skeletal muscle was not a characteristic feature in young (<22 weeks) mutant tRNA^{Ala} mice, detected at only moderate levels in 2 out of 8 mice for both. COX deficiency is a common feature of muscle biopsies of patients with mtDNA disease, and indeed those with mt-tRNA^{Ala} mutations (Sciocco M 1994; Swalwell, Deschauer et al. 2006; McFarland, Swalwell et al. 2008) and as such the initial findings in young animals could question the validity of the tRNA^{Ala} mutant mouse as a model of disease. Despite the lack of respiratory chain deficiency, young mutant tRNA^{Ala} mice with high heteroplasmy, did show evidence of decreased body mass, indicating a muscle phenotype, as well as evidence of cardiomyopathy

characterised by an increased heart to body mass ratio and elevated levels of atrial natriuretic factor (ANF), a sensitive indicator of cardiac pathogenesis (Vikstrom, Bohlmeier et al. 1998) (James Stewart, unpublished results). Given that the heart and skeletal muscle are post-mitotic tissues, in which clonal expansion is not as rapid as the colon (Taylor and Turnbull 2005; Fellous, McDonald et al. 2009), the absence of routine respiratory chain deficiency may simply be due to the fact that more time is needed for the mutation to reach the critical threshold level to precipitate a biochemical defect. Indeed this would appear to be the case, with the discovery that 70 week old tRNA^{Ala} mutant mice displayed evidence of COX deficiency in the heart, thigh and calf. Furthermore, pyrosequencing of COX deficient and COX positive colonic smooth muscle fibers revealed a higher m.5024C>T threshold level (~84%) for COX deficiency. As such it would appear that muscle tissues have a higher threshold level for an impairment of the respiratory chain to ensue, and therefore take longer to become afflicted.

Even though evidence of COX deficiency was documented in the heart and skeletal muscle of 70 week old mutant tRNA^{Ala} mice, this was only moderate in both tissues, and could be argued as too low for a model of mtDNA disease. This may be attributable to species specific differences as mtDNA defects tend to be tolerated fairly well in both mouse heart and muscle, as evidenced by normal respiratory chain function in the heart and plastic properties of muscle, in tissue specific TFAM knockout mice (Wredenberg, Wibom et al. 2002; Freyer, Park et al. 2010). Furthermore mouse muscle relies much more on glycolysis than OXPHOS for energy production (Ibrahim, Zweber et al. 1981) and so may not be as severely affected by respiratory chain dysfunction as human muscle. Alternatively, however it may simply be that respiratory chain deficient muscle fibers with high levels of the m.5024C>T mutation undergo apoptosis, as studies in rats have previously shown that respiratory chain deficiency in muscle fibers was associated with muscle atrophy (Herbst, Pak et al. 2007). Indeed some of the 70 week old mutant tRNA^{Ala} mice with high tail heteroplasmy did display signs of muscle wasting when they were sacrificed (James Stewart, personal communication). The magnitude of COX deficiency that was detected in the heart and skeletal muscle as well as the colonic smooth muscle fibers of 70 week old tRNA^{Ala} mutant mice did not correlate with the m.5024 C>T heteroplasmy recorded in tail clippings. This may simply be due to the limited number of tissues this was completed on and the inherent variability that would occur between mice, especially given that the incidence only varied by a few percent.

Alternatively, this may be due to the fact that the incidence of COX deficiency in tissues does not always correlate with the clinical presentation and disease severity in mtDNA disease patients (Betts, Jaros et al. 2006; McFarland, Swalwell et al. 2008). This leads on to the primary limitation of this study, being that COX/SDH histochemistry was the only screen used to identify mitochondrial dysfunction in tissues of the mutant tRNA^{Ala} mice. Histological abnormalities in muscle, such as enlarged mitochondria and the presence of ragged red fibers are also typical of patients with mitochondrial disease caused by mt-tRNA mutations and are used in diagnosis (Hirano 1994; Finnilä, Tuisku et al. 2001; Taylor and Turnbull 2005). Furthermore combined respiratory chain defects, including a loss of complex I activity, is also common in patients with mt-tRNA mutations (Bonilla, Sciacco et al. 1992; Ciafaloni, Ricci et al. 1992; Swalwell, Deschauer et al. 2006; McFarland, Swalwell et al. 2008). As such evidence of mitochondrial dysfunction and tissue phenotypes cannot simply be judged by COX deficiency in tissues of tRNA^{Ala} mutant mice.

An interesting observation in this study was that the m.5024C>T mutation segregated promptly in colonic crypts of young mutant tRNA^{Ala} mice, but was selectively lost from the colonic epithelium of aged animals, which actually displayed segregation of the mutation in the colonic smooth muscle. Not only does this demonstrate varied segregation of the mutation in different cell types within the same tissue but it also indicates a selective loss of the pathogenic mutation in mitotic, actively dividing cells. This was further supported by the fact that post mitotic tissues of aged animals maintained constant heteroplasmy. This data suggests that colonic crypts are not as permissive as originally thought and that respiratory chain deficient colonic crypt stem cells are not able to survive with high levels of a markedly pathogenic mtDNA point mutation after a certain length of time. It could therefore be hypothesised that COX deficiency decreases the half-life of a crypt, such that a stem cell harbouring high levels of a markedly pathogenic m.5024C>T mutation may become arrested in a senescent state or undergo apoptosis. As such these stem cells would no longer fulfil their purpose and repopulate the crypt, giving an absence of progeny cells with high levels of the mutation. Only those stem cells with low levels/ an absence of the mutation would be able to replicate and repopulate the crypt. In this case the actively dividing nature and the low mtDNA copy number of intestinal stem cells (Barker, Van Es et al. 2007) coupled with the marked pathogenicity of the m.5024C>T mutation could make colonic crypt stem cells highly vulnerable to the mutation and unable to fulfil their purpose.

This would therefore account for the loss of the mutation from the colonic epithelium and the high incidence of partial COX deficient crypts in aged animals. Contrastingly post mitotic tissues contain 1000s of copies of the mtDNA genome (Lightowlers, Chinnery et al. 1997) and so more mutant mtDNA genomes can be tolerated before a biochemical defect and mitochondrial dysfunction ensues, as demonstrated with the higher threshold level in the COX deficient colonic smooth muscle fibers of aged mutant tRNA^{Ala} mice. The high threshold coupled with random replication of 1000s of copies of the mtDNA genome could maintain heteroplasmy at a constant level in post mitotic tissues.

The selective loss of a mt-tRNA point mutation in actively dividing stem cells in human disease is not uncommon. Patients with MELAS (m.3243A>G in tRNA^{Leu} (UUR)) typically display higher heteroplasmy in post-mitotic tissues than mitotic, actively dividing tissues (Ciafaloni, Ricci et al. 1992) and more importantly they frequently show a selective loss of the m.3243A>G mutation in blood over time (Chinnery, Zwijnenburg et al. 1999; Rahman, Poulton et al. 2001). Furthermore analysis of COX activity in colon biopsies of a few patients with MELAS has revealed an absence of COX deficiency in the colonic crypts but the colonic smooth muscle was almost entirely COX deficient (unpublished data from this lab). However, the selective elimination of mt-tRNA point mutations in actively dividing stem cells is not a characteristic feature of all patients with mt-tRNA point mutations, where heteroplasmy can remain constant across all tissues, as seen in MERRF patients with the tRNA^{Lys} mutation (Lombès, Diaz et al. 1992). Given that the MERRF mt-tRNA^{Lys} mutation is relatively benign in terms of pathogenicity and the resulting biochemical defect, it is likely that the selective loss of a mutation in mitotic tissues is influenced by the pathogenicity of the mutation and the degree of mitochondrial dysfunction that ensues. Thus for mt-tRNA mutations this may depend on the deformation of the tRNA and the subsequent defect in protein translation. Indeed this could account for the loss of the m.5024C>T mutation, which is predicted to be highly pathogenic, given the predicted significant deformation in the acceptor stem (see earlier). Alternatively, given that the OriL is critical for mtDNA replication (Wanrooij, Miralles Fusté et al. 2012), if a mutation caused problems at the OriL, this could also contribute to the selective loss during mtDNA replication, occurring at a much faster rate in actively dividing tissues. Interestingly studies in humans have shown that those mt-tRNA point mutations that display an overriding phenotype in dividing cells and are selectively lost, are least likely to be inherited

(Elson, Swalwell et al. 2009). As such the selective loss of the pathogenic m.5024 C>T mutation that we see in actively dividing colonic crypts of tRNA^{Ala} mutant mice could hold implications for the transmission of this mutation, explaining the threshold level observed in offspring.

The overriding, long term aim of this study was to determine whether the m.5024 C>T mutant tRNA^{Ala} mice could serve as a model of mtDNA disease and be used to uncover disease mechanisms associated with heteroplasmic point mutations. This mouse demonstrates routine evidence of respiratory chain deficiency, with which the m.5024 C>T mutation segregates, demonstrating pathogenicity of the mutation. Aged animals also become more afflicted, displaying phenotypic evidence of mitochondrial respiratory chain dysfunction in the heart, skeletal muscle and colonic smooth muscle, which is representative of disease caused by mt-tRNA point mutations (Taniike, Fukushima et al. 1992; Taylor, Giordano et al. 2003; Swalwell, Deschauer et al. 2006; McFarland, Swalwell et al. 2008). Moreover aged mutant tRNA^{Ala} mice with high heteroplasmy also show routine evidence of cardiomyopathy (enlarged hearts), as well as elevated levels of fibroblast growth factor (FGF-21), a serum marker of muscle mitochondrial respiratory chain deficiencies (Suomalainen 2013) with a few high level animals showing evidence of muscle difficulties and hind limb myopathy (James Stewart, unpublished results). Moreover these mice also display characteristic features of patients harbouring mt-tRNA point mutations, including different threshold levels for different cell types, mitotic segregation of the mutation and the selective loss in actively dividing cells (Chinnery, Zwijnenburg et al. 1999; Rahman, Poulton et al. 2001). The data presented here therefore suggests that the m.5024C>T tRNA^{Ala} mutant mouse is the first mouse model to harbour a pathogenic heteroplasmic mtDNA point mutation, that displays mitochondrial respiratory chain dysfunction, differential segregation of the mutation and tissue phenotypes that are representative of mitochondrial disease caused by an mt-tRNA point mutation.

5.6.1 Future work

Given that aged mutant tRNA^{Ala} mice routinely demonstrate evidence of cardiomyopathy, it would be useful to complete pyrosequencing of COX deficient and COX positive cardiac muscle fibers to directly associate pathogenicity of the mutation with the phenotype. Given that the colonic crypts and smooth muscle fibers displayed different threshold levels for COX deficiency, this would also uncover the threshold necessary for COX deficiency in the heart, and whether this is even higher, as is often

the case in humans (Bates, Bourke et al. 2012). Preliminary experiments suggest that pyrosequencing would require substantial optimisation, given the overlapping nature of cardiac muscle fibers, to ensure that only COX deficient fibers and no COX positive fibers are present in a sample, and vice versa. Reducing section thickness and collecting more fibers will be necessary in order to optimise this technique successfully for heart tissue.

Future work would undoubtedly involve looking for other evidence of mitochondrial dysfunction in muscle and heart samples from the m.5024 C>T tRNA^{Ala} mutant mice. A Gomori Trichrome stain to look for the presence of ragged red fibers and mitochondrial hyperproliferation could be used in skeletal muscle as well as using immunohistochemistry/ immunofluorescence to look for complex I deficiency in the muscle and heart. Complex I defects often precede a loss of complex IV activity in patients with mt-tRNA point mutations (Bonilla, Sciacco et al. 1992; Ciafaloni, Ricci et al. 1992), and so the incidence of complex I deficiency may be higher than the observed COX deficiency in these tissues. Complex I screening will be especially interesting in the heart, given that biochemical analysis of mutant tRNA^{Ala} mice also shows a down regulation in complex I activity (James Stewart, personal communication). Screening for complex I defects may also be useful in the brain of these mice, given that neurological features and complex I defects in the brain are also common in mtDNA disease (Tanji, Kunimatsu et al. 2001).

Whilst the loss of the m.5024 C>T mutation in the colonic crypts suggests a loss of the mutation in actively dividing stem cell tissues, it would be useful to confirm this in the blood. Mutation load quantification, by either pyrosequencing or RFLP, from blood samples taken from animals 22 weeks old and then again, at multiple stages throughout lifespan (40 weeks and then >65 weeks) would determine whether the m.5024 C>T mutation is generally lost from mitotic tissues of these mice.

Future work will also involve using these mice to uncover disease mechanisms, by ageing them further to determine how the disease phenotypes progress and how severely afflicted the mice become, as well as examining transmission of pathogenic mt-tRNA point mutations further. Quantification of m.5024 C>T heteroplasmy from oocytes and embryos from mothers could be performed to help determine whether the breeding threshold occurs during the germline, due to the genetic bottleneck or whether there is embryo reabsorption of the allele/ early embryo loss in those with very high

m.5024 C>T heteroplasmy. Furthermore rescue experiments with leucyl tRNA synthetase, could be used to see if steady state levels of tRNA^{Ala} are maintained, due to stabilization of the tRNA and prevention of degradation, in an attempt mitigate mitochondrial dysfunction and develop strategies to manage/ treat disease.

5.7 Conclusions

In this study I have shown that COX/SDH histochemistry in the colon correlated a genotype to a phenotype in young m.5024 C>T tRNA^{Ala} mutant mice before the onset of high heteroplasmy and disease like phenotypes in aged mice. This therefore provides evidence that this is a useful early experimental screening tool for the detection of pathogenic mtDNA point mutations in the breeding of mouse lineages. Furthermore the m.5024 C>T tRNA^{Ala} mutant mice appear to be a reasonably good model of a pathogenic heteroplasmic mt-tRNA point mutation in disease; demonstrating evidence of mitochondrial dysfunction and tissue phenotypes which become progressively worse over time and from which we are already uncovering certain disease mechanisms regarding mitotic segregation and transmission of the allele. This therefore suggests that this mouse model will be a valuable tool for understanding factors that govern disease progression caused by mt-tRNA point mutations, disease presentation and the development of potential treatments.

Chapter 6

Chapter 6. Final Discussion

The overarching aim of this thesis was to further our understanding of the clonal expansion of mtDNA point mutations and resulting respiratory chain deficiency that occurs during ageing and the mechanisms associated with disease heterogeneity, using mice that harbour mtDNA point mutations. Establishing good mouse models is fundamental to enable more detailed phenotyping of the effects of mtDNA point mutations upon cellular functions and processes to uncover how they contribute to the ageing process and to understand the mechanisms that drive the progression and transmission of mtDNA disease.

The study in the *PolgA*^{+/*mut*} mouse colon provided evidence for a conserved mechanism for the clonal expansion of somatic mtDNA point mutations by random genetic drift, without any selective constraints, resulting in age-related respiratory chain deficiency in colonic epithelial tissue of both *PolgA*^{+/*mut*} mice and ageing humans. Establishing the *PolgA*^{+/*mut*} mouse as a good model of age-related mitochondrial dysfunction therefore enabled the RNA sequencing study to begin to uncover the potential functional consequences of somatic mtDNA point mutations upon cellular processes. This study provided novel preliminary data suggesting that age-related COX deficiency in colonic crypts could be associated with alterations in: the cell cycle and proliferation; DNA maintenance and repair; cell adhesion and tight junction formation; the adaptive immune response and energy metabolism. Furthermore this study revealed a number of interesting potential associations between age-related respiratory chain deficiency and a predisposition to cancer in the colonic crypts and the pathogenesis of inflammatory bowel disease.

Regarding the study in the m.5024C>T tRNA^{Ala} mice I demonstrated that COX/SDH histochemistry in colonic epithelial tissue is a useful early experimental screening tool for the detection of pathogenic mtDNA point mutations in the breeding of mouse lineages. Moreover I presented evidence that the m.5024C>T tRNA^{Ala} mouse appears to be a good model of a pathogenic mt-tRNA point mutation in mtDNA disease as: the m.5024C>T mutation was shown to be pathogenic; mice displayed phenotypic evidence of respiratory chain deficiency; aged mice displayed evidence of disease progression; different cell types showed different biochemical thresholds and mitotic segregation was observed, with a preferential loss of the mutation in actively dividing cells. To my knowledge this is the first study to present evidence for a good mouse model of a

pathogenic heteroplasmic mtDNA point mutation in disease and will therefore be invaluable for understanding factors that govern mtDNA disease progression, presentation, transmission and the development of potential treatments.

6.1 Segregation of mtDNA point mutations: why is there a selective loss?

Interestingly the data in this thesis highlighted a difference in the accumulation of mtDNA point mutations in colonic crypts over time. Deleterious mutations were able to clonally expand and cause an increase in COX deficiency in the ageing *PolgA*^{+/*mut*} mouse colonic epithelium, yet the m.5024C>T mutation was selectively eliminated from colonic crypts in mutant tRNA^{Ala} mice over time. This therefore begs the question why some mtDNA point mutations are lost from the stem cell pool and others are not?

Whilst the m.5024C>T mutation is predicted to be highly deleterious and cause a significant deformation in the tRNA, the elimination of this mutation cannot simply be attributable to pathogenicity. Equally pathogenic, non-synonymous mtDNA point mutations and STOP codons have also been detected in mt-tRNA genes and protein encoding genes in the ageing colonic epithelium of both the *PolgA*^{+/*mut*} mouse (chapter 3 and (Baines, Stewart et al. 2014)) and ageing human colon (Greaves, Elson et al. 2012). An alternative argument could be the origin and occurrence of the mtDNA point mutation within the stem cells and the subsequent time taken for clonal expansion. In the m.5024C>T tRNA^{Ala} mouse the mutation was already present at high levels in the germline, whereas somatic mtDNA point mutations are only believed to occur during early development and have to clonally expand throughout adulthood (Coller, Khrapko et al. 2001; Elson, Samuels et al. 2001; Greaves 2014). This could mean that the m.5024C>T mutation was lost, simply because it accumulated to higher levels quicker in the colonic crypts. However, this would not explain why somatic mtDNA point mutations are still detected at high heteroplasmy (>75%) and in the homoplasmic state in COX deficient colonic crypts in both the *PolgA*^{+/*mut*} mouse (chapter 3 and (Baines, Stewart et al. 2014)) and human colon (Greaves, Elson et al. 2012).

The incidence of clonally expanding mtDNA point mutations in the ageing colonic epithelium, in combination with the pathogenicity of the mutation, could be an alternative and more plausible hypothesis to explain segregation and the loss of certain pathogenic point mutations from stem cell populations. In the ageing human colon it takes ~20 years for the first somatic mtDNA point mutations to clonally expand and cause COX deficiency (Taylor, Barron et al. 2003). Over time there is an exponential

increase in COX deficiency in the colonic epithelium, with different COX deficient crypts displaying different clonally expanded somatic mtDNA point mutations (Taylor, Barron et al. 2003; Greaves, Elson et al. 2012; Baines, Stewart et al. 2014). Indeed, an increase in the frequency of clonally expanded somatic mtDNA point mutations has recently been reported in the ageing human colonic epithelium (Greaves 2014). It could therefore be possible that all markedly pathogenic clonally expanded mtDNA point mutations are lost from colonic crypts after a certain amount of time, as stem cells carrying such mutations become arrested/ undergo apoptosis and are unable to repopulate the crypt. If this were the case clonally expanded somatic mtDNA mutations and an increase in COX deficiency would simply be observed in the colon of ageing humans and *PolgA*^{+/*mut*} mice, due to an increase in clonally expanded mtDNA point mutations that occur with age (Greaves 2014). This hypothesis could explain why I saw a loss of the m.5024C>T mutation in mutant tRNA^{Ala} mice where I was just examining the expansion of the one notably pathogenic mutation (Figure 6-1a); unlike in the *PolgA*^{+/*mut*} mouse and ageing human colon where the overall incidence of clonally expanded somatic mtDNA point mutations is examined, which will constantly increase with age and include a number of pathogenic mutations (Figure 6-1b) (Greaves, Elson et al. 2012; Baines, Stewart et al. 2014; Greaves 2014). As such this hypothesis suggests that the selective loss of a mtDNA point mutation would be governed by both the pathogenicity of the mutation and the incidence of clonal expansions.

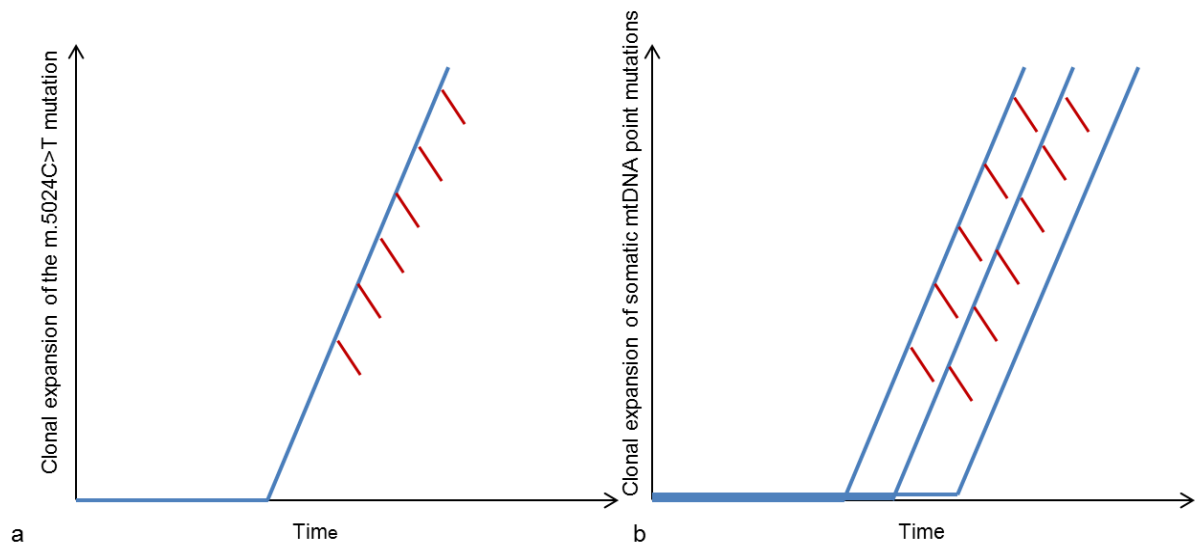


Figure 6-1: The accumulation of mtDNA point mutations in colonic crypts is affected by the incidence of clonal expansions.

(a) In the m.5024C>T tRNA^{Ala} mice colonic epithelium, the half-life of a COX deficient crypt is decreased and so a stem cell becomes arrested or undergoes apoptosis after harbouring high levels of the m.5024C>T mutation for a certain length of time. Colonic crypts are only repopulated by stem cells with low levels of the mutation that have survived and so the mutation is lost from the colonic epithelium over time. (b) In the ageing colonic epithelium high level, clonally expanded mtDNA point mutations are still lost from the stem cell pool by causing growth arrest/apoptosis, however the increased frequency of clonal expansions means that clonally expanded somatic mtDNA mutations are increasingly detected in colonic crypts, overriding the loss. Blue lines represent the clonal expansion of an mtDNA point mutation and red lines represent loss of the mutation from the stem cell pool.

6.2 The colon: a model replicative tissue

The data in this thesis confirms that mtDNA point mutations undergo high rates of clonal expansion in the colon (Taylor, Barron et al. 2003; Fellous, McDonald et al. 2009), and convincingly shows that mitochondrial dysfunction presents much earlier in the colon than in other tissues. This is most likely due to the hypothesised low mtDNA copy number in colonic crypt stem cells (Barker, Van Es et al. 2007). Interestingly, however, data from these studies indicates for the first time that the colonic crypts may not be as permissive stem cell environment as originally thought. Data from the mutant tRNA^{Ala} mice suggests that respiratory chain deficient colonic crypt stem cells cannot survive and repopulate crypts for extended periods of time, but eventually become arrested. This therefore questions the use of mtDNA point mutations as benign stem cell markers used in cell lineage tracing and understanding stem cell dynamics (Fellous, McDonald et al. 2009). Nevertheless the data presented does support the use of the colonic epithelium as a model replicative tissue for studying stem cell populations. The defined architecture of the crypts and the fact that all cells are derived from the stem cells in the crypt base was crucial in understanding the prevalence of partially COX

deficient crypts in the colon of aged mutant tRNA^{Ala} mice to form the above hypothesis in an attempt to explain the selective loss and segregation of mtDNA point mutations.

6.3 Use of mouse models

Species specific differences and the breeding of mice in a controlled environment, with a lack of exposure to environmental stresses will always be a disadvantage of using mouse models to study the mechanisms involved in ageing and disease. This was the reason for such extensive phenotypic and genotypic characterisation of the respiratory chain deficiency and mtDNA point mutations, at the cellular level, in the two mouse models used in this thesis, so that extensive comparisons could be made to human processes. Mouse models are invaluable for studying the ageing process and disease progression, quite simply due to the ability to collect tissues at multiple stages throughout their lifespan, allowing processes to be monitored over time in a relatively large number of samples. Moreover multiple tissues can be collected from the same mouse, which is often not possible for humans. The implications of this were paramount in the study on mutant tRNA^{Ala} mice, and the discovery that the m.5024C>T mutation was selectively eliminated from the colonic epithelium, but maintained at constant levels in post-mitotic tissues of aged animals. Mitotic segregation is a hallmark of human mtDNA disease, and contributes to disease heterogeneity (Taylor and Turnbull 2005) and as such this mouse will be valuable for monitoring the effects of this on disease progression and prognosis. Finally, the extensive homology between the human and mouse mtDNA genomes (Bibb, Van Etten et al. 1981), renders them an ideal mammalian model in which to study the effects of mtDNA defects in ageing and disease.

6.4 Implications for ageing and disease

The studies in this thesis confirmed that COX/SDH histochemistry is useful for identifying the presence of mtDNA defects in cells in both disease and ageing, which was fundamental in characterising the *PolgA*^{+/*mut*} mouse and the m.5024C>T tRNA^{Ala} mouse as good models of mitochondrial dysfunction in ageing and disease. Indeed, the *PolgA*^{+/*mut*} mouse is already proving valuable for uncovering the potential functional consequences of age-related respiratory chain deficiency upon cellular processes and normal tissue homeostasis in colonic crypts, with potential implications for the development of age-related disease, namely cancer. However, much further research still needs to be done to determine how mtDNA point mutations cause alterations in these cellular processes. Mechanisms have been suggested in this thesis concerning:

alterations in ROS production and signalling; defective energy production affecting energy requiring cellular processes; and disturbed Ca^{2+} homeostasis and signalling. However, experiments targeted to answering this question still need to be developed and will be fundamental to categorically establish a role for somatic mtDNA point mutations in the ageing of replicative tissues.

Research using the m.5024C>T tRNA^{Ala} mouse is also proving valuable for studying certain disease mechanisms that influence the heterogeneity of mtDNA disease, progression and transmission including: mitotic segregation of the mutation and a selective loss from actively dividing cells; different biochemical thresholds in different cell types and a non-random transmission of the mutation. Further characterisation of the extent of mitochondrial dysfunction in these mice, such as complex I deficiency and muscle histology, will be crucial to categorically determine the mtDNA disorder this mouse is most representative of. Indeed the use of these mice to study mtDNA disease extends much further beyond disease presentation and progression, with the potential to use this mouse to test novel treatments prior to their use in humans. For example there are future plans to treat these mice with restriction endonuclease enzymes targeted to the mitochondria (mitoTALENs) to see if the mtDNA mutation can be cleaved from the mtDNA genome. Furthermore there is the potential to use a modified tRNA synthetase, such as leucyl tRNA synthetase, to see if this would stabilise and rescue levels of tRNA^{Ala}, thus preventing the mitochondrial dysfunction in these mice. Moreover these mice could be bred on different nuclear backgrounds, to determine how the interaction between the nuclear and mtDNA genomes plays a role in mtDNA disease heterogeneity in patients that harbour the same mtDNA point mutation (Jacobs 2003). Undoubtedly the potential that these mice hold for mtDNA disease research is extensive and the detailed molecular characterisation performed in this thesis will prove fundamental for the continued monitoring of disease progression/presentation and determining the efficacy of treatments in rescuing these phenotypes.

6.5 Concluding remarks

In conclusion the data presented in this thesis has characterised the *PolgA*^{+/mut} mouse and the m.5024C>T tRNA^{Ala} mutant mice as good representative models of the mitochondrial dysfunction we see in human ageing and disease. Already the characterisation of these mice and functional analyses are providing valuable insights for understanding the role of mtDNA point mutations in the ageing process and the mechanisms involved in disease progression and transmission. Using mouse models to

understand these mechanisms is crucial if we ever aim to rescue tissue phenotypes and improve survival to benefit human health and well-being.

Appendices

Chapter 7. Appendices

7.1 Appendix A: Mice used in this study

<i>Details of PolgA^{+/mut} mice used for detection of clonally expanded somatic mtDNA point mutations in single colonic crypts</i>		
Mouse number	Age	Tissue
Hz1346	18 weeks	Colon
Hz1140	30 weeks	Colon
Hz539	40 weeks	Colon
Hz576	40 weeks	Colon
Hz21	48 weeks	Colon
Hz27	48 weeks	Colon
Hz160	59 weeks	Colon
Hz1059	81 weeks	Colon
Hz1136	81 weeks	Colon
Hz1137	81 weeks	Colon

<i>Details of PolgA^{mut/mut} used for COX deficiency calculations for modelling</i>			
Mouse number	Genotype	Age	Tissue
LPA194	<i>PolgA^{mut/mut}</i>	3 months	Colon
LPA195	<i>PolgA^{mut/mut}</i>	3 months	Colon
Polg215	<i>PolgA^{mut/mut}</i>	3 months	Colon
Polg220	<i>PolgA^{mut/mut}</i>	3 months	Colon
Polg221	<i>PolgA^{mut/mut}</i>	3 months	Colon
Polg126	<i>PolgA^{mut/mut}</i>	6 months	Colon
Polg129	<i>PolgA^{mut/mut}</i>	6 months	Colon

Polg150	<i>PolgA^{mut/mut}</i>	6 months	Colon
Polg194	<i>PolgA^{mut/mut}</i>	6 months	Colon
Polg196	<i>PolgA^{mut/mut}</i>	6 months	Colon
Polg73	<i>PolgA^{mut/mut}</i>	9 months	Colon
Polg88	<i>PolgA^{mut/mut}</i>	9 months	Colon
Polg115	<i>PolgA^{mut/mut}</i>	9 months	Colon
Polg118	<i>PolgA^{mut/mut}</i>	9 months	Colon
Polg158	<i>PolgA^{mut/mut}</i>	9 months	Colon
Polg161	<i>PolgA^{mut/mut}</i>	9 months	Colon
Polg199	<i>PolgA^{mut/mut}</i>	9 months	Colon
Polg137	<i>PolgA^{mut/mut}</i>	11.5 months	Colon
Polg163	<i>PolgA^{mut/mut}</i>	11 months	Colon
Polg63	<i>PolgA^{mut/mut}</i>	12 months	Colon
Polg74	<i>PolgA^{mut/mut}</i>	12 months	Colon
Polg78	<i>PolgA^{mut/mut}</i>	12 months	Colon
Polg85	<i>PolgA^{mut/mut}</i>	12 months	Colon

M.5024 tRNA^{Ala} mutant and control mice				
Mouse number	Age	Tail m.5024C>T heteroplasmy	Mutant/Control	Tissues
111	83 weeks	29%	Mutant	Colon
112	83 weeks	24%	Mutant	Colon
471	72 weeks	45%	Mutant	Colon
472	72 weeks	18%	Mutant	Colon
483	71 weeks	39%	Mutant	Colon
1180	49 weeks	11%	Mutant	Colon
1181	14 weeks	54%	Mutant	Colon
1183	48 weeks	55%	Mutant	Colon
1184	48 weeks	59%	Mutant	Colon

1622	22 weeks	74%	Mutant	Colon
1623	21 weeks	75%	Mutant	Colon
1624	21 weeks	64%	Mutant	Colon
1625	21 weeks	69%	Mutant	Colon
1626	21 weeks	72%	Mutant	Colon
1734	20 weeks	60%	Mutant	Colon, Muscle, Heart
1764	20 weeks	66%	Mutant	Colon, Muscle, Heart
2265	20 weeks	60%	Mutant	Colon, Muscle, Heart
2266	20 weeks	53%	Mutant	Colon, Muscle, Heart
2267	20 weeks	77%	Mutant	Colon, Muscle, Heart
2268	20 weeks	66%	Mutant	Colon, Muscle, Heart
2269	20 weeks	74%	Mutant	Colon, Muscle, Heart
2307	12 weeks (culled)	51%	Mutant	Colon, Muscle, Heart
1299	10 weeks	50%	Mutant	Colon
1305	10 weeks	12%	Mutant	Colon
2191	22 weeks	10%	Control	Colon, Muscle, Heart
2192	22 weeks	20%	Control	Muscle, Heart
2489	21 weeks	7%	Control	Colon, Muscle, Heart
2430	22 weeks	24%	Control	Colon, Muscle, Heart
2431	22 weeks	7%	Control	Muscle, Heart
2432	22 weeks	13%	Control	Colon, Muscle, Heart

2241	65.9 weeks	68%	Mutant	Colon
2242	65.9 weeks	65%	Mutant	Colon
2261	64.9 weeks	64%	Mutant	Colon
2199	68 weeks	61%	Mutant	Colon
2200	68 weeks	58%	Mutant	Colon
2262	64.9 weeks	52%	Mutant	Colon
2264	64.9 weeks	60%	Mutant	Colon
9831	65.7 weeks	WT	Control	Colon
10045	62.7 weeks	WT	Control	Colon
2884	70 weeks	66%	Mutant	Colon, Muscle, Heart
2885	70 weeks	26%	Mutant	Colon, Muscle, Heart
2887	70 weeks	51%	Mutant	Colon, Muscle, Heart
17066	69 weeks	WT	Control	Colon, Muscle, Heart
17369	68 weeks	WT	Control	Colon, Muscle, Heart
TN139		0%	Positive control	Colon

<i>Details of PolgA^{+mut} mice used for RNA sequencing</i>			
Mouse number	Genotype	Age	Tissue
Polg23	<i>PolgA^{+mut}</i>	12 months	Colon
Polg25	<i>PolgA^{+mut}</i>	12 months	Colon
Polg42	<i>PolgA^{+mut}</i>	12 months	Colon
Polg44	<i>PolgA^{+mut}</i>	12 months	Colon
Polg45	<i>PolgA^{+mut}</i>	12 months	Colon

7.2 Appendix B: Primer sequences and positions for molecular biology techniques

Polg POP PCR Primers		
Primers	Primer Position	Size (incl primer)
POLG58Forward	1114-1134	294
POLG59Reverse	1407-1386	

Polg POP PCR Primers	
Primer	Sequence
POLG58Forward	5'-GCCTCGCTTTCTCCGTGACT-3'
POLG59Reverse	5'-GGATGTGGCCCAGGCTGTA ACTCA-3'

Primers used for amplification of the entire mitochondrial genome			
Primers	Primer Position		Size (incl primer)
1	1081-1101	2314-2294	1234
2	2666-2685	3840-3821	1175
3	4241-4260	5516-5498	1276
4	5904-5926	7135-7116	1232
5	7638-7658	8832-8811	1195
6	9377-9396	10162-10143	786
7	10628-10647	11868-11848	1241
8	12404-12424	13685-13665	1282
9	14190-14209	15334-15314	1145
10	15774-15794	676-657	1198
11	54-74	1217-1198	1164
12	1629-1648	2757-2738	1129
13	3132-3151	4372-4353	1241

Primers used for amplification of the entire mitochondrial genome			
14	5181-5200	6250-6231	1070
15	6432-6452	7787-7769	1356
16	8192-8214	9487-9464	1296
17	9822-9844	10735-10716	914
18	11131-11150	12493-12473	1363
19	12996-13015	14317-14298	1322
20	14682-14701	15898-15879	1217
21	556-575	1745-1725	1190
22	2116-2135	3330-3311	1215
23	3757-3776	5177-5157	1421
24	5406-5424	6558-6539	1153
25	7026-7045	8293-8217	1268
26	8745-8765	9824-9799	1080
27	10060-10079	11269-11250	1210
28	11773-11793	13142-13123	1370
29	13609-13629	14818-14799	1210
30	15141-15161	132-113	1287

Primers used for amplification of the entire mitochondrial genome	
Primer	Sequence
1 Forward	TGTAAAACGACGGCCAGTATGAACACTCTGAACTAATCC
1 Reverse	CAGGAAACAGCTATGACCACTTTGACTTGTAAGTCTAGG
2 Forward	TGTAAAACGACGGCCAGTAGAGAAGGTTATTAGGGTGG
2 Reverse	CAGGAAACAGCTATGACCGGATAAGGTGTTTAGGTAGC
3 Forward	TGTAAAACGACGGCCAGTCCATTCCACTTCTGATTACC
3 Reverse	CAGGAAACAGCTATGACCAAAGCATGGGCAGTTACG
4 Forward	TGTAAAACGACGGCCAGTCTGCTCCTATTATCACTACC
4 Reverse	CAGGAAACAGCTATGACCGATATAGAGGACTAAGGAGC

Primers used for amplification of the entire mitochondrial genome	
5 Forward	TGTA AACGACGGCCAGTTGTCCTAGAAATGGTTCCAC
5 Reverse	CAGGAAACAGCTATGACCGTACAATAGGAGTGTGGTGGCC
6 Forward	TGTA AACGACGGCCAGTTTGATGAGGATCTTACTCCC
6 Reverse	CAGGAAACAGCTATGACCGTAGGTTGAGATTTTGGACG
7 Forward	TGTA AACGACGGCCAGTAATCGGTTCTATTCCACTGC
7 Reverse	CAGGAAACAGCTATGACCAGAATTTGATTGATGTGGTGG
8 Forward	TGTA AACGACGGCCAGTAGGAAAATCAGCACAATTTGG
8 Reverse	CAGGAAACAGCTATGACCATGATGTTGGAGTTATGTTGG
9 Forward	TGTA AACGACGGCCAGTCACTCATTTCATTGACCTACC
9 Reverse	CAGGAAACAGCTATGACCTCATTTTCAGGTTTACAAGACC
10 Forward	TGTA AACGACGGCCAGTGAAACTTTATCAGACATCTGG
10 Reverse	CAGGAAACAGCTATGACCGCTGAATTAGCAAGAGATGG
11 Forward	TGTA AACGACGGCCAGTTGTATCCCATAAACACAAAGG
11 Reverse	CAGGAAACAGCTATGACCTGCGGTACTAGTTCTATAGC
12 Forward	TGTA AACGACGGCCAGTAGAAAGCGTTCAAGCTCAAC
12 Reverse	CAGGAAACAGCTATGACCAGAACACTATTAGGGAGAGG
13 Forward	TGTA AACGACGGCCAGTTCACTATTCGGAGCTTTACG
13 Reverse	CAGGAAACAGCTATGACCGATAGTAGAGTTGAGTAGCG
14 Forward	TGTA AACGACGGCCAGTAATGGCGGTAGAAGTCTTAG
14 Reverse	CAGGAAACAGCTATGACCGCTGATGTAAAGTAAGCTCG
15 Forward	TGTA AACGACGGCCAGTGATACATACTATGTAGTAGCC
15 Reverse	CAGGAAACAGCTATGACCTTGATGTATCTAGTTGTGG
16 Forward	TGTA AACGACGGCCAGTCACATACATTTACACCTACTACC
16 Reverse	CAGGAAACAGCTATGACCTTAATGAAGATAACAGTGTACAGG
17 Forward	TGTA AACGACGGCCAGTAAAAAATTAATGATTTGACTC
17 Reverse	CAGGAAACAGCTATGACCCATGAAGCGTCTAAGGTGTG
18 Forward	TGTA AACGACGGCCAGTCATCATCACTCCTATTCTGC
18 Reverse	CAGGAAACAGCTATGACCGTACTTGAGTGTAGTAGTGCT

Primers used for amplification of the entire mitochondrial genome	
19 Forward	TGTAAAACGACGGCCAGTACAGCTATGTACAGCATAACG
19 Reverse	CAGGAAACAGCTATGACCTCTGATGTGTAGTGTATGGC
20 Forward	TGTAAAACGACGGCCAGTGCTTTCCACTTCATCTTACC
20 Reverse	CAGGAAACAGCTATGACCCACAGTTATGTTGGTCATGG
21 Forward	TGTAAAACGACGGCCAGTAGAGAACTACTAGCCATAGC
21 Reverse	CAGGAAACAGCTATGACCTACTCATACTAACAGTGTTGC
22 Forward	TGTAAAACGACGGCCAGTTTGACCTTTCAGTGAAGAGG
22 Reverse	CAGGAAACAGCTATGACCTTGTTTCTGCTAGGGTTGAG
23 Forward	TGTAAAACGACGGCCAGTCAAGCCCTCTTATTTCTAGG
23 Reverse	CAGGAAACAGCTATGACCTTTTTTTCGGCGGTAGAAGTAG
24 Forward	TGTAAAACGACGGCCAGTGGAATAGTGGGTACTGCAC
24 Reverse	CAGGAAACAGCTATGACCTTGCTCATGTGTCATCTAGG
25 Forward	TGTAAAACGACGGCCAGTTCCAACCTTGGTCTACAAGAC
25 Reverse	CAGGAAACAGCTATGACCGTTTTTAGTTTGTGTCGGAAGCC
26 Forward	TGTAAAACGACGGCCAGTCTACTACCAATATCCTCAC
26 Reverse	CAGGAAACAGCTATGACCTTTTAAACTAATTG
27 Forward	TGTAAAACGACGGCCAGTACCATCTTAGTTTTTCGCAGC
27 Reverse	CAGGAAACAGCTATGACCGCTAGATTAGCTAGACTTGC
28 Forward	TGTAAAACGACGGCCAGTTCTTCATTCTTCTACTATCCC
28 Reverse	CAGGAAACAGCTATGACCGACAAATCCTGCAAAGATGC
29 Forward	TGTAAAACGACGGCCAGTTACTACCATCATTCAAGTAGC
29 Reverse	CAGGAAACAGCTATGACCGTATAGTAGGGGTGAAATGG
30 Forward	TGTAAAACGACGGCCAGTCTTATCTTAACCTGAATTGGG
30 Reverse	CAGGAAACAGCTATGACCTCTATGGAGGTTTGCATGTG

M.5024 First round PCR Primers		
Primers	Primer Position	Size (incl primer)
2Forward	2666-2685	4470

M.5024 First round PCR Primers	
4Reverse	7135-7116

M.5024 First round PCR Primers	
Primer	Sequence
2 Forward	TGTA AACGACGGCCAGTAGAGAAGGTTATTAGGGTGG
4 Reverse	CAGGAAACAGCTATGACCGATATAGAGGACTAAGGAGC

M.5024 Second round PCR Primers		
Primers	Primer Position	Size (incl primer)
3Forward	4241-4260	1276
3Reverse	5516-5498	

M.5024 Second round PCR Primers	
Primer	Sequence
3 Forward	TGTA AACGACGGCCAGTCCATTCCACTTCTGATTACC
3 Reverse	CAGGAAACAGCTATGACCAAAGCATGGGCAGTTACG

Pyrosequencing PCR primers		
Primers	Primer Position	Size (incl primer)
5024 Forward biotinylated	4891-4913	224
5024 Reverse	5114-8091	

Pyrosequencing PCR primers

Pyrosequencing PCR primers	
Primer	Sequence
5024 Forward biotinylated	Biosg/TTCCACCCTAGCTATCATAAGC
5024 Reverse	CGTAGGTTTAATTCCTGCCAATCT

Long-range PCR (1st und)		
Primer	Primer position	Size (incl primer)
L272	272-301	16 042
H16283	16283-16312	

Long-range PCR (1st round)	
Primer	Sequence
L272	GACTAAGTTATACCTCTTAGGGTTGGTAAA
H16283	CTGAATAGAGTATGATTAGAGTTTTGGTTC

Long-range PCR (2nd round)		
Primer	Primer position	Size (incl primer)
L1275	1275-1304	14 530
H15833	15833-15804	

Long-range PCR (2nd round)	
Primer	Sequence
L1275	TTTTGCATAATGAACTAACTAGAAACTTC
H15833	GTATGGGCGATAACGCATTTGATGGCCCTG

7.3 Appendix C-Somatic mtDNA point mutations detected in the *PolgA*^{+/*mut*} mouse colonic crypts.

Crypts and mutations highlighted in blue were those detected in COX deficient colonic crypts from two 48 week old *PolgA*^{+/*mut*} mice (Holly Baines, MRes Project)

Crypt	COX Histochemistry	Mutation	WT base	Mutant base	Heteroplasmy level	Gene	Codon change	Amino acid change	Substitution type
1	Deficient	m.4892 T>C	T	C	100%	<i>MT-ND2</i>	TTC	Phe-Phe	syn
	Deficient	m.6779 T>C	T	C	25%	<i>MT-CO1</i>	CCA	Ser-Pro	ns
2	Deficient	m.4892 T>C	T	C	100%	<i>MT-ND2</i>	TTC	Phe-Phe	syn
	Deficient	m.5831 T>C	T	C	50%	<i>MT-CO1</i>	ACT	Ile-Thr	ns
	Deficient	m.7413 C>T	C	T	50%	<i>MT-CO2</i>	TGA	Arg-Trp	ns
	Deficient	m.9740 T>C	T	C	100%	<i>MT-ND3</i>	CCA	Leu-Pro	ns
	Deficient	m.10392 A>G	A	G	25%	<i>MT-ND4</i>	CTG	Leu-Leu	syn
	Deficient	m.13817 G>T	G	T	25%	<i>MT-ND6</i>	AAA	Asn-Lys	ns
3	Deficient	m.13852 C>T	C	T	50%	<i>MT-ND6</i>	ACT	Ala-Thr	ns
3	Deficient	m.6098 T>A	T	A	75%	<i>MT-CO1</i>	GAA	Val-Glu	ns
4	Deficient	m.986 G>A	G	A	50%	<i>MT-16SrRNA</i>	-	-	
	Deficient	m.2283 G>T	G	T	50%	<i>MT-16SrRNA</i>	-	-	
	Deficient	m.6024 G>A	G	A	75%	<i>MT-CO1</i>	CAA	Gln-Gln	syn
5	Deficient	m.1214 C>G	C	G	75%	<i>MT-16SrRNA</i>	-		
	Deficient	m.5695 G>A	G	A	100%	<i>MT-CO1</i>	AGA	Gly-Gly	syn
	Deficient	m.6835 C>T	C	T	75%	<i>MT-CO1</i>	TAC	His-Tyr	ns
	Deficient	m.6919 C>T	C	T	100%	<i>MT-tRNA^{Ser}</i>	-		
	Deficient	m.7641 G>A	G	A	100%	<i>MT-CO2</i>	ATC	Val-Ile	ns
6	Deficient	m.506 C>T	C	T	75%	<i>MT-12SrRNA</i>	-	-	
	Deficient	m.812 C>G	C	G	75%	<i>MT-12SrRNA</i>	-	-	
	Deficient	m.2424 C>T	C	T	50%	<i>MT-16SrRNA</i>	-	-	

	Deficient	m.2446 C>T	C	T	75%	<i>MT-16ArRNA</i>	-	-	
	Deficient	m.4946 A>G	A	G	75%	<i>MT-ND2</i>	GCC	Thr-Ala	ns
	Deficient	m.11539 C>T	C	T	25%	<i>MT-ND4</i>	ATA	Thr-Met	ns
	Deficient	m.15243 C>T	C	T	50%	<i>MT-CYB</i>	TCA	Pro-Ser	ns
7	Deficient	m.3429 G>A	G	A	75%	<i>MT-ND1</i>	AAG	Glu-Lys	ns
	Deficient	m.5713 A>G	A	G	25%	<i>MT-CO1</i>	TGC	Tyr-Cys	ns
	Deficient	m.5894 T>A	T	A	75%	<i>MT-CO1</i>	CTA	Leu_leu	syn
	Deficient	m.6444 G>C	G	C	50%	<i>MT-CO1</i>	CTA	Val-Leu	ns
	Deficient	m.14400 G>A	G	A	25%	<i>MT-CYB</i>	AGA	Gly-Null	ns
	Deficient	m.16254 G>A	G	A	50%	<i>ctrl region</i>	-	-	-
8	Deficient	m.847 T>A	T	A	50%	<i>MT-12SrRNA</i>	-	-	
	Deficient	m.2537 G>A	G	A	50%	<i>MT-16SrRNA</i>	-	-	
	Deficient	m.4143 A>T	A	T	25%	<i>MT-ND2</i>	ATC	Asn-Ile	ns
	Deficient	m.5959 C>T	C	T	50%	<i>MT-CO1</i>	ATA	Thr-Met	ns
	Deficient	m.8126 C>T	C	T	50%	<i>MT-ATP6</i>	ATA	Thr-Met	ns
	Deficient	m.8744 C>T	C	T	75%	<i>MT-CO3</i>	GGT	Gly-Gly	syn
9	Deficient	m.1181 A>G	A	G	25%	<i>MT-16SrRNA</i>	-		
	Deficient	m.6305 C>T	C	T	25%	<i>MT-CO1</i>	ACT	Thr-Thr	syn
	Deficient	m.11402 T>A	T	A	50%	<i>MT-ND4</i>	ATA	Ile-Met	ns
	Deficient	m.12015 G>A	G	A	25%	<i>MT-ND5</i>	ATA	Val-Met	ns
10	Deficient	m.221 C>T	C	T	75%	<i>MT-12SrRNA</i>			
	Deficient	m.2649 C>T	C	T	50%	<i>MT-16SrRNA</i>			
	Deficient	m.2807 C>T	C	T	75%	<i>MT-ND1</i>	TTT	Phe-Phe	syn
	Deficient	m.2970 G>A	G	A	75%	<i>MT-ND1</i>	ACA	Ala-Thr	ns
	Deficient	m.6402 T>C	T	C	75%	<i>MT-CO1</i>	CCC	Ser-Pro	ns

	Deficient	m.7533 C>T	C	T	50%	<i>MT-CO2</i>	GTC	Ala-Val	ns
	Deficient	m.10360 T>C	T	C	25%	<i>MT-ND4</i>	TCA	Leu-Ser	ns
	Deficient	m.15357 C>T	C	T	75%	<i>Mt-tRNA P</i>			
11	Deficient	m.4925 C>T	C	T	25%	<i>MT-ND2</i>	TCC	Pro-Ser	ns
	Deficient	m.5714 C>T	C	T	25%	<i>MT-CO1</i>	TAT	Tyr-Tyr	syn
	Deficient	m.5977 C>T	C	T	25%	<i>MT-CO1</i>	ATA	Thr-Met	ns
12	Deficient	m.212 G>A	G	A	25%	<i>MT-12SrRNA</i>			
	Deficient	m.366 C>T	C	T	75%	<i>MT-12SrRNA</i>			
	Deficient	m.2745 C>T	C	T	100%	<i>MT-tRNA L1</i>			
	Deficient	m.3053 G>A	G	A	75%	<i>MT-ND1</i>	GGA	Gly-Gly	syn
	Deficient	m.4830 C>T	C	T	25%	<i>MT-ND2</i>	CTA	Pro-Leu	ns
	Deficient	m.6640 G>A	G	A	75%	<i>MT-CO1</i>	CAA	Arg-Gln	ns
	Deficient	m.6886 C>T	C	T	75%	<i>MT-tRNA S1</i>			
	Deficient	m.8489 C>T	C	T	75%	<i>MT-ATP6</i>	ATA	Thr-Met	ns
	Deficient	m.9268 G>A	G	A	75%	<i>MT-CO3</i>	CAA	Gln-STOP	ns
	Deficient	m.10165 C>T	C	T	25%	<i>MT-ND4 L</i>	TAA	Ala-Val	ns
	Deficient	m.11062 C>T	C	T	50%	<i>MT-ND4</i>	GTA	Ala-Val	ns
	Deficient	m.11643 C>T	C	T	75%	<i>MT- tRNA S2</i>			
	Deficient	m.12862 G>A	G	A	75%	<i>MT-ND5</i>	GAA	Val-Glu	ns
	Deficient	m.12946 G>A	G	A	75%	<i>MT-ND5</i>	TAC	Cys-Tyr	ns
	Deficient	m.13268 A>G	A	G	25%	<i>MT-ND5</i>	ATG	Met-Met	syn
12	Deficient	m.14471 T>C	T	C	75%	<i>MT-CYB</i>	TTC	Phe-Phe	syn
13	Deficient	m.4966 C>T	C	T	75%	<i>MT-tRNA W</i>			
	Deficient	m.5440 G>A	G	A	75%	<i>MT-CO1</i>	CAA	Arg-Gln	ns
	Deficient	m.10387 C>T	C	T	25%	<i>MT-ND4</i>	CTA	Pro-Leu	ns

	Deficient	m.10420 A>G	A	G	50%	<i>MT-ND4</i>	AGA	Lys-Null	ns
	Deficient	m.14309 C>T	C	T	50%	<i>MT-CYB</i>	TAT	Tyr-Tyr	syn
	Deficient	m.14326 C>T	C	T	50%	<i>MT-CYB</i>	ATA	Thr-Met	ns
	Deficient	m.15632 C>T	C	T	25%	<i>Ctrl region</i>			
14	Deficient	m.239 C>T	C	T	25%	<i>MT-12SrRNA</i>			
	Deficient	m. 2461 G>T	G	T	50%	<i>MT-16SrRNA</i>			
	Deficient	m.3278 G>A	G	A	25%	<i>MT-ND1</i>	CTA	Leu-Leu	syn
	Deficient	m. 3649 T>A	T	A	50%	<i>MT-ND1</i>	TAA	Leu-STOP	ns
	Deficient	m.5580 C>T	C	T	50%	<i>MT-CO1</i>	TTA	Leu-Leu	syn
	Deficient	m.7486 C>T	C	T	25%	<i>MT-CO2</i>	GAT	Asp-Asp	syn
	Deficient	m.12241 C>T	C	T	25%	<i>MT-ND5</i>	GTA	Ala-Val	ns
	Deficient	m.12986 C>T	C	T	25%	<i>MT-ND5</i>	GCT	Ala-Ala	syn
	Deficient	m.12997 C>T	C	T	25%	<i>MT-ND5</i>	ATA	Thr-Met	ns
	Deficient	m.14617 C>T	C	T	75%	<i>MT-CYB</i>	ATA	Thr-Met	ns
15	Deficient	m.9077 c>T	C	T	25%	<i>MT-CO3</i>	AAT	Asn-Asn	syn
	Deficient	m.14537 C>T	C	T	25%	<i>MT-CYB</i>	TAT	Tyr-Tyr	syn
	Deficient	m.15529 A>T	A	T	25%	<i>Ctrl Region / ETAS2</i>			
16	Deficient	m.491 G>T	G	T	50%	<i>MT-12SrRNA</i>			
	Deficient	m.501 C>T	C	T	25%	<i>MT-12SrRNA</i>			
	Deficient	m.1001 A>T	A	T	25%	<i>MT-12SrRNA</i>			
	Deficient	m.2411 C>T	C	T	25%	<i>MT-16SrRNA</i>			
	Deficient	m.6186 G>A	G	A	25%	<i>MT-CO1</i>	ATA	Val-Met	ns
	Deficient	m.6418 A>T	A	T	75%	<i>MT-CO1</i>	GTC	Asp-Val	ns
	Deficient	m.7772 C>T	C	T	50%	<i>MT-ATP8</i>	TAA	Gln-STOP	ns

	Deficient	m.8109 C>T	C	T	50%	<i>MT-ATP6</i>	CAT	His-His	syn
17	Deficient	m.5032 C>T	C	T	75%	<i>MT-tRNA A</i>			
	Deficient	m.9430 T>C	T	C	75%	<i>MT-tRNA G</i>			
	Deficient	m.9666 G>A	G	A	75%	<i>MT-ND3</i>	ACT	Ala-Thr	ns
	Deficient	m.11317 C>T	C	T	75%	<i>MT-ND4</i>	TTA	ser-Leu	ns
	Deficient	m.12218 C>T	C	T	75%	<i>MT-ND5</i>	TAT	Tyr-Tyr	syn
	Deficient	m.13403 C>T	C	T	75%	<i>MT-ND5</i>	GAT	Asp-Asp	syn
	Deficient	m.15005 A>T	A	T	25%	<i>MT-CYB</i>	AAT	Lys-Asn	ns
	Deficient	m.15298 G>A	G	A	75%	<i>MT-tRNA T</i>			
18	Deficient	m.5718 C>T	C	T	50%	<i>MT-CO1</i>	TCT	Pro-ser	ns
	Deficient	m.11508 A>T	A	T	50%	<i>MT-ND4</i>	TCT	Thr-Ser	ns
	Deficient	m.13783 C>T	C	T	75%	<i>MT-ND6</i>	GTA	Val-Val	syn
19	Deficient	m.5976 A>T	A	T	25%	<i>MT-CO1</i>	TCA	Thr-Ser	ns
20	Deficient	m.2083 G>A	G	A	75%	<i>MT-16SrRNA</i>			
	Deficient	m.2386 A>T	A	T	50%	<i>MT-16SrRNA</i>			
	Deficient	m.4879 C>T	C	T	25%	<i>MT-ND2</i>	CCT	Pro-Pro	syn
	Deficient	m.5096 G>A	G	A	75%	<i>MT-tRNA N</i>			
	Deficient	m.5647 C>T	C	T	75%	<i>MT-CO1</i>	CTA	Pro-Leu	ns
	Deficient	m.6241 T>C	T	C	50%	<i>MT-CO1</i>	TCT	Phe-Ser	ns
	Deficient	m.6850 C>T	C	T	50%	<i>MT-CO1</i>	CTA	Pro-Leu	ns
	Deficient	m.8864 C>G	C	G	75%	<i>MT-CO3</i>	TTG	Phe-Leu	ns
	Deficient	m.9985 G>A	G	A	75%	<i>MT-ND4L</i>	ATA	Val-Met	ns
	Deficient	m.11710 C>T	C	T	75%	<i>MT-tRNA I2</i>			
	Deficient	m.13789 C>T	C	T	50%	<i>MT-ND6</i>	TTA	Leu-Leu	syn
	Deficient	m.13967 C>T	C	T	75%	<i>MT-ND6</i>	AAT	Ser-Asn	ns

21	Deficient	m.14808 C>T	C	T	100%	<i>MT-CYB</i>	TCC	Pro-Ser	ns
	Deficient	m.14818 C>T	C	T	25%	<i>MT-CYB</i>	ATA	Thr-Met	ns
	Deficient	m.14925 C>T	C	T	100%	<i>MT-CYB</i>	TCA	Pro-Ser	ns
	Deficient	m.14938 C>T	C	T	25%	<i>MT-CYB</i>	CTA	Pro-Leu	ns
22	Deficient	m.5536 T>A	T	A	75%	<i>MT-CO1</i>	GAA	Val-Glu	ns
	Deficient	m.6964 C>T	C	T	75%	<i>MT-tRNA D</i>	-		-
	Deficient	m.7164 C>T	C	T	75%	<i>MT-CO2</i>	ATA	Thr-met	ns
	Deficient	m.9520 C>T	C	T	75%	<i>MT-ND3</i>	GTA	Ala-Val	ns
	Deficient	m.16166 A>T	A	T	75%	<i>ctrl region</i>	-		-
	Deficient	m.16286 A>G	A	G	75%	<i>ctrl region</i>	-		-
23	Deficient	m.2679 A>T	A	T	100%	<i>MT-tRNA L1</i>	-		-
	Deficient	m.4890 T>A	T	A	50%	<i>MT-ND1</i>	TAT	Phe-Tyr	ns
	Deficient	m.5686 C>T	C	T	25%	<i>MT-CO1</i>	GTA	Ala-Val	ns
	Deficient	m.6342 C>T	C	T	75%	<i>MT-CO1</i>	TTA	Leu-Leu	syn
	Deficient	m.11012 A>T	A	T	100%	<i>MT-ND4</i>	TTT	Leu-Phe	ns
	Deficient	m.11429 C>T	C	T	25%	<i>MT-ND4</i>	AAT	Asn-Asn	syn
	Deficient	m.12080 C>T	C	T	100%	<i>MT-ND5</i>	AAT	Asn-Asn	syn
	Deficient	m.12143 C>T	C	T	100%	<i>MT-ND5</i>	GCT	Ala-Ala	syn
24	Deficient	m.2078 A>T	A	T	100%	<i>MT-16SrRNA</i>			
	Deficient	m.4885 A>T	A	T	75%	<i>MT-ND2</i>	CTT	Leu-Leu	syn
	Deficient	m.6472 C>T	C	T	75%	<i>MT-CO1</i>	TTA	ser-Leu	ns
	Deficient	m.9203 G>A	G	A	75%	<i>MT-CO3</i>	ATA	Met-Met	syn
	Deficient	m.11951 C>T	C	T	100%	<i>MT-ND5</i>	ACT	Thr-Thr	syn
	Deficient	m.14905 A>G	A	G	75%	<i>MT-CYB</i>	GGC	Asp-Gln	ns
	Deficient	m.15921 T>A	T	A	100%	<i>Ctrl Region</i>			

	Deficient	m.1776 T>A	T	A	75%	<i>MT-16SrRNA</i>	-		-
	Deficient	m.5521 T>C	T	C	50%	<i>MT-CO1</i>	ACA	Met-Thr	ns
	Deficient	m.5931 C>A	C	A	75%	<i>MT-CO1</i>	ATA	leu-Met	ns
	Deficient	m.6484 T>A	T	A	75%	<i>MT-CO1</i>	GAG	Val-Glu	ns
	Deficient	m.8627 A>G	A	G	50%	<i>MT-CO3</i>	GCG	Ala-Ala	syn
	Deficient	m.8631 C>T	C	T	50%	<i>MT-CO3</i>	TAC	His-Tyr	ns
	Deficient	m.8650 C>T	C	T	50%	<i>MT-CO3</i>	CTA	Pro-Leu	ns
	Deficient	m.9505 A>G	A	G	50%	<i>MT-ND3</i>	AGG	Thr-Null	ns
	Deficient	m.11172 C>T	C	T	75%	<i>MT-ND4</i>	TGG	Arg-Trp	ns
	Deficient	m.11698 G>A	G	A	25%	<i>MT-tRNA L2</i>	-		-
	Deficient	m.12218 C>T	C	T	50%	<i>MT-ND5</i>	TAT	Tyr-Tyr	syn
	Deficient	m.12706 C>T	C	T	25%	<i>MT-ND5</i>	CTA	Pro-Leu	ns
25	Deficient	m.14462 A>T	A	T	50%	<i>MT-CYB</i>	TCT	Ser-Ser	syn
	Deficient	m.192 A>G	A	G	50%	<i>MT-12SrRNA</i>	-		-
	Deficient	m.424 G>T	G	T	25%	<i>MT-12SrRNA</i>	-		-
	Deficient	m.3497 C>T	C	T	50%	<i>MT-ND1</i>	ATT	Ile-Ile	syn
	Deficient	m.3553 C>T	C	T	50%	<i>MT-ND1</i>	TTA	Ser-Leu	ns
	Deficient	m.3609 C>T	C	T	25%	<i>MT-ND1</i>	TAT	His-Tyr	ns
	Deficient	m.5697 A>G	A	G	75%	<i>MT-CO1</i>	GCA	Thr-Ala	ns
	Deficient	m.6047 C>T	C	T	75%	<i>MT-CO1</i>	CAT	His-His	syn
	Deficient	m.6386 A>G	A	G	75%	<i>MT-CO1</i>	CTG	Leu-Leu	syn
	Deficient	m.6444 G>A	G	A	75%	<i>MT-CO1</i>	ATA	Val-Met	ns
26	Deficient	m.15323 A>G	A	G	25%	<i>MT-tRNA T</i>	-		-
27	Deficient	m.13033 C>T	C	T	25%	<i>MT-ND5</i>	ATA	Thr-Met	ns

	Deficient	m.14024 C>T	C	T	25%	<i>MT-ND6</i>	AAA	Cys-Lys	ns
28	Deficient	m.4879 C>T	C	T	25%	<i>MT-ND2</i>	CCT	Pro-Pro	syn
	Deficient	m.5096 G>A	G	A	50%	<i>MT-tRNA N</i>			
	Deficient	m.13457 C>T	C	T	25%	<i>MT-ND5</i>	AAT	Asn-Asn	syn
29	Deficient	m.568 G>A	G	A	100%	<i>MT-12SrRNA</i>			
	Deficient	m.635 C>T	C	T	75%	<i>MT-12SrRNA</i>			
	Deficient	m.655 C>T	C	T	75%	<i>MT-12SrRNA</i>			
	Deficient	m.2357 G>A	G	A	75%	<i>MT-16SrRNA</i>			
	Deficient	m.2712 A>T	A	T	75%	<i>MT-tRNA LI</i>			
	Deficient	m.2898 G>A	G	A	75%	<i>MT-ND1</i>	ACA	Ala-Thr	ns
	Deficient	m.5357 C>T	C	T	100%	<i>MT-CO1</i>	ACT	Thr-Thr	syn
	Deficient	m.6147 G>A	G	A	75%	<i>MT-CO1</i>	ATA	Val-Met	ns
	Deficient	m.6486 T>A	T	A	75%	<i>MT-CO1</i>	ATT	Phe-Ile	ns
	Deficient	m.10449 T>C	T	C	75%	<i>MT-ND4</i>	CAC	Tyr-His	ns
	Deficient	m.11236 C>T	C	T	75%	<i>MT-ND4</i>	ATA	Thr-Met	ns
	Deficient	m.12829 C>T	C	T	25%	<i>MT-ND5</i>	ATA	Thr-Met	ns
1	Positive	m.3716 C > G	C	G	50%	<i>MT-tRNA I</i>	disrupts DHU stem		-
1	Positive	m.7961 C > T	C	T	50%	<i>MT-ATP8/6</i>	TAA	Pro-Leu/Gln- STOP	ns/ns
	Positive	m.13224 G>A	G	A	50%	<i>MT-ND5</i>	ATA	Val-Met	ns
	Positive	m.15116 G>A	G	A	25%	<i>MT-CYB</i>	TTA	Leu-Leu	syn
2	Positive	m.2291 T>C	T	C	50%	<i>MT-16SrRNA</i>			-
3	Positive	m.5957 A>G	A	G	25%	<i>MT-CO1</i>	CTG	Leu-Leu	syn

	Positive	m.12723 C>T	C	T	25%	<i>MT-ND5</i>	TAC	His-Tyr	ns
	Positive	m.12783 C>T	C	T	75%	<i>MT-ND5</i>	TAT	His-Tyr	ns
4	Positive	m.3084T>C	T	C	25%	<i>MT-ND1</i>	CCA	Ser-Pro	ns
	Positive	m.8578 G>A	G	A	75%	<i>MT-ATP6</i>	ATA	Val-Met	ns
	Positive	m.11970 A>G	A	G	75%	<i>MT-ND5</i>	GAA	Lys-Glu	ns
	Positive	m.12783 C>T	C	T	50%	<i>MT-ND5</i>	TAT	His-Tyr	ns
	Positive	m.13200 A>T	A	T	50%	<i>MT-ND5</i>	TAA	Lys-STOP	ns
	Positive	m.15164 C>T	C	T	50%	<i>MT-CYB</i>	GGT	Gly-Gly	syn
5	Positive	m.381 A>T	A	T	75%	<i>MT-16SrRNA</i>			-
	Positive	m.6265 C>T	C	T	50%	<i>MT-CO1</i>	GTA	Ala-Val	ns
	Positive	m.7860 C>T	C	T	25%	<i>MT-ATP8</i>	ATA	Thr-Met	ns
	Positive	m.8079 A>T	A	T	50%	<i>MT-ATP6</i>	AAT	Lys-Asn	ns
	Positive	m.8126 C>T	C	T	50%	<i>MT-ATP6</i>	ATA	Thr-Met	ns
	Positive	m.10717 A>T	A	T	50%	<i>MT-ND4</i>	CTC	His-Leu	ns
	Positive	m.12105 A>T	A	T	75%	<i>MT-ND5</i>	TCA	Thr-Ser	ns
	Positive	m.12353 C>T	C	T	75%	<i>MT-ND5</i>	TCT	Ser-Ser	syn
	Positive	m.12592 C>T	C	T	75%	<i>MT-ND5</i>	ATC	Thr-Ile	ns
	Positive	m.14658 A>T	A	T	75%	<i>MT-CYB</i>	TAA	Lys-STOP	ns
6	Positive	m.3541 T>C	T	C	50%	<i>MT-ND1</i>	CCA	Leu-Pro	ns
	Positive	m.5966 C>T	C	T	25%	<i>MT-CO1</i>	CGT	Arg-Arg	syn
	Positive	m.8048 G>A	G	A	25%	<i>MT-ATP6</i>	CAT	Arg-His	ns
	Positive	m.8489 C>T	C	T	50%	<i>MT-ATP6</i>	ATA	Thr-Met	ns
	Positive	m.11001 C>T	C	T	25%	<i>MT-ND4</i>	TAA	Gln-STOP	ns
	Positive	m.11113 T>C	T	C	50%	<i>MT-ND4</i>	ACA	Met-Thr	ns

	Positive	m.11180 C>T	C	T	25%	<i>MT-ND4</i>	CAT	His-His	syn
	Positive	m.13403 C>T	C	T	75%	<i>MT-ND5</i>	GAT	Asp-Asp	syn
	Positive	m.3908 G>A	G	A	50%	<i>MT-tRNA M</i>	A:G Mismatch to A:A in AA stem		-
	Positive	m.8518 C>A	C	A	75%	<i>MT-ATP6</i>	ATA	Leu-Met	ns
	Positive	n.12088 G>T	G	T	25%	<i>MT-ND5</i>	CTA	Arg-Leu	ns
7	Positive	m.12211 G>A	G	A	25%	<i>MT-ND5</i>	TAA	Trp-STOP	ns
8	Positive	m.13033 C>T	C	T	25%	<i>MT-ND5</i>	ATA	Trp-Met	ns
	Positive	m.5499 G>A	G	A	50%	<i>MT-CO1</i>	ATA	Val-Met	ns
	Positive	m.8065 C>T	C	T	25%	<i>MT-ATP6</i>	TAC	His-Tyr	ns
9	Positive	m.13435 C>T	C	T	25%	<i>MT-ND5</i>	TTC	Ser-Phe	ns
	Positive	m.2525 C>T	C	T	25%	<i>MT-16SrRNA</i>			-
	Positive	m.3226 C>T	C	T	75%	<i>MT-ND1</i>	TTC	Ser-Phe	ns
	Positive	m.5668 C>T	C	T	75%	<i>MT-CO1</i>	GTA	Ala-Val	ns
	Positive	m.6960 A>G	A	G	50%	<i>MT-tRNA D</i>	DHU Loop		-
	Positive	m.7881 C>T	C	T	25%	<i>MT-ATP8</i>	CTA	Pro-Leu	ns
	Positive	m.8955 C>T	C	T	25%	<i>MT-CO3</i>	TCT	pro-Ser	ns
	Positive	m.9780 C>T	C	T	75%	<i>MT-ND3</i>	TAA	Gln-STOP	ns
	Positive	m.10549 C>T	C	T	25%	<i>MT-ND4</i>	CTA	Pro-Leu	ns
	Positive	m.10939 C>T	C	T	75%	<i>MT-ND4</i>	GTA	Ala-Val	ns
	Positive	m.11066 A>T	A	T	25%	<i>MT-ND4</i>	TCT	Ser-Ser	syn
10	Positive	m.12942 A>T	A	T	75%	<i>MT-ND5</i>	TCC	Thr-Ser	ns
11	Positive	m.10466 C>T	C	T	50%	<i>MT-ND4</i>	ATT	Ile-Ile	syn

	Positive	m.14447 C>T	C	T	75%	<i>MT-CYB</i>	GGT	Gly-Gly	syn
	Positive	m.15191 C>T	C	T	75%	<i>MT-CYB</i>	ATT	Ile-Ile	syn
	Positive	m.15202 T>C	T	C	75%	<i>MT-CYB</i>	CCA	Leu-Pro	ns
12	Positive	none	none	none	none	none	none	none	none

7.4 Appendix D: Incidence of COX deficiency in different tissues of mutant and control tRNA^{Ala} mice

Mouse code	Age	m.5024C>T Tail heteroplasmy	COX –ve colonic crypts	Partial colonic crypts	COX +ve colonic crypts
111	83 weeks	29%	1%	21%	78%
112	83 weeks	24%	1%	15%	84%
471	72 weeks	45%	4%	10%	86%
472	72 weeks	18%	1%	10%	89%
483	71 weeks	39%	1%	17%	82%
1180	49 weeks	11%	-	14%	86%
1181	14 weeks	54%	-	6%	94%
1183	48 weeks	55%	-	16%	84%
1184	48 weeks	59%	1%	11%	88%
1622	22 weeks	74%	1%	12%	87%
1623	21 weeks	75%	2%	16%	82%
1624	21 weeks	64%	-	17%	83%
1625	21 weeks	69%	-	27%	73%
1626	21 weeks	72%	-	15%	85%
1734	20 weeks	60%	-	19%	81%
1764	20 weeks	66%	-	21%	79%
2265	20 weeks	60%	0%	6%	94%
2266	20 weeks	53%	0%	6%	94%
2267	20 weeks	77%	5%	20%	75%
2268	20 weeks	66%	0%	11%	89%
2269	20 weeks	74%	0%	13%	87%
2307	12 weeks (culled)	51%	0%	7%	93%
1299	10 weeks	50%	-	11%	89%
1305	10 weeks	12%	-	2%	98%
2191	22 weeks	10%	0%	0%	100%
2489	21 weeks	7%	0%	0%	100%
2430	22 weeks	24%	0%	0%	100%
2432	22 weeks	13%	0%	0%	100%

Mouse code	Age	M.5024C>T tail heteroplasmy	COX -ve colonic crypts	Partial colonic crypts	COX +ve colonic crypts	COX-ve colon smooth muscle	COX +ve colon smooth muscle
2241	65.9 weeks	68%	0%	9%	91%	1%	99%
2242	65.9 weeks	65%	0%	4%	96%	4%	96%
2261	64.9 weeks	64%	0%	8%	92%	1%	99%
2262	64.9 weeks	52%	0%	8%	92%	-	-
2264	64.9 weeks	60%	0%	7%	93%	-	-
2199	68 weeks	61%	0%	17%	83%	-	-
2200	68 weeks	58%	0%	24%	76%	4%	96%
2884	70 weeks	66%	2%	23%	75%	2%	98%
2885	70 weeks	26%	3%	47%	50%	0%	100%
2887	70 weeks	51%	2%	28%	70%	2%	98%

Mouse code	Age	M.5024C>T Tail heteroplasmy	COX -ve SKM fibers	Intermediate SKM fibers	Transitional SKM fibers	COX +ve SKM fibers	COX -ve Heart fibers	COX -ve Heart fibers
2884	70 weeks	66%	Thigh 0% Calf 1%	Thigh 1% Calf 3%	Thigh 1% Calf 1%	Thigh 98% Calf 95%	9%	91%
2885	70 weeks	26%	Thigh 0% Calf 0%	Thigh 3% Calf 2%	Thigh 2% Calf 3%	Thigh 95% Calf 95%	5%	95%
2887	70 weeks	51%	Thigh 0% Calf 0%	Thigh 2% Calf 2%	Thigh 3% Calf 3%	Thigh 95% Calf 95%	3%	97%

Chapter 8. References

- Acín-Pérez, R., P. Fernández-Silva, et al. (2008). "Respiratory Active Mitochondrial Supercomplexes." *Molecular Cell* **32**(4): 529-539.
- Agarwal, S. and R. S. Sohal (1996). "Relationship between susceptibility to protein oxidation, aging, and maximum life span potential of different species." *Experimental Gerontology* **31**(3): 365-372.
- Ahlqvist, K. J., R. H. Hämäläinen, et al. (2012). "Somatic progenitor cell vulnerability to mitochondrial DNA mutagenesis underlies progeroid phenotypes in polg mutator mice." *Cell Metabolism* **15**(1): 100-109.
- Al Rawi, S., S. Louvet-Vallée, et al. (2011). "Postfertilization autophagy of sperm organelles prevents paternal mitochondrial DNA transmission." *Science* **334**(6059): 1144-1147.
- Alberts, B., Johnson, A., Lewis, J., Raff, M., Roberts, K. and Walter, P. (2002). *Molecular Biology of the Cell*, New York: Garland Science.
- Anders, S., P. T. Pyl, et al. (2014). "HTSeq—A Python framework to work with high-throughput sequencing data." *bioRxiv*.
- Anderson, S., A. T. Bankier, et al. (1981). "Sequence and organization of the human mitochondrial genome." *Nature* **290**(5806): 457-465.
- Ardail, D., J. P. Privat, et al. (1990). "Mitochondrial contact sites: Lipid composition and dynamics." *Journal of Biological Chemistry* **265**(31): 18797-18802.
- Baines, H. L., J. B. Stewart, et al. (2014). "Similar patterns of clonally expanded somatic mtDNA mutations in the colon of heterozygous mtDNA mutator mice and ageing humans." *Mechanisms of Ageing and Development* **139**(1): 22-30.
- Baines, H. L., D. M. Turnbull, et al. (2014). "Human stem cell aging: Do mitochondrial DNA mutations have a causal role?" *Ageing Cell* **13**(2): 201-205.
- Balaban, R. S., S. Nemoto, et al. (2005). "Mitochondria, Oxidants, and Aging." *Cell* **120**(4): 483-495.
- Barker, N., J. H. Van Es, et al. (2007). "Identification of stem cells in small intestine and colon by marker gene Lgr5." *Nature* **449**(7165): 1003-1007.
- Baron, S. (1996). *Medical Microbiology*.
- Barrell, B. G., S. Anderson, et al. (1980). "Different pattern of codon recognition by mammalian mitochondrial tRNAs." *Proceedings of the National Academy of Sciences of the United States of America* **77**(6 I): 3164-3166.
- Bates, M. G. D., J. P. Bourke, et al. (2012). "Cardiac involvement in mitochondrial DNA disease: Clinical spectrum, diagnosis, and management." *European Heart Journal* **33**(24): 3023-3033.
- Bender, A., K. J. Krishnan, et al. (2006). "High levels of mitochondrial DNA deletions in substantia nigra neurons in aging and Parkinson disease." *Nature Genetics* **38**(5): 515-517.
- Berg, R. D. (1996). "The indigenous gastrointestinal microflora." *Trends in Microbiology* **4**(11): 430-435.
- Betts, J., E. Jaros, et al. (2006). "Molecular neuropathology of MELAS: Level of heteroplasmy in individual neurones and evidence of extensive vascular involvement." *Neuropathology and Applied Neurobiology* **32**(4): 359-373.
- Biao-Xue, R., C. Xi-Guang, et al. (2011). "EphA2-dependent molecular targeting therapy for malignant tumors." *Current Cancer Drug Targets* **11**(9): 1082-1097.
- Bibb, M. J., R. A. Van Etten, et al. (1981). "Sequence and gene organization of mouse mitochondrial DNA." *Cell* **26**(2 PART 2): 167-180.
- Biroccio A, C.-V. J., Augereau A, Pinte S, Bauwens S, Ye J, Simonet T, Horard B, Jamet K, Cervera L, Mendez-Bermudez A, Poncet D, Grataroli R, de Rodenbeeke CT, Salvati E, Rizzo A, Zizza P, Ricoul M, Cognet C, Kuilman T, Duret H, Lépinasse F, Marvel J, Verhoeven E, Cosset FL, Peeper D, Smyth MJ, Londoño-Vallejo A, Sabatier L, Picco V, Pages G, Scoazec JY, Stoppacciaro A, Leonetti C, Vivier E, Gilson E. (2013). "TRF2 inhibits a cell-extrinsic pathway through which natural killer cells eliminate cancer cells." *Nat Cell Biol* **15**(7): 818-828.

- Bjorksten, J. and H. Tenhu (1990). "The crosslinking theory of aging - Added evidence." Experimental Gerontology **25**(2): 91-95.
- Blackwood, J. K., S. C. Williamson, et al. (2011). "In situ lineage tracking of human prostatic epithelial stem cell fate reveals a common clonal origin for basal and luminal cells." Journal of Pathology **225**(2): 181-188.
- Blakely, E. L., H. Swalwell, et al. (2007). "Sporadic myopathy and exercise intolerance associated with the mitochondrial 8328G > A tRNA(Lys) mutation." Journal of Neurology **254**(9): 1283-1285.
- Boerries, M., P. Most, et al. (2007). "Ca²⁺-dependent interaction of S100A1 with F₁-ATPase leads to an increased ATP content in cardiomyocytes." Molecular and Cellular Biology **27**(12): 4365-4373.
- Bogenhagen, D. and D. A. Clayton (1977). "Mouse l cell mitochondrial DNA molecules are selected randomly for replication throughout the cell cycle." Cell **11**(4): 719-727.
- Bogenhagen, D. F. (1999). "Repair of mtDNA in vertebrates." American Journal of Human Genetics **64**(5): 1276-1251.
- Bonilla, E., M. Sciacco, et al. (1992). "New morphological approaches to the study of mitochondrial encephalomyopathies." Brain Pathology **2**(2): 113-119.
- Bonnefoy, N. and T. D. Fox (2001). Genetic transformation of *Saccharomyces cerevisiae* mitochondria. Methods in Cell Biology: 381-396.
- Booth, D. and C. S. Potten (2001). "Protection against mucosal injury by growth factors and cytokines." Journal of the National Cancer Institute. Monographs(29): 16-20.
- Boulet L, K. G., Shoubridge EA. (1992). "Distribution and threshold expression of the tRNA(Lys) mutation in skeletal muscle of patients with myoclonic epilepsy and ragged-red fibers (MERRF)." Am J Hum Genet. 1992 Dec;**51**(6):1187-200. **51**: 1187-1200.
- Bowmaker, M., M. Y. Yang, et al. (2003). "Mammalian Mitochondrial DNA Replicates Bidirectionally from an Initiation Zone." Journal of Biological Chemistry **278**(51): 50961-50969.
- Brändén, G., R. B. Gennis, et al. (2006). "Transmembrane proton translocation by cytochrome c oxidase." Biochimica et Biophysica Acta - Bioenergetics **1757**(8): 1052-1063.
- Brierley, E. J., M. A. Johnson, et al. (1998). "Role of mitochondrial DNA mutations in human aging: Implications for the central nervous system and muscle." Annals of Neurology **43**(2): 217-223.
- Bua, E., J. Johnson, et al. (2006). "Mitochondrial DNA-deletion mutations accumulate intracellularly to detrimental levels in aged human skeletal muscle fibers." American Journal of Human Genetics **79**(3): 469-480.
- Cahalan, M. D. and K. G. Chandy (2009). "The functional network of ion channels in T lymphocytes." Immunological Reviews **231**(1): 59-87.
- Cai, S., Y. Xu, et al. (2005). "Mitochondrial targeting of human O6-methylguanine DNA methyltransferase protects against cell killing by chemotherapeutic alkylating agents." Cancer Research **65**(8): 3319-3327.
- Carew, J. S. and P. Huang (2002). "Mitochondrial defects in cancer." Molecular Cancer **1**.
- Carroll, M. (1989). Organelles, Macmillan Education Ltd.
- Cavalli, L. R. and B. C. Liang (1998). "Mutagenesis, tumorigenicity, and apoptosis: Are the mitochondria involved?" Mutation Research - Fundamental and Molecular Mechanisms of Mutagenesis **398**(1-2): 19-26.
- Cech, T. R. (2004). "Beginning to Understand the End of the Chromosome." Cell **116**(2): 273-279.
- Cerritelli, S. M., E. G. Frolova, et al. (2003). "Failure to produce mitochondrial DNA results in embryonic lethality in Rnaseh1 null mice." Molecular Cell **11**(3): 807-815.
- Chance, B., Sies, H. and Boveris, A. (1979). "Hydroperoxide metabolism in mammalian organs." Physiol Rev **59**: 527-605.
- Chance, B. a. W., G.R. (1956). "Respiratory enzymes in oxidative phosphorylation. VI. The effects of adenosine diphosphate on azide-treated mitochondria." J Biol Chem. **221**(1): 477-489.
- Chen, L. B. (1988). "Mitochondrial membrane potential in living cells." Annu Rev Cell Biol **4**: 155-181.

- Chinnery, P. F., P. J. G. Zwijnenburg, et al. (1999). "Nonrandom tissue distribution of mutant mtDNA." American Journal of Medical Genetics **85**(5): 498-501.
- Chomyn, A., A. Martinuzzi, et al. (1992). "MELAS mutation in mtDNA binding site for transcription termination factor causes defects in protein synthesis and in respiration but no change in levels of upstream and downstream mature transcripts." Proceedings of the National Academy of Sciences of the United States of America **89**(10): 4221-4225.
- Ciafaloni, E., E. Ricci, et al. (1992). "MELAS: Clinical features, biochemistry, and molecular genetics." Annals of Neurology **31**(4): 391-398.
- Clayton, D. A. (1982). "Replication of animal mitochondrial DNA." Cell **28**(4): 693-705.
- Clayton, D. A. (1991). "Replication and transcription of vertebrate mitochondrial DNA." Annu Rev Cell Biol **7**: 453-478.
- Clayton DA, D. J., Friedberg EC. (1974). "The Absence of a Pyrimidine Dimer Repair Mechanism in Mammalian Mitochondria." Proc Natl Acad Sci U S A. **71**: 2777-2781.
- Clément-Ziza, M., A. Munnich, et al. (2008). "Stabilization of RNA during laser capture microdissection by performing experiments under argon atmosphere or using ethanol as a solvent in staining solutions." RNA **14**(12): 2698-2704.
- Coller, H. A., K. Khrapko, et al. (2001). "High frequency of homoplasmic mitochondrial DNA mutations in human tumors can be explained without selection." Nature Genetics **28**(2): 147-150.
- Coller, H. A., K. Khrapko, et al. (2005). "Clustering of mutant mitochondrial DNA copies suggests stem cells are common in human bronchial epithelium." Mutation Research - Fundamental and Molecular Mechanisms of Mutagenesis **578**(1-2): 256-271.
- Cookson, J. C. a. L., C. A. (2009). "The levels of telomere-binding proteins in human tumours and therapeutic implications." Eur J Cancer **45**(4): 536-550.
- Cortopassi, G. A. and N. Arnheim (1990). "Detection of a specific mitochondrial DNA deletion in tissues of older humans." Nucleic Acids Research **18**(23): 6927-6933.
- Cortopassi, G. A., D. Shibata, et al. (1992). "A pattern of accumulation of a somatic deletion of mitochondrial DNA in aging human tissues." Proceedings of the National Academy of Sciences of the United States of America **89**(16): 7370-7374.
- Cottrell, D. A., E. L. Blakely, et al. (2001). "Cytochrome C oxidase deficient cells accumulate in the hippocampus and choroid plexus with age." Neurobiology of Aging **22**(2): 265-272.
- Cree, L. M., D. C. Samuels, et al. (2008). "A reduction of mitochondrial DNA molecules during embryogenesis explains the rapid segregation of genotypes." Nature Genetics **40**(2): 249-254.
- Croft, D., A. F. Mundo, et al. (2014). "The Reactome pathway knowledgebase." Nucleic acids research **42**(D1): D472-D477.
- Cuervo, A. M., Dice, J. F. (2000). "Age-related decline in chaperone-mediated autophagy." J Biol Chem. **275**: 31505-31513.
- Cummins, J. (1998). "Mitochondrial DNA in mammalian reproduction." Reviews of Reproduction **3**(3): 172-182.
- Cummins, J. M., T. Wakayama, et al. (1997). "Fate of microinjected sperm components in the mouse oocyte and embryo." Zygote **5**(4): 301-308.
- Dairaghi, D. J., G. S. Shadel, et al. (1995). "Addition of a 29 residue carboxyl-terminal tail converts a simple HMG box-containing protein into a transcriptional activator." Journal of Molecular Biology **249**(1): 11-28.
- Davies, A. M., S. Hershman, et al. (2003). "A Ca²⁺-induced mitochondrial permeability transition causes complete release of rat liver endonuclease G activity from its exclusive location within the mitochondrial intermembrane space. Identification of a novel endonuclease activity residing within the mitochondrial matrix." Nucleic Acids Research **31**(4): 1364-1373.
- De Grey, A. D. N. J. (1997). "A proposed refinement of the mitochondrial free radical theory of aging." BioEssays **19**(2): 161-166.
- De Luca, C., C. Besagni, et al. (2006). "Mutations in yeast mt tRNAs: Specific and general suppression by nuclear encoded tRNA interactors." Gene **377**(1-2): 169-176.
- de Souza-Pinto, N. C., P. A. Mason, et al. (2009). "Novel DNA mismatch-repair activity involving YB-1 in human mitochondria." DNA Repair **8**(6): 704-719.

- Denton, R. M. (2009). "Regulation of mitochondrial dehydrogenases by calcium ions." Biochimica et Biophysica Acta **1787**: 1309-1316.
- Diaz, F., M. P. Bayona-Bafaluy, et al. (2002). "Human mitochondrial DNA with large deletions repopulates organelles faster than full-length genomes under relaxed copy number control." Nucleic Acids Research **30**(21): 4626-4633.
- DiMauro, S. and E. A. Schon (2001). "Mitochondrial DNA mutations in human disease." American Journal of Medical Genetics - Seminars in Medical Genetics **106**(1): 18-26.
- DiMauro, S. and E. A. Schon (2003). "Mitochondrial respiratory-chain diseases." New England Journal of Medicine **348**(26): 2656-2668.
- Dobin, A., C. A. Davis, et al. (2013). "STAR: ultrafast universal RNA-seq aligner." Bioinformatics **29**(1): 15-21.
- Dormoy, V., K. Tormanen, et al. (2013). "Par6 γ is at the mother centriole and controls centrosomal protein composition through a Par6 α -dependent pathway." Journal of Cell Science **126**(3): 860-870.
- Duchen, M. R. (2000). "Mitochondria and calcium: From cell signalling to cell death." Journal of Physiology **529**(1): 57-68.
- Dunbar, D. R., P. A. Moonie, et al. (1995). "Different cellular backgrounds confer a marked advantage to either mutant or wild-type mitochondrial genomes." Proceedings of the National Academy of Sciences of the United States of America **92**(14): 6562-6566.
- Durham, S. E., D. C. Samuels, et al. (2006). "Is selection required for the accumulation of somatic mitochondrial DNA mutations in post-mitotic cells?" Neuromuscular Disorders **16**(6): 381-386.
- Edgar, D., I. Shabalina, et al. (2009). "Random Point Mutations with Major Effects on Protein-Coding Genes Are the Driving Force behind Premature Aging in mtDNA Mutator Mice." Cell Metabolism **10**(2): 131-138.
- Ekstrand, M. I., M. Terzioglu, et al. (2007). "Progressive parkinsonism in mice with respiratory-chain-deficient dopamine neurons." Proceedings of the National Academy of Sciences of the United States of America **104**(4): 1325-1330.
- Elliott, H. R., D. C. Samuels, et al. (2008). "Pathogenic Mitochondrial DNA Mutations Are Common in the General Population." American Journal of Human Genetics **83**(2): 254-260.
- Elson, J. L., D. C. Samuels, et al. (2001). "Random intracellular drift explains the clonal expansion of mitochondrial DNA mutations with age." American Journal of Human Genetics **68**(3): 802-806.
- Elson, J. L., H. Swalwell, et al. (2009). "Pathogenic mitochondrial tRNA mutations - Which mutations are inherited and why?" Human Mutation **30**(11): E984-E992.
- Elson, J. L., D. M. Turnbull, et al. (2004). "Comparative Genomics and the Evolution of Human Mitochondrial DNA: Assessing the Effects of Selection." American Journal of Human Genetics **74**(2): 229-238.
- Falcon, S. and R. Gentleman (2007). "Using GOstats to test gene lists for GO term association." Bioinformatics **23**(2): 257-258.
- Falkenberg, M., M. Gaspari, et al. (2002). "Mitochondrial transcription factors B1 and B2 activate transcription of human mtDNA." Nature Genetics **31**(3): 289-294.
- Falkenberg, M., N. G. Larsson, et al. (2007). DNA replication and transcription in mammalian mitochondria. Annual Review of Biochemistry. **76**: 679-699.
- Fan, W., K. G. Waymire, et al. (2008). "A mouse model of mitochondrial disease reveals germline selection against severe mtDNA mutations." Science **319**(5865): 958-962.
- Fayet, G., M. Jansson, et al. (2002). "Ageing muscle: Clonal expansions of mitochondrial DNA point mutations and deletions cause focal impairment of mitochondrial function." Neuromuscular Disorders **12**(5): 484-493.
- Fellous, T. G., S. Islam, et al. (2009). "Locating the stem cell niche and tracing hepatocyte lineages in human liver." Hepatology **49**(5): 1655-1663.
- Fellous, T. G., S. A. C. McDonald, et al. (2009). "A methodological approach to tracing cell lineage in human epithelial tissues." Stem Cells **27**(6): 1410-1420.
- Ferguson, S. J. (2010). "ATP synthase: From sequence to ring size to the P/O ratio." Proceedings of the National Academy of Sciences of the United States of America **107**(39): 16755-16756.

- Ferlay, J., Bray, P., Pisani, P. et al., . (2001). "Globoscan 2000: Cancer incidence, mortality and prevalence worldwide, version 1.0."
- Finch, C. E. and R. E. Tanzi (1997). "Genetics of aging." *Science* **278**(5337): 407-411.
- Finnilä, S., S. Tuisku, et al. (2001). "A novel mitochondrial DNA mutation and a mutation in the Notch3 gene in a patient with myopathy and CADASIL." *Journal of Molecular Medicine* **79**(11): 641-647.
- Fiocchi, C. (1998). "Inflammatory bowel disease: Etiology and pathogenesis." *Gastroenterology* **115**(1): 182-205.
- Fisher, R. P., J. N. Topper, et al. (1987). "Promoter selection in human mitochondria involves binding of a transcription factor to orientation-independent upstream regulatory elements." *Cell* **50**(2): 247-258.
- Fleischer, S., Klouwen, H. and Brierley, G. (1961). "Studies of the electron transfer system." *The Journal of Biological Chemistry* **236**(11): 36-41.
- Fleury, C., B. Mignotte, et al. (2002). "Mitochondrial reactive oxygen species in cell death signaling." *Biochimie* **84**(2-3): 131-141.
- Fox, R. G., S. Magness, et al. (2012). "Mitochondrial DNA polymerase editing mutation, PolgD257A, disturbs stem-progenitor cell cycling in the small intestine and restricts excess fat absorption." *American Journal of Physiology - Gastrointestinal and Liver Physiology* **302**(9): G914-G924.
- Freya, T. G. and C. A. Mannellab (2000). "The internal structure of mitochondria." *Trends in Biochemical Sciences* **25**(7): 319-324.
- Freyer, C., L. M. Cree, et al. (2012). "Variation in germline mtDNA heteroplasmy is determined prenatally but modified during subsequent transmission." *Nature Genetics* **44**(11): 1282-1285.
- Freyer, C., C. B. Park, et al. (2010). "Maintenance of respiratory chain function in mouse hearts with severely impaired mtDNA transcription." *Nucleic Acids Research* **38**(19): 6577-6588.
- Fu, L., H. Pelicano, et al. (2002). "The circadian gene Period2 plays an important role in tumor suppression and DNA damage response in vivo." *Cell* **111**(1): 41-50.
- Fukui, H. and C. T. Moraes (2009). "Mechanisms of formation and accumulation of mitochondrial DNA deletions in aging neurons." *Human Molecular Genetics* **18**(6): 1028-1036.
- Funk, S. D. and A. W. Orr (2013). "Ephs and ephrins resurface in inflammation, immunity, and atherosclerosis." *Pharmacological Research* **67**(1): 42-52.
- Gattoni, A., A. Parlato, et al. (2006). "Interferon- γ : Biologic functions and HCV therapy (type I/II) (1 of 2 parts)." *Clinica Terapeutica* **157**(4): 377-386.
- Giles, R. E., H. Blanc, et al. (1980). "Maternal inheritance of human mitochondrial DNA." *Proceedings of the National Academy of Sciences of the United States of America* **77**(11 I): 6715-6719.
- Gohil, V. M., R. Nilsson, et al. (2010). "Mitochondrial and nuclear genomic responses to loss of LRPPRC expression." *Journal of Biological Chemistry* **285**(18): 13742-13747.
- Goldstein, J. C., N. J. Waterhouse, et al. (2000). "The coordinate release of cytochrome c during apoptosis is rapid, complete and kinetically invariant." *Nature Cell Biology* **2**(3): 156-162.
- Gong, Y., C. He, et al. (2013). "Association of two ERCC4 tagSNPs with susceptibility to atrophic gastritis and gastric cancer in Chinese." *Gene* **519**(2): 335-342.
- Gorfu, G., J. Rivera-Nieves, et al. (2010). " β 7 integrin deficiency suppresses B cell homing and attenuates chronic ileitis in SAMP1/YitFc mice." *Journal of Immunology* **185**(9): 5561-5568.
- Goto, Y. I., I. Nonaka, et al. (1990). "A mutation in the tRNA(Leu(UUR)) gene associated with the MELAS subgroup of mitochondrial encephalomyopathies." *Nature* **348**(6302): 651-653.
- Gray, H. and W. Tai Wai (1992). "Purification and identification of subunit structure of the human mitochondrial DNA polymerase." *Journal of Biological Chemistry* **267**(9): 5835-5841.

- Greaves, L. C., M. J. Barron, et al. (2011). "Differences in the accumulation of mitochondrial defects with age in mice and humans." Mechanisms of Ageing and Development **132**(11-12): 588-591.
- Greaves, L. C., M. J. Barron, et al. (2010). "Defects in multiple complexes of the respiratory chain are present in ageing human colonic crypts." Experimental Gerontology **45**(7-8): 573-579.
- Greaves, L. C., J. L. Elson, et al. (2012). "Comparison of Mitochondrial Mutation Spectra in Ageing Human Colonic Epithelium and Disease: Absence of Evidence for Purifying Selection in Somatic Mitochondrial DNA Point Mutations." PLoS Genetics **8**(11): e1003082. doi: 1003010.1001371/journal.pgen.1003082. Epub 1002012 Nov 1003015.
- Greaves, L. C., J. L. Elson, et al. (2012). "Comparison of Mitochondrial Mutation Spectra in Ageing Human Colonic Epithelium and Disease: Absence of Evidence for Purifying Selection in Somatic Mitochondrial DNA Point Mutations." PLoS Genetics **8**(11).
- Greaves, L. C., Nooteboom, M., Elson, J.L., Tuppen, H.A.L., Taylor, G. A., Commane, D.M., Arasaradnam, R.P., Khrapko, K., Taylor, R.W., Kirkwood, T.B.L., Mathers, J.C. and Turnbull, D.M. (2014). "Clonal expansion of early to mid-life mitochondrial DNA point mutations drives mitochondrial dysfunction during human ageing." PLoS Genetics: e1004620.
- Greaves, L. C., S. L. Preston, et al. (2006). "Mitochondrial DNA mutations are established in human colonic stem cells, and mutated clones expand by crypt fission." Proceedings of the National Academy of Sciences of the United States of America **103**(3): 714-719.
- Grizzi, F., A. Di Ieva, et al. (2006). "Cancer initiation and progression: An unsimplifiable complexity." Theoretical Biology and Medical Modelling **3**.
- Guliaeva, N. A., E. A. Kuznetsova, et al. (2006). "Proteins associated with mitochondrial DNA protect it against the action of X-rays and hydrogen peroxide." Biofizika, **51**(4): 692-697.
- Gutierrez-Gonzalez, L., M. Deheragoda, et al. (2009). "Analysis of the clonal architecture of the human small intestinal epithelium establishes a common stem cell for all lineages and reveals a mechanism for the fixation and spread of mutations." Journal of Pathology **217**(4): 489-496.
- Hackenbrock, C. R. (1968). "Chemical and physical fixation of isolated mitochondria in low-energy and high-energy states." Proceedings of the National Academy of Sciences of the United States of America **61**(2): 598-605.
- Hafner, C., S. Meyer, et al. (2005). "Ephrin-B reverse signaling induces expression of wound healing associated genes in IEC-6 intestinal epithelial cells." World Journal of Gastroenterology **11**(29): 4511-4518.
- Hägerhäll, C. (1997). "Succinate: Quinone oxidoreductases. Variations on a conserved theme." Biochimica et Biophysica Acta - Bioenergetics **1320**(2): 107-141.
- Hamanaka, R. B. and N. S. Chandel (2010). "Mitochondrial reactive oxygen species regulate cellular signaling and dictate biological outcomes." Trends in Biochemical Sciences **35**(9): 505-513.
- Harley, C. B., Vaziri, H., Counter, C. M., Allsopp, R. C. (1992). "The telomere hypothesis of cellular aging." Exp Gerontol. **27**: 375-382.
- Harman, D. (1956). "Aging: a theory based on free radical and radiation chemistry." J Gerontol. **11**: 298-300.
- Harman, D. (1972). "The biologic clock: the mitochondria?" Journal of the American Geriatrics Society **20**(4): 145-147.
- Hart, R. W., Setlow, R. B. (1974). "Correlation between deoxyribonucleic acid excision-repair and life-span in a number of mammalian species." Proc Natl Acad Sci U S A. **71**: 2169-2173.
- Hatefi, Y. (1985). "The mitochondrial electron transport and oxidative phosphorylation system." Annu. Rev. Biochem **54**: 1015-1069.
- Hauser, D. N., A. A. Dillman, et al. (2014). "Post-translational decrease in respiratory chain proteins in the polg mutator mouse brain." PLoS ONE **9**(4).
- Hayashi, J. I., S. Ohta, et al. (1991). "Introduction of disease-related mitochondrial DNA deletions into HeLa cells lacking mitochondrial DNA results in mitochondrial

- dysfunction." Proceedings of the National Academy of Sciences of the United States of America **88**(23): 10614-10618.
- He, Y., J. Wu, et al. (2010). "Heteroplasmic mitochondrial DNA mutations in normal and tumour cells." Nature **464**(7288): 610-614.
- Health, N. I. (2006). "What You Need To Know About Cancer of the Colon and Rectum."
- Herbener, G. H. (1976). "A morphometric study of age dependent changes in mitochondrial populations of mouse liver and heart." Journals of Gerontology **31**(1): 8-12.
- Herbst, A., J. W. Pak, et al. (2007). "Accumulation of mitochondrial DNA deletion mutations in aged muscle fibers: Evidence for a causal role in muscle fiber loss." Journals of Gerontology - Series A Biological Sciences and Medical Sciences **62**(3): 235-245.
- Herrero, A. and G. Barja (1997). "Sites and mechanisms responsible for the low rate of free radical production of heart mitochondria in the long-lived pigeon." Mechanisms of Ageing and Development **98**(2): 95-111.
- Hewitt, G., D. Jurk, et al. (2012). "Telomeres are favoured targets of a persistent DNA damage response in ageing and stress-induced senescence." Nature Communications **3**.
- Hinttala, R., R. Smeets, et al. (2006). "Analysis of mitochondrial DNA sequences in patients with isolated or combined oxidative phosphorylation system deficiency." Journal of Medical Genetics **43**(11): 881-886.
- Hirano, M. a. P., S.G. (1994). "Mitochondrial myopathy,encephalopathy, lactic acidosis, and stroke-like episodes (MELAS): current concepts." J Child Neurol **9**: 4-13.
- Hofer, A. M., S. Curci, et al. (2000). "Intercellular communication mediated by the extracellular calcium-sensing receptor." Nature Cell Biology **2**(7): 392-398.
- Hollander, D. (1992). "The intestinal permeability barrier: an hypothesis as to its regulation and involvement in Crohn's disease." Scand J Gastroenterol **27**: 721-726.
- Holt, I. J., A. E. Harding, et al. (1988). "Deletions of muscle mitochondrial DNA in patients with mitochondrial myopathies." Nature **331**(6158): 717-719.
- Holt, I. J., H. E. Lorimer, et al. (2000). "Coupled Leading- and Lagging-Strand Synthesis of Mammalian Mitochondrial DNA." Cell **100**(5): 515-524.
- Houshmand, M., C. Lindberg, et al. (1999). "A novel heteroplasmic point mutation in the mitochondrial tRNA(Lys) gene in a sporadic case of mitochondrial encephalomyopathy: De novo mutation and no transmission to the offspring." Human Mutation **13**(3): 203-209.
- Hubbard, M. J. and N. J. McHugh (1996). "Mitochondrial ATP synthase F1- β -subunit is a calcium-binding protein." FEBS Letters **391**(3): 323-329.
- Hwang-Verslues, W. W., P. H. Chang, et al. (2013). "Loss of corepressor PER2 under hypoxia up-regulates OCT1-mediated EMT gene expression and enhances tumor malignancy." Proceedings of the National Academy of Sciences of the United States of America **110**(30): 12331-12336.
- Ibrahim, G. A., B. A. Zweber, et al. (1981). "Remote tumor effects on lactic dehydrogenase of mouse muscle fibers with different glycolytic-oxydative metabolic potentials." Proceedings of the Society for Experimental Biology and Medicine **168**(1): 119-122.
- Inoue, K., K. Nakada, et al. (2000). "Generation of mice with mitochondrial dysfunction by introducing mouse mtDNA carrying a deletion into zygotes." Nature Genetics **26**(2): 176-181.
- Itzkovitz, S., A. Lyubimova, et al. (2012). "Single-molecule transcript counting of stem-cell markers in the mouse intestine." Nature Cell Biology **14**(1): 106-114.
- Ivanova, R., V. Lepage, et al. (1998). "Mitochondrial DNA sequence variation in human leukemic cells." International Journal of Cancer **76**(4): 495-498.
- Jacobs, H. T. (2003). "Disorders of mitochondrial protein synthesis." Human Molecular Genetics **12**(REV. ISS. 2): R293-R301.
- Jayasena, C. S., L. A. Trinh, et al. (2011). "Live imaging of endogenous periodic tryptophan protein 2 gene homologue during zebrafish development." Developmental Dynamics **240**(11): 2578-2583.
- Jensen, L. E. and A. S. Whitehead (2003). "Expression of alternatively spliced interleukin-1 receptor accessory protein mRNAs is differentially regulated during inflammation and apoptosis." Cellular Signalling **15**(8): 793-802.

- Jenuth, J. P., A. C. Peterson, et al. (1996). "Random genetic drift in the female germline explains the rapid segregation of mammalian mitochondrial DNA." Nature Genetics **14**(2): 146-151.
- Jenuth, J. P., A. C. Peterson, et al. (1997). "Tissue-specific selection for different mtDNA genotypes in heteroplasmic mice." Nature Genetics **16**(1): 93-95.
- Jerónimo, C., S. Nomoto, et al. (2001). "Mitochondrial mutations in early stage prostate cancer and bodily fluids." Oncogene **20**(37): 5195-5198.
- Johansson, M. E. V., M. Phillipson, et al. (2008). "The inner of the two Muc2 mucin-dependent mucus layers in colon is devoid of bacteria." Proceedings of the National Academy of Sciences of the United States of America **105**(39): 15064-15069.
- Johns, D. R. (1995). "Seminars in medicine of the Beth Israel Hospital, Boston. Mitochondrial DNA and disease." N Engl J Med; **333**: 638-644.
- Johns, D. R., M. J. Neufeld, et al. (1992). "An ND-6 mitochondrial DNA mutation associated with Leber hereditary optic neuropathy." Biochemical and Biophysical Research Communications **187**(3): 1551-1557.
- Joshi-Tope, G., M. Gillespie, et al. (2005). "Reactome: a knowledgebase of biological pathways." Nucleic acids research **33**(suppl 1): D428-D432.
- Joshi, B., L. Li, et al. (1999). "Apoptosis induction by a novel anti-prostate cancer compound, BMD188 (A fatty acid-containing hydroxamic acid), requires the mitochondrial respiratory chain." Cancer Research **59**(17): 4343-4355.
- Kaguni, L. S. (2004). DNA polymerase γ , the mitochondrial replicase. Annual Review of Biochemistry. **73**: 293-320.
- Kaido, M., H. Fujimura, et al. (1995). "Focal cytochrome c oxidase deficiency in the brain and dorsal root ganglia in a case with mitochondrial encephalomyopathy (tRNA(Ile) 4269 mutation): Histochemical, immunohistochemical, and ultrastructural study." Journal of the Neurological Sciences **131**(2): 170-176.
- Kanehisa, M. and S. Goto (2000). "KEGG: kyoto encyclopedia of genes and genomes." Nucleic acids research **28**(1): 27-30.
- Kanehisa, M., S. Goto, et al. (2006). "From genomics to chemical genomics: new developments in KEGG." Nucleic acids research **34**(suppl 1): D354-D357.
- Karam, S. M. (1999). "Lineage commitment and maturation of epithelial cells in the gut." Frontiers in bioscience : a journal and virtual library **4**: D286-298.
- Kasahara, A., K. Ishikawa, et al. (2006). "Generation of trans-mitochondrial mice carrying homoplasmic mtDNAs with a missense mutation in a structural gene using ES cells." Human Molecular Genetics **15**(6): 871-881.
- Kataoka, H., H. Igarashi, et al. (2004). "Correlation of EPHA2 overexpression with high microvessel count in human primary colorectal cancer." Cancer Science **95**(2): 136-141.
- Kelleher, F. C., A. Rao, et al. (2014). "Circadian molecular clocks and cancer." Cancer Letters **342**(1): 9-18.
- Khrapko, K., N. Bodyak, et al. (1999). "Cell-by-cell scanning of whole mitochondrial genomes in aged human heart reveals a significant fraction of myocytes with clonally expanded deletions." Nucleic Acids Research **27**(11): 2434-2441.
- Khrapko, K., Y. Kraytsberg, et al. (2006). "Does premature aging of the mtDNA mutator mouse prove that mtDNA mutations are involved in natural aging?" Aging Cell **5**(3): 279-282.
- Kim, I. and J. J. Lemasters (2011). "Mitophagy selectively degrades individual damaged mitochondria after photoirradiation." Antioxidants and Redox Signaling **14**(10): 1919-1928.
- Kim, I., S. Rodriguez-Enriquez, et al. (2007). "Selective degradation of mitochondria by mitophagy." Archives of Biochemistry and Biophysics **462**(2): 245-253.
- King, M. P. and G. Attardi (1989). "Human cells lacking mtDNA: Repopulation with exogenous mitochondria by complementation." Science **246**(4929): 500-503.
- Kirichok, Y., G. Krapivinsky, et al. (2004). "The mitochondrial calcium uniporter is a highly selective ion channel." Nature **427**(6972): 360-364.
- Kirkwood, T. B. (1995). What can evolution theory tell us about the mechanisms of ageing? Molecular Aspects of ageing

- Kirkwood, T. B. L. (1977). "Evolution of ageing." *Nature* **270**(5635): 301-304.
- Kirkwood, T. B. L. (2008). "Understanding ageing from an evolutionary perspective." *Journal of Internal Medicine* **263**(2): 117-127.
- Kolesar, J. E., Safdar, A., Abadi, A., Mac Neil, L.G., Crane, J.D., Tarnopolsky, M.A. and Kaufman, B.A. (2014). "Defects in mitochondrial DNA replication and oxidative damage in muscle of mtDNA mutator " *Free Radic Biol Med*. **Epub ahead of print**.
- Kopsidas, G., S. A. Kovalenko, et al. (1998). "An age-associated correlation between cellular bioenergy decline and mtDNA rearrangements in human skeletal muscle." *Mutation Research - Fundamental and Molecular Mechanisms of Mutagenesis* **421**(1): 27-36.
- Korhonen, J. A., M. Gaspari, et al. (2003). "TWINKLE has 5' → 3' DNA helicase activity and is specifically stimulated by mitochondrial single-stranded DNA-binding protein." *Journal of Biological Chemistry* **278**(49): 48627-48632.
- Korr, H., C. Kurz, et al. (1998). "Mitochondrial DNA synthesis studied autoradiographically in various cell types in vivo." *Brazilian Journal of Medical and Biological Research* **31**(2): 289-298.
- Kowald, A. and T. B. L. Kirkwood (2000). "Accumulation of defective mitochondria through delayed degradation of damaged organelles and its possible role in the ageing of post-mitotic and dividing cells." *Journal of Theoretical Biology* **202**(2): 145-160.
- Kowald, A. and T. B. L. Kirkwood (2013). "Mitochondrial mutations and aging: random drift is insufficient to explain the accumulation of mitochondrial deletion mutants in short-lived animals." *Aging Cell* **12**(4): 728-731.
- Kozar, S., E. Morrissey, et al. (2013). "Continuous Clonal Labeling Reveals Small Numbers of Functional Stem Cells in Intestinal Crypts and Adenomas." *Cell Stem Cell* **13**(5): 626-633.
- Kraytsberg, Y., E. Kudryavtseva, et al. (2006). "Mitochondrial DNA deletions are abundant and cause functional impairment in aged human substantia nigra neurons." *Nature Genetics* **38**(5): 518-520.
- Kraytsberg, Y., D. K. Simon, et al. (2009). "Do mtDNA deletions drive premature aging in mtDNA mutator mice?" *Aging Cell* **8**(4): 502-506.
- Krishnan, K. J., A. K. Reeve, et al. (2008). "What causes mitochondrial DNA deletions in human cells?" *Nature Genetics* **40**(3): 275-279.
- Kujoth, C. C., A. Hiona, et al. (2005). "Mitochondrial DNA mutations, oxidative stress, and apoptosis in mammalian aging." *Science* **309**(5733): 481-484.
- Kukat, A. and A. Trifunovic (2009). "Somatic mtDNA mutations and aging - Facts and fancies." *Experimental Gerontology* **44**(1-2): 101-105.
- Kukat, C. and N. G. Larsson (2013). "MtDNA makes a U-turn for the mitochondrial nucleoid." *Trends in Cell Biology* **23**(9): 457-463.
- Kunkel, T. A. (1986). "Frameshift mutagenesis by eucaryotic DNA polymerases in vitro." *Journal of Biological Chemistry* **261**(29): 13581-13587.
- Larsson, N. G. and D. A. Clayton (1995). Molecular genetic aspects of human mitochondrial disorders. *Annual Review of Genetics*. **29**: 151-178.
- Larsson, N. G., H. G. Eiken, et al. (1992). "Lack of transmission of deleted mtDNA from a woman with Kearns-Sayre syndrome to her child." *American Journal of Human Genetics* **50**(2): 360-363.
- Larsson, N. G., M. H. Tulinius, et al. (1992). "Segregation and manifestations of the mtDNA tRNA^{Lys} A→G(8344) mutation of myoclonus epilepsy and ragged-red fibers (MERRF) syndrome." *American Journal of Human Genetics* **51**(6): 1201-1212.
- Larsson, N. G., J. Wang, et al. (1998). "Mitochondrial transcription factor A is necessary for mtDNA maintenance and embryogenesis in mice." *Nature Genetics* **18**(3): 231-236.
- Larsson, N. G. C., D. A. (1995). "Molecular genetic aspects of human mitochondrial disorders." 151-178.
- Lee, H. C., P. H. Yin, et al. (2005). Mitochondrial genome instability and mtDNA depletion in human cancers. *Annals of the New York Academy of Sciences*. **1042**: 109-122.
- Li, M., A. Schönberg, et al. (2010). "Detecting heteroplasmy from high-throughput sequencing of complete human mitochondrial DNA genomes." *American Journal of Human Genetics* **87**(2): 237-249.

- Li, Z., K. I. Okamoto, et al. (2004). "The importance of dendritic mitochondria in the morphogenesis and plasticity of spines and synapses." *Cell* **119**(6): 873-887.
- Liang, Q. and P. C. Dedon (2001). "Cu(II)/H₂O₂-induced DNA damage is enhanced by packaging of DNA as a nucleosome." *Chemical Research in Toxicology* **14**(4): 416-422.
- Lièvre, A., C. Chapusot, et al. (2005). "Clinical value of mitochondrial mutations in colorectal cancer." *Journal of Clinical Oncology* **23**(15): 3517-3525.
- Lightowlers, R. N., P. F. Chinnery, et al. (1997). "Mammalian mitochondrial genetics: Heredity, heteroplasmy and disease." *Trends in Genetics* **13**(11): 450-455.
- Lin, C. S., M. S. Sharpley, et al. (2012). "Mouse mtDNA mutant model of Leber hereditary optic neuropathy." *Proceedings of the National Academy of Sciences of the United States of America* **109**(49): 20065-20070.
- Lin, S. J., M. Kaeberlein, et al. (2002). "Calorie restriction extends *Saccharomyces cerevisiae* lifespan by increasing respiration." *Nature* **418**(6895): 344-348.
- Ling, C., M. Ishiai, et al. (2007). "FAAP100 is essential for activation of the Fanconi anemia-associated DNA damage response pathway." *EMBO Journal* **26**(8): 2104-2114.
- Liu, J., J. Yan, et al. (2012). "Site-specific ubiquitination is required for relieving the transcription factor Miz1-mediated suppression on TNF- α -induced JNK activation and inflammation." *Proceedings of the National Academy of Sciences of the United States of America* **109**(1): 191-196.
- Liu, L. and T. A. Rando (2011). "Manifestations and mechanisms of stem cell aging." *Journal of Cell Biology* **193**(2): 257-266.
- Liu, P. and B. Dimple (2010). "DNA repair in mammalian mitochondria: Much more than we thought?" *Environmental and Molecular Mutagenesis* **51**(5): 417-426.
- Liu, P., L. Qian, et al. (2008). "Removal of oxidative DNA damage via FEN1-dependent long-patch base excision repair in human cell mitochondria." *Molecular and Cellular Biology* **28**(16): 4975-4987.
- Liu, V. W. S., C. Zhang, et al. (1997). "Quantitative allele-specific PCR: Demonstration of age-associated accumulation in human tissues of the A \rightarrow G mutation at nucleotide 3243 in mitochondrial DNA." *Human Mutation* **9**(3): 265-271.
- Liu, X., C. N. Kim, et al. (1996). "Induction of apoptotic program in cell-free extracts: Requirement for dATP and cytochrome c." *Cell* **86**(1): 147-157.
- Logan, A., I. G. Shabalina, et al. (2014). "In vivo levels of mitochondrial hydrogen peroxide increase with age in mtDNA mutator mice." *Aging Cell* **13**(4): 765-768.
- Lombès, A., C. Diaz, et al. (1992). "Analysis of the tissue distribution and inheritance of heteroplasmic mitochondrial DNA point mutation by denaturing gradient gel electrophoresis in merrf syndrome." *Neuromuscular Disorders* **2**(5-6): 323-330.
- Love, M. I., W. Huber, et al. (2014). "Moderated estimation of fold change and dispersion for RNA-Seq data with DESeq2. bioRxiv preprint, 2014." URL: <http://dx.doi.org/10.1101/002832>.
- Ma, C. Y., C. P. Zhang, et al. (2011). "Decreased expression of profilin 2 in oral squamous cell carcinoma and its clinicopathological implications." *Oncology Reports* **26**(4): 813-823.
- Macmillan, C., B. Lach, et al. (1993). "Variable distribution of mutant mitochondrial DNAs (tRNA^{Leu}[3243]) in tissues of symptomatic relatives with MELAS: The role of mitotic segregation." *Neurology* **43**(8): 1586-1590.
- Majamaa, K., J. S. Moilanen, et al. (1998). "Epidemiology of A3243G, the mutation for mitochondrial encephalomyopathy, lactic acidosis, and strokelike episodes: Prevalence of the mutation in an adult population." *American Journal of Human Genetics* **63**(2): 447-454.
- Mankertz, J. and J. D. Schulzke (2007). "Altered permeability in inflammatory bowel disease: Pathophysiology and clinical implications." *Current Opinion in Gastroenterology* **23**(4): 379-383.
- Margulis, L. (1971). "The origin of plant and animal cells." *American Scientist* **59**(2): 230-235.
- Martin, W. and M. Müller (1998). "The hydrogen hypothesis for the first eukaryote." *Nature* **392**(6671): 37-41.

- Maslov, A. Y., T. A. Barone, et al. (2004). "Neural Stem Cell Detection, Characterization, and Age-Related Changes in the Subventricular Zone of Mice." Journal of Neuroscience **24**(7): 1726-1733.
- Mason, P. A., E. C. Matheson, et al. (2003). "Mismatch repair activity in mammalian mitochondria." Nucleic Acids Research **31**(3): 1052-1058.
- Matsutani N, Y. H., Tahara E, et al. (2001). "Expression of telomeric repeat binding factor 1 and 2 and TRF1-interacting nuclear protein 2 in human gastric carcinomas." Int J Oncol **19**: 507-512.
- Mazzoccoli, G., A. Piepoli, et al. (2012). "Altered expression of the clock gene machinery in kidney cancer patients." Biomedicine and Pharmacotherapy **66**(3): 175-179.
- McCord, J. M., Fridovich. I. (1969). "Superoxide dismutase. An enzymic function for erythrocyte hemocuprein (hemocuprein)." J Biol Chem. **244**: 6049-6055.
- McDaniel, L. D. and R. A. Schultz (2008). XPF/ERCC4 and ERCC1: Their products and biological roles. Advances in Experimental Medicine and Biology. **637**: 65-82.
- McDonald, S. A. C., L. C. Greaves, et al. (2008). "Mechanisms of Field Cancerization in the Human Stomach: The Expansion and Spread of Mutated Gastric Stem Cells." Gastroenterology **134**(2): 500-510.
- McDonald, S. A. C., S. L. Preston, et al. (2006). "Clonal expansion in the human gut: Mitochondrial DNA mutations show us the way." Cell Cycle **5**(8): 808-811.
- McFarland, R., J. L. Elson, et al. (2004). "Assigning pathogenicity to mitochondrial tRNA mutations: When 'definitely maybe' is not good enough." Trends in Genetics **20**(12): 591-596.
- McFarland, R., H. Swalwell, et al. (2008). "The m.5650G > A mitochondrial tRNAAla mutation is pathogenic and causes a phenotype of pure myopathy." Neuromuscular Disorders **18**(1): 63-67.
- McFarland, R., R. W. Taylor, et al. (2007). Mitochondrial Disease-Its Impact, Etiology, and Pathology. **77**: 113-155.
- McKay, D. M. (2005). "Good bug, bad bug: In the case of enteric inflammatory disease does the epithelium decide?" Memorias do Instituto Oswaldo Cruz **100**(SUPPL. 1): 205-210.
- Medawar, P. B. (1952). An unsolved problem in biology. London.
- Meyer, R., V. Fofanov, et al. (2009). "Overexpression and mislocalization of the chromosomal segregation protein separase in multiple human cancers." Clinical Cancer Research **15**(8): 2703-2710.
- Meyerson, M., C. M. Counter, et al. (1997). "hEST2, the putative human telomerase catalytic subunit gene, is up-regulated in tumor cells and during immortalization." Cell **90**(4): 785-795.
- Michikawa, Y., F. Mazzucchelli, et al. (1999). "Aging-dependent large accumulation of point mutations in the human mtDNA control region for replication." Science **286**(5440): 774-779.
- Miquel, J., A. C. Economos, et al. (1980). "Mitochondrial role in cell aging." Experimental Gerontology **15**(6): 575-591.
- Mita, S., B. Schmidt, et al. (1989). "Detection of 'deleted' mitochondrial genomes in cytochrome-c oxidase-deficient muscle fibers of a patient with Kearns-Sayre syndrome." Proceedings of the National Academy of Sciences of the United States of America **86**(23): 9509-9513.
- Mithieux, G., F. Rajas, et al. (2004). "A novel role for glucose 6-phosphatase in the small intestine in the control of glucose homeostasis." Journal of Biological Chemistry **279**(43): 44231-44234.
- Miyaki, M., K. Yatagai, et al. (1977). "Strand breaks of mammalian mitochondrial DNA induced by carcinogens." Chemico-Biological Interactions **17**(3): 321-329.
- Montanari, A., C. Besagni, et al. (2008). "Yeast as a model of human mitochondrial tRNA base substitutions: Investigation of the molecular basis of respiratory defects." RNA **14**(2): 275-283.
- Moraes, C. T., S. DiMauro, et al. (1989). "Mitochondrial DNA deletions in progressive external ophthalmoplegia and Kearne-Sayre syndrome." New England Journal of Medicine **320**(20): 1293-1299.

- Moreno-Lastres, D., F. Fontanesi, et al. (2012). "Mitochondrial complex I plays an essential role in human respirasome assembly." Cell Metabolism **15**(3): 324-335.
- Moretta, L., Ciccone, E., Mingari, M. C., Biassoni, R. and Moretta, A. (1994). "Human natural killer cells: origin, clonality, specificity, and receptors." Adv Immunol. **55**: 341-380.
- Morris, A. A., Jackson, M. J., Bindoff, L. A., and Turnbull, D. M. (1995). "The investigation of mitochondrial respiratory chain disease." J R Soc Med **88**: 217p-222p.
- Morris, R. L. and P. J. Hollenbeck (1993). "The regulation of bidirectional mitochondrial transport is coordinated with axonal outgrowth." Journal of Cell Science **104**(3): 917-927.
- Muller-Hocker, J. (1989). "Cytochrome-c-oxidase deficient cardiomyocytes in the human heart: An age-related phenomenon. A histochemical ultracytochemical study." American Journal of Pathology **134**(5): 1167-1173.
- Muller-Hocker, J. (1990). "Cytochrome c oxidase deficient fibres in the limb muscle and diaphragm of man without muscular disease: An age-related alteration." Journal of the Neurological Sciences **100**(1-2): 14-21.
- Munscher, C., T. Rieger, et al. (1993). "The point mutation of mitochondrial DNA characteristic for MERRF disease is found also in healthy people of different ages." FEBS Letters **317**(1-2): 27-30.
- Nakahata, S. and K. Morishita (2012). "CADM1/TSLC1 is a novel cell surface marker for adult T-cell leukemia/lymphoma." Journal of clinical and experimental hematopathology : JCEH **52**(1): 17-22.
- Nass, M. M. (1966). "The circularity of mitochondrial DNA." Proceedings of the National Academy of Sciences of the United States of America **56**(4): 1215-1222.
- Neckelmann, N., K. Li, et al. (1987). "cDNA sequence of a human skeletal muscle ADP/ATP translocator: lack of a leader peptide, divergence from a fibroblast translocator cDNA, and coevolution with mitochondrial DNA genes." Proceedings of the National Academy of Sciences of the United States of America **84**(21): 7580-7584.
- Nekhaeva, E., N. D. Bodyak, et al. (2002). "Clonally expanded mtDNA point mutations are abundant in individual cells of human tissues." Proceedings of the National Academy of Sciences of the United States of America **99**(8): 5521-5526.
- Neri, P., L. Ren, et al. (2011). "Integrin β 7-mediated regulation of multiple myeloma cell adhesion, migration, and invasion." Blood **117**(23): 6202-6213.
- Newmeyer, D. D. and S. Ferguson-Miller (2003). "Mitochondria: Releasing power for life and unleashing the machineries of death." Cell **112**(4): 481-490.
- Nishikawa, M., N. Oshitani, et al. (2005). "Accumulation of mitochondrial DNA mutation with colorectal carcinogenesis in ulcerative colitis." British Journal of Cancer **93**(3): 331-337.
- Nishimura, E. K., S. R. Granter, et al. (2005). "Mechanisms of hair graying: Incomplete melanocyte stem cell maintenance in the niche." Science **307**(5710): 720-724.
- Noah, T. K., B. Donahue, et al. (2011). "Intestinal development and differentiation." Experimental Cell Research **317**(19): 2702-2710.
- Noji, H., R. Yasuda, et al. (1997). "Direct observation of the rotation of F1-ATPase." Nature **386**(6622): 299-302.
- Nomoto, S., K. Yamashita, et al. (2002). "Mitochondrial D-loop mutations as clonal markers in multicentric hepatocellular carcinoma and plasma." Clinical Cancer Research **8**(2): 481-487.
- Nooteboom, M., R. Johnson, et al. (2010). "Age-associated mitochondrial DNA mutations lead to small but significant changes in cell proliferation and apoptosis in human colonic crypts." Aging Cell **9**(1): 96-99.
- Norddahl, G. L., C. J. Pronk, et al. (2011). "Accumulating mitochondrial DNA mutations drive premature hematopoietic aging phenotypes distinct from physiological stem cell aging." Cell Stem Cell **8**(5): 499-510.
- Norris, M. D., J. Smith, et al. (2005). "Expression of multidrug transporter MRP4/ABCC4 is a marker of poor prognosis in neuroblastoma and confers resistance to irinotecan in vitro." Molecular Cancer Therapeutics **4**(4): 547-553.

- Old, S. L. and M. A. Johnson (1989). "Methods of microphotometric assay of succinate dehydrogenase and cytochrome c oxidase activities for use on human skeletal muscle." Histochemical Journal **21**(9-10): 545-555.
- Orrenius, S., B. Zhivotovsky, et al. (2003). "Regulation of cell death: The calcium-apoptosis link." Nature Reviews Molecular Cell Biology **4**(7): 552-565.
- Palade, G. E. (1953). "An electron microscope study of the mitochondrial structure." The journal of histochemistry and cytochemistry : official journal of the Histochemistry Society **1**(4): 188-211.
- Park, J. S., L. K. Sharma, et al. (2009). "A heteroplasmic, not homoplasmic, mitochondrial DNA mutation promotes tumorigenesis via alteration in reactive oxygen species generation and apoptosis." Human Molecular Genetics **18**(9): 1578-1589.
- Park, S. J. and P. Schimmel (1988). "Evidence for interaction of an aminoacyl transfer RNA synthetase with a region important for the identity of its cognate transfer RNA." Journal of Biological Chemistry **263**(32): 16527-16530.
- Passos, J. F., G. Saretzki, et al. (2007). "Mitochondrial dysfunction accounts for the stochastic heterogeneity in telomere-dependent senescence." PLoS Biology **5**(5): 1138-1151.
- Patel, J. H. and S. B. McMahon (2007). "BCL2 is a downstream effector of MIZ-1 essential for blocking c-MYC-induced apoptosis." Journal of Biological Chemistry **282**(1): 5-13.
- Payne, B. A. I., I. J. Wilson, et al. (2013). "Universal heteroplasmy of human mitochondrial DNA." Human Molecular Genetics **22**(2): 384-390.
- Peterson, L. W. and D. Artis (2014). "Intestinal epithelial cells: Regulators of barrier function and immune homeostasis." Nature Reviews Immunology **14**(3): 141-153.
- Phua, L. C., M. Mal, et al. (2013). "Investigating the role of nucleoside transporters in the resistance of colorectal cancer to 5-fluorouracil therapy." Cancer Chemistry and Pharmacology **71**(3): 817-823.
- Pinz, K. G. and D. F. Bogenhagen (1998). "Efficient repair of abasic sites in DNA by mitochondrial enzymes." Molecular and Cellular Biology **18**(3): 1257-1265.
- Polyak, K., Y. Li, et al. (1998). "Somatic mutations of the mitochondrial genome in human colorectal tumours." Nature Genetics **20**(3): 291-293.
- Potten, C. S. (1998). "Stem cells in gastrointestinal epithelium: Numbers, characteristics and death." Philosophical Transactions of the Royal Society B: Biological Sciences **353**(1370): 821-830.
- Potten, C. S., J. A. O'Shea, et al. (2001). "The effects of repeated doses of keratinocyte growth factor on cell proliferation in the cellular hierarchy of the crypts of the murine small intestine." Cell Growth and Differentiation **12**(5): 265-275.
- Pozzan, T., P. Magalhães, et al. (2000). "The comeback of mitochondria to calcium signalling." Cell Calcium **28**(5-6): 279-283.
- Prakash, L. (1975). "Repair of pyrimidine dimers in nuclear and mitochondrial DNA of yeast irradiated with low doses of ultraviolet light." Journal of Molecular Biology **98**(4): 781-795.
- Rahman, S., J. Poulton, et al. (2001). "Decrease of 3243 A→G mtDNA mutation from blood in MELAS syndrome: A longitudinal study." American Journal of Human Genetics **68**(1): 238-240.
- Rahman, S., J. W. Taanman, et al. (1999). "A missense mutation of cytochrome oxidase subunit II causes defective assembly and myopathy." American Journal of Human Genetics **65**(4): 1030-1039.
- Rea, S. L., N. Ventura, et al. (2007). "Relationship between mitochondrial electron transport chain dysfunction, development, and life extension in *Caenorhabditis elegans*." PLoS Biology **5**(10).
- Rebelo, A. P., L. M. Dillon, et al. (2011). "Mitochondrial DNA transcription regulation and nucleoid organization." Journal of Inherited Metabolic Disease **34**(4): 941-951.
- Reddel, R. R. (2014). "Telomere Maintenance Mechanisms in Cancer: Clinical Implications." Curr Pharm Des. Epub ahead of print.
- Richter C, P. J., Ames BN. (1988). "Normal oxidative damage to mitochondrial and nuclear DNA is extensive.
- ." Proc Natl Acad Sci U S A. **85**: 6465-6467.

- Roberti, M., F. Bruni, et al. (2006). "MTERF3, the most conserved member of the mTERF-family, is a modular factor involved in mitochondrial protein synthesis." Biochimica et Biophysica Acta - Bioenergetics **1757**(9-10): 1199-1206.
- Ross, J. M., J. B. Stewart, et al. (2013). "Germline mitochondrial DNA mutations aggravate ageing and can impair brain development." Nature **501**(7467): 412-415.
- Rossi, D. J., D. Bryder, et al. (2005). "Cell intrinsic alterations underlie hematopoietic stem cell aging." Proceedings of the National Academy of Sciences of the United States of America **102**(26): 9194-9199.
- Rotig, A., V. Cormier, et al. (1990). "Pearson's marrow-pancreas syndrome. A multisystem mitochondrial disorder in infancy." Journal of Clinical Investigation **86**(5): 1601-1608.
- Saito, T., N. Masuda, et al. (2004). "Expression of EphA2 and E-cadherin in colorectal cancer: Correlation with cancer metastasis." Oncology Reports **11**(3): 605-611.
- Samorajski, T., R. L. Friede, et al. (1971). "Age differences in the ultrastructure of axons in the pyramidal tract of the mouse." Journals of Gerontology **26**(4): 542-551.
- Samuels, D. C., E. A. Schon, et al. (2004). "Two direct repeats cause most human mtDNA deletions." Trends in Genetics **20**(9): 393-398.
- Schaefer, A. M., R. McFarland, et al. (2008). "Prevalence of mitochondrial DNA disease in adults." Annals of Neurology **63**(1): 35-39.
- Schägger, H. and K. Pfeiffer (2000). "Supercomplexes in the respiratory chains of yeast and mammalian mitochondria." EMBO Journal **19**(8): 1777-1783.
- Schimanski, C. C., G. Schmitz, et al. (2005). "Reduced expression of Hugel-1, the human homologue of Drosophila tumour suppressor gene lgl, contributes to progression of colorectal cancer." Oncogene **24**(19): 3100-3109.
- Schmidt, G. H., D. J. Winton, et al. (1988). "Development of the pattern of cell renewal in the crypt-villus unit of chimaeric mouse small intestine." Development **103**(4): 785-790.
- Schon, E. A., R. Rizzuto, et al. (1989). "A direct repeat is a hotspot for large-scale deletion of human mitochondrial DNA." Science **244**(4902): 346-349.
- Schriner, S. E., N. J. Linford, et al. (2005). "Medicine: Extension of murine life span by overexpression of catalase targeted to mitochondria." Science **308**(5730): 1909-1911.
- Schroeder, A., O. Mueller, et al. (2006). "The RIN: An RNA integrity number for assigning integrity values to RNA measurements." BMC Molecular Biology **7**.
- Schultz, B. E. and S. I. Chan (2001). Structures and proton-pumping strategies of mitochondrial respiratory enzymes. Annual Review of Biophysics and Biomolecular Structure. **30**: 23-65.
- Schwartz, M. and J. Vissing (2002). "Paternal inheritance of mitochondrial DNA." New England Journal of Medicine **347**(8): 576-580.
- Sciacco M, B. E., Schon EA, DiMauro S, Moraes CT. (1994). "Distribution of wild-type and common deletion forms of mtDNA in normal and respiration-deficient muscle fibers from patients with mitochondrial myopathy." Hum Mol Genet **3**: 13-19.
- Shadel, G. S. and D. A. Clayton (1997). Mitochondrial DNA maintenance in vertebrates. Annual Review of Biochemistry. **66**: 409-436.
- Shanahan, F. (2002). "The host-microbe interface within the gut." Best Practice & Research Clinical Gastroenterology **16**(6): 915-931.
- Shao, L., H. Li, et al. (2011). "Reactive oxygen species and hematopoietic stem cell senescence." International Journal of Hematology **94**(1): 24-32.
- Sharpless, N. E. and R. A. DePinho (2007). "How stem cells age and why this makes us grow old." Nature Reviews Molecular Cell Biology **8**(9): 703-713.
- Shay, J. W. and S. Ishii (1990). "Unexpected nonrandom mitochondrial DNA segregation in human cell hybrids." Anticancer Research **10**(2 A): 279-284.
- Shi, T. Y., J. He, et al. (2012). "Association between XPF polymorphisms and cancer risk: A meta-analysis." PLoS ONE **7**(7).
- Shimizu, A., T. Mito, et al. (2014). "Transmitochondrial mice as models for primary prevention of diseases caused by mutation in the tRNALys gene." Proceedings of the National Academy of Sciences of the United States of America **111**(8): 3104-3109.
- Shoffner, J. M., M. T. Lott, et al. (1990). "Myoclonic epilepsy and ragged-red fiber disease (MERRF) is associated with a mitochondrial DNA tRNA(Lys) mutation." Cell **61**(6): 931-937.

- Shoffner, J. M., M. T. Lott, et al. (1989). "Spontaneous Kearns-Sayre/chronic external ophthalmoplegia plus syndrome associated with a mitochondrial DNA deletion: A slip-replication model and metabolic therapy." Proceedings of the National Academy of Sciences of the United States of America **86**(20): 7952-7956.
- Shokolenko, I., N. Venediktova, et al. (2009). "Oxidative stress induces degradation of mitochondrial DNA." Nucleic Acids Research **37**(8): 2539-2548.
- Shoubridge, E. A. (2001). "Nuclear genetic defects of oxidative phosphorylation." Human Molecular Genetics **10**(20): 2277-2284.
- Shoubridge, E. A., G. Karpati, et al. (1990). "Deletion mutants are functionally dominant over wild-type mitochondrial genomes in skeletal muscle fiber segments in mitochondrial disease." Cell **62**(1): 43-49.
- Shui, J. W., M. W. Steinberg, et al. (2011). "Regulation of inflammation, autoimmunity, and infection immunity by HVEM-BTLA signaling." Journal of Leukocyte Biology **89**(4): 517-523.
- Silva, J. P., M. Köhler, et al. (2000). "Impaired insulin secretion and β -cell loss in tissue-specific knockout mice with mitochondrial diabetes." Nature Genetics **26**(3): 336-340.
- Simon, D. K., M. T. Lin, et al. (2004). "Somatic mitochondrial DNA mutations in cortex and substantia nigra in aging and Parkinson's disease." Neurobiology of Aging **25**(1): 71-81.
- Singh, K. K., J. Russell, et al. (1999). "Mitochondrial DNA determines the cellular response to cancer therapeutic agents." Oncogene **18**(48): 6641-6646.
- Smeitink, J. and L. Van Den Heuvel (1999). "Human mitochondrial complex I in health and disease." American Journal of Human Genetics **64**(6): 1505-1510.
- Smits, P., J. Smeitink, et al. (2010). "Mitochondrial translation and beyond: Processes implicated in combined oxidative phosphorylation deficiencies." Journal of Biomedicine and Biotechnology **2010**.
- Sohal, R. S., I. Svensson, et al. (1989). "Superoxide anion radical production in different animal species." Mechanisms of Ageing and Development **49**(2): 129-135.
- Soták, M., L. Polidarová, et al. (2013). "An association between clock genes and clock-controlled cell cycle genes in murine colorectal tumors." International Journal of Cancer **132**(5): 1032-1041.
- Spelbrink, J. N., F. Y. Li, et al. (2001). "Human mitochondrial DNA deletions associated with mutations in the gene encoding Twinkle, a phage T7 gene 4-like protein localized in mitochondria." Nature Genetics **28**(3): 223-231.
- Srivastava, S. and C. T. Moraes (2005). "Double-strand breaks of mouse muscle mtDNA promote large deletions similar to multiple mtDNA deletions in humans." Human Molecular Genetics **14**(7): 893-902.
- St-Pierre, J., J. A. Buckingham, et al. (2002). "Topology of superoxide production from different sites in the mitochondrial electron transport chain." Journal of Biological Chemistry **277**(47): 44784-44790.
- Starkov, A. A. (2008). The role of mitochondria in reactive oxygen species metabolism and signaling. Annals of the New York Academy of Sciences. **1147**: 37-52.
- Starkov, A. A. (2008). "The Role of Mitochondria in Reactive Oxygen Species Metabolism and Signaling." Annals of the New York Academy of Sciences **1147**(1): 37-52.
- Steinbach, D., J. Lengemann, et al. (2003). "Response to chemotherapy and expression of the genes encoding the multidrug resistance-associated proteins MRP2, MRP3, MRP4, MRP5, and SMRP in childhood acute myeloid leukemia." Clinical Cancer Research **9**(3): 1083-1086.
- Stewart, J. B., C. Freyer, et al. (2008). "Strong purifying selection in transmission of mammalian mitochondrial DNA." PLoS Biology **6**(1).
- Stewart, J. B., C. Freyer, et al. (2008). "Strong purifying selection in transmission of mammalian mitochondrial DNA." PLoS Biol **6**(1): e10.
- Subramanian, A., P. Tamayo, et al. (2005). "Gene set enrichment analysis: a knowledge-based approach for interpreting genome-wide expression profiles." Proceedings of the National Academy of Sciences of the United States of America **102**(43): 15545-15550.
- Sugioka, K., M. Nakano, et al. (1988). "Mechanism of O-2 generation in reduction and oxidation cycle of ubiquinones in a model of mitochondrial electron transport systems." BBA - Bioenergetics **936**(3): 377-385.

- Sui, G., S. Zhou, et al. (2006). "Mitochondrial DNA mutations in preneoplastic lesions of the gastrointestinal tract: A biomarker for the early detection of cancer." Molecular Cancer **5**.
- Suomalainen, A. (2013). "Fibroblast growth factor 21: A novel biomarker for human muscle-manifesting mitochondrial disorders." Expert Opinion on Medical Diagnostics **7**(4): 313-317.
- Susin, S. A., H. K. Lorenzo, et al. (1999). "Molecular characterization of mitochondrial apoptosis-inducing factor." Nature **397**(6718): 441-446.
- Sutovsky, P., R. D. Moreno, et al. (2000). "Ubiquitinated sperm mitochondria, selective proteolysis, and the regulation of mitochondrial inheritance in mammalian embryos." Biology of Reproduction **63**(2): 582-590.
- Swalwell, H., M. Deschauer, et al. (2006). "Pure myopathy associated with a novel mitochondrial tRNA gene mutation." Neurology **66**(3): 447-449.
- Swerdlow, R. H. (2007). "Mitochondria in cybrids containing mtDNA from persons with mitochondrialriopathies." Journal of Neuroscience Research **85**(15): 3416-3428.
- Szakács, G., J. P. Annereau, et al. (2004). "Predicting drug sensitivity and resistance: Profiling ABC transporter genes in cancer cells." Cancer Cell **6**(2): 129-137.
- Szilard, L. (1959). "ON THE NATURE OF THE AGING PROCESS." Proc Natl Acad Sci U S A. **45**(1): 30-45.
- Takai, H., A. Smogorzewska, et al. (2003). "DNA damage foci at dysfunctional telomeres." Current Biology **13**(17): 1549-1556.
- Tan, D. J., R. K. Bai, et al. (2002). "Comprehensive scanning of somatic mitochondrial DNA mutations in breast cancer." Cancer Research **62**(4): 972-976.
- Taniike, M., H. Fukushima, et al. (1992). "Mitochondrial tRNAlle mutation in fatal cardiomyopathy." Biochemical and Biophysical Research Communications **186**(1): 47-53.
- Tanji, K., T. Kunimatsu, et al. (2001). "Neuropathological features of mitochondrial disorders." Seminars in Cell and Developmental Biology **12**(6): 429-439.
- Tarasov, A. I., E. J. Griffiths, et al. (2012). "Regulation of ATP production by mitochondrial Ca²⁺." Cell Calcium **52**(1): 28-35.
- Taylor, R. W., M. J. Barron, et al. (2003). "Mitochondrial DNA mutations in human colonic crypt stem cells." Journal of Clinical Investigation **112**(9): 1351-1360.
- Taylor, R. W., C. Giordano, et al. (2003). "A homoplasmic mitochondrial transfer ribonucleic acid mutation as a cause of maternally inherited hypertrophic cardiomyopathy." Journal of the American College of Cardiology **41**(10): 1786-1796.
- Taylor, R. W. and D. M. Turnbull (2005). "Mitochondrial DNA mutations in human disease." Nat Rev Genet **6**(5): 389-402.
- Temperley, R., R. Richter, et al. (2010). "Hungry codons promote frameshifting in human mitochondrial ribosomes." Science **327**(5963): 301.
- Tian, Q., J. Zhang, et al. (2005). "Human multidrug resistance associated protein 4 confers resistance to camptothecins." Pharmaceutical Research **22**(11): 1837-1853.
- Tomkinson, A. E., R. T. Bonk, et al. (1988). "Mitochondrial endonuclease activities specific for apurinic/apyrimidinic sites in DNA from mouse cells." Journal of Biological Chemistry **263**(25): 12532-12537.
- Toyokuni, S. K., Okamoto, J., Yodoi et al., (1995). "Persistant Oxidative stress in Cancer." FEBS Lett **358**: 1-3.
- Trifunovic, A., A. Hansson, et al. (2005). "Somatic mtDNA mutations cause aging phenotypes without affecting reactive oxygen species production." Proceedings of the National Academy of Sciences of the United States of America **102**(50): 17993-17998.
- Trifunovic, A., A. Wredenberg, et al. (2004). "Premature ageing in mice expressing defective mitochondrial DNA polymerase." Nature **429**(6990): 417-423.
- Tuppen, H. A. L., E. L. Blakely, et al. (2010). "Mitochondrial DNA mutations and human disease." Biochimica et Biophysica Acta (BBA) - Bioenergetics **1797**(2): 113-128.
- Turrens, J. F. and A. Boveris (1980). "Generation of superoxide anion by the NADH dehydrogenase of bovine heart mitochondria." Biochemical Journal **191**(2): 421-427.
- Twig, G., A. Elorza, et al. (2008). "Fission and selective fusion govern mitochondrial segregation and elimination by autophagy." EMBO Journal **27**(2): 433-446.

- Tyynismaa, H., K. P. Mjosund, et al. (2005). "Mutant mitochondrial helicase Twinkle causes multiple mtDNA deletions and a late-onset mitochondrial disease in mice." Proceedings of the National Academy of Sciences of the United States of America **102**(49): 17687-17692.
- Valko, M., D. Leibfritz, et al. (2007). "Free radicals and antioxidants in normal physiological functions and human disease." International Journal of Biochemistry and Cell Biology **39**(1): 44-84.
- van der Giezen, M. and J. Tovar (2005). "Degenerate mitochondria." EMBO Reports **6**(6): 525-530.
- Van Goethem, G., B. Dermaut, et al. (2001). "Mutation of POLG is associated with progressive external ophthalmoplegia characterized by mtDNA deletions." Nature Genetics **28**(3): 211-212.
- Varlamov, D. A., A. P. Kudin, et al. (2002). "Metabolic consequences of a novel missense mutation of the mtDNA CO I gene." Human Molecular Genetics **11**(16): 1797-1805.
- Venyo, A. K. G. (2014). "Lymphoma of the Urinary bladder." Advances in Urology.
- Verbsky, J. and P. W. Majerus (2005). "Increased levels of inositol hexakisphosphate (InsP6) protect HEK293 cells from tumor necrosis factor α - and Fas-induced apoptosis." Journal of Biological Chemistry **280**(32): 29263-29268.
- Vermulst, M., J. H. Bielas, et al. (2007). "Mitochondrial point mutations do not limit the natural lifespan of mice." Nature Genetics **39**(4): 540-543.
- Vermulst, M., J. Wanagat, et al. (2008). "DNA deletions and clonal mutations drive premature aging in mitochondrial mutator mice." Nat Genet **40**(4): 392-394.
- Vernoche, C., A. Mourier, et al. (2012). "Adipose-specific deletion of TFAM increases mitochondrial oxidation and protects mice against obesity and insulin resistance." Cell Metabolism **16**(6): 765-776.
- Vikstrom, K. L., T. Bohlmeier, et al. (1998). "Hypertrophy, pathology, and molecular markers of cardiac pathogenesis." Circulation Research **82**(7): 773-778.
- Vogel, F., C. Bornhövd, et al. (2006). "Dynamic subcompartmentalization of the mitochondrial inner membrane." Journal of Cell Biology **175**(2): 237-247.
- Vousden, K. H. (2002). "Switching from life to death: The Miz-ing link between Myc and p53." Cancer Cell **2**(5): 351-352.
- Wallace, D., C., Singh, G., Lott, J.A., Schurr, T.G., Lezza, A.M., Elsas II, L.J. and Nikoskelainen, E.K. (1988). "Mitochondrial DNA mutation associated with Lebers hereditary optic neuropathy." Science **242**: 1427-1430.
- Wallace, D. C. (1989). "Mitochondrial DNA mutations and neuromuscular disease." Trends in Genetics **5**(1): 9-13.
- Wallace, D. C. (1999). "Mitochondrial diseases in man and mouse." Science **283**(5407): 1482-1488.
- Wallace, D. C., J. Ye, et al. (1987). "Sequence analysis of cDNAs for the human and bovine ATP synthase β subunit: mitochondrial DNA genes sustain seventeen times more mutations." Current Genetics **12**(2): 81-90.
- Wallace, D. C., Lott, M.T. and Procaccio, V. (2007). Emery and Rimoin's principles and practice of medical genetics.
- Wang, G. J., L. M. Nutter, et al. (1997). "Insensitivity of cultured rat cortical neurons to mitochondrial DNA synthesis inhibitors. Evidence for a slow turnover of mitochondrial DNA." Biochemical Pharmacology **54**(1): 181-187.
- Wang, J. and K. Pantopoulos (2011). "Regulation of cellular iron metabolism." Biochemical Journal **434**(3): 365-381.
- Wang, Z., M. Gerstein, et al. (2009). "RNA-Seq: A revolutionary tool for transcriptomics." Nature Reviews Genetics **10**(1): 57-63.
- Wanrooij, S., J. Miralles Fusté, et al. (2012). "In vivo mutagenesis reveals that OriL is essential for mitochondrial DNA replication." EMBO Reports **13**(12): 1130-1137.
- Warburg, O. (1930). Metabolism of tumors, Arnold Constable, London.
- Wilcken, B. (2010). "Fatty acid oxidation disorders: Outcome and long-term prognosis." Journal of Inherited Metabolic Disease **33**(5): 501-506.
- Williams (1957). "Pleiotropy, natural selection, and the evolution of senescence." Evolution **11**: 398-411.

- Williams, M. D., H. Van Remmen, et al. (1998). "Increased oxidative damage is correlated to altered mitochondrial function in heterozygous manganese superoxide dismutase knockout mice." Journal of Biological Chemistry **273**(43): 28510-28515.
- Williams, R. S., S. Salmons, et al. (1986). "Regulation of nuclear and mitochondrial gene expression by contractile activity in skeletal muscle." Journal of Biological Chemistry **261**(1): 376-380.
- Wilson, P. D. and L. M. Franks (1975). "The effect of age on mitochondrial ultrastructure." GERONTOLOGIA **21**(2): 81-94.
- Wilson, P. D. and L. M. Franks (1975). "The effect of age on mitochondrial ultrastructure and enzyme cytochemistry." Biochemical Society Transactions **3**(1): 126-128.
- Winge, D. R. (2012). "Sealing the Mitochondrial Respirasome." Molecular and Cellular Biology **32**(14): 2647-2652.
- Wood, P. A., X. Yang, et al. (2008). "Period 2 mutation accelerates ApcMin/+ tumorigenesis." Molecular Cancer Research **6**(11): 1786-1793.
- Wredenberg, A., C. Freyer, et al. (2006). "Respiratory chain dysfunction in skeletal muscle does not cause insulin resistance." Biochemical and Biophysical Research Communications **350**(1): 202-207.
- Wredenberg, A., R. Wibom, et al. (2002). "Increased mitochondrial mass in mitochondrial myopathy mice." Proceedings of the National Academy of Sciences of the United States of America **99**(23): 15066-15071.
- Yakubovskaya, E., Z. Chen, et al. (2006). "Functional human mitochondrial DNA polymerase γ forms a heterotrimer." Journal of Biological Chemistry **281**(1): 374-382.
- Yakubovskaya, E., E. Mejia, et al. (2010). "Helix unwinding and base flipping enable human MTERF1 to terminate mitochondrial transcription." Cell **141**(6): 982-993.
- Yang, X., X. He, et al. (2012). "Mammalian PER2 regulates AKT activation and DNA damage response." Biochemistry and Cell Biology **90**(6): 675-682.
- Yarham, J. W., M. Al-Dosary, et al. (2011). "A comparative analysis approach to determining the pathogenicity of mitochondrial tRNA mutations." Human Mutation **32**(11): 1319-1325.
- Yasukawa, T., A. Reyes, et al. (2006). "Replication of vertebrate mitochondrial DNA entails transient ribonucleotide incorporation throughout the lagging strand." EMBO Journal **25**(22): 5358-5371.
- Yasukawa, T., T. Suzuki, et al. (2000). "Defect in modification at the anticodon wobble nucleotide of mitochondrial tRNA(Lys) with the MERRF encephalomyopathy pathogenic mutation." FEBS Letters **467**(2-3): 175-178.
- Yasukawa, T., T. Suzuki, et al. (2000). "Modification defect at anticodon wobble nucleotide of mitochondrial tRNAs(Leu)(UUR) with pathogenic mutations of mitochondrial myopathy, encephalopathy, lactic acidosis, and stroke-like episodes." Journal of Biological Chemistry **275**(6): 4251-4257.
- Yokota, M., H. Shitara, et al. (2010). "Generation of trans-mitochondrial mito-mice by the introduction of a pathogenic G13997A mtDNA from highly metastatic lung carcinoma cells." FEBS Letters **584**(18): 3943-3948.
- Yoneda, M., A. Chomyn, et al. (1992). "Marked replicative advantage of human mtDNA carrying a point mutation that causes the MELAS encephalomyopathy." Proceedings of the National Academy of Sciences of the United States of America **89**(23): 11164-11168.
- Yu-Wai-Man, P., J. Lai-Cheong, et al. (2010). "Somatic mitochondrial DNA deletions accumulate to high levels in aging human extraocular muscles." Investigative Ophthalmology and Visual Science **51**(7): 3347-3353.
- Zamzami, N. and G. Kroemer (2001). "The mitochondrion in apoptosis: How Pandora's box opens." Nature Reviews Molecular Cell Biology **2**(1): 67-71.
- Zeviani, M., C. T. Moraes, et al. (1988). "Deletions of mitochondrial DNA in Kearns-Sayre syndrome." Neurology **38**(9): 1339-1346.
- Zhang, C., A. W. Linnane, et al. (1993). "Occurrence of a particular base substitution (3243 A to G) in mitochondrial DNA of tissues of ageing humans." Biochemical and Biophysical Research Communications **195**(2): 1104-1110.

- Zhang, H., J. M. Barceló, et al. (2001). "Human mitochondrial topoisomerase I." Proceedings of the National Academy of Sciences of the United States of America **98**(19): 10608-10613.
- Zhang, N., G. Ge, et al. (2008). "Overexpression of Separase induces aneuploidy and mammary tumorigenesis." Proceedings of the National Academy of Sciences of the United States of America **105**(35): 13033-13038.
- Zheng, L., M. Zhou, et al. (2008). "Human DNA2 Is a Mitochondrial Nuclease/Helicase for Efficient Processing of DNA Replication and Repair Intermediates." Molecular Cell **32**(3): 325-336.
- Zheng, W., K. Khrapko, et al. (2006). "Origins of human mitochondrial point mutations as DNA polymerase γ -mediated errors." Mutation Research - Fundamental and Molecular Mechanisms of Mutagenesis **599**(1-2): 11-20.